

# Sheffield Hallam University

*Changes in chondroitin sulphate proteoglycan in multiple sclerosis : A role for ADAMTS-9.*

ABUNEEZA, Esadawi.

Available from the Sheffield Hallam University Research Archive (SHURA) at:

<http://shura.shu.ac.uk/20613/>

## A Sheffield Hallam University thesis

This thesis is protected by copyright which belongs to the author.

The content must not be changed in any way or sold commercially in any format or medium without the formal permission of the author.

When referring to this work, full bibliographic details including the author, title, awarding institution and date of the thesis must be given.

Please visit <http://shura.shu.ac.uk/20613/> and <http://shura.shu.ac.uk/information.html> for further details about copyright and re-use permissions.

Learning and IT Services  
Collegiate Learning Centre  
Collegiate Crescent Campus  
Sheffield S10 2BP

1445

102 156 560 1



**REFERENCE**

ProQuest Number: 10701260

All rights reserved

INFORMATION TO ALL USERS

The quality of this reproduction is dependent upon the quality of the copy submitted.

In the unlikely event that the author did not send a complete manuscript and there are missing pages, these will be noted. Also, if material had to be removed, a note will indicate the deletion.



ProQuest 10701260

Published by ProQuest LLC (2017). Copyright of the Dissertation is held by the Author.

All rights reserved.

This work is protected against unauthorized copying under Title 17, United States Code  
Microform Edition © ProQuest LLC.

ProQuest LLC.  
789 East Eisenhower Parkway  
P.O. Box 1346  
Ann Arbor, MI 48106 – 1346

**Changes in Chondroitin Sulphate Proteoglycan in  
Multiple Sclerosis: a role for ADAMTS-9**

**Esadawi Abuneeza**

**A thesis submitted in partial fulfilment of the requirement of Sheffield  
Hallam University for the degree of Doctor of Philosophy**

**December 2015**

## Abstract

Multiple Sclerosis (MS) is an inflammatory demyelinating disease of the central nervous system (CNS) causing neurological disability in young adults, characterised by discrete acute and chronic lesions that are predominantly located in the CNS white matter. The role the extracellular matrix (ECM) has been widely studied as it is thought to be implicated in the pathogenesis of MS. Components such as chondroitin sulphate proteoglycans (CSPGs) are up-regulated in response to injury and inflammation and participate in the formation of sclerotic lesions. Research into the role of a disintegrin and metalloproteinase with thrombospondin motifs (ADAMTS) in CNS injury and inflammation has demonstrated that this protease may aid the recovery process by cleaving CSPGs, which are inhibitory to neurite outgrowth and axonal regeneration.

*In vivo* studies were carried out investigating the distribution and expression of aggrecan and versican by dual label immunohistochemistry (IHC) and western blotting (WB) using antibodies which specially recognise cleavage-derived aggrecan and versican neopeptides and intact protein. ADAMTS-9 expression was assessed by real time PCR (qRT-PCR), IHC and western blotting. In active lesions, both IHC and WB indicated that intact versican and aggrecan as well as their neopeptides and ADAMTS-9 expression were all increased in areas of myelin thinning with ongoing demyelination and macrophage activation, compared to control and normal appearing white matter (NAWM) brain tissue. Immunostaining for CSPG neopeptide was particularly strong at the plaque border in chronic active lesions (CAL) compared to chronic inactive lesions (CL), NAWM and control brain tissue, suggesting active enzymatic cleavage of intact protein. IHC studies demonstrated that ADAMTS-9 was expressed predominantly by astrocytes, endothelium, macrophages and neurons with increased expression within MS active lesions. qRT-PCR studies confirmed ADAMTS-9 expression in MS tissue. In summary this study provides evidence that ADAMTS-9 plays an important role in cleavage of the ECM CSPGs, aggrecan and versican, in active lesions in MS.

The role of CSPGs in neurite outgrowth from human neurons has been largely untested but is critical for understanding of regeneration following CNS injury. This thesis aimed to assess the effect of the ECM components, aggrecan, on neurite outgrowth of neuroblastoma cell line (SHSY-5Y) and expression of ADAMTS-9. This was achieved by several methods including qRT-PCR, ICC and WB. These data provided evidence that neurite outgrowth from SHSY-5Y cells is inhibited by aggrecan, this inhibition was associated with high level expression of ADAMTS-9.

This thesis also aimed to investigate the expression of ADAMTS-9 by cells of the CNS to gain a better understanding of how these enzymes might be regulated and their possible role in the pathogenesis of MS. Cells were treated with pro-inflammatory cytokines *in vitro*, to mimic *in vivo* inflammatory conditions, and following this, ICC and WB data demonstrated that ADAMTS-9 was constitutively expressed by primary human astrocytes, microglia (CHME3) and neuronal (SHSY-5Y) cell lines *in vitro*, under basal condition. In primary astrocytes, ADAMTS-9 expression was increased following treatment with 10ng/mL interferon- $\gamma$  compared to control untreated cells. In contrast, dual treatment with interleukin-1 and tumour necrosis factor resulted in down regulation of ADAMTS-9. Thus illustrating the external inflammatory milieu influences the expression of ADAMTS-9 in lesions in MS, which in turn influences the degradation of the ECM components aggrecan and versican, which are also upregulated in lesions. Further work to understand how these changes in the ECM influence CNS repair is needed.

## Acknowledgements

The work described within this thesis would not have been possible without the assistance and guidance of many people to whom I owe thanks.

To my supervisors Prof Nicola Woodroffe, Dr Rowena Bunning, Dr Alison Cross and Dr Gail Haddock, whose encouragement, guidance and assistance were invaluable.

To all the members of staff and students of the BMRC (past and present), for all their help, encouragement, and making the last three years so memorable, especially Abbie Binch, Abbey Thorpe, Abdurrahman Eswayah, Salah Enbaia, Hasan Aldewachi, Jodi Brookes, Mariam Sheilabi, Mowafag Elazzauzi, Mohamed Elzayat, Mootaz Salman, Nicola Wright, Rebecca Day, Umarat Srisawat and Yasin Al-Luabi. I would like to kindly acknowledge the generous contribution of David Owen who has helped with some of my IHC slides and confocal imaging.

The undertaking of this study would not have been possible without the financial backing of both the Ministry of Higher Education and Scientific Research-Libya. The MS Society Tissue Bank provided the human brain samples used in this thesis and are gratefully acknowledged.

Also, thanks to Drs Caroline Dalton, Christine Le Maitre and Susan Campbell for their valuable advice and support. I wish to extend heartfelt appreciation to Daniel English, Marguerite Lyons, Sarah Nile, and Karin Glockle. I will forever be grateful for your time and kindness shown during my stay in the BMRC. Thank you to all my friends in Libya; especially Adnan Salama, Mohamed Elrowemi and Walid Alnaas.

Lastly but not least, my family: father, mother, wife, children, brother and sisters as always, have been superb. Words cannot possibly describe how much tribute I must pay to you for your endless patience, tolerance, care, motivation, support and love. This not only enables me to survive during the recent terrible events in Libya but also would encourage me to take on any future challenge. Thank you from down deep in my heart and soul.

# Contents

Abstract.....	i
Acknowledgements.....	ii
Contents.....	iii
List of Figures.....	vii
List of Tables.....	x
Abbreviations.....	xi
Chapter 1 : Introduction.....	1
1 Multiple sclerosis .....	2
1.1 Clinical symptoms and disease course in MS.....	2
1.2 Diagnosis of MS .....	4
1.3 Aetiology of MS .....	4
1.3.1 Environmental factors.....	4
1.3.2 Genetics in MS.....	5
1.4 Pathology of MS .....	6
1.5 Cellular constituents of the CNS and their role in MS.....	7
1.5.1 Glial cells in MS .....	7
1.5.2 Microglia in MS .....	8
1.5.3 Astrocytes.....	10
1.5.4 Oligodendrocytes .....	10
1.5.5 Cerebral endothelia and the BBB.....	11
1.6 BBB dysfunction.....	13
1.7 Autoimmune mechanisms in MS .....	13
1.8 The CNS extracellular matrix in MS.....	17
1.8.1 Chondroitin Sulphate Proteoglycans .....	18
1.8.2 CSPG expression changes in demyelination and remyelination in MS.....	20
1.8.3 Molecular mechanism of CSPG inhibition of neurite outgrowth .....	26
1.9 Matrix metalloproteinases .....	27
1.9.1 Matrix metalloproteinase family proteins .....	27
1.9.2 MMPs in MS .....	30
1.10 ADAM family proteins.....	30
1.10.1 ADAM-17 in MS.....	31
1.11 ADAMTSs.....	31

1.11.1	Overview of ADAMTS.....	31
1.11.2	Basic domain structure and functions of ADAMTSs .....	32
1.11.3	Function of ADAMTSs subgroups.....	36
1.11.4	ADAMTS proteoglycanases in the physiology of the CNS.....	39
1.11.5	ADAMTS proteoglycanases in the pathological CNS.....	39
1.11.6	ADAMTSs in MS.....	40
1.12	The aims and objective of this study .....	43
2	Chapter 2 : Material and methods .....	44
2.1	Human brain tissue.....	45
2.1.1	Histopathology of frozen brain tissue.....	48
2.1.2	Immunohistochemistry on normal and MS brain sections.....	50
2.1.3	Image capture and analysis.....	53
2.1.4	Quantitation of immunostaining and data analysis.....	53
2.2	Western Blotting .....	54
2.2.1	Sodium dodecyl sulphate polyacrylamide gel electrophoresis (SDS- PAGE) .....	54
2.2.2	Protein Extraction .....	57
2.2.3	Estimation of total protein concentration by using Bradford assay.....	57
2.2.4	SDS-PAGE .....	58
2.2.5	Protein electroblotting.....	58
2.2.6	Immunoprobng the membrane .....	60
2.2.7	Determination of molecular weight of proteins migrated on SDS-PAGE.	60
2.3	Quantitative Reverse Transcriptase Polymerase Chain Reaction (qRT-PCR) .....	63
2.3.1	Overview of qRT-PCR .....	63
2.3.2	The amplification plot .....	63
2.3.3	Total RNA Extraction .....	65
2.3.4	Agarose gel electrophoresis of RNA products .....	65
2.3.5	cDNA Synthesis.....	66
2.3.6	Primer design and housekeeping genes for qRT-PCR validation .....	66
2.3.7	Comparative CT method of data analysis .....	67
2.4	Cell culture.....	69
2.4.1	Overview .....	69

2.4.2	Sub-culture of cells.....	69
2.4.3	Cell counting.....	70
2.4.4	Cryopreservation of cells .....	70
2.4.5	Aggrecan coating of plasticware for cell culture .....	70
2.4.6	Cytokine treatment of cells.....	72
2.4.7	Mycoplasma Testing .....	72
2.4.8	Determination of cell viability by MTT assay.....	73
2.4.9	Immunocytochemistry of the CNS cells.....	73
3	Chapter 3: Expression of white matter ECM CSPGs and neoepitope in MS.....	76
3.1	Introduction.....	77
3.1.1	Aims of the study .....	79
	The aims of this study were .....	79
3.2	Results .....	82
3.2.1	Tissue grading.....	82
3.2.2	Classification of the human brain tissue blocks.....	83
3.2.3	Expression of versican isoforms and versican neoepitope in human brain tissue .....	101
3.3	Discussion .....	110
3.4	Conclusion .....	113
4	Chapter 4: Expression of ADAMTS-9 in the CNS in MS; a pathological role.....	114
4.1	Introduction.....	115
4.1.1	Aim of study .....	116
4.2	Results .....	117
4.2.1	ADAMTS-9 immunoreactivity within control and MS CNS white matter .....	117
4.2.2	qRT-PCR analysis of mRNA expression of ADAMTS-9 in MS AL, MS NAWM and normal control brain tissue.....	125
4.3	Discussion .....	132
4.4	Conclusion .....	136
5	Chapter 5: ADAMTS-9 expression and modulation in CNS cells <i>in vivo</i> .....	137
5.1	Introduction.....	138
5.1.1	Aims of the study .....	139
5.2	Methods .....	140
5.2.1	Neuroblastoma cell line differentiation with retinoic acid.....	140

5.2.2	The effect of aggrecan on expression of ADAMTS-9 in the SHSY-5Y cells using in cell ELISA .....	140
5.3	Results .....	142
5.3.1	The effect of CSPGs on neurite outgrowth of the neuroblastoma cell line .....	142
5.3.2	Effect of pro-inflammatory cytokines on ADAMTS-9 protein expression in CNS cells .....	152
5.4	Discussion .....	168
5.4.1	Effect of aggrecan on neuronal phenotype; impact of ADAMTS-9 .....	168
5.4.2	Effect of pro-inflammatory cytokines on ADAMTS-9 expression in CNS cells .....	171
5.5	Conclusion .....	173
6	Chapter 6: General discussion .....	174
6.1	Implications of this study .....	175
6.2	Postmortem studies .....	175
6.3	<i>In vitro</i> studies .....	178
6.4	Future Directions .....	179
6.5	Conclusion .....	181
7	Chapter 7: References .....	184
8	Appendices .....	223

## List of Figures

Figure 1-1: Summary of the clinical classification of MS subtypes.....	3
Figure 1-2: Schematic diagram of the major cellular components of the BBB.....	12
Figure 1-3 Schematic of cellular events occurring in the immunopathogenesis of MS .....	15
Figure 1-4: Structural models of the CNS extracellular matrix.....	21
Figure 1-5: Strategies to overcome the CSPG-mediated inhibition of remyelination .....	24
Figure 1-6: Molecular mechanisms of CSPG inhibition of neurite outgrowth.....	28
Figure 1-7: Structural organisation of MMPs, ADAMs and ADAMTS .....	33
Figure 1-8: Domain structure of ADAMTS proteins.....	37
Figure 1-9: Proteolytic cleavage sites of CSPG.....	42
Figure 2-1: Schematic diagram showing the coronal slicing of brain and preparation of tissue blocks by the UK Multiple Sclerosis Society Tissue Bank. ....	46
Figure 2-2: Protein detection on western blots.....	55
Figure 2-3: Bradford assay standard curve .....	59
Figure 2-4: Measurement of the molecular weight of sample protein .....	62
Figure 2-5: qRT-PCR amplification plot.....	64
Figure 2-6: Modified from Promega. Luminescent reaction to detect ATP in mycoplasma test. ....	72
Figure 3-1: Aggrecan structure and ADAMTS cleavage sites.....	80
Figure 3-2: Haematoxylin and eosin staining showing the different grades of inflammation observed in CNS MS and control white matter.....	85
Figure 3-3: ORO staining showing the different grades of lipid-laden macrophages in white matter CNS tissue.....	87
Figure 3-4: MOG and HLA-DR expression in normal control (NC) and active MS lesion brain tissue .....	89
Figure 3-5: Comparison of expression of aggrecan and its neoepitope between MS and control brain tissue by IHC.....	95
Figure 4-1: Detection of ADAMTS-9 in MS and control human brain tissue using IHC	118
Figure 4-2: Dual label immunofluorescence of ADAMTS-9 and vWF in MS AL brain tissue sections .....	121

Figure 4-3: Dual label immunofluorescence of ADAMTS-9 and HLA-DR in MS AL brain tissue .....	122
Figure 4-4: Dual label immunofluorescence of ADAMTS-9 and NF in MS AL brain tissue .....	123
Figure 4-5 Dual label immunofluorescence of ADAMTS-9 and GFAP in MS AL brain tissue .....	124
Figure 4-6: Western blot analysis of ADAMTS-9 protein expression in MS and control CNS white matter protein extracts .....	127
Figure 4-7: Agarose gel electrophoresis pattern of total RNA extracted from control and MS human brain tissue .....	128
Figure 4-8: Amplification plots from qRT-PCR data for housekeeping genes in MS and control human brain tissue .....	129
Figure 4-9: Expression of ADAMTS-9 mRNA in human control and MS brain tissue assessed by qRT-PCR.....	131
Figure 5-1: Morphological effects of RetA on neuroblastoma cell line SHSY-5Y.....	141
Figure 5-2: Effect of aggrecan coating concentration on the viability of SHSY-5Y differentiated cells .....	143
Figure 5-3: Agarose gel electrophoresis of total RNA extracted from differentiated SHSY-5Y cells .....	144
Figure 5-4: ADAMTS-9 mRNA expression when differentiated SHSY-5Y cells were grown on various concentrations of aggrecan.....	146
Figure 5-5: Immunocytochemical detection of NF-L and ADAMTS-9 in differentiated SHSY-5Y cells grown on aggrecan .....	148
Figure 5-6: Effect of aggrecan on ADAMTS-9 and NF-L protein expression using an in cell ELISA.....	150
Figure 5-7: Effect of pro-inflammatory cytokines on the viability of CNS cells <i>in vitro</i>	153
Figure 5-8: Effect of pro-inflammatory cytokines on ADAMTS-9 expression in CHME3 cells.....	156
Figure 5-9: Effect of pro-inflammatory cytokine interferon- $\gamma$ on ADAMTS-9 expression in human primary astrocytes .....	158
Figure 5-10: Statistical analysis of the effect of pro-inflammatory cytokines on ADAMTS-9 expression in CHME3 cells and primary human astrocytes using ICC.....	160

Figure 5-11: Effect of Pro-inflammatory cytokines on expression of ADAMTS-9 in CNS cells assessed by western blotting.....163

Figure 5-12: Statistical analysis of the effect of pro-inflammatory cytokine treatment on expression of ADAMTS-9 in CNS cells assessed by western blotting .....165

Figure 6-1: CSPG Deposition in CNS lesions .....176

Figure 6-2: Modulation of ADAMTS-9 expression in the CNS.....182

## List of Tables

Table 1-1: CSPG isoforms and their interactions with hyaluronan receptors in CNS extracellular matrix.....	19
Table 2-1: Case details of post mortem brains used in this study.....	49
Table 2-2: Details of primary and secondary antibodies used in immunohistochemistry .....	52
Table 2-3: Details of the primary and secondary antibodies used in western blotting .....	61
Table 3-4: Primers utilised in qRT-PCR experiments for analysis of ADAMTS-9 mRNA expression levels .....	68
Table 2-5: Human primary cells and secondary cell lines used in this study and their culture medium composition .....	79
Table 2-6: Details of primary and secondary antibodies used for dual immunocytochemical detection of GFAP, NF-L and ADAMTS-9 in the CNS cells .....	75
Table 3-1: Human CNS tissue classification of MS and control blocks based on immunohistochemical studies used in this study.....	90
Table 3-2: Summary of extracellular matrix proteoglycan immunohistochemistry .....	109
Table 5-1: Summary of the effect of pro-inflammatory cytokines on ADAMTS-9 proteins by different CNS cell types .....	167

## Abbreviations

Ab	Antibody
ADAM	A disintegrin and metalloproteinase
ADAMTS	A disintegrin and metalloproteinase with thrombospondin motif
ADP	adenosine diphosphate
AL	Active lesion
AMPA	$\alpha$ -amino-3-hydroxy-5-methyl-4 isoxazolepropionic acid
APCs	Antigen-presenting cells
ATP	adenosine triphosphate
BBB	Blood brain barrier
BRAL1	Brain link protein -1
BSA	Bovine serum albumin
CAL	Chronic active lesion
CAM	Cell adhesion molecule
CCL20	Chemokine (C-C motif) ligand 20
CCR6	Chemokine (C-C) receptor 6
CD4	Cluster of differentiation 4
CD8	Cluster of differentiation 8
cDNA	Complementary DNA
CL	Chronic lesion
CNPase	2, 3-Cyclic nucleotide-3-phosphohydrolase
CNS	Central nervous system
CRD	Cysteine rich domain
CRP	Complement repeat protein
CRTL-1	Cartilage link protein1
CSF	Cerebrospinal fluid
CSLM	Confocal scanning laser microscopy
CSPGs	Chondroitin sulphate proteoglycans
CT	Cycle threshold
CUB	Cubilin domain
CX3CL1	Chemokine (C-X <sub>3</sub> -C motif) ligand 1
CX3CR1	Chemokine (C-X <sub>3</sub> -C) receptor 1
CXCL12	Chemokine (C-X-C motif) ligand 12
CXCR4	Chemokine (C-X-C motif) receptor 4
CYP27B1	Cytochrome P450 family 27 subfamily B1
Da	Dalton
DAPI	4,6 Diamidino-2-phenylindole
dATP	Deoxyadenosine triphosphate
dCTP	Deoxycytidine triphosphate
dGTP	Deoxyguanosine triphosphate
dH <sub>2</sub> O	Distilled water
DMEM	Dulbecco's Modified Eagle's Medium

DMSO	dimethyl sulphoxide
DNA	Deoxyribonucleic acid
dNTPs	Deoxynucleotide triphosphates
DPBS	Dulbecco's phosphate-buffered saline
DPX	Di-N-Butyl phthalate in xylene
DSPGs	Dermatan sulphate proteoglycans
DTT	Dithiothreitol
dTTP	Deoxythymidine triphosphate
EBV	Epstein-Barr virus
ECM	Extracellular matrix
EDTA	Ethylenediaminetetraacetic acid
EGF	Epidermal growth factor
ELISA	Enzyme-linked immunosorbent assay
ERK	Extracellular signal-regulated kinase
EVI5	Ecotropic viral integration-5
FGF	Fibroblast growth factor
FN-III	Fibronectin-3
GAG	Glycosaminoglycan
GalC	Galactocerebroside
GAPDH	Glyceraldehyde 3-phosphate dehydrogenase
GEP	Glutamyl endopeptidase
GFAP	Glial fibrillary acidic protein
GSK-3B	Glycogen synthesis kinase 3 beta
GWAS	Genome-wide association study
H&E	Haematoxylin and eosin
HA	Hyaluronan
HIFCS	heated-inactivated foetal calf serum
HPRT-1	Hypoxanthine phosphoribosyltransferase 1
HSPGs	Heparin sulphate proteoglycans
ICAM-1	Intracellular adhesion molecule-1
ICC	Immunocytochemistry
Ig	Immunoglobulin
IGF	Insulin-like growth factor
IHC	Immunohistochemistry
IL-1 $\beta$	Interleukin-1 $\beta$
IMSGC	International MS Genetic Consortium
INF- $\gamma$	Interferon-gamma
KIF1 $\beta$	Kinesin family member 1 $\beta$
KSPGs	Keratin sulphate proteoglycans
LAR	Leukocyte antigen receptor
LFA-1	Leukocyte function antigen-1
MALT1	Mucosa-associated lymphoid translocation protein 1

MAP	Mitogen activated protein
MBP	Myelin basic protein
MHC	Major histocompatibility complex
MMP	Matrix metalloproteinase
MOG	Myelin oligodendrocyte glycoprotein
Mr	Relative molecular weight
MRI	Magnetic resonance imaging
mRNA	Messenger ribonucleic acid
MS	Multiple sclerosis
MT-MMP	Membrane type metalloproteinase
MTT	3-(4, 5-Dimethylthiazol-2yl)-2, 5- diphenyltetrazolium bromide, atetrazole
MW	molecular weight
NAWM	normal appearing white matter
NC	normal control
NCM	Nitrocellulose membrane
Neo	Neoepitopes
NFDM	Non-fat dried milk
NF-L	Neurofilament light
NG2	Neural/glia antigen 2
NgR-1/3	Nogo-66 receptor-1/3
NLRs	Nuclear oligomerisation domain like receptors
NO	Nitric oxide
OCB	Oligoclonal band
OLG	Oligodendrocyte
OPC	Oligodendrocyte precursor cell
ORO	Oil Red O
PAGE	Polyacrylamide gel electrophoresis
PAMP	Pathogen associated molecule pattern
PBMC	Peripheral blood mononuclear cell
PBS	Phosphate buffered saline
PBS-T	Phosphate buffered saline -Tween
PCs	Pericyte cells
PFA	Paraformaldehyde
PG	Proteoglycan
PLAC	Protease and lacunin
PLP	Proteolipid protein
PMI	Post-mortem interval
PPIA	Peptidylprolyl isomerase A
PPMS	Primary progressive multiple sclerosis
PNN	Perineuronal net
PRMS	Progressive remitting multiple sclerosis

PSD-95	Postsynaptic density protein-95
PTP- $\beta$	Protein tyrosine phosphate -beta
PVDF	Polyvinylidene difluoride
qRT-PCR	Quantitative reverse transcriptase polymerase chain reaction
RetA	Retinoic acid
RGS1	Regulator of G-protein signalling 1
Rho A	Ras homolog gene family, member A
RNA	Ribonucleic acid
ROCK	Rho-associated protein kinase
ROI	Region of interest
ROS	Reactive oxygen species
RRMS	Relapsing -remitting multiple sclerosis
RT	Room temperature
SBB	Sudan black B
SDS	Sodium dodecyl sulphate
SEM	Standard error of the mean
siRNA	Small interfering RNA
SNAP-25	Synaptosomal associated protein-25
SPMS	Secondary progressive multiple sclerosis
STAT3	Signal transducer and activator of transcription 3
TAGAP	T-cell activation RhoGTPase activating
TEP	Triethyl phosphate
TGF- $\alpha$	Transforming growth factor alpha
TIMP	Tissue inhibitor metalloproteinase
TJ	Tight junction
TLR	Toll-like receptor
Tmcao	transient middle cerebral artery occlusion
TNF- $\alpha$	Tumour necrosis factor alpha
TNFRSF1A	Tumour necrosis factor receptor superfamily member 1A
T-R	Tenascin-R
TSR	Thrombospondin repeat like domain
TYK2	Tyrosine kinase 2
UVR	Ultraviolet radiation
UTP	Uridine triphosphate
V1	Versican-1
VAM-1	Vascular adhesion molecule-1
VEGF	Vascular endothelial growth factor
VLA-4	Very late antigen-4
vWF	Von Willebrand factor
WB	Western blotting
WTCCC2	Wellcome Trust case control consortium 2
ZBM	Zinc binding motif

## **1 Multiple sclerosis**

Multiple sclerosis (MS) is a complex disease displaying several pathological features including demyelination, inflammation, axonal/neuronal damage, changes in the immune system and blood brain barrier (BBB) dysfunction, affecting mainly the white matter of the central nervous system (CNS) (Lucchinetti *et al.*, 2011; Polman *et al.*, 2011). Demyelination of axons and the formation of inflammatory lesions (plaques) leads to the disruption of nerve conduction within the CNS typically associated with specific symptoms displayed by the patient (lessmann *et al.*, 2012). MS can result in a range of severe neurological deficits generally leading to disability for the individual. The development of MS is influenced by environmental factors, genetic factors and predisposition to autoimmunity in general (Altmann *et al.*, 2004; Milo & Kahana, 2010). The MS Trust has estimated that approximately 2.5 million people in the world have MS; 100,000 of these cases are in the UK (Gourraud *et al.*, 2012). MS has a personal, social and economic load on society, which was estimated to be ~£1 million per MS patient (Orton *et al.*, 2006).

### **1.1 Clinical symptoms and disease course in MS**

Typically the first symptoms experienced by people with MS occurs between the ages of 20-40 years, but they may commence as early as 3 years and as late as the seventh decade. Women are affected twice as often as men (Lublin and Reingold *et al.*, 1996; Huijbregts *et al.*, 2006). Symptoms occur in specific parts of the body dependent on which areas of CNS are damaged, which includes memory problems, depression, emotional changes, tremor and visual disturbance (Shivane & Charabarty, 2007). MS patients usually present with relapse-remitting symptoms with repeated neurologic episodes, each of which is usually followed by either partial or complete recovery with a period free of new symptoms known as relapse remitting MS (RRMS). Around 50-60% patients with RRMS ultimately develop to secondary progressive MS (SPMS). Approximately 10% of patients follow a primary progressive (PPMS) course, with a progressive neurologic deterioration from the onset (Pender *et al.*, 2007; Antel *et al.*, 2012). The classification of MS and the time course of neurological disability in the different forms of MS are illustrated in Figure (1-1).

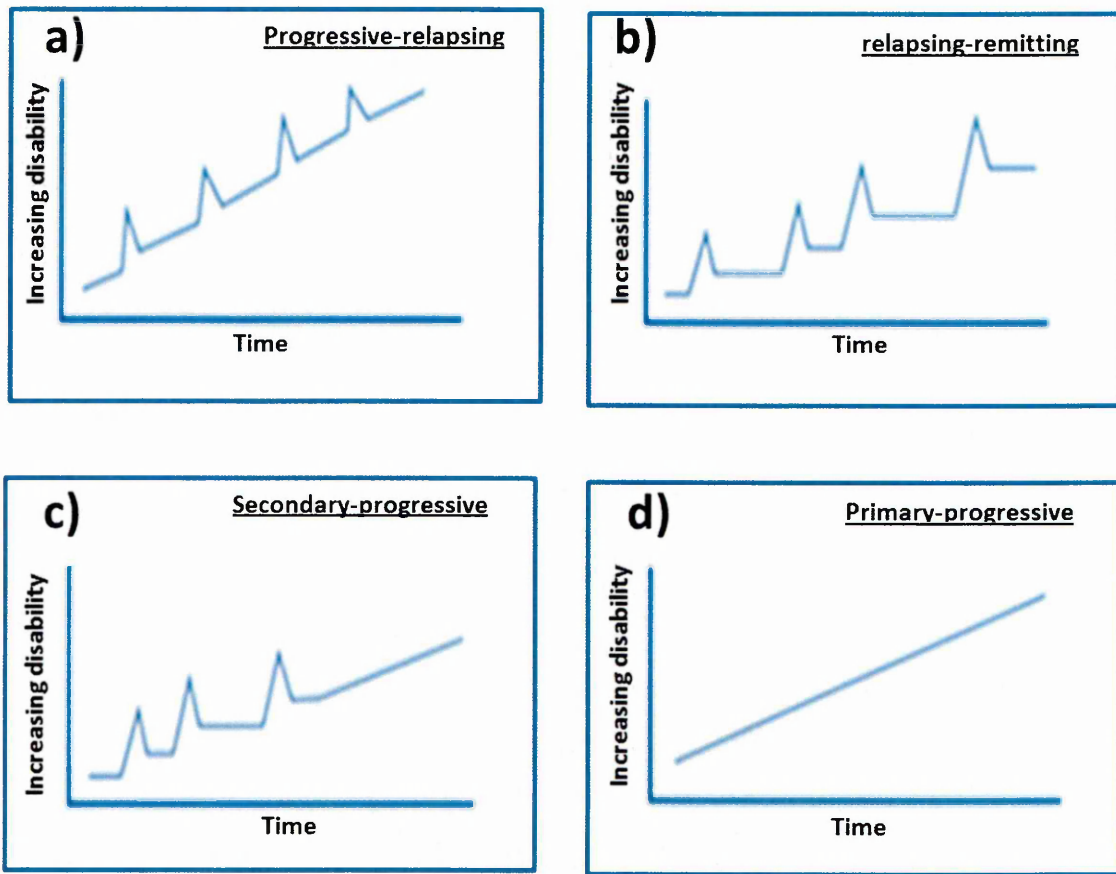


**Figure 1-1: Summary of the clinical classification of MS subtypes**

Progressive relapsing (PRMS) (a); Disease progression from the beginning, characterized by steady progression of the clinical neurological damage with relapse and remissions, is a very rare condition. Around 80-90% of MS patients show relapse-remitting symptoms that begin with period of varying neurological impairment interspersed with periods of remission (RRMS) (b). Around half of MS patients with RRMS will go onto development secondary-progressive MS (SPMS) which is characterized by fewer attacks and incomplete recovery as the disease becomes more progressive (c). Around 10-20% of patients present as primary-progressive MS (PPMS) which is characterised by an increase in disability from onset over time in the absence of improvement and remissions (d). Figure adapted from Zuvich *et al.*, (2009).

## 1.2 Diagnosis of MS

MS can be misdiagnosed as other conditions can imitate it, e.g. neuromyelitis optica. There are also no specific tests that can determine entirely if a patient has MS or is likely to have it in the future (Charil *et al.*, 2006; Kuhmann, 2013). Current diagnosis of definite MS is supported by both clinical investigations and by laboratory testing including the sampling of cerebrospinal fluid (CSF) for presence of oligoclonal bands (OCB) recognising an immune reaction within the brain and the use of magnetic resonance imaging (MRI) for lesion identification (Barazini *et al.*, 2009; Reynolds *et al.*, 2011).

MRI shows white matter lesions in more than 95% of MS patients. The most recent McDonald criteria formally integrate data from MRI and focusing on early diagnosis of patients presenting with a clinically isolated syndrome (CIS) suggestive of MS (Miller *et al.*, 2008). Patients suspected of having MS may have neurological symptoms upon initial examination that are clinically monofocal (no dissemination in space, for which a single CNS lesion can explain signs and symptoms) or multifocal (dissemination in space, for which symptoms and signs can only be explained by at least two lesions in separate parts of the CNS) (Polman *et al.*, 2011).

## 1.3 Aetiology of MS

### 1.3.1 Environmental factors

The aetiology of MS remains unclear, but is thought to involve exposure to environmental factors in those with genetic susceptibility (Olson *et al.*, 2001; Handel *et al.*, 2010; Sadovnick, 2013). This includes smoking (Pittas *et al.*, 2009; Hedstrom *et al.*, 2013), obesity (Hedstrom *et al.*, 2012; Munger, 2013) and lack of ultraviolet radiation (UVR), indicating that environmental factors play a crucial role in the development of MS (Lucas *et al.*, 2011). As the geographical distribution of MS prevalence is linked to exposure to sunlight, which relates to vitamin D synthesis, this is also associated consistently with an increased risk of developing MS (Goldberg *et al.*, 1986; Ascherio *et al.*, 2010; Burton *et al.*, 2010).

Viral infections have been implicated with either the aetiology or progression of MS such as Epstein-Barr virus (EBV), and human herpes virus (Libbey *et al.*, 2007; Tselis, 2012). Bacterial infections in addition to *Borrelia burgdorferi* have been proposed to

play a role in MS aetiology. The common respiratory pathogen *Chlamydia pneumonia* is known to infect endothelial cells, which is believed to assist in the migration of leukocytes into brain parenchyma (Stratton *et al.*, 2006; Contini *et al.*, 2010).

### 1.3.2 Genetics in MS

Susceptibility to MS is determined by a complex interaction of susceptibility genes in an individual; the incidence of MS in relatives of people with MS is twenty times higher than in the general population, indicative of a genetic link. Similarly studies of dizygotic twins have demonstrated a concordance rate of less than 5% and monozygotic twins show a concordance rate of approximately 30% (Taylor, 2011), again indicative of a genetic association. The major histocompatibility complex (MHC) located on chromosomes 6; 17p11, 3q21-24 and 18p11 were the first genes described as potential regions linked to MS (Sotgiu *et al.*, 2004). The previously completed GWAS and follow-up projects have identified 110 independent SNPs outside the HLA locus showing genome wide significant association with MS risk (Lill *et al.*, 2015), in particular inheritance of the HLA-DRB\*1501, DRB5\*0101, DQB1\*0602 and DQA1\*0102 haplotypes (Kaushansky *et al.*, 2015; Lima *et al.*, 2015) is linked to increased likelihood of developing MS.

A genome-wide association study (GWAS) identified more than 10,000 additional risk loci as part of the Wellcome Trust case control consortium 2 (WTCCC2) project (Sawcer *et al.*, 2014; Dankowski *et al.*, 2015). Cases were recruited through the International MS Genetic Consortium (IMSGC) and compared with the WTCCC2 common control set (IMSG, 2011). The study implicated a multitude of genes coding for cytokine and chemokine pathways [CXCR5, IL2RA, IL-7R, IL-7, IL12RB1, IL22RA2, IL12A, IL12B, IRF8 (interferon regulatory factors 8), TNFRSF1A (tumour necrosis factor receptor superfamily member 1A)] co-stimulatory molecules (CD37, CD40, CD58, CD80, CD86) and signal transduction proteins [MALT1 (mucosa-associated lymphoid translocation protein1), RGS1 (regulator of G-protein signalling1), STAT3 (signal transducer and activator of transcription 3), TAGAP (T-cell activation RhoGTPase activating), TYK2 (tyrosine kinase 2)] (IMSG, 2011; Bashinskaya *et al.*, 2015). All these genes coded for molecules with immunological relevance, in keeping with the autoimmune proposed aetiology of MS.

Genes were also identified which were linked to previously reported environmental factors which influence the incidence of MS, such as vitamin D deficiency [CYP27B1, (cytochrome P450 family 27 subfamily B1) (Bahlo *et al.*, 2009; Pierrot-Deseilligny & Souberbielle, 2010). The gene encoding vascular cell adhesion molecule (VCAM1) was also identified as a susceptibility gene, which correlated with effective treatment of MS patients with natalizumab, a therapeutic antibody, which blocks VCAM1 preventing migration of inflammatory cells into the CNS, reducing relapse rates considerably (Steinman, 2009).

Other genes have also been reported as being MS susceptibility loci associated with single nucleotide polymorphisms such as interleukin-7 receptor, interleukin-2 receptor, ecotropic viral integration site 5 (EVI5) and kinesin family member 1 $\beta$  (KIF1 $\beta$ ) (Aulchenko *et al.*, 2008; Hoppenbrouwers *et al.*, 2008; Maier *et al.*, 2009; Haas *et al.*, 2011). The IL-7R and IL-2R cytokine receptors were also identified as susceptibility loci in the GWAS study, reinforcing the importance of this family of cytokines and receptors in MS pathogenesis (IMSGC, 2011; Bashinskaya *et al.*, 2015).

#### **1.4 Pathology of MS**

In 1868, Charcot first described the pathological hallmark of MS including, inflammation and infiltration of immune cells within the CNS, mainly in the white matter, but grey matter is also involved (Lucchinetti *et al.*, 2005). The affected areas of brain tissue in MS are known as lesions or plaques which are usually localised around post capillary vessels (Shivane & Chakrabarty, 2007). The distribution of lesions is more common in specific areas including optic nerve, spinal cord, periventricular regions, and brainstem (Akenami *et al.*, 2000). Pathological features include; oligodendrocyte damage, demyelination, axonal damage, BBB leakage, glial scar formation and the presence of inflammatory infiltrates that mainly consist of lymphocytes and macrophages (Sospedra & Martin, 2005). The classification of MS lesions is quite difficult to fully define due to the nature of MS as a disease. Numerous attempts to identify lesion types based on aggressiveness, ranging from gradually to quickly developing severe chronic lesions have been reported (Bruck *et al.*, 1995; Lucchinetti *et al.*, 2000). MS lesions can be typically staged into four different categories active/acute lesion, chronic active, chronic inactive and normal appearing white matter (NAWM) (Brosnan & John, 2009).

Active lesions (AL) contain activated macrophages, containing myelin debris as a result of the demyelination process, assembled oligodendrocyte precursor cells (OPCs) at the edge of some initial acute plaques in an attempt to repair damaged oligodendrocytes (Chang *et al.*, 2002; Patani *et al.*, 2007). The typical active lesion can be sub divided into two different types;

Acute MS plaques are referred to as the early active lesions that contain an even distribution of macrophages/ activated microglia throughout the whole lesion, with disrupted myelin (Lassmann, 2011).

Chronic active plaques (CAL) also referred to as the late active lesion, contain foamy macrophages digesting myelin in the advanced edge; axonal damage can be seen, reactive astrocytes, demyelination is found in the lesion core. The chronic inactive plaque is also known as a silent plaque, is hypo-cellular (few macrophages and lymphocytes are seen), reduction in OPCs, reactive astrocytes with extensive gliosis, and myelin loss is clearly marked (Trapp *et al.*, 1998; Hickey *et al.*, 1999).

## **1.5 Cellular constituents of the CNS and their role in MS**

The CNS consists of the cerebral endothelium, astrocytes, oligodendrocytes, microglia and neurons. The cells within the CNS communicate through various transporter mechanisms, ion channels and signalling pathways to maintain homeostasis within the CNS (Bear *et al.*, 2007; Higgins *et al.*, 2013). Glial stem cells/ progenitor cells, described as self-renewing, are also present in the CNS which are multipotent cells that generate all cells types including astrocytes and oligodendrocytes (Purves *et al.*, 2008).

### **1.5.1 Glial cells in MS**

Virchow in 1846 first described the term neuroglia; this term has been used since the 1850s as a generic name of CNS cells (Kettenman& Verkhratsky, 2008). Glial cells form the protective and supportive network of the CNS in a number of ways and including oligodendrocytes (OLGs) providing insulation of neurons with myelin, and macroglia (astrocytes) providing maintenance and participation in signal transmission. Microglia act as macrophages and form the basis of the immune system in the CNS (Love *et al.*, 2008). They also produce many molecules with inflammatory and immune function, such as cytokines, chemokines and proteases (Minager *et al.*, 2002).

### 1.5.2 Microglia in MS

Microglia are the resident macrophages of the CNS and are small cells derived from progenitor cells in the embryonic yolk sac, which are spaced evenly throughout white and grey matter (Ginhoux *et al.*, 2013). There are significantly more microglia in white matter versus grey matter (Mittelbronn *et al.*, 2001). Microglia represent approximately 20% of the total cells in the CNS (Brodell, 2010; de Pablos *et al.*, 2013). In healthy nervous tissue, microglia are able to participate in both innate and adaptive immunity. Following immune stimulation, microglia become activated, migrate to the injured area, and regulate expression of levels of MHC II antigens which have the ability to activate lymphocytes in an immune response. Microglia can be found in three states resting, reactive (activated non-phagocytic) and activated phagocytic (Jack *et al.*, 2005; Boche *et al.*, 2013). Microglia can be distinguished by their activation state, resting cells have typical ramified morphology. In comparison, microglia under insult are enlarged and spherical in shape known as amoeboid cells (Loughlin *et al.*, 1993; Nimmerjahn *et al.*, 2005).

Microglia are also important in embryogenesis through secretion of neurotrophic factors such as nerve growth factors (NGF), brain-derived neurotrophic factor (BDNF), insulin-like growth factor (IGF) and neurotrophin-3 in response to both physiological and pathological stimulation (Ransohoff, 2011; Wake *et al.*, 2011). Microglia can express  $\alpha$ -amino-3-hydroxy-5-methyl-4 isoxazolepropionic acid (AMPA) receptors to glutamate (Noda *et al.*, 2000), P2 purinoceptors in response to ATP (Koizumi *et al.*, 2007), and a range of cytokines and growth factors that can affect neural circuits and brain homeostasis or disease (Wake *et al.*, 2011). These signals facilitate the recruitment of microglia, including the release of nucleotide adenosine triphosphate (ATP) and uridine triphosphate (UTP) from damaged neurons, which have been shown to be key mediators in the recruitment of microglia through activation of P2 purinoceptors following injury, leading to the removal of dying cells or their debris (Davalos *et al.*, 2005; Haynes *et al.*, 2006). Activated microglia can also eliminate neurotoxins and reactive oxygen species (ROS) through their expression of catalases such as superoxide dismutase, along with the removal of cellular debris (Wang *et al.*, 2004; Stables *et al.*, 2010).

Microglial cells express Toll-like receptors (TLRs) which are the first line of defence mediated by the recognition of pathogen associated molecules patterns (PAMPs) expressed by microbes (Jack *et al.*, 2007; Aravalli *et al.*, 2007). Upon PAMP binding to specific TLRs, activation of signalling pathways occurs, mediated by transcription factors and protein kinases, leading to activation of cytotoxic and inflammatory mediators e.g. cytokines such as IL-1 $\beta$  and IL-6, chemokines such as CCL2 and CCL5 and complement proteins and cell killing by release of nitric oxide (NO) and superoxide radicals (Von Bernhandi & Ramirez, 2001; Takeda & Akira, 2005; Glezer *et al.*, 2007). In addition to TLRs, microglia express nuclear oligomerisation domain-like receptors (NLRs) that are able to detect pathogens including viruses and bacterial products within the cytoplasm. NLRs also activate signalling pathways leading to activation of caspase-1 via inflammation which in turn leads to increased expression of cytokines such as IL-1 and IL-18 (Fukata *et al.*, 2009; Zhong *et al.*, 2013).

Microglia are highly motile under normal physiological conditions and interactions between synapses and microglia occur in the brain with implications for synapse homeostasis, development and disease. Both presynaptic (SNAP-25) and postsynaptic (PSD95) reactivity could be detected inside microglia during normal cortical development that is associated with changes in the morphology of the postsynaptic spine (Poalicelli *et al.*, 2011). Activation of microglia results in ATP release that subsequently activates astrocytes' purinoceptors (P2Y<sub>12</sub>) to release glutamate and activate presynaptic mGluRs to enhance glutamate activation of AMPA receptors (Wake *et al.*, 2011).

Microglia undergo a process called reactive microgliosis in response to inflammation whereby microglia proliferate extensively and up-regulate the expression of ECM protein involved in glial scar formation including CSPGs. There are many members of the CSPGs and individual CSPGs are synthesised by different cell types and at different time points following injury. Reactive astrocytes synthesise brevican, neurocan and phosphocan, while reactive microglia account for increased expression of aggrecan and versican (Siebert *et al.*, 2014).

### 1.5.3 Astrocytes

Astrocytes are the major cellular constituent of the CNS outnumbering neurons 10:1 (Okada *et al.*, 2005). There are two different subtypes of astrocytes: protoplasmic astrocytes which are located in grey matter and fibrous astrocytes which are found in white matter (Purves *et al.*, 2008). In the healthy CNS, astrocytes play a vital role in many functions including homeostasis of extracellular matrix fluid, removal of excess ions (in particular potassium) from the external environment of neurons, regulate intracellular  $\text{Ca}^{++}$ , recycling of neurotransmitters and are involved in the uptake of glucose and glutamate (Pellerin & Magistretti, 2005; Sofroniew & Vinters, 2010; Moore *et al.*, 2011). Astrocytes also play a crucial role in the formation and maintenance of the BBB through the glia limitans (Hamm *et al.*, 2004). Astrocytes can be detected *in vivo* by using antibodies against intermediate filament proteins including glial fibrillary acidic protein (GFAP) and S-100 $\beta$  (Zheng *et al.*, 2000; Roelofs *et al.*, 2005).

Astrocytes do not have the potential to release free radicals, but they are known to attract T cells through the production of cytokines (Constantinescu *et al.*, 2005), MMPs (Larsen *et al.*, 2003; Crocker *et al.*, 2006) and chemokines (Choi *et al.*, 2014) that contribute to MS pathogenesis. Supporting a role for astrocytes in the immune response, they produce IL-12 and IL-23, which helps to initiate both Th1 and Th17 T cells which play a crucial role in MS pathogenesis (Constantinescu *et al.*, 2005). Others indicate that cytokines produced by astrocytes, including IL-1, IL-6, TNF and IL-10, can drive and determine the immune response in demyelinating disease (Benveniste *et al.*, 1995). *In vitro* studies have shown that astrocytes produce pro-inflammatory cytokines including IL-9, IL-10, IL-11 by activation of TLRs on astrocytes (Nair *et al.*, 2008; Bsibsi *et al.*, 2006). In contrast, astrocytes express IL-4 receptors and upon exposure to IL-4 they express neutrophins, nerve growth factor which support axonal growth (Minager *et al.*, 2002; Pellerin & Magistretti, 2005).

### 1.5.4 Oligodendrocytes

Oligodendrocytes (OLGs) are a type of glial cell that are responsible for synthesis of myelin, each OLG is able to myelinate more than 40 axons (Funfschilling *et al.*, 2012; Nave *et al.*, 2010). OLGs are the end products of many stages of proliferation and differentiation of OLG precursor cells (OPCs). Throughout the CNS, OLGs have been

distinguished at different stages of maturation expressing individual phenotypes including expression of chondroitin sulphate proteoglycan (neural/glia antigen-2; NG2), surface gangliosides (A2B5), proteolipid protein (PLP), myelin basic protein (MBP), galactocerebroside (GalC) and 2, 3-cyclic nucleotide-3-phosphohydrolase (CNPase) (Armstrong *et al.*, 1992; Norton *et al.*, 1996; Levine *et al.*, 2001). The proliferation and differentiation of OLGs are controlled by many factors including cytokines and growth factors. An additional role of OLGs is that they are essential for long term integrity and survival of axons (Kassmann & Nava, 2008; Edgar *et al.*, 2004; Lappe-Siefke *et al.*, 2003).

### **1.5.5 Cerebral endothelia and the BBB**

The blood brain barrier (BBB) is a term used for the separation of the brain parenchyma from the blood circulation which acts as a filter, allowing the transport of substances which are less than 0.5 kDa (e.g. glucose) into the CNS and blocking large molecules including cells from entering (Petty *et al.*, 2002; Abbott *et al.*, 2010). The BBB is comprised of capillary endothelial cells adjacent to a thin but multilayered basement membrane which separates them from closely adherent pericytes, perivascular macrophages and the astrocyte foot-processes termed the glia limitans (Francis *et al.*, 2003).

Basement membrane and astrocyte end-feet which are opposed to the outer endothelial cell (EC) surface act as a structural support for the tight junctions and acts as a two way signalling pathway between the endothelium and the surrounding neuroenvironment (Luissint *et al.*, 2012). The tight junctions consist of three main proteins (claudin, occludin and junction adhesion molecules). Astrocyte end-feet play a vital role in proteoglycan synthesis resulting in an increase in human brain microvascular endothelial cell charge selectivity (Carvey *et al.*, 2009; Persidsky *et al.*, 2006).

Pericytes (PCs) are also cells that wrap around ECs providing structural support and vasodynamic capacity to the microvascular tube. PCs play a key role in angiogenesis, maintaining structural integrity and differentiation of the vessel, and formation of endothelial TJs (Daneman *et al.*, 2010). Figure (1-2) shows a schematic diagram of the BBB.

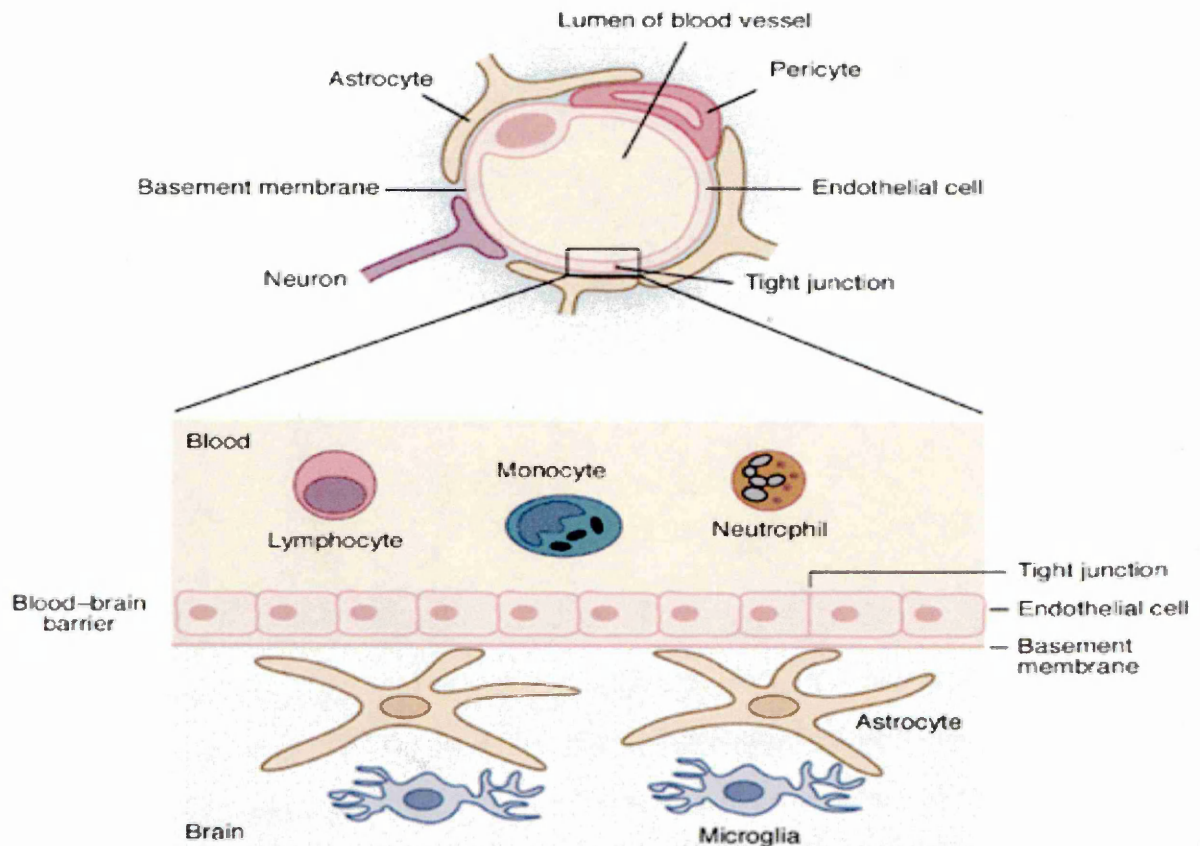


**Figure 1-2: Schematic diagram of the major cellular components of the BBB**

The CNS presents three main barriers to penetration by cells or substances, the first is mainly created by brain endothelial cells which adhere to each other through the formation of tight junctions (TJ) consist of three main proteins (claudin, occludin and junction adhesion molecules) (outlined within in the box), the basement membrane (BM) that consists of proteins (collagen, elastin, fibronectin and laminin), pericytes within the BM and astrocytic end feet also contribute to the composition of the BBB. This protects the CNS from infiltration of immune cells, pathogens and antibody mediated immune responses. Figure adapted from Francis *et al.*, (2003).

## 1.6 BBB dysfunction

Dysfunction of the BBB is believed to be one of the early events in MS pathogenesis, prior to lesion formation; this can be identified by MRI and through investigation of post-mortem tissue (Alvarez *et al.*, 2011; Larochelle *et al.*, 2011). Numerous aspects of BBB dysfunction have been implicated in MS, including TJ abnormalities (McQuaid *et al.*, 2009), degradation of the BBB by MMPs (Minagar & Alexander 2003; Daneman, 2012) and downregulation of laminin expression in the basal lamina (Oki *et al.*, 2004). As mentioned previously, soluble mediators including, NO (Hill *et al.*, 2004), mast-cell-derived histamine (Kruger, 2001), chemokines (Holman *et al.*, 2011), metalloproteinases (Yang *et al.*, 2007) and cytokines (Wojcick-Stothard *et al.*, 1998) act as inflammatory mediators in the breakdown of the BBB. For instance, infiltrating macrophages express IL-1 $\beta$  that has been shown to induce MMP-9 expression, an enzyme responsible for cleavage of TJ proteins (Lleo *et al.*, 2007; Yang *et al.*, 2007). Others consider breakdown of the BBB and increased permeability in MS to be advantageous, enhancing self-repair, allowing anti-inflammatory cells into the CNS to reduce inflammation (Larochelle *et al.*, 2011).

## 1.7 Autoimmune mechanisms in MS

Leukocyte infiltration occurs in numerous disorders of the CNS, including intracerebral haemorrhage (Ma *et al.*, 2011), hyperglycaemia following transient ischemia (Luitse *et al.*, 2012) and autoimmune diseases such as MS (Tullman *et al.*, 2013). The exact mechanisms involved in cell migration across the BBB are still not fully understood. But it is known that the exposure of the endothelial cells to pro-inflammatory cytokines such as interleukin (IL-1 $\beta$ ), tumour necrosis factor (TNF) and interferon- $\gamma$  (IFN- $\gamma$ ) disturb the BBB by disorganising cell-cell junctions, and enhance leukocyte and endothelial adhesion molecule expression at the BBB (Martins *et al.*, 2011). Adhesion molecules expressed by ECs include E-selectin, intracellular adhesion molecule-1 (ICAM-1) and vascular cell adhesion molecule-1 (VCAM-1), which interact with ligands on peripheral blood mononuclear cell (PBMCs), namely carbohydrate epitopes, leukocyte function antigen-1 (LFA-1) and very late antigen-4 (VLA-4) respectively (Kohm & Miller, 2003; Serres *et al.*, 2011; Linnartz *et al.*, 2012), to enhance cell migration into the CNS.

Chemokines and their receptors are also implicated in the chemoattraction of leukocytes into injured tissue. Chemokine receptors belong to the superfamily of seven-transmembrane domain receptors that signal through heterotrimeric GTP-binding proteins. One chemokine can activate more than one receptor and conversely. However, unique chemokine-chemokine receptor relationships do occur, e.g. CX3CL1-CX3CR1, CCL20-CCR6 and CXCL12-CXCR4 (Holman *et al.*, 2011; Roy *et al.*, 2014).

MMPs are proteolytic enzymes not only implicated in BBB disruption by degrading the ECM and basement membrane but also have a role in demyelination, cytokine activation and axonal damage (Comabella & Khoury, 2012). CSF and peripheral blood levels of MMP-2 and MMP-9 have been reported to be elevated in MS patients correlating with clinical and radiological disease activities (Alexander *et al.*, 2010).

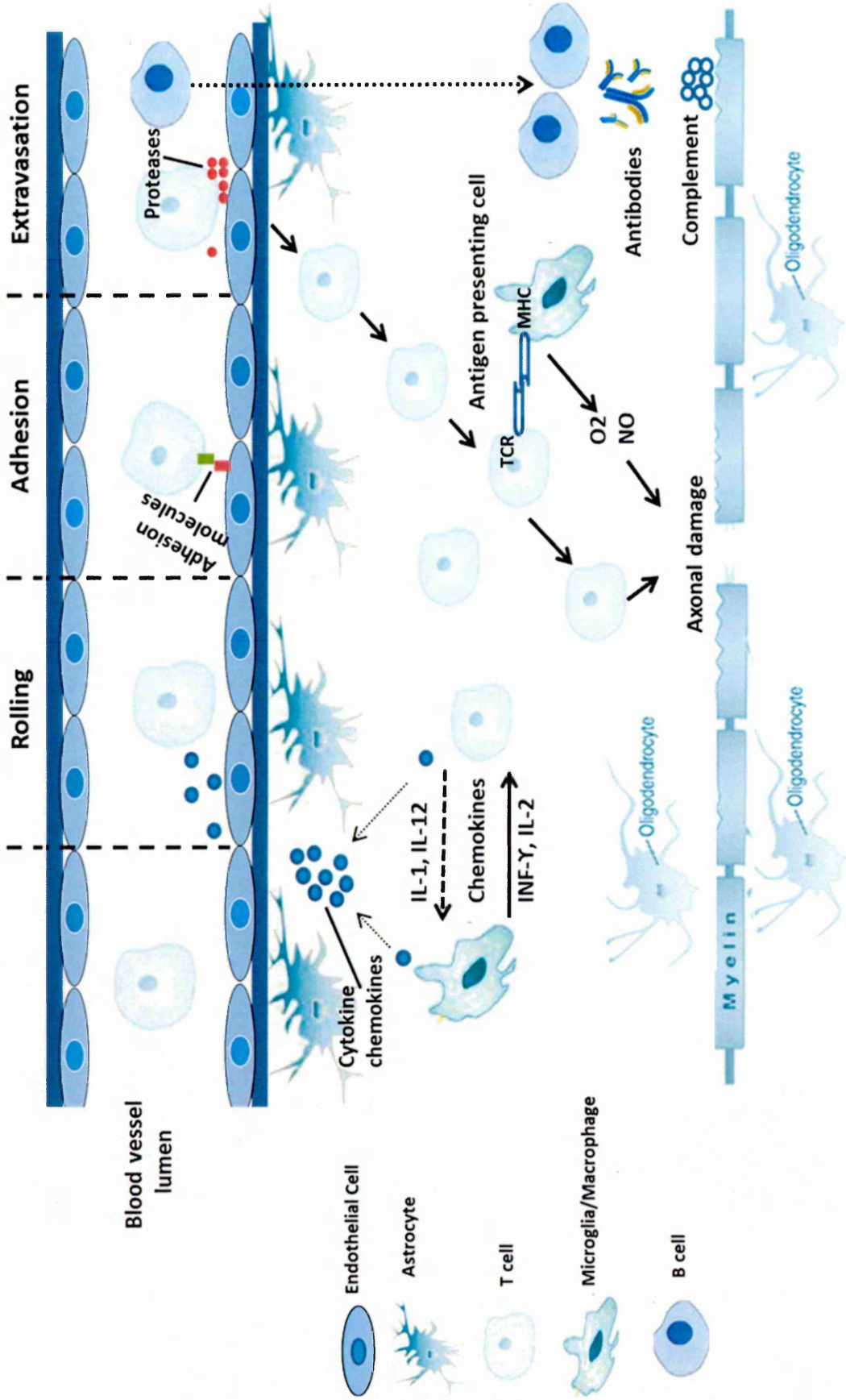
Until recently, MS research has mostly focused on the role of CD4+ T cells in disease pathogenesis. Myelin-specific CD4+ T cells are reactivated in the peripheral blood via myelin antigen presented in the context of HLA class II molecules in conjunction with accessory molecules on the surface of antigen presenting cells (APC) on macrophages and microglia (Comabella & Khoury, 2012). Reactivation triggers the release of pro-inflammatory cytokines, chemokines and soluble mediators that stimulate chemotaxis resulting in a second large wave of inflammatory cells recruitment into the CNS as described in figure (1-3).

Naïve T cells differentiate into various T cell populations with different effector functions following activation. Th1 cells release pro-inflammatory cytokines such as INF- $\gamma$  which activates macrophages to kill intracellular pathogens (Engelhardt *et al.*, 2005; Prat & Antel, 2005). IL-23 produced by macrophages and dendritic cells causes expansion of Th17 cells that synthesis the pro-inflammatory cytokines IL-17, IL-21 and IL-22 (McFarland & Martin, 2007, Constantinescu *et al.*, 2011).

CD8+ (cytotoxic) T cells increase tissue damage through further cytokine synthesis as well as granzyme and perforin production, leading to transection of axons (Fletcher *et al.*, 2010). CD8+ T cells are present at the edge of lesions as well as in perivascular regions, while, CD4+ cell are generally only present at the lesion edge (McFarland & Martin, 2007). In addition, there is a higher frequency of CD8+ T cells recognising myelin proteins in patients with MS compared with healthy controls.

### **Figure 1-3 Schematic of cellular events occurring in the immunopathogenesis of MS**

Initiation of MS is believed to involve CD4<sup>+</sup> T cells becoming activated in the periphery; through antigen-presenting cells (APCs) presenting CNS related antigens. Activated auto-reactive T cells with high levels of adhesion molecules in the periphery are then attracted to the endothelial cells, mediated by chemokines and chemokine receptor interactions. The increased expression of cell adhesion molecules (CAM) on the cell surfaces and their ligands on the endothelial cells, as well as increased expression of MMPs by the T cells enables them to cross the blood brain barrier. T cells interact with microglial cells that present antigen (localized APCs) which activate T cells further, triggering an inflammatory response involving release of cytokines, chemokines, nitric oxide (NO) and glutamate which eventually cause damage to myelin, oligodendrocytes (OLGs) and neurons. B cells and macrophages are also present in the perivascular area as a result of inflammation; they produce inflammatory mediators, MMPs and autoantibodies that damage myelin and neurons. Figure adapted from Markovic-Plese *et al.*, (2004).



It is indicated that CD4+ cells initiate the MS lesion, followed by clonal expansion of CD8 + T cells that amplify and mediate the damage (Medana et al., 2001, Constantinescu *et al.*, 2011).

There is much evidence for an autoimmune pathogenesis in MS and the most likely targets are myelin proteins including myelin basic protein (MBP), myelin oligodendrocyte glycoprotein (MOG) and proteolipid protein (PLP). Indeed, increased circulating T cells with reactivity to amino acid residues 184-209 and 143-168 of both PLP and MBP respectively were found in patients with MS (Pender *et al.*, 2007).

B cells are found within the perivascular space within inflammatory lesions, which release antibodies that in turn opsonise antigens expressed on oligodendrocytes and myelin (Alter *et al.*, 2003). B cells also present antigens to T cells and secrete cytokines, which impact on the immune response within lesions. Several findings indicate that B cells undergo rapid division in the CNS in the affected areas, as short-lived plasmablasts are found in the inflamed CSF (Alter *et al.*, 2003; Haider *et al.*, 2011). Currently there is controversy over the presence of ectopic B cell follicles associated with the meninges, which are implicated in cortical demyelination (Aloisi *et al.*, 2010).

## **1.8 The CNS extracellular matrix in MS**

The extracellular matrix (ECM) is a complex structure which surrounds and supports cells in all tissue types and includes collagens, non-collagen protein, glycoproteins and proteoglycans. The components of the ECM vary greatly between tissue types and the CNS ECM lacks collagen, fibronectin and laminin, giving the brain a soft structure compared to other tissues (Yamaguchi, 2000; Barros *et al.*, 2011). The ECM constitutes approximately 10-20% of the normal brain tissue and forms perineuronal nets (PNN). The ECM exists free or in aggregates bound to cell receptors, and is synthesised by both neurons and glial cells. It has been indicated that during maturation of the CNS, distinctive alterations in the composition of the molecules of ECM (lectican, tenascins and link protein) occurs in the brain (Mohan *et al.*, 2010; Wiese *et al.*, 2012). The ECM within PNNs helps regulate many physiological brain processes including development, migration of precursor cells, proliferation, repair and cell signalling (Bellail *et al.*, 2004; Lau *et al.*, 2013).

The PNN consists of a condensed layer of mesh-like matrix composed largely of hyaluronan, proteoglycans (PGs), tenascin R (TR) and link proteins that surround neuronal bodies and proximal dendrites (Kwok *et al.*, 2011). PGs consist of a core protein to which glycosaminoglycan (GAG) side chains attach. Individual PGs differ in the composition of either their core protein or the number and types of GAG side chains; that is, they determine whether the molecule is a dermatan sulphate proteoglycan (DSPGs), chondroitin sulphate proteoglycan (CSPGs), keratin sulphate proteoglycan (KSPGs) or a heparan sulphate proteoglycan (HSPGs) (Jones & Tuszynski, 2002 ; Van Horsen *et al.*, 2007; Shute, 2012).

### **1.8.1 Chondroitin Sulphate Proteoglycans**

#### **1.8.1.1 Structure and function in the CNS**

Chondroitin sulphate proteoglycans (CSPGs) are expressed in various tissues; those expressed in the CNS fall into three families: lecticans (aggrecan, versican, neurocan and brevican), phosphacan known as protein tyrosine phosphatase- $\beta$  (RPTP- $\beta$ ) and neuron-gial antigen 2 (NG2) (Sugahara *et al.*, 2007; Pendleton *et al.*, 2013). Three major nervous tissue specific CSPGs including, neurocan, phosphacan and brevican have been described (Kurazono *et al.*, 2001; Inatani *et al.*, 2001). CSPGs are a family of single-core protein PGs with attached side chains of GAG as shown in figure (1-4). Lecticans share a tridomain structure; an N-terminal domain (G1) that binds to hyaluronan through link proteins such as brain link protein-1 (BRAL-1), a central domain that can be glycanated to various degrees and a C-terminal domain (G3) that binds to other ECM proteins such as TR (Galtery *et al.*, 2007; Lau *et al.*, 2013).

The core protein of aggrecan has an additional domain, G2, consisting of two link proteins. GAGs have considerable heterogeneity within the lectican family and the full length core protein ranges in size from 90KDa to 400KDa, and the number of GAG side chains ranges from 20-200 (Table 1-1) (Schaefer *et al.*, 2010). NG2 is the only transmembrane CSPG and is expressed on oligodendrocyte precursor cells (Biname *et al.*, 2013). Alternative splicing of mRNA that encodes GAG binding regions generates versican into four isoforms including V0 (contains all domains), V1 (contains GAG-B), V2 (contains GAG- $\alpha$ ), and V3 consist of G1/G2) (Zako *et al.*, 1995; Wu *et al.*, 2005).

**Table 1-1: CSPG isoforms and their interactions with hyaluronan receptors in CNS extracellular matrix**

CSPGs	GAGs	CNS-Specific	Link Protein	GAG number	core protein size KDa
Aggrecan	CS/KS	NO	CRTL1	~100	224
Versican V0	CS	NO	BRAL1	17-23	370
Versican V1	CS	NO	BRAL1	12-15	262
Versican V2	CS	NO	BRAL1	5-8	180
Neurocan	CS	Yes	BRAL1	3	133
Brevican	CS	Yes	BRAL2	0-5	79
Phosphacan	CS/KS	Yes	No HA binding	3-4	173

CS; Chondroitin sulphate, CSPGs; Chondroitin sulphate proteoglycan, GAGs; Glycosaminoglycans, KS; Keratin sulphate; CRTL; Cartilage link protein; BRAL; Brain link protein; HA; Hyaluronan. Table adapted from Galtrey *et al.*, (2007).

Besides the distribution of lectican indicated in figure (1-4), CSPGs are also present in the perinodal matrix surrounding nodes of Ranvier in myelinated axons (Bekku *et al.*, 2010). It has been reported that there are distinctive changes in the ECM molecules during maturation of the CNS. In the adult brain, brevican, versican V2, aggrecan, Tenascin-R (TR) are major ECM components while neurocan, versican V1, and tenascin-C are characteristic components of developing brain ECM (Hirakawa *et al.*, 2000). The main functions of CSPGs are dependent on their interactions with components of several receptor systems, including leukocyte common antigen-related phosphate (Fisher *et al.*, 2011), protein tyrosine phosphate (Shen *et al.*, 2009), epidermal growth factor receptors (Koprivica *et al.*, 2005), Toll-like receptors (Jiang *et al.*, 2007; Kim *et al.*, 2009), CD44 and Nogo receptor family members (Nogo receptors) NgR1 and NgR3 (Dickendesher *et al.*, 2012). However, the roles of CSPGs in developing brain ECM might differ from that in the injured adult CNS and over expression in injured brain may lead to inhibition of neurite outgrowth and axonal regeneration (Niето-Sampedro, 1999; Deller *et al.*, 2000; Schmalfeld *et al.*, 2000; Levine *et al.*, 2001). Lectican expression is affected by a variety of stimuli, including cytokines, chemokines and adhesion molecules (Jander *et al.*, 2000; Asher *et al.*, 2000; Viapiano & Matthews, 2006).

### **1.8.2 CSPG expression changes in demyelination and remyelination in MS**

Failure of remyelination is a critical impediment to recovery in demyelinating diseases such as MS (Patrikio *et al.*, 2006; Albert *et al.*, 2007). Within MS lesions, oligodendrocyte precursor cells (OPCs) can be found in areas with demyelinated axons, yet many of these do not go on to form compact myelin (Chang *et al.*, 2002; Kuhlmann *et al.*, 2008). CSPGs have been reported to accumulate also in MS lesions and inhibit remyelination by impairing OPCs (Figure 1-5) (Back *et al.*, 2005; Gregg *et al.*, 2007; Sloane *et al.*, 2010). PNNs are also lost around neurons in demyelinated regions, and many of the affected neurons appear to be compromised, as indicated by accumulation of phosphorylated neurofilament protein in their cell bodies. It is unknown whether these changes in PNNs affect synaptic plasticity and function (Gray *et al.*, 2008).

## Figure 1-4: Structural models of the CNS extracellular matrix

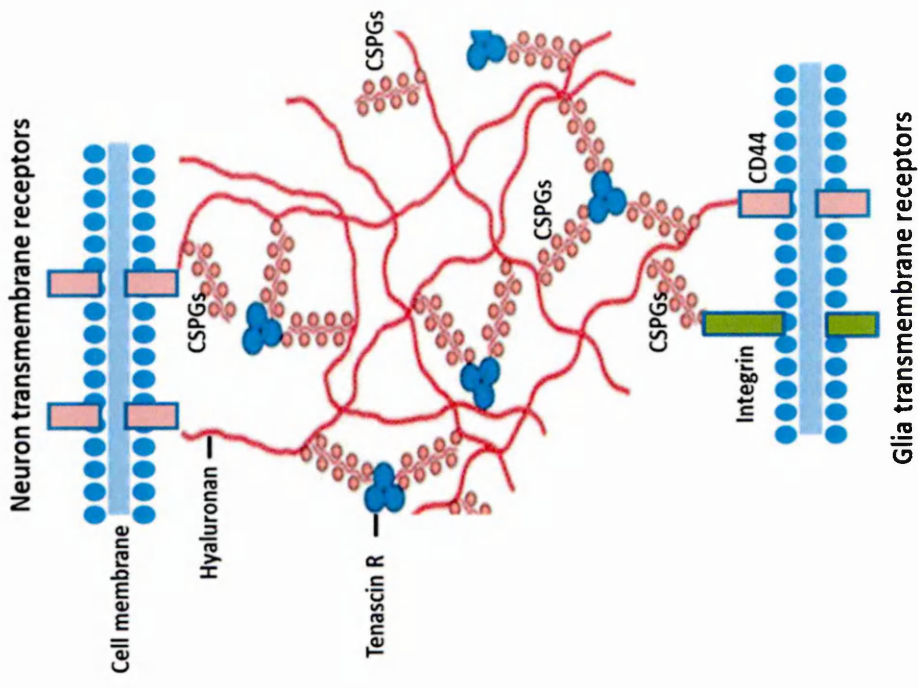
### (a) Basic structure of the lectican

Structural model of lectican composed of an N-terminal domain (G1) that binds to hyaluronan, chondroitin sulphate (CS) attachment regions and C-terminal domain (G3). G1 contains an immunoglobulin like (Ig-like) domain, while G3 contains epidermal growth factor domain (EGF), C-type lectican like domain and complement repeat protein like domain (CRP). Figure adapted from Maeda *et al.*, (2015).

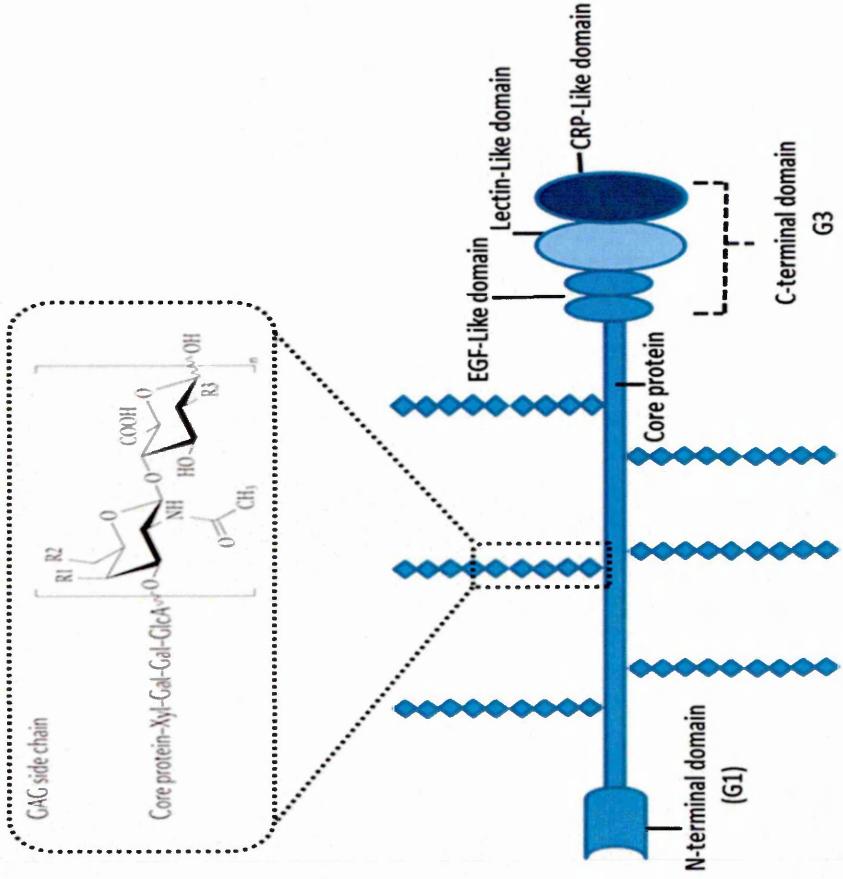
### (b) Schematic view of the perineuronal net (PNN)

Lecticans form complexes with hyaluronan (HA) and tenascin-R (TR) in the ECM and occupy the spaces between neuronal and glial cells. The lectican family binds to hyaluronan by their N-terminus and hyaluronan is attached to neuronal and glial cells by CD44. Interactions between both hyaluronan and lectican are stabilized by link proteins. TRs exist as trimers and CSPGs bind to TR by their C-terminal domain. Figure adapted from Bonneh *et al.*, (2009).

**b**



**a**



There is now considerable evidence indicating that the CSPGs affect oligodendrocyte lineage cells, including their proliferation, survival, migration, differentiation, process extension and myelination (Sherman *et al.*, 2008; Lin *et al.*, 2011). Cell culture studies have emphasised that CSPGs inhibit the spreading and survival of oligodendrocytes by interacting with  $\beta$ 1 integrin to trigger signalling cascades. Treatment of human neuronal cells with chondroitinase ABC increased the number of OPCs in the surrounding lesion, and the addition of growth factors promoted the differentiation of transplanted OPCs into mature oligodendrocytes (Karimi *et al.*, 2012).

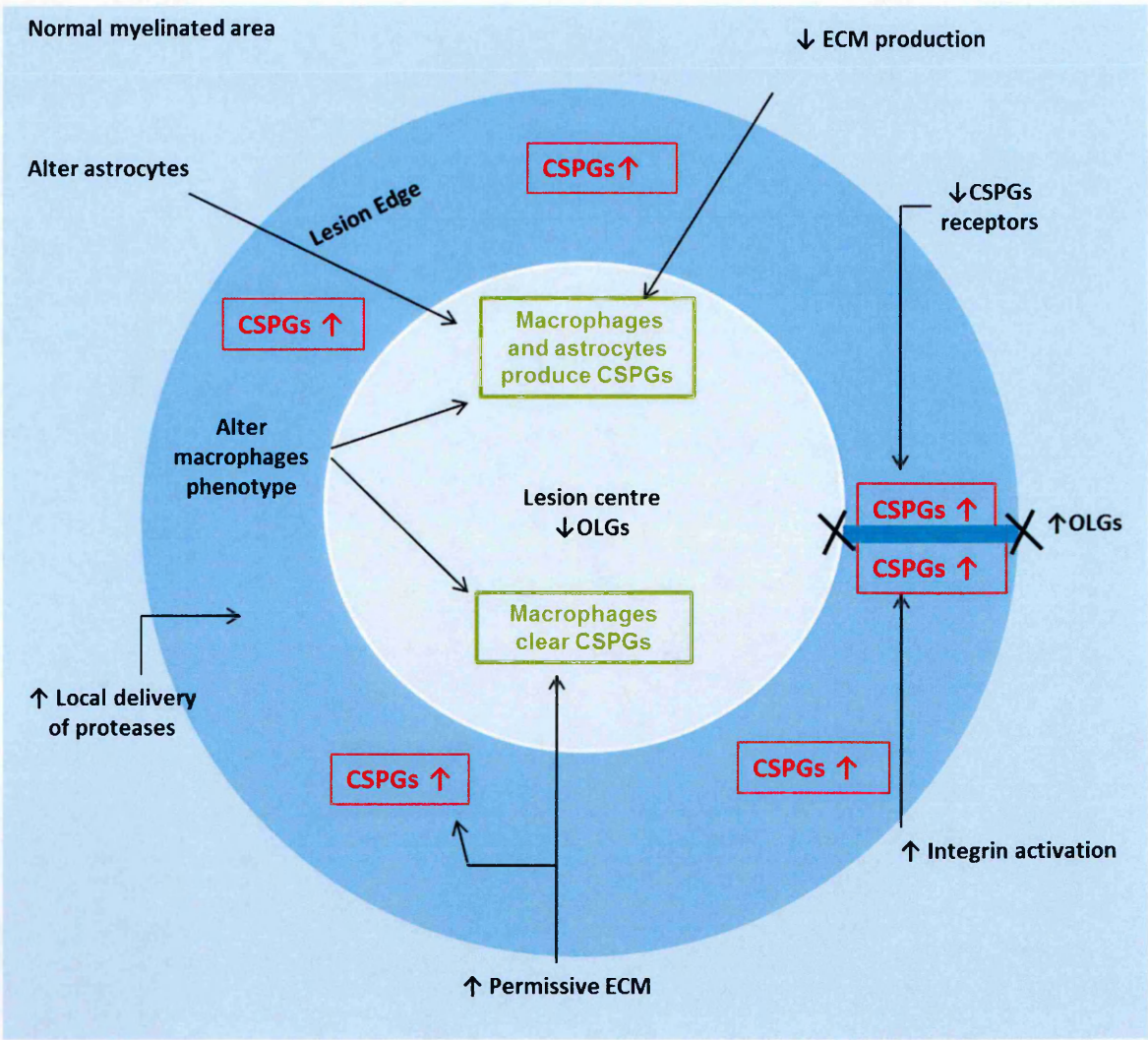
CSPG biosynthesis is catalysed by a series of intracellular enzymes including xylosyltransferase-1, which is required during CSPG synthesis to form xylose-galactose-galactose-glucuronic acid which initiates GAG polymerisation on the core protein. Notably, targeting of xylosyltransferase-1 mRNA with locally applied mRNA knockdown disrupted CSPG production in the ECM, resulting in increased axonal regeneration around lesion in mouse model of MS (Grimpe *et al.*, 2004; Lau *et al.*, 2013).

Another enzymatic approach are MMPs, a disintegrin and metalloproteinase (ADAM) and a disintegrin and metalloproteinase with thrombospondin motifs (ADAMTSs) that clear deposited CSPGs and maintain the dynamic nature of the PPNs which relies upon constitutive remodelling by numerous factors (Yong *et al.*, 2005; Apte, 2009; Sorokin *et al.*, 2010; Rodriguez *et al.*, 2010; Kucharova *et al.*, 2011).

A subgroup of the ADAMTSs has glutamyl endopeptidase (GEP) activity and they have the ability to cleave CSPGs and are also upregulated in MS lesions (Westling *et al.*, 2004; Induklenmesi *et al.*, 2014). These enzymes probably influence the lesion microenvironment during remyelination as several members of this protein family cleave laminin, CSPGs and ECM receptors such as integrins (Sternlicht & Werb *et al.*, 2001; Rodriguez *et al.*, 2010). For instance; in mouse models of spinal cord injury, increased ADAMTS-4 expression reduced glial scarring and improved locomotor recovery associated with axon regeneration (Tauchi *et al.*, 2012).

### **Figure 1-5: Strategies to overcome the CSPG-mediated inhibition of remyelination**

This schematic depicts a demyelinated CNS MS lesion (white circle), such as that observed in MS. Chondroitin sulphate proteoglycan (CSPG) is observed in the ECM at the lesion edge (red box), while macrophages containing CSPG immunoreactive material are encountered in the lesion core (Green box), presumably because these cells have phagocytosed CSPGs previously and because macrophages and activated microglia as well as reactive astrocytes can be a source of CSPGs. There is a high number of OPCs in normal appearing white matter, but these may be unable to repopulate in the lesion core owing in part to the non-permissive CSPG barrier. High levels of CSPGs are implicated in inhibition of re-myelination and digestion products of CSPGs by particular proteases have been reported to retard myelin repair (Tauchi *et al.*, 2012). Several mechanisms have been proposed to enhance the repair of myelin and neurite outgrowth in demyelinating diseases such as MS. These include enzymatic clearance of deposited ECM [matrix metalloproteinase (MMPs), a disintegrin and metalloproteinase (ADAMs) and a disintegrin and metalloproteinase with thrombospondin motifs (ADAMTSs)], enzymatic removal of the GAG chains of CSPGs (chondroitinase ABC), reducing the synthesis of inhibitory molecules of neurite outgrowth by blocking of xylosyltransferase-1 which is required during CSPG synthesis. An increase in expression is indicated with a ↑ arrow and a decrease in expression is indicated with a ↓ arrow. Figure adapted from Lau *et al.*, (2013).



### 1.8.3 Molecular mechanism of CSPG inhibition of neurite outgrowth

Neurite outgrowth is a key process during neuronal migration and differentiation, and is a complex process that occurs in three stages (1) "sprouting" initiation of neurite formation, (2) "path finding" elongation of neurite over long distances and guidance of their axons to the appropriate target and (3) synapse information and functional maturation of the newly formed connection (Johnson & Michell, 2015; Khodosevich & Monyer, 2010). Axon elongation, formation of synapses, axon regeneration and signal connection between neuronal cells are essential processes for maintenance of the CNS, and many molecules are involved in neurite outgrowth from cytoskeleton constituents to membrane receptors (Johnson & Michell, 2015). However, in the new-born and even in the mature animal, axon injury leads to severe functional deficits, as in patients with MS (Sharma *et al.*, 2012).

The failure of destroyed axons to repair and regenerate after CNS injury has been described as due to two factors; a developmental reduction in the intrinsic growth factors and environmental factors (Ibanze & Simi, 2012; Kwok *et al.*, 2012; Dick *et al.*, 2013) . It is now clear that the intrinsic growth capacity relies on expression and activation of numerous independent cell molecules that are implicated in signalling by both classes of growth promoting and growth inhibitory environmental factors (Park *et al.*, 2010). An important classes of extrinsic growth inhibitory is the CSPGs, myelin associated growth factors and chemo-repulsive guidance molecules which are components of the ECM comprising the PNNs (Liu *et al.*, 2006; Piaton *et al.*, 2011; Tong *et al.*, 2013).

In fact, several general mechanisms involving receptors have been reported in the inhibition of neurite outgrowth via GSPGs including, integrins (Asfari *et al.*, 2010; Tan *et al.*, 2011), and leukocyte antigen receptors (LAR) (Fry *et al.*, 2010; Takashashi *et al.*, 2013) and NgR1 / NgR3 (nogo-66 receptor-1/3)(Shen *et al.*, 2009; Fisher *et al.*, 2011; Dickendeshner *et al.*, 2012). The intracellular effects of most axon growth-suppressing proteins are mediated by activation of the GPI-binding protein, RhoA, which is a signalling molecule regulating neuronal morphogenesis by interaction with several other enzymes such as serine threonine kinases, lipid kinase, oxidase tyrosine kinase (Luo, 2000; Mueller *et al.*, 2005, Walker *et al.*, 2005; Rollof *et al.*, 2015). Reaction of GPI-binding protein with RhoA leads immediately to activate Rho kinase (ROCK), which

leads to phosphorylation of several target proteins, including myosin light chains and mediating cytoskeletal rearrangement and disassembly in neurons and collapse of growth cones (Mckerracher *et al.*, 2012; Forgione & Fehling, 2014). Further strategies to overcome CSPG and hyaluronan-mediated inhibition of neurite outgrowth include semaphorins (Sema 5 A) (Hilario *et al.*, 2009; Dick *et al.*, 2013), neutrotrophins (Liu *et al.*, 2010), and protein tyrosine phosphate (PTP) (Chien *et al.*, 2013) and calcium channels (Ca<sup>++</sup>) (Hrabetova *et al.*, 2009; Kadomatus & Sakamoto, 2014) as described in figure (1-6).

## **1.9 Matrix metalloproteinases**

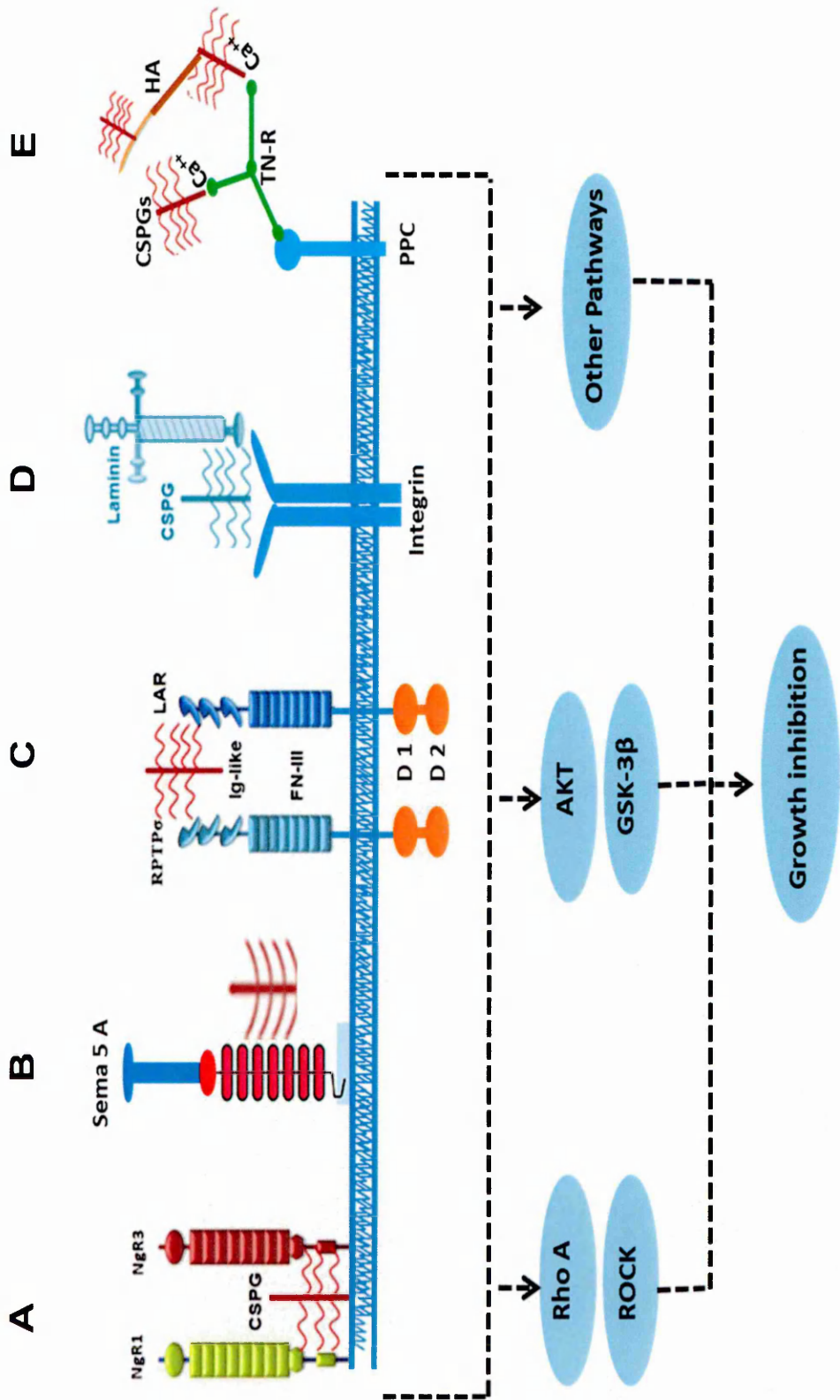
### **1.9.1 Matrix metalloproteinase family proteins**

The matrix metalloproteinase (MMP) family consisting of 25 members is a group of Zn-dependent proteolytic enzymes that are implicated in the remodelling of the ECM in a variety of physiological and pathological processes (Rosenberg *et al.*, 2002; Mandal *et al.*, 2003; Lui & Rosenberg, 2005). Based upon their main substrate specificity, they are divided into collagenases, gelatinases, stromelysins and membrane type (MT)-MMPs, which are capable of degrading ECM components; collagen, proteoglycan, elastin, laminin and fibronectin (Leppert *et al.*, 2001; Szabo *et al.*, 2004).

MMPs are synthesised as proenzymes secreted from cells as zymogens with an inhibitory N-terminal pro-peptide sequence which are activated in the ECM via cleavage by serine family protease enzymes such as plasmin (Gingras *et al.*, 2000; Rosenberg, 2002). MMPs play pathological and detrimental roles in MS including breakdown of the BBB and myelin sheath (Chandler *et al.*, 1997; Kouwenhoven *et al.*, 2001; Larochelle *et al.*, 2011; Sato *et al.*, 2012). MMPs can be regulated at four levels; pro-enzyme activation, gene expression, enzyme secretion and by tissue inhibitors of MMP (TIMPs) which are reported to be constitutively expressed in normal brain (Leppert *et al.*, 2001).

### **Figure 1-6: Molecular mechanisms of CSPG inhibition of neurite outgrowth**

Schematic diagram showing the major factors which regulate neurite outgrowth including, (A) Nogo receptor (NgR1 and NgR3) binding, (B) CSPGs have the potential to inhibit semaphorin 5 A by altering it from an attractive form to an inhibitory one, (C) Leukocyte antigen receptor (LAR) which are a subfamily of transmembrane protein tyrosine phosphate (PTP) composed of two intracellular domain immunoglobulin domain (Ig) and fibronectin domain (FN-III), (D) CSPGs may suppress axon growth by blocking function of growth-promoting molecules including laminin and its receptors integrins. (E) CSPGs are implicated in the formation of PNN and interaction with TN-R, dependent on calcium, CSPGs may regulate neurite growth by altering influx of calcium into neurons. Intracellularly, several signalling pathways mediate the activity of CSPG inhibition including RhoA, Akt and other signalling proteins are also implicated in neurite outgrowth. FN-III: fibronectin type III domain, HA: hyaluronan, Rho A: Ras homolog gene family; member A, ROCK: Rho-associated protein kinase; GSK-3 $\beta$ : glycogen synthesis kinase 3 beta, PPC: phosphacan. Figure adapted from Sharma *et al.*, (2012).



### 1.9.2 MMPs in MS

In the CNS, gelatinases, stromelysins and MT-MMPs make up the majority of MMPs present, with MMPs 2, 3 and 9, being the most significant (Muir *et al.*, 2002; Verslegers *et al.*, 2013). MMP3 is known to activate MMP-9 via causing removal of the peptidase that maintains the activity of the zinc binding site (Gu *et al.*, 2002). MMP2 and 9 act on fewer ECM substrates than MMP3, but process important components of the basal lamina (Yong *et al.*, 2001; Yang & Rosenberg, 2011). It has been indicated that up-regulation of MMPs and a relative decrease in their TIMP inhibitor, may produce persistent proteolysis, resulting in the neuronal loss that represents the steady advance of symptoms of secondary chronic progression in MS (Lindberg *et al.*, 2001). The serum, CSF and brain tissue of MS patients all showed an increase in MMPs 1, 2, 3, 7, 9 and 12. MMPs in particular, are thought to assist with T cell migration into the CNS, high levels of MMPs are detected in astrocytes and macrophages in demyelinating lesions and in the CSF of MS patients (Szabo *et al.*, 2004; Kurzepa *et al.*, 2005; Brosnan *et al.*, 2013).

### 1.10 ADAM family proteins

The ADAMs comprise the adamalysin subfamily of the metazincins (Killar *et al.*, 1999; Rawling *et al.*, 2013), and are important in regulating cell phenotype by their effect on growth factors, cytokines, cell adhesion molecules and cell immigration (Andreini *et al.*, 2005; Klein & Bischoff, 2011). ADAMs are transmembrane proteins which are implicated in pathological processes including cancer metastasis and inflammatory diseases such as MS (Plumb *et al.*, 2006; Shiomi *et al.*, 2010). The ADAM family of proteins include the adamalysin subfamily of the metzincins along with the snake venom metalloproteinase. ADAMs are similar to matrixins in that the metalloproteinase consists of a multi-domain protein with pro-domain, metalloproteinase, disintegrin, cysteine-rich, epidermal growth factor (EGF)-like, transmembrane and cytoplasmic tail domains (Weber *et al.*, 2013) (Figure 1-7). ADAM 17 is mainly implicated in CNS inflammatory disorders, through cleavage of a wide variety of proteins including; chemokine, amyloid precursor protein, transforming growth factors (TGF- $\alpha$ ), TNF and TNF receptors (Garton *et al.*, 2001; Allinson *et al.*, 2003; Scott *et al.*, 2011).

### **1.10.1 ADAM-17 in MS**

ADAM-17 is a membrane bound enzyme that cleaves cell surface proteins. It is a polypeptide of 824 amino acids and its gene is found on chromosome 2p25. ADAM-17 has the ability to take part in a broad range of functions and has immune-mediated functions through modulation of shedding of proteins vital to the immune response (Holdt *et al.*, 2008; Gooz, 2010). Within normal brain, ADAM-17 expression has been observed in both neuronal and endothelial cells (Goddard *et al.*, 2001). In MS white matter, ADAM-17 expression is upregulated in neuronal cells, endothelial cells and macrophages and CD3 T lymphocytes (Keiseier *et al.*, 2003; Plumb *et al.*, 2006). Previous findings indicated that ADAM-17 is implicated in the pathogenesis of MS via cleavage of membrane bound TNF, releasing soluble TNF, which has several pro-inflammatory effects including, up regulation of cell adhesion leading to increased endothelial cell attachment of immune cells, induction of chemokines, and subsequent migration and BBB disruption (Scheller *et al.*, 2011; Kaltsonoudis *et al.*, 2014). Abnormally upregulated ADAM-17 may induce a beneficial immune response by producing apoptosis of autoreactive T cells (Probert & Akassoglou, 2001; Weishaupt *et al.*, 2004).

## **1.11 ADAMTSs**

### **1.11.1 Overview of ADAMTS**

ADAMTSs (a disintegrin and metalloproteinase with thrombospondin motifs) were first described in mice by Kuno and colleagues in 1997. ADAMTSs are also part of the adamalysin subfamily of metalloproteinases, thus they contain zinc and have highly conserved thrombospondin motifs with some molecules having substantial proteoglycanase and anti-angiogenic activity (Andreini *et al.*, 1997; Bornstein, 1992; Tang, 2001). Nineteen distinct human ADAMTS genes have been identified, numbered 1-20, and their functions are limited to a few specific members in the CNS. Many orphan ADAMTSs, their substrates and activities are still not known. ADAMTS-1, -4, -5 and -9 express strong proteoglycanase activity against large aggregating CSPGs and their activity can be inhibited by TIMP-3 (Porter *et al.*, 2005; Rivera *et al.*, 2010).

### **1.11.2 Basic domain structure and functions of ADAMTSs**

The structure of ADAMTSs and ADAMs is highly conserved and the main difference between them is that ADAMTSs are secreted proteins, while ADAMs are transmembrane proteins. As illustrated in Figure (1-8) the detailed structure of ADAMTS domains are shared with ADAMs, with the prodomain followed by the catalytic active site and metalloproteinase domain containing the zinc binding site. ADAMTS molecules are characterized by various numbers of thrombospondin like repeats (TSR-1) and at their C-terminal lack transmembrane and cytoplasmic domains (Paulissen *et al.*, 2009; Lin & Liu, 2010).

ADAMTSs can be expressed in multiple isoforms due to their alternative gene splicing, and they are translated originally as inactive pre-proenzymes, whose structure includes; a signal peptide, a pro-domain, a catalytic domain, a disintegrin-like domain, a central thrombospondin type-1 like (TS) repeat, a cysteine-rich domain, a spacer region and a variable number of C-terminal TS repeats (Kuno *et al.*, 2000; Porter *et al.*, 2005).

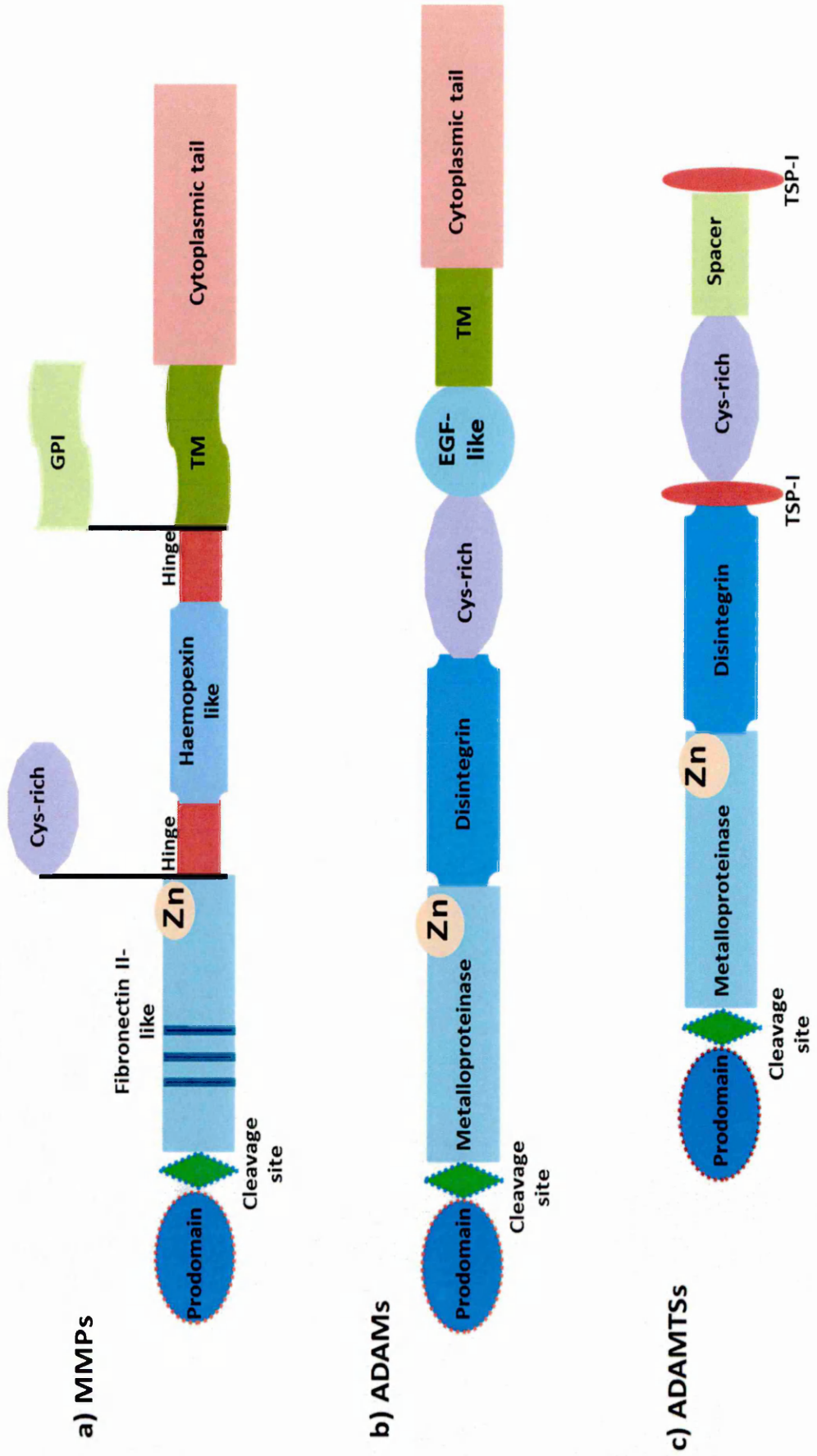
As seen in Figure (1-8), the C-terminal of ADAMTS-20 possesses a 14 TSR-1 repeat that is important for the ability of ADAMTS-20 to bind to different molecules of the ECM. ADAMTS-4 lacks the C-terminal (TS) repeat and has the ability to bind to ECM molecules by its spacer region (which correlates with the C-terminal of fibronectin) (Tortorella *et al.*, 2000; Hashimoto *et al.*, 2004).

#### **1.11.2.1 Signal peptide and prodomain of ADAMTSs**

The N-terminus of ADAMTSs contains a signal sequence that directs its post-translation transport into the secretory pathway by the endoplasmic reticulum. Signal peptides vary in length between the ADAMTSs (5-30 amino acids), very short in ADAMTS-13, and is removed from the protein prior to secretion (Dunn *et al.*, 2006; Tauchi *et al.*, 2013).

### Figure 1-7: Structural organisation of MMPs, ADAMs and ADAMTS

Schematic representation of the domain organisation of (a) matrix metalloproteinases (MMPs), (b) a disintegrin and metalloproteinase (ADAMs) and (c) a disintegrin and metalloproteinase with thrombospondin motifs (ADAMTS). Note that most MMPs have an additional C-terminal extension domain containing a catalytic metalloproteinase domain with fibronectin type II and hemopexin-like domain. The common structure of ADAMs is a pro-domain, a cleavage site for furin or furin like protein, a metalloproteinase domain, a disintegrin domain, epidermal growth factor repeats (EGF-like domain), a transmembrane domain (TS) and a cytoplasmic tail domain. ADAMTSs do not have a transmembrane (TM) domain and bear various numbers of thrombospondin type-1 motifs (TSP-1) at their C-terminal extremity. Cys-rich: cysteine-rich repeats, GPI: glycosylphatidylinositol. Figure adapted from Paulissen *et al.*, (2009) and Shimoda & Khokha, (2013).



The signal peptide is followed by the pro-domain that keeps the metalloproteinase site of ADAMTSs in the inactive form. The pro-domain exhibits a high level of similarity between ADAMTSs (220-300 amino acids), the exclusion to this rule is ADAMTS-13 which has 74 amino acids (Cao *et al.*, 2000; Longpre & Leduc, 2004). The prodomain possesses cleavage sites for a furin cleavage consensus motif. Thus, it is generally believed that zymogen forms of ADAMTSs are cleaved intracellularly and then the protein is produced in its mature forms. This process of maturation was supported by studies of ADAMTS-1 and -4, which identified that furin interacts with the pro-form of these ADAMTSs to co-localise within the trans-Golgi network (Longpre & Leduc, 2004; Wang *et al.*, 2004). However, not all ADAMTSs increase in catalytic activity when cleaved, as seen in ADAMTS-9, which is resistant to furin cleavage in the secretory pathway (Koo *et al.*, 2007) as well as ADAMTS-13, which does not require prodomain cleavage for cleavage of von Willbrand factor (vWF) (Majerus *et al.*, 2003).

#### **1.11.2.2 Metalloproteinase domain of ADAMTSs**

The catalytic domain of ADAMTSs shares a high degree of similarity and has a zinc-binding sequence HEXXHXXG that distinguishes the ADAMTS and ADAM family from MMPs ("X" = any amino acid residue). It is essential for the zinc ion to be bound to the histidine residues within the catalytic domain in order for ADAMTSs to be active, this known as the zinc binding motif (ZBM). The zinc activates water molecules by reduction of hydrogen atoms, rendering it a reactive nucleophile with the ability to attack peptide carbonyl groups. The glutamate (E) has been shown to have an essential role in this process by polarising the water molecules through hydrogen bonding (Andrein *et al.*, 2005; Gottschall & Howell, 2015).

#### **1.11.2.3 Ancillary domain of ADAMTSs**

The C-terminal domains of the ADAMTSs are known as the ancillary domains. The catalytic domain of all ADAMTSs is followed by a highly conserved 60-90 amino acid domain with the primary sequence having similarity to snake venom disintegrins known as the disintegrin-like domain. These primary sequences have an integrin recognition sequence, arginine/glycine/aspartic acid (RGD), which binds to the superfamily adhesion molecule integrins. Unlike ADAMs, the C-terminal to the disintegrin like domain is highly conserved, with a 45-54 amino acid central TSP-1

domain. TSP-1 is a glycoprotein proven to have an essential role in wound healing, inflammation and angioinhibition. This is followed by a cysteine rich domain and spacer regions (Porter *et al.*, 2005; Takeda *et al.*, 2012).

The cysteine rich domain (CRD) is highly homologous between all ADAMTSs and consists of ten cysteine residues. The CRD is believed to promote cell adhesion molecules through interacting with ECM proteins including fibronectin and syndecans (Rivera *et al.*, 2010). The next domain downstream to the CRD is a cysteine-free spacer region; both are implicated in the binding to CSPGs (Stanton *et al.*, 2011). The spacer domain on ADAMTS-4 is believed to interact with the GAG side chains on aggrecan allowing proteolysis to take place (Kashiwagi *et al.*, 2004). Following the spacer region, a variable number of TSP repeats from 1 to 14 and further domains on certain ADAMTS enzymes are present (Figure 1-8).

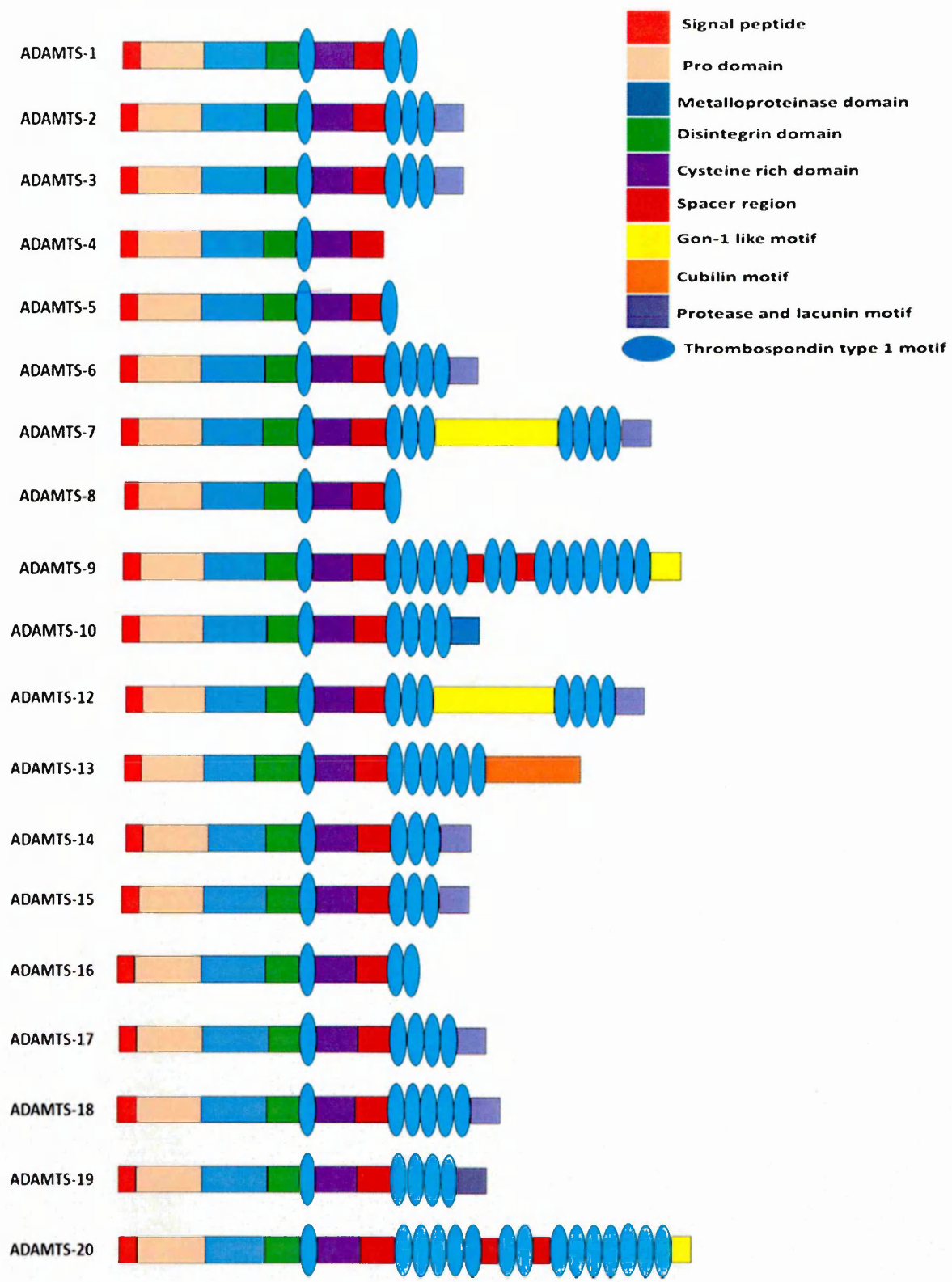
### **1.11.3 Function of ADAMTSs subgroups**

Phylogenetic tests of the ADAMTSs indicated that family members could be divided into three subgroups on the basis of their sequence similarities and, where known, their cleavage of target substrates, which are specific ECM macromolecules as follows (Lemarchant *et al.*, 2013): proteoglycans (ADAMTS-1, -4, -5, -8, -9 and -15 and -20), pro-collagen (ADAMTS-2, -3 and -14), or von Willebrand factor (ADAMTS-13), which is implicated in blood coagulation homeostasis (Grawley *et al.*, 2011). ADAMTS-13 is least like any other ADAMTSs as shown in figure (1-8). All members of the subgroup consisting of ADAMTS-1, -4, -5, -8, -9, -15 and -20 have all been shown to cleave lecticans and have thus been termed as hyalactanase "aggrecanases". There is subdivision into two further groups, one composed of ADAMTS-9 and 20 and the other of ADAMTS-1, -4, -5, -8 and -15. Though ADAMTS-9 is classified as Gon-ADAMTS with ADAMTS-20, it is able to cleave versican (Isik *et al.*, 2015).

Several ADAMTSs including ADAMTS-2, -3, -10, -14, -17 and -19 have protease and lacunin (PLAC) containing domains with six conserved cysteine residues that are found

### **Figure 1-8: Domain structure of ADAMTS proteins**

A schematic representation of the structure of the distinct human ADAMTS family. The ADAMTSs have the same general structure in that they all contain a signal peptide, a pro-domain, a metalloproteinase domain, disintegrin-like domain, a central TSP-1, a cysteine rich domain (CRD), a spacer domain and a variable number of C-terminus TSP-1 motifs. Additional domains are present at the C-terminal of particular ADAMTSs including protease and lacunin motif (PLAC), Gon-1 domain and cubulin domain motif (CUB). Figure adapted from Porter *et al.*, (2005).



in some protein convertases and their function is still not known (Gottschall & Howell, 2015). A C-terminal extension comprising a distinctive embedded PLAC domain is found in ADAMTS-2, -3 and -14 (Colige, 2010; Jones & Riley, 2005). Additional C-terminal domains are present in ADAMTS-13 includes two cubilin domains (CUB). In addition to proteoglycan cleavage, ADAMTS-1 and -8 have the ability to regulate and inhibit angiogenesis via suppressing growth factors including fibroblast growth factor-2 (FGF) and vascular endothelial growth factor (VEGF) (Vong & Kalluri, 2011; Kumer *et al.*, 2012).

#### **1.11.4 ADAMTS proteoglycanases in the physiology of the CNS**

ADAMTS proteoglycanases are present in several CNS structures including the cortex, the hippocampus, striatum and the spinal cord (Lemarchant *et al.*, 2013). While it is clear that neurons and glia express ADAMTS proteoglycanases *in vitro* and *in vivo*, their presence in neuronal cells under physiological condition is controversial. Evidence exists for the presence of ADAMTS-1, -4 and ADAMTS-cleaved brevican fragment in physiological rat brain, particularly in regions such as the hippocampus, suggesting the involvement of the ADAMTS in the plasticity of PNNs (Gottschall & Matthew, 2015).

Hamel *et al.*, (2008) indicated active ADAMTS-4 promoted neurite outgrowth of cortical neurons *in vitro* by; i) breakdown of CSPGs by its proteolytic activity, and by ii) activating the mitogen activated protein (MAP) and extracellular signal-regulated kinase (ERK) signalling pathways, presumably due to the activation of tyrosine kinase receptors by the TSP-1 domain of ADAMTS-4 (Hamel *et al.*, 2008). The expression of synaptic proteins, such as synaptosomal associated protein 25 (SNAP-25), postsynaptic density protein (PSD-95) and synaptophysin, was down-regulated in developing frontal cortex of ADAMTS-1 deficient mice, suggesting specific involvement of ADAMTS-1 in synaptic plasticity (Howell *et al.*, 2012). Others indicated that ADAMTS-4 and ADAMTS-5 are capable of cleaving Reelin, which is involved in neurodevelopment and in synaptic plasticity induced learning and memory processes (Krstic *et al.*, 2012).

#### **1.11.5 ADAMTS proteoglycanases in the pathological CNS**

ADAMTS breakdown of the ECM can be both beneficial and harmful in various pathological states of the CNS including, ischemic stroke and spinal cord injury (Lemarchant *et al.*, 2013). An increased synthesis of ADAMTS-4, -5 and -9 by

astrocytes was reported after transient middle cerebral artery occlusion (tMCAO) (Reid *et al.*, 2009; Zamanian *et al.*, 2012). Several cytokines including, IL-1 $\beta$ , IL-6, INF- $\gamma$ , transforming growth factor (TGF) and TNF have previously been described to upregulate the expression of ADAMTS proteoglycanases in CNS cell types. IL-1 $\alpha$  in combination with the IL-1 receptor promoted ADAMTS-1 transcription in N1E-115 neuroblastoma cell line *in vitro* and in motoneurons after nerve injury *in vivo* (Sasaki *et al.*, 2001).

ADAMTS-4 mRNA and protein expression was increased by TNF in human astrocytes *in vitro*, whereas only up-regulation of ADAMTS-1 mRNA and ADAMTS-5 protein level was upregulated under the same conditions (Cross *et al.*, 2006). TNF- $\alpha$  and INF- $\gamma$  increased the expression of ADAMTS-4 in macrophages induced by differentiation of human monocyte cell line THP1 (Wagsater *et al.*, 2008). In experimental autoimmune encephalomyelitis (EAE), differential expression of ADAMTS-1, -4, -5 and TIMP-3 was seen at various stages of disease progression. There have been a limited number of reports in other CNS disorders focusing on ADAMTS involvement. ADAMTS-1 expression was demonstrated to be up-regulated in Down's syndrome, Pick's and Alzheimer's disease (Miguel *et al.*, 2005).

#### **1.11.6 ADAMTSs in MS**

ADAMTS-1, -4, -5, -8, -9 and 15 are glutamate endopeptidase (GEPs), cleaving peptide bonds at the carboxyl end of the glutamate residues, and can cleave the major cartilage proteoglycan (Porter *et al.*, 2005). ADAMTS-1 is expressed in all human tissues with high expression in heart, thyroid, skeletal muscle and placenta. ADAMTS-1 can cleave both aggrecan and versican and is up-regulated by pro-inflammatory cytokines (Demircan *et al.*, 2013; Ren *et al.*, 2013). Other reports indicate that ADAMTS-1 cleaves aggrecan *in vitro* and the spacer region is essential for this (Kuno *et al.*, 2000). Most studies are reported on aggrecanases ADAMTS-4 and 5 which cleave aggrecan at the GLu373-Ala374 bond, and at the four other sites within the GAG-attachment region between The G2 and G3 globular domain including GLu1480-Gly1481, Glu1667-Gly1668, Glu1771-Ala1772 and Glu1871-Leu1782 as shown in Figure (1-9). Aggrecan neoepitopes produced by cleavage at all of these sites by ADAMTS-4 and ADAMTS-5 have been detected in bovine articular cartilage explants treated with pro-inflammatory cytokines to enhance aggrecan release (Tortorella *et al.*, 2001).

ADAMTS-4 and 5 can also cleave brevican, predominantly expressed in CNS tissue (Matthews *et al.*, 2000). In addition, differential expression of ADAMTS-1, 4 and 5 were identified during different lesion stages in MS which may contribute to ECM degradation in disease progression (Tauchi *et al.*, 2012). Previous studies in our laboratory emphasise the up-regulation of ADAMTS-4 in active lesions of MS (Cross *et al.*, 2006).

ADAMTS-9 was also identified as an aggrecanase and versicanase, cleaving aggrecan at the Glu373-Ala374 bond and versican at the Glu441- Ala442 bond (Somerville *et al.*, 2003). ADAMTS-9 was produced by astrocytes and was also up regulated after spinal cord injury in mice (Demircan *et al.*, 2013).

Despite the fact ADAMTS-9 is clearly expressed in abundance in the CNS (Ried *et al.*, 2009), no studies have focussed specifically on the protein expression in the brain.

ADAMTS-9 may also degrade other CSPGs proteins brevican and neurocan, on which the peptidase has yet to be tested. Therefore ADAMTS-9 could be implicated in normal ECM turnover e.g. cleaning a path for the migration of precursor cells. Other studies have demonstrated that ADAMTS-9 is up-regulated in response to pro-inflammatory cytokines, in particular IL-1 $\beta$ , TNF and INF- $\gamma$  (Reid *et al.*, 2009). However, anti-inflammatory mediators, for example TGF- $\beta$ 1, have been shown to down-regulate ADAMTS-9 in neuronal cell lines (Cross *et al.*, 2005). Following astrogliosis which accompanies neuronal injury, ADAMTS-9 has the ability to degrade HSPGs present in glial scars (Trendelenburg & Dirnagl, 2005). As ADAMTS-9 has a number of roles in both normal and injured CNS tissues, it is important to analyse the expression profile and modulation of ADAMTS-9 in the brain to provide a better understanding of its role in MS.

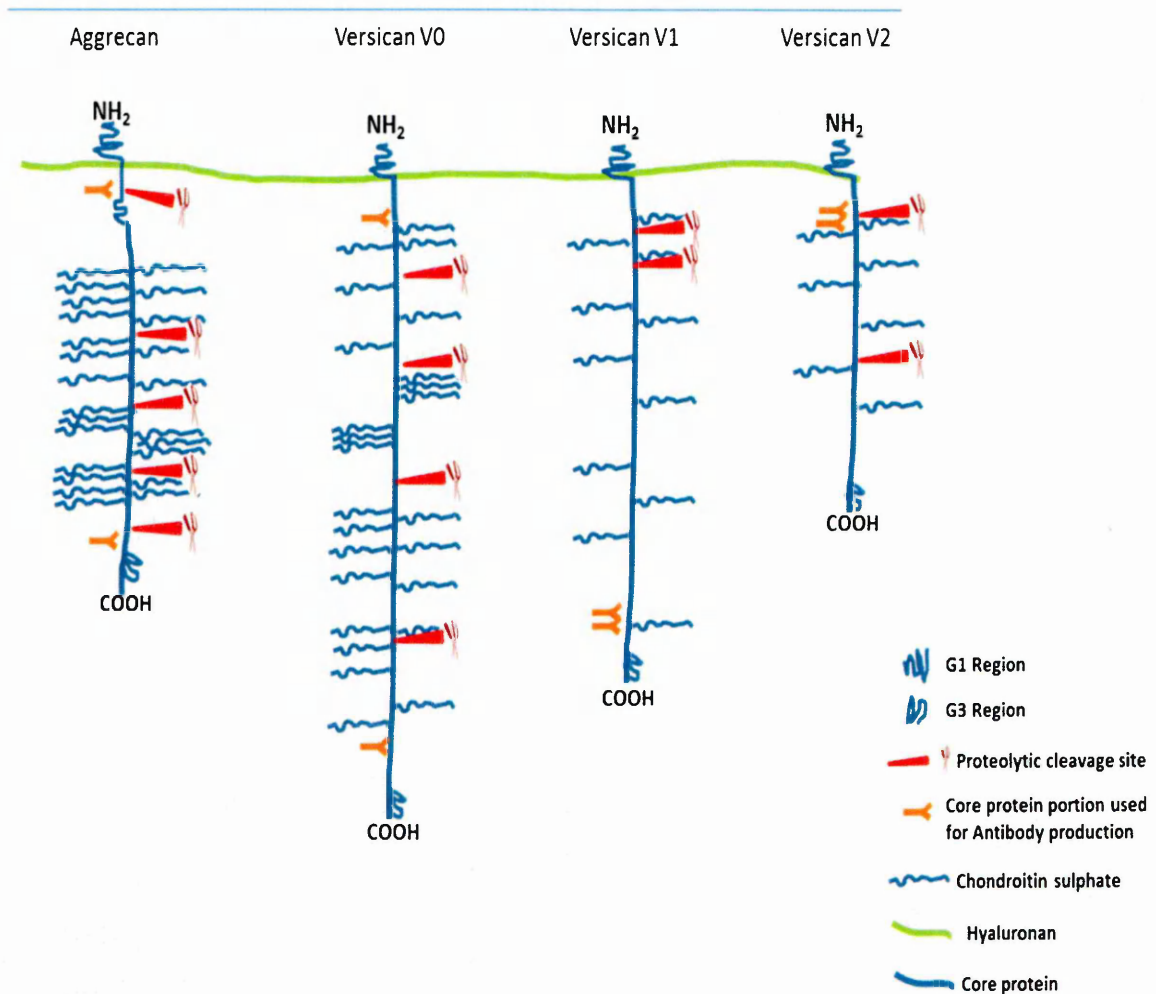


**Figure 1-9: Proteolytic cleavage sites of CSPG**

Structural models of aggrecan and versican isoforms (V0, V1 and V3) share the same feature of large CSPGs with G1 and G3 domain with GAG region in between, ADAMTS cleavage site and binding regions of the polyclonal antibodies used in immunohistochemical studies in this thesis are displayed in the figures. Figure adapted from Zimmermann & Dours-Zimmermann (2008).

## 1.12 The aims and objective of this study

### Hypotheses:

- CSPGs are up-regulated in MS and contribute to lack of neuronal regeneration by preventing migration of oligodendrocyte precursor cells. Breakdown of CSPGs by ADAMTSs may enable axonal outgrowth and repair. Conversely, it may assist the access of inflammatory cells and the secretion of cytokines which may promote axonal damage.
- Increased ADAMTS-9 activity in the brain causes breakdown of ECM components in MS
- Neuronal ADAMTS-9 expression is modulated in response to proinflammatory cytokines *in vitro*.

### Objectives

- To determine the distribution of CSPGs; aggrecan and versican in CNS *in vivo* in control white matter, MS NAWM and MS lesions using immunohistochemistry (IHC) and western blotting (WB).
- To detect CSPG degradation by ADAMTSs *in vivo* by the detection of neoepitopes of ECM components in normal and MS CNS tissue using IHC and WB.
- Determination of expression of ADAMTS-9 within MS and control white matter at the protein level by immunofluorescence and western blotting and at the mRNA level by qRT-PCR.
- To assess the impact of aggrecan on neurite outgrowth using in-cell ELISA, immunocytochemistry (ICC) and WB detection of neurofilament-L (NF-L) expression.
- To analyse the modulation of ADAMTS-9 expression by cytokines relevant to CNS inflammation in MS in microglia, astrocytes and neuronal cells *in vitro*.

**Chapter 2**  
**Materials and Methods**

## **Chapter 3**

**Expression of white matter extracellular  
matrix chondroitin sulphate proteoglycans  
and their neoepitopes in the CNS in multiple  
sclerosis and controls**

## 2.1 Human brain tissue

The UK MS Society Tissue Bank, situated at Imperial College School of Medicine at Hammersmith Hospital, London, was established in 2007 by the Multiple Sclerosis Society to co-ordinate the collection of tissue from donors, and distributes high quality CNS tissue samples to MS researchers.

Snap-frozen autopsy brain tissue from twenty eight clinically and neuropathologically confirmed MS cases, together with eight normal control cases were received from the UK MS Society Tissue Bank. Informed consent and ethical approval for the MS Tissue Bank was obtained through multi-centre research ethics approval (MREC; 08/MRE09/31) (Appendix I). Snap-frozen brain blocks were transported on dry ice, before being stored in airtight containers in a -80°C freezer until required. Control tissues were matched to MS tissue as closely as possible, in terms of the corresponding region of the brain.

The MS cases included 17 females, mean age 54.52 years (range 39-77) and 11 males with a mean age of 60.54 years (range 38-75), while control cases included five males, mean age of 67.8 (range 35-88) and 3 females, mean age of 68.3 (range 50-77). 24 of the MS cases had a confirmed diagnosis of secondary progressive MS (SPMS), 2 were diagnosed as primary progressive MS, one was diagnosed as relapsing-remitting MS and one was not specified, this study only included SPMS cases. Table (2-2) summarises the clinical details of all the individual cases used in this study and the mean time from death to freezing (post-mortem interval) for each case.

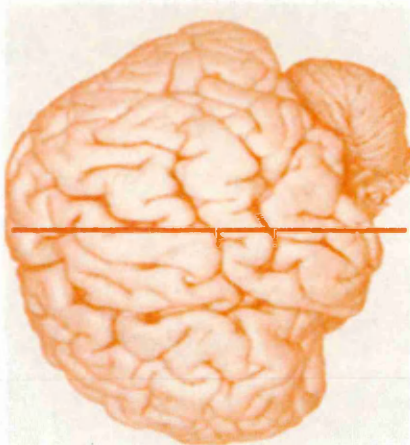
After the brain was removed from the deceased donor, it was dissected according to an approved protocol by staff at the tissue bank. Tissue blocks were prepared by cutting a whole brain into anterior and posterior halves by a single cut through the mammillary bodies. One centimetre thick coronal slices were then cut through the entire brain. The slices were then numbered, based on whether they were taken anteriorly (frontal pole) or posteriorly (occipital pole) to the mammillary bodies (Figure 2-1). The former were numbered A1, A2 etc and the latter were numbered P1, P2 etc.

The coronal slices were laid on a grid and cut into two cm<sup>2</sup> blocks, which were frozen by immersion in isopentane, precooled on dry ice and then stored at -80 °C.

**Figure 2-1: Schematic diagram showing the coronal slicing of brain and preparation of tissue blocks by the UK Multiple Sclerosis Society Tissue Bank.**

The whole brain was first divided into the anterior and posterior segments (a), following this, each segment was then coronally sliced into one centimetre thick slices (b). Slices were the numbered on whether they were cut anterior or posterior to the mammillary bodies, the first slice anterior to the mammillary bodies was labelled A1, the next A2, etc., and the first slice posterior was labelled P1, the next P2, etc (c). Finally, each slice was placed onto a grid for further cutting into two centimetre square blocks and then given a number based on the co-ordinates on the grid from which the block was cut.

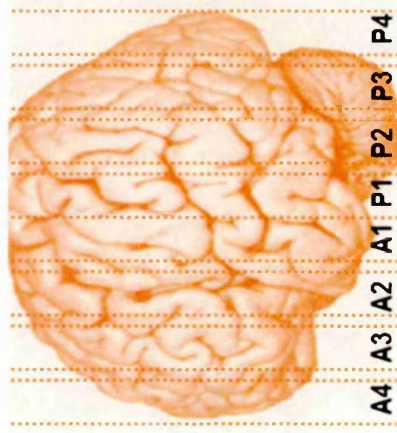
**a**



**b**



**c**



**d**



In addition, each patient was given an ID code and the four digits following that related to the coronal sections and the grid reference where the tissue blocks was taken from. e.g. MS076 A1E3, the patient's code is MS076, and the coronal slice is A1 and therefore derived from the first section anterior to the mammillary bodies, and the block was taken from grid co-ordinate E3.

## **2.1.1 Histopathology of frozen brain tissue**

### **2.1.1.1 Haematoxylin and Eosin staining**

Haematoxylin and eosin (H&E) is a histological stain that uses the basic dye haematoxylin to stain basophilic structures, such as the nucleus, ribosomes, and RNA-rich cytoplasmic regions to produce a blue/purple colour shade. Whereas, the acidic dye, eosin Y stains eosinophilic structures, typically the cytoplasm, connective tissue and collagen pink (Ross & Pawlina, 2006).

Prior to staining, frozen tissue sections were fixed in 4% paraformaldehyde (PFA) (Appendix II) for 15 mins at room temperature (RT). Sections were immersed in filtered Harris's haematoxylin (Sigma-Aldrich, UK) for 2 mins followed by rinsing with running tap water until the water ran clear. Then sections were stained with eosin (1%) (Sigma-Aldrich, UK) for 1 min followed by rinsing in tap water. Following this, slides were subjected to dehydration in increasing concentrations of ethanol (50, 70, 80, 95, and 100%) for 2 mins at each concentration. Slides were placed in xylene (Sigma-Aldrich, UK) for 5 mins and then mounted with Di-N-Butyl phthalate (DPX) in Xylene (Sigma-Aldrich, UK). Slides were then left to harden in the fume hood for at least 1h and then examined using light microscopy with an Olympus BX60 microscope with Cool SNAP-Pro (media Cybernetics) imaging system.

### **2.1.1.2 Oil Red O staining**

Oil Red O (ORO) is a neutral lipid dye which indicates regions of myelin breakdown via staining myelin debris engulfed by macrophages (Suvarna *et al.*, 2013). ORO solution was prepared by adding 1g of ORO powder (Sigma-Aldrich, UK) to 60mL of triethyl phosphate (TEP) (Sigma-Aldrich, UK) and 40mL of distilled water (dH<sub>2</sub>O), heating to 100°C for 5mins whilst stirring continuously on a magnetic stirrer. The ORO solution was filtered through filter paper (Fisher Scientific, UK) whilst hot, and again, when cold.

**Table 2-1: Case details of post mortem brains used in this study**

Case	Sex	Died Age (Yrs)	initial symptoms age(Yrs)	PMI (hrs)	Diagnosis	Cause of death
MS049	Male	75	38	8	SPMS	Aspiration Pneumonia, Cerebrovascular accident, MS
MS050	Female	72	41	8	SPMS	Bronchopneumonia, MS
MS051	Female	73	43	19	PPMS	Bronchopneumonia
MS057	Female	77	44	9	SPMS	General deterioration, lung infection, treatment withheld
MS058	Female	51	21	15	PPMS	MS
MS060	Male	55	43	16	SPMS	Aspiration of gastric, MS
MS062	Female	49	19	10	SPMS	Respiratory infection
MS074	Female	64	36	7	SPMS	Gastrointestinal bleed/obstruction, Aspiration Pneumonia
MS076	Female	49	18	31	SPMS	Chronic renal failure, heart disease, general decline
MS079	Female	49	23	7	SPMS	Bronchopneumonia, MS
MS080	Female	71	35	24	SPMS	Bowel blockage then post-operative complication, heart failure
MS081	Male	72	47	23	SPMS	Bronchopneumonia
MS090	Male	62	39	17	SPMS	MS
MS092	Female	37	17	26	SPMS	MS
MS094	Female	42	6	11	SPMS	Bronchopneumonia, MS
MS100	Male	46	8	7	SPMS	Pneumonia
MS102	Male	73	52	20	SPMS	Left ventricular failure, Pneumonia, Pleural effusion
MS103	Female	77	21	7	SPMS	Pneumonia
MS104	Male	53	11	12	No Specified	Advanced Multiple Sclerosis, urinary tract infections
MS105	Male	73	46	8	SPMS	Pneumonia
MS106	Female	39	21	18	SPMS	Bronchopneumonia
MS107	Male	38	16	19	PRMS	Aspiration pneumonia, Pulmonary oedema
MS121	Female	49	14	24	SPMS	MS
MS122	Male	44	10	16	SPMS	Bronchopneumonia
MS126	Male	75	32	22	SPMS	Pneumonia
MS153	Female	50	-	12	SPMS	MS
MS154	Female	34	22	12	SPMS	MS
MS160	Female	44	-	18	SPMS	Aspiration pneumonia, MS
CO014	Male	64	Normal	18	Normal	Cardiac failure
CO022	Female	77	Normal	20	Normal	Pneumonia
CO025	Male	35	Normal	22	Normal	Carcinoma of the tongue
CO026	Female	78	Normal	33	Normal	Myeloid Leukaemia
CO032	Male	88	Normal	22	Normal	Prostate cancer, bone metastases
CO036	Male	68	Normal	30	Normal	Coronary artery, fibrosing alveolitis, heart failure
CO037	Male	84	Normal	5	Normal	bladder cancer, Pneumonia
CO039	Female	50	Normal	8	Normal	Cardiac failure

CO, control, PMI, post-mortem interval; SPMS, secondary progress multiple sclerosis; PPMS, primary progress multiple sclerosis; PRMS, progress remitting multiple sclerosis.

Frozen sections were prepared for ORO staining by fixation in 4% PFA at RT for 15 mins. Following fixation, slides were washed in tap water, briefly rinsed in 60% TEP, and stained in filtered ORO solution for 10-15 mins at room temperature (RT). Stained slides were then briefly rinsed in 60% TEP, and given a further rinse in tap water. Nuclei were counterstained with Harris's haematoxylin (diluted with dH<sub>2</sub>O to 20% v/v); the slides were washed in dH<sub>2</sub>O, and mounted using 22X50 mm coverslips (Fisher Scientific, UK) with the aqueous mountant glycerol gelatine (Sigma-Aldrich, UK).

## **2.1.2 Immunohistochemistry on normal and MS brain sections**

### **2.1.2.1 Single label immunofluorescence stainings of brain sections**

Prior to immuno staining, sections were fixed in ice-cold acetone in Coplin jars for 10 mins at RT and then air-dried for 5 mins. After fixation, the tissue area of the slides was defined to contain the antibody solution by drawing a wax circle around it with an "ImmEdge" pen (Vector Lab, UK). Slides were then treated either with 3% goat serum (Abcam, UK) or donkey serum (Abcam, UK) or rabbit serum (Abcam, UK) dependent on the species of the antibodies used for stains diluted in 1% bovine serum albumin (BSA) (Sigma-Aldrich, UK) for 30 mins at RT to prevent non-specific binding of the primary and secondary antibodies. Table (2-2) provides a summary of the primary and secondary antibodies used in this study.

Tissue sections were characterized using antibodies to cell markers for the detection of endothelial cells of blood vessels using antibodies to Von Willebrand factor (VWF, Dako, UK), human leukocyte antigen (HLA-DR, Leica, UK) for activated macrophages/microglia, myelin oligodendrocyte glycoprotein (MOG, gift from Prof C Linington, Glasgow University) for regions of demyelination, glial fibrillary acidic protein (GFAP, Millipore, UK) for astrocytes, and neurofilaments (Cell Signalling, UK) for neurons. Primary antibodies were initially optimised by selecting a range of dilutions based on an initial recommendation by the manufacturer.

To identify CNS white matter CSPG alterations in normal control and MS sections, polyclonal rabbit anti-CSPG antibodies (Abcam, UK) to the core protein of two lecticans (aggrecan and versican), and their corresponding neoepitopes (Thermo, UK) were used. Prior to acetone fixation, a deglycosylation step was required for CSPGs to remove the

glycosylation and unmask the antigen. Thus, sections were treated with chondroitinase ABC (0.25IU/ml, Appendix II) (Sigma-Aldrich, UK) for 90 mins at RT.

Primary antibodies (180µL) were applied in PBS, and slides incubated in a humid chamber for 2h at RT. Negative controls with omission of the primary antibodies were also performed. Unbound antibody was removed by 3 x 2min PBS washes, on an orbital shaker. Secondary antibodies were incubated and washed off in the same way as primary antibodies, and then Sudan Black B (SBB) staining was performed as described in (2.1.2.2), prior to mounting in DAPI mountant (Vector Labs, UK).

### **2.1.2.2 Sudan Black B**

Brain tissue sections are susceptible to autofluorescence caused by the fluorescent pigment lipofuscin, which accumulates with age in the cytoplasm of cells, and is detrimental when using fluorescence microscopy, it is therefore often necessary to treat sections to reduce lipofuscin-like autofluorescence to enable detection of specific fluorescence from antibody and antigen reaction (Yao *et al.*, 2003; Viegas *et al.*, 2009).

Sudan Black B (SBB) is a fat soluble dye used for staining neutral triglyceride and lipids blue black on frozen sections. SBB solution was prepared by adding 1g of SBB powder (Sigma-Aldrich, UK) to 70mL of ethanol and 30mL of dH<sub>2</sub>O. The solution was stirred on a magnetic stirrer in the dark for 2h at RT. It was then filtered, and stored at 4°C for a maximum of one month. Following the final wash to remove unbound secondary antibody, slides were immersed in 1% SBB in the dark for 5 mins at RT, and mounted using 4', 6-diamidino-2-phenylindole (DAPI) mountant with a 22 X 50mm coverslip.

### **2.1.2.3 Dual label immunofluorescence**

Dual-label immunofluorescence was performed with rabbit polyclonal antibodies to CSPGs (versican and aggrecan) and their neoepitopes together with mouse monoclonal anti-HLA-DR and anti-MOG antibodies for indication of inflammation and demyelination respectively. To determine the cellular origin of ADAMTS-9 expression; dual labelling immunofluorescence was also performed with specific cell markers (vWF, HLA-DR, GFAP and NF-L). Briefly, sections were incubated with goat polyclonal antibody to ADAMTS-9 overnight at 4°C and then detected by incubating in Alexa fluor 568/488 conjugated secondary at RT for 90mins.

**Table 2-2: Details of the primary and secondary antibodies used in immunohistochemistry**

Immunogen	Primary antibodies			Secondary antibodies	
	Antibody Class	Working dilution	Supplier	Secondary antibody	working dilution
<b>HLA-DR</b>	Mouse (IgG2b)	1 in 50	Leica, UK	Goat anti-mouse Alexa fluor 568 Rabbit anti-mouse Alexa fluor 488	1 in 500
<b>MOG</b>	Mouse	1 in 100	A Gift from Prof C.Linington Glasgow University	Goat anti-mouse Alexa fluor 568 Rabbit anti-mouse Alexa fluor 488	1 in 1000
<b>VWF</b>	Mouse (IgG)	1 in 500	Dako, UK	Goat anti-mouse Alexa fluor 568 Rabbit anti-mouse Alexa fluor 488	1 in 1000
<b>NF-L</b>	Rabbit (IgG)	1:100	Cell Signalling Technology, UK	Donkey anti-rabbit Alexa fluor 488	1 in 1000
<b>GFAP</b>	Mouse (IgG1)	1:1000	Millipore, UK	Directly conjugated	1 in 500
<b>Aggrecan</b>	Rabbit (IgG1)	1 in 50	Abcam, UK	Donkey anti-rabbit Alexa fluor 488	1 in 500
<b>Aggrecan Neo</b>	Rabbit (IgG)	1 in 100	Thermo, UK	Donkey anti-rabbit Alexa fluor 488	1 in 500
<b>Versican</b>	Rabbit (IgG)	1 in 50	Abcam, UK	Donkey anti-rabbit Alexa fluor 488	1 in 500
<b>Versican Neo</b>	Rabbit (IgG)	1 in 50	Thermo, UK	Donkey anti-rabbit Alexa fluor 488	1 in 500
<b>ADAMTS-9</b>	Goat (IgG)	1in100	Santa Cruz, UK	Donkey anti-goat Alexa fluor 568/488	1 in 1000

ADAMTS-9; a disintegrin and metalloproteinase with thrombospondin motifs-9, GFAP; glial fibrillary acidic protein, HLA-DR; human leukocyte antigen, MOG; myelin oligodendrocyte glycoprotein, NF-L; neurofilament light, IgG; immunoglobulin G, Neo; neopeptides. All secondary antibodies were from Invitrogen, UK.

Following 3 X 5min washes in PBS, sections were further incubated with monoclonal antibody for 2h at RT. Sections were washed in PBS as previously and incubated in Alexa fluor 568/488 conjugated secondary antibody for a further 90 mins (Table 2-2). After the final secondary antibody had been washed off, sections were treated with SBB (2.1.2.2) to quench autofluorescence of the tissue, and mounted using DAPI mountant.

Various controls were performed alongside the sections that were dual labelled, including single labelling with primary antibodies for serial sections, omission of the first or second primary antibodies in turn, and incubation of one primary antibody with both secondary antibodies.

### **2.1.3 Image capture and analysis**

#### **2.1.3.1 Light and fluorescence microscopy**

Images of immunofluorescence on sections to assess expression of CSPGs were taken using an upright Olympus BX60 with cool-snap pro (cybernetics) digital camera. Fluorophores were excited at wavelengths of either 488 or 568nm. Composite images were stored and transferred into Microsoft PowerPoint without further manipulation.

#### **2.1.3.2 Confocal scanning laser microscopy**

Immunofluorescence images to determine co-localization of ADAMTS-9 were captured using a Zeiss 510 confocal scanning laser microscope (CSLM) equipped with a krypton/argon laser. Fluorophores were excited at wavelengths of either 488 or 568nm. Co-localization studies of the dual-labelled sections utilized the co-localization software available with the Zeiss 510 CSLM. Individual pixels were scanned for each channel within set intensity thresholds, which were consistent for all analyses. Co-localised pixels were represented as yellow in the composite image.

### **2.1.4 Quantitation of immunostaining and data analysis**

Statistical significance of any increase or decrease in expression level of CSPGs and their neopeptides in particular regions was performed using Image J software. The region of interest (ROI) was drawn with a drawing tool on captured images and then the mean density of staining was measured based on the MOG staining pattern on serial sections. All statistical analysis of data was performed via Kruskal-Wallis, where

\*P<0.05, \*\*P<0.01 and P<0.001. All data was expressed as mean  $\pm$  SEM for normal control samples and MS lesion brain tissue blocks.

## 2.2 Western Blotting

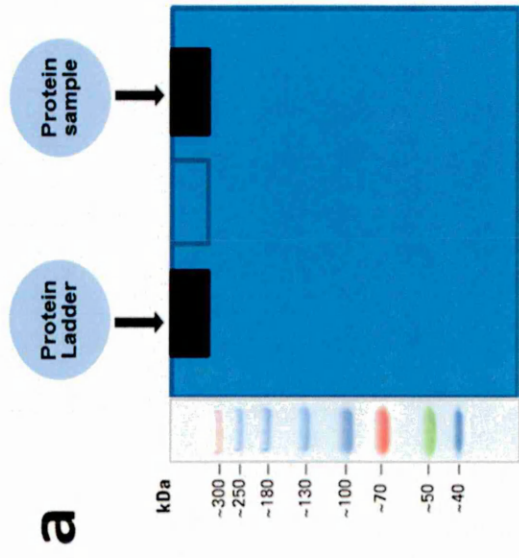
### 2.2.1 Sodium dodecyl sulphate polyacrylamide gel electrophoresis (SDS-PAGE)

A mixture of proteins in a sample can be separated by SDS-PAGE on the basis of molecular weight (*MW*) via migration through a polyacrylamide gel as a support medium, in the presence of a current by electrostatic attraction of the negative charge (caused by SDS binding to the protein) to the anode. Negatively charged SDS coated proteins migrate in the gel relative to their size only and not to their charge. A *MW* marker containing proteins of known *MW* is run in parallel to enable determination of the *MW* of protein in the test sample (Figure 2-2). Following SDS-PAGE, the presence of a protein within a sample can be confirmed by using instant blue stain (Sigma-Aldrich, UK) (Schutz-Geschwender, 2004).

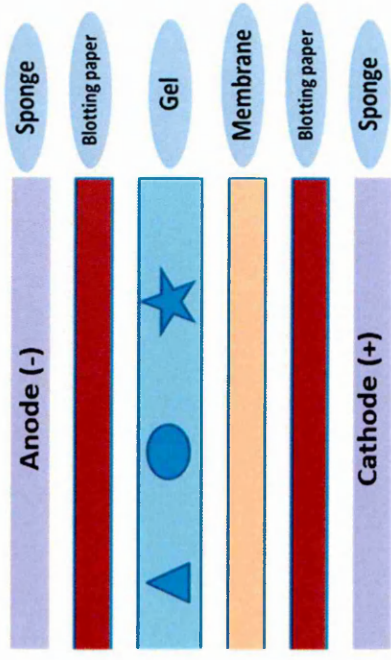
Western blotting (WB) is a well-established and widely used technique for the detection and analysis of specific proteins. The western blotting technique was first described in 1979 and has since become one of the most commonly used techniques in life science research (Renart *et al.*, 1979). Proteins are separated by SDS-PAGE and are then transferred onto nitrocellulose or polyvinylidene difluoride (PVDF) membrane where they are probed with antibodies specific to a target protein. Although there are a number of membrane types, nitrocellulose is the most commonly used. PVDF membranes have high protein binding capacity and are strong; however they are expensive and have a short shelf-life. A nitrocellulose membrane has a low binding capacity and is often brittle when dry, but is relatively inexpensive and has the longest shelf-life. Supported nitrocellulose membrane such as Hybond-C-extra (GE Healthcare LTD, UK), have improved mechanical strength thereby making them less brittle (Figure 2-2). Specific antibody binding is then detected using a range of methods, e.g. chemiluminescence with an enzyme labelled secondary antibody, or a fluorescently labelled secondary antibody (Figure 2-2) (Kurien *et al.*, 2011).

### **Figure 2-2: Protein detection on western blots**

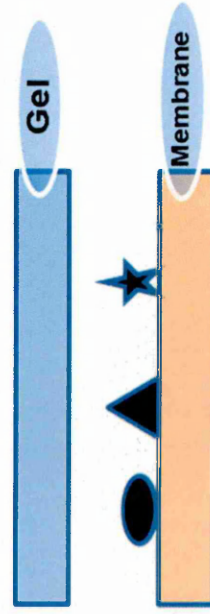
Schematic representation of SDS-PAGE, western blotting and detection procedure: a) protein denatured by SDS is loaded into the wells of an SDS-PAGE gel along side a protein ladder containing standards of known molecular weight (Spectra multicolour high range protein ladder) (Thermo Scientific, UK). b) Western blotting sandwich, the gel is electroblotted onto a membrane, c) resulting in the transfer of all proteins onto the membrane. d) The resulting blot is then immunoprobed with a primary antibody specific to the target protein, followed by incubation with a fluorescently labelled secondary antibody specific for the antibody species of the primary antibody. The target fluorescent labelled protein bands are then visualised using the Li-COR Odyssey® system.



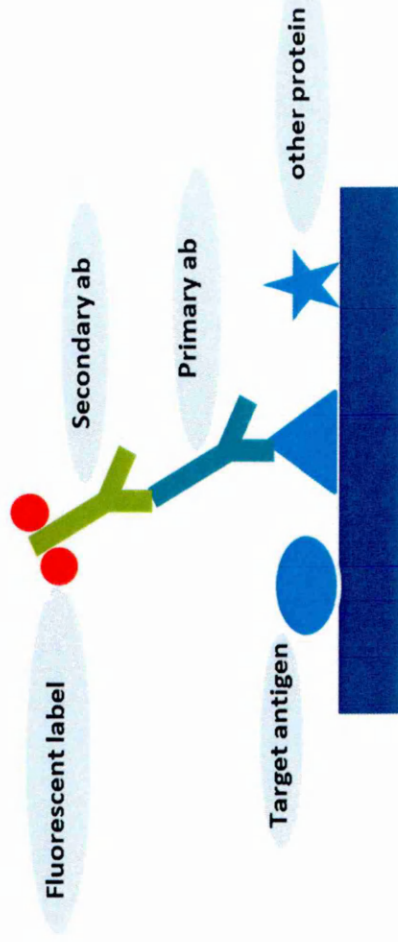
**b**



**c**



**d**



## **2.2.2 Protein Extraction**

### **2.2.2.1 Tissue protein extraction**

The human brain tissue blocks were stored at -80°C immediately after collection from the MS Society Tissue Bank. The region brain tissue of interest (ROI) was cut based on IHC results for active lesions, NAWM and normal control white matter. The tissues were then weighted and an appropriate amount of cellLytic™ Mammalian Tissue Lysis/Extraction Reagent (Sigma-Aldrich, UK) and protease inhibitor cocktail (Sigma-Aldrich, UK) used. For this procedure, a ratio of tissue to cellLytic™ reagent of 1:10 (1gram of tissue/ 10 ml of reagent) was used. Each tissue sample was transferred to a pre-chilled microhomogenizer, where it was homogenized at 4°C. The pellet was discarded and the supernatant was centrifuged at 20,000 g for 10 mins at 4°C. The supernatant was stored at -20°C in 500µl aliquots.

### **2.2.2.2 Cellular protein extraction**

In accordance with the manufacturer's protocol (Sigma-Aldrich, UK) protein was extracted from neuroblastoma cells line (SHSY-5Y), human foetal microglia cell line (CHME3) and human primary astrocytes using CellLytic™ reagent. Cells were grown on 24 well plate in triplicate and 150µl of CellLytic™ reagent added to each well (4X10<sup>5</sup> cells per/well). Prior to adding CellLytic™ reagent, the growth medium were removed from the cells and then cells rinsed once with DPBS, being careful not to dislodge the cells attached to the plate. The cells were incubated for 15 mins on shaker at RT and the lysed cells centrifuged for 10 mins at 12,000 g to pellet the cellular debris. Finally, the protein-containing supernatant was transferred to a chilled Eppendorf tube and stored at -20°C until used.

### **2.2.3 Estimation of total protein concentration by using Bradford assay**

Following protein extraction, the protein concentration was determined using a quick start Bradford dye™ reagent kit (Bio-Rad, UK) according to the manufacturer's instructions. 5µL of bovine serum albumin (BSA, Sigma Aldrich, UK) protein standard in PBS (ranging from 0.1 to 200mg/ml) along side 5µl of extracted protein sample in triplicate were pipetted into a 96 well plate. 200µL of Bradford dye reagent was added to each well. The plate was incubated for 30 mins at RT and the absorbance was read

with a Victor Wallac<sup>2</sup> plate reader at 570nm. A standard curve was drawn in excel and protein concentration was determined using the trend line of the equation of the standard curve (Figure 2-3):

$Y = aX + b$  where (Y) corresponds to absorbance, (a) corresponds to the slope of the trend line; (X) corresponds to the concentration of protein in the sample and (b) corresponds to the intercept point with the X-axis.

#### **2.2.4 SDS-PAGE**

All reagents and materials were from Invitrogen, Paisley, UK, unless stated otherwise. The extracted proteins from tissue blocks were fractionated on pre-cast 7% Tris acetate gels, 1mm thick with 10 wells, in the presence of Nupage Tris Acetate running buffer (Appendix II). 15-30µg of each protein sample was loaded per well along side 10µl of multicolour high molecular weight markers standard (range 40-300kDa, Thermo Scientific, UK) and electrophoresis carried out at 130 voltages and 200 mA for approximately 1h, until the dye front reached the bottom of the gel.

#### **2.2.5 Protein electroblotting**

Separated proteins were transferred onto Hybond-C nitrocellulose membrane (GE Healthcare, UK) in order to make the proteins accessible to antibody. A piece of nitrocellulose membrane was soaked for 5 mins in cold transfer buffer (Appendix II), along with two pieces of blotting paper and two pieces of sponge per mini-gel. One sponge was placed on the open transfer cassette, followed by a piece of blotting paper and the gel, nitrocellulose membrane (NCM), a second piece of blotting paper and another sponge.

Proteins were transferred from the SDS-PAGE gel to the NCM at 100 V for 1h (Figure 2-2). To verify the protein had transferred successfully onto the membrane, the gel was immersed in instant blue (Sigma Aldrich, UK) and the NCM in Ponceau red (Sigma Aldrich, UK) in order to visualise the protein.

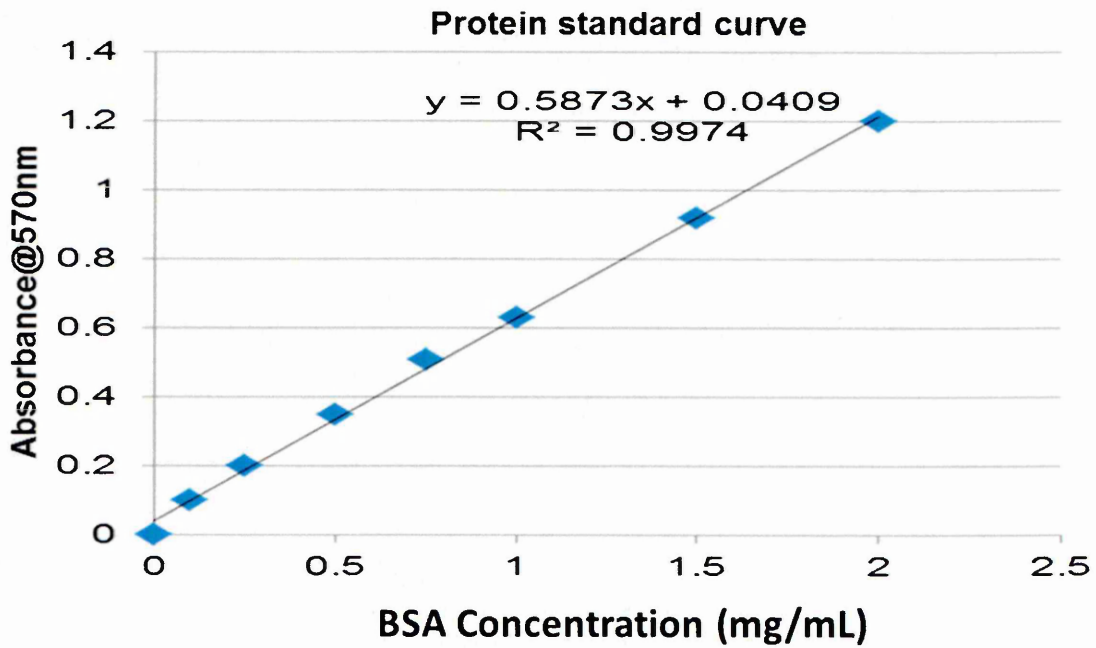


**Figure 2-3: Bradford assay standard curve**

An example of a standard curve used in the determination of protein concentration of an unknown cell or tissue extract sample using bovine serum albumin (BSA) as standard. Sample absorbances at 570nm were read and plotted as illustrated in the graph above. Equation of chart line and  $R^2$  value of the chart are given.

## 2.2.6 Immunoprobng the membrane

Following transfer of protein to the NCM, it was immediately placed in blocking solution [5% non-fat milk in PBS-T (phosphate buffered saline containing 0.02% Tween)]. Following this, the membrane was washed three times for 5 mins each in PBS, with gentle agitation on a platform shaker. The primary antibodies were then diluted in 10mL of PBS and added to the membrane and incubated overnight at 4°C (Table 2-3). For negative controls, primary antibody was omitted and the membrane was incubated with PBS alone. Following three washes of the membrane with PBS for 5 mins each, labelled secondary antibody was then diluted in PBS (Table 2-3) and incubated for 1h with gentle agitation at RT. The membrane was then washed twice for 5 mins each in PBS on the shaker followed by one final wash for 5 mins in PBS only with gentle agitation.

## 2.2.7 Determination of molecular weight of proteins migrated on SDS-PAGE

Molecular weight markers (spectra multicolour high range protein ladder (40-300kDa), Thermo, UK) were used to identify the approximate mass of a protein run on a gel; using the principle that molecular weight is inversely proportion to migration distance through a gel matrix. Consequently, once used in gel electrophoresis, markers effectively provide a logarithmic scale by which to estimate the size of the protein (Figure 2-4) (Choi *et al.*, 2009). In order to determine the mass of a protein band on western blotting, a marker lane was always included. The distance migrated by the protein markers was measured and a standard curve constructed using a plot of  $\log^{10}$  mass versus relative mobility (distance migrated by band/distance migrated by dye). The molecular weight (MW) of the unknown protein band was then determined by using the equation of the line using Microsoft Excel.

**Table 2-3: Details of the primary and secondary antibodies used in western blotting**

Target antigen	Primary antibodies			Secondary antibodies	
	Species	Working dilution	source	Species	working dilution
<b>β -Actin</b>	Mouse (IgG2b)	1:1000	Cell Signalling Technology, UK	Goat IRDye® 680 LT	1 in 10,000
<b>NF-L</b>	Rabbit (IgG)	1:1000	Cell Signalling Technology, UK	Donkey IRDye® 800 CW	1 in 10,000
<b>Aggrecan</b>	Rabbit (IgG1)	1 in 50	Abcam, UK	Donkey IRDye® 800 CW	1 in 20,000
<b>Aggrecan Neo</b>	Rabbit (IgG)	1 in 100	Thermo, UK	Donkey IRDye® 800 CW	1 in 20,000
<b>Versican</b>	Rabbit (IgG)	1 in 50	Abcam, UK	Donkey IRDye® 800 CW	1 in 20,000
<b>Versican Neo</b>	Rabbit (IgG)	1 in 50	Thermo, UK	Donkey IRDye® 800 CW	1 in 20,000
<b>ADAMTS-9</b>	Goat (IgG)	1 in 100	Santa Cruz, UK	Donkey IRDye® 800 CW	1 in 10,000

ADAMTS-9; a disintegrin and metalloproteinase with thrombospondin motif-9, NF-L; neurofilament light, IgG; immunoglobulin G, Neo; neoepitopes. All secondary antibodies were supplied from Li-COR Bioscience, UK.

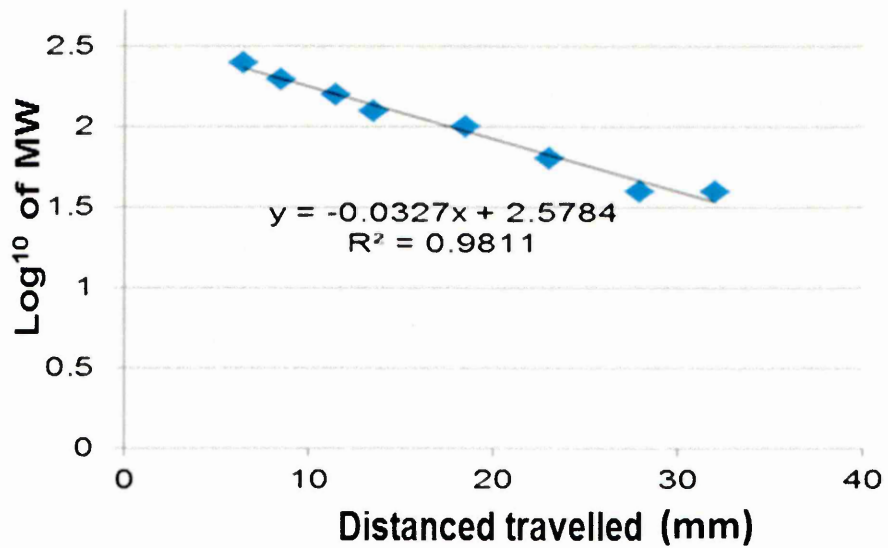


**Figure 2-4: Measurement of the molecular weight of sample protein**

Determination of the MW of the protein sample on SDS-PAGE using a known molecular weight marker (spectra multicolour high range protein ladder, Thermo Scientific, UK). A standard curve generated by plotting log molecular weight (MW) versus migration distance ( $R_f$ ) of each band of the protein ladder marker through an SDS-PAGE gel.

## **2.3 Quantitative Reverse Transcriptase Polymerase Chain Reaction (qRT-PCR)**

### **2.3.1 Overview of qRT-PCR**

Quantitative reverse transcriptase polymerase chain reaction is widely used in gene expression studies in order to detect and quantify expression specific genes of interest. Prior to PCR, mRNA is converted to complementary DNA (cDNA) through the action of the enzyme reverse transcriptase, which elongates and copies the single-stranded RNA using deoxynucleotide triphosphates (dNTPs) to make single cDNA sequences of the entire length of RNA (Bustin *et al.*, 2002). This double-stranded DNA product, or amplicon, then undergoes many repeats of thermal cycling, which consist of heating to denature the hydrogen bonds of the alpha-DNA helix thus separating the strands, and cooling to anneal primers and encouraging polymerization, resulting in the synthesis of copies of target DNA exponentially (Wong & Medrano, 2006).

### **2.3.2 The amplification plot**

As amplification proceeds, the amplification is plotted by the instrument after every cycle using fluorescent intensity related to the amount of amplicon, and is converted into a RT-PCR graph. qRT-PCR consists of three amplification stages, exponential, linear and plateau (cycles 28-40) (Figure 2-5). The amount of product doubles in each cycle of PCR, resulting in an exponential increase in fluorescence throughout the amplification reaction. However, as the reaction progresses the reagents are consumed and the reaction slows and thus at an endpoint the reaction stops (plateau phase). qRT-PCR allows accurate and precise detection and quantification of product during the exponential phase (Wong & Medrano, 2006).

Within the exponential phase, a threshold is set; the RT-PCR cycle at which the sample reaches this threshold is called the cycle threshold (CT). The CT value is used in downstream quantitation and depends on the amount of target, the larger the amount of template DNA in the reaction the fewer amplification cycles is needed to form a significant fluorescent signal. In contrast, a small amount of target will require more amplification cycles for the fluorescence signal to generate a detectable fluorescence signal (Orlando *et al.*, 1998).

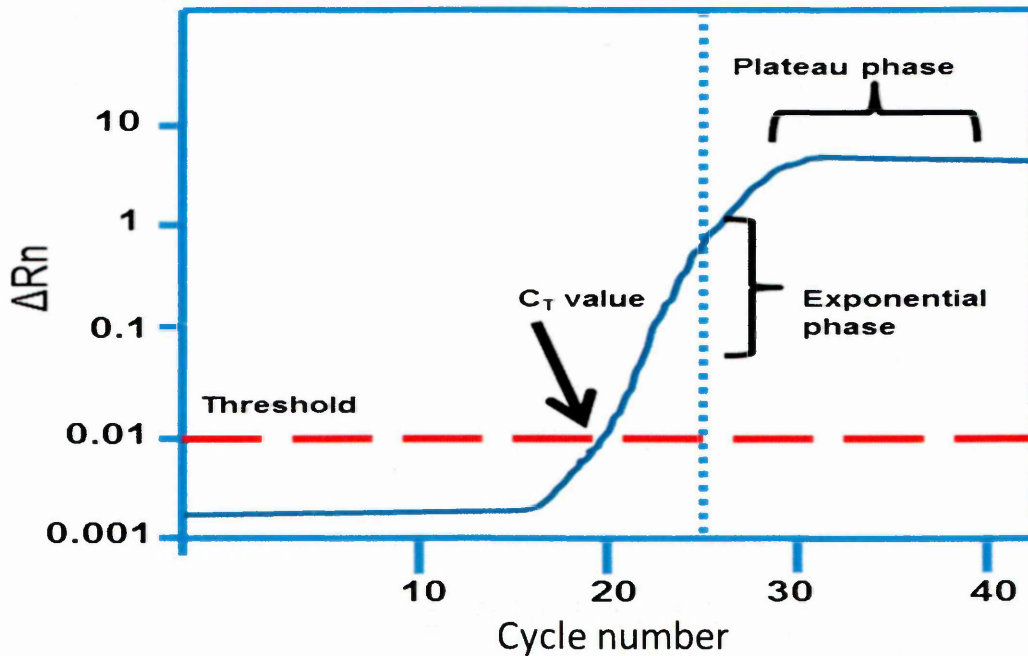


**Figure 2-5: qRT-PCR amplification plot**

This plot shows the exponential and plateau phases of qRT-PCR amplification. The PCR cycle number is shown on the X-axis and changes in fluorescence from the amplification, which is proportional to the amount of the amplified products, is shown on the Y-axis. In the exponential phase, reagents are in abundance with PCR product doubling every cycle. During the plateau phase these reagents begin to deplete and the PCR reaction begins to slow down.

**Key:** CT; cycle threshold

### **2.3.3 Total RNA Extraction**

#### **2.3.3.1 Brain tissue RNA extraction**

RNA was extracted from characterized human brain tissue blocks using Tri-reagent following the manufacturer's instructions (Sigma Aldrich, UK). Samples were left in Tri-reagent for 5 minutes at room temperature to dissociate nucleoprotein complexes.

#### **2.3.3.2 RNA extraction from cell culture**

In accordance with the manufacturer's protocol (Sigma-Aldrich, UK) mRNA was extracted from SHSY-5Y cells using Tri-reagent. Cells were grown in 24 well plates in triplicate and 1mL of Tri-reagent added to each well ( $4 \times 10^5$  cells/well). Prior to addition of Tri-reagent, the growth medium was removed from the cells, and then the cells rinsed once with DPBS, being careful not to dislodge any of the cells. RNA extraction was performed as described below (2.3.3.3).

#### **2.3.3.3 RNA extraction using Tri-reagent**

Following incubation of cells/tissue with Tri-reagent for 5mins, 0.2ml of chloroform was added; samples were mixed by vortexing for 15 seconds and incubated at room temperature for 3 mins prior to centrifugation at 12,000g for 15 mins at 4°C. Following centrifugation the upper aqueous phase (RNA containing) was removed to a clean 1.5ml Eppendorf tube and 500µl isopropanol added. RNA samples were incubated for 10 mins at RT and then centrifuged at 12,000g for 10 mins. The supernatant was carefully removed and discarded, and then 1ml of 75% ethanol added to each pellet. Tubes were centrifuged at 8,000g for 5 mins. 75% ethanol was removed and the pellet re-suspended in nuclease free water (30µl) (Sigma Aldrich, UK). The RNA samples were stored at -80°C prior to use.

#### **2.3.4 Agarose gel electrophoresis of RNA products**

A 1% agarose gel was made up by heating 0.5g of agarose (Bioline, UK) in 50ml Tris-acetate-EDTA (TAE) buffer (89mM Tris-HCL pH 7.8, 89 mM borate, 2mM EDTA) for 2 mins or until the agarose had dissolved entirely. The 1% gel solution was allowed to cool for several minutes and 10µl of ethidium bromide (10mg/ml-stock solution) (Sigma Aldrich, UK) was added. The solution was then poured into a casting tray and an 8 well comb inserted. The gel was allowed to set for 30 mins. Once the gel had set, the

comb was removed and the gel was placed in an electrophoresis tank filled with 1x TAE buffer. 2.5µl of loading buffer (Thermo Scientific, UK) was added to 2.5µl of RNA products and carefully loaded into each well of the agarose gel. The electrophoresis was then run at 100 volts for 40 mins. Images were captured by UVP Bio-imaging system Epi II in the dark room using LabWorks software version 4.0.

### **2.3.5 cDNA Synthesis**

Extracted mRNA cannot serve as a template for real-time PCR and therefore it is used to synthesise cDNA with the enzyme reverse transcriptase (RT). All reagents were from Invitrogen, unless otherwise specified. The synthesis of the first stand of cDNA requires a primer in order for the RT to extend the cDNA. The cDNA synthesis was performed with RNase/DNase free tips, tubes, gloves and surfaces were cleaned with alcohol wipes. The total reaction volume for each RNA sample was 19µl including: Superscript II RT (1µL), 5X first strand buffer (4µL), dithiothreitol (DTT) (2µL), RNaseout ribonuclease inhibitor (0.5µL), random hexamers (0.5µL) and 1µL dNTP mix containing 12.5% dATP, 12.5% dCTP, 12.5% dGTP and 12.5% dTTP (Bioline, London, UK), RNA sample (1µL) and molecular grade water (9µL). The reaction was performed at 42°C for 1 h in a heat block. The reaction was stopped by heating the samples at 95°C for 5 mins in a heat block, to inactivate the enzyme. For each cDNA synthesis preparation, two samples were included as negative controls, one lacking RT and the other mRNA template (replaced by RNase/DNase free water) (Sigma Aldrich, UK). The prepared cDNA samples were stored at -20°C prior to use as a template for real-time PCR.

### **2.3.6 Primer design and housekeeping genes for qRT-PCR validation**

PCR primers for the RT-PCR step should ideally be designed to span exon-exon junctions, with one of the amplification primers potentially spanning the actual exon-intron boundary. This design plays a crucial role in reducing the risk of false positives from amplification of contaminating genomic DNA. If primers cannot be designed to separate exons or exons boundaries, it is necessary to treat the RNA samples with RNase-free DNase in order to remove contaminating genomic DNA (Gunson *et al.*, 2006). The primers utilized in this study were designed using primer express and purchased from Applied Biosystems, UK. To achieve accurate relative quantification of an mRNA target, it is necessary to normalise to at least one reference gene, which is

constitutively expressed and is not affected by the experimental treatment under study, and therefore can be used to correct for differences in the amount of total nucleic acid added to each reaction (Vandesompele *et al.*, 2002). Table (2-4) lists details of the fully optimised and validated primers utilized in this study. Human housekeeping genes, glyceraldehyde 3-phosphate dehydrogenase (GAPDH), hypoxanthine phosphoribosyltransferase 1 (HPRT-1), cyclophilin A (PPIA) as well as human ADAMTS-9 were validated and optimised previously by Cross *et al.*, 2006, Ried *et al.*, 2009 and Gibrel, 2012), and expression of ADAMTS-9 was normalized against expression of these housekeeping genes. According to the manufacturer's information primer efficiencies of the target and reference genes were approximately 100%.

Synthesised cDNA was used as a template for qRT-PCR and was diluted 1:10 in nuclease free water. All qRT-PCR reactions were prepared on ice. Amplification was carried out using the ABI Prism sequence detection system (Applied Biosystems, UK). Real-time PCR was carried out with 10 $\mu$ L reaction volume in triplicate. The reaction mixture consisted of 5 $\mu$ L 2X Taqman mastermix, 3.5 $\mu$ L nuclease free water, 0.5 $\mu$ L of forward and reverse primers and 1 $\mu$ L cDNA.

### 2.3.7 Comparative CT method of data analysis

Real-time PCR data was expressed as an amplification plot for each individual gene detected. Baseline and threshold values were manually determined on each amplification plot for each target and reference gene. Thresholds were set within the exponential phase of the amplification plot and maintained across all samples investigated. Measured CT values of the mean of each triplicate target and housekeeping gene was exported to an excel file for analysis by the  $2^{-\Delta\Delta CT}$  method (Livak *et al.*, 2001). Briefly, analysis was performed by the arithmetical mean target CT value of each sample being normalized to the mean CT values of three housekeeping genes resulting in the CT value, as follows:

**Calculation:** Step 1:  $\Delta C_T = C_T \text{ target gene} - C_T \text{ reference gene}$

Step 2:  $\Delta\Delta C_T \text{ values} = \Delta C_T \text{ of test sample} - \Delta C_T \text{ control sample}$

Step 3:  $2^{-\Delta\Delta CT} = \text{relative fold increase}$

**Table 2-4: Primers utilised in qRT-PCR experiments for analysis of ADAMTS-9 mRNA expression levels**

Gene	Gene Name	Interrogated sequence Ref sequence	exon boundary	product size (base pairs)
GAPDH	glyceraldehyde 3-phosphate dehydrogenase	NM_002046.4	3-3	122
HPRT-1	hypoxanthine phosphoribosyltransferase-1	NM_000194.2	6-7	100
PPIA	peptidylprolyl isomerase A	NM_021130.3	4-5	98
ADAMTS-9	a disintegrin and metalloproteinase with thrombospondin motif-9	NM_182920.1	19-20	90

In order to perform statistical analysis on RT-PCR data, statistical significance of  $2^{-\Delta\Delta CT}$  values representing the relative levels of ADAMTS-9 expression between samples was compared using Stats Direct software (Kruskal-Wallis). Results were considered statistically significant when \*P<0.05, \*\*P<0.01 and \*\*\*P<0.001.

## **2.4 Cell culture**

### **2.4.1 Overview**

The growth of particular mammalian cells *in vitro* allows the analysis of target protein/mRNA (e.g. ADAMTS-9) expression levels to be measured under experimental conditions, which mimic a particular physiological or pathological state. By controlling or modifying the culture medium, the effect on the cell of one variable from a complex disease process can be analysed e.g. a cytokine. All cell culture procedures were carried out under sterile conditions in a Hera Safe class II laminar flow cabinet. Three human CNS cell types [primary astrocytes, neuroblastoma cell line (SHSY-5Y) and foetal microglia cell line (CHME3)] were used in this study and details including culture medium are listed in Table (2-5). All cell types have an adherent mode of growth and were incubated at 37°C in 5% CO<sub>2</sub>/95% air in a humid environment in a Hera cell incubator (Heraeus Instruments, Kandro Laboratory Products, Germany). Culture media was changed every 3 days.

### **2.4.2 Sub-culture of cells**

Monolayer cultures were maintained up to 80-90% confluence before passaging. Culture media was removed and cells were washed twice with sterile PBS to remove any remaining serum. Cultures were incubated for 3 mins at 37°C with 3mL 0.05% trypsin-ethylene diamine tetra acetic acid (EDTA) (Gibco, UK) until the cells began to detach from the surface of the flask. The addition of an equivalent volume of complete media caused inactivation of the trypsin. Cells and media were harvested and then centrifuged in Sorvall RT7 plus centrifuge (Kandro Laboratory Products, Germany) at 1,200 rpm for 10 mins and the pellet was re-suspended in fresh media. Cells were either divided into new flasks or counted for plating out in experiments.

### **2.4.3 Cell counting**

Trypan blue stain was used to quantify the number of live and dead cells in the suspension. Trypan blue is based on the principle that live cells have an intact cell membrane and therefore do not take up certain dyes. In contrast dead cells do not have an intact and functional membrane and therefore do take up the dye from their surrounding medium (Strober *et al.*, 2001). 10µl of the cell suspension was mixed thoroughly with 10µl trypan blue solution (0.4%) (Sigma, Aldrich, UK) and 10µl of the mixture was pipetted carefully onto a Countess® slide. Cells were counted using a Countess® Automated Cell Counter (Invitrogen, UK) and total cell count value, live cell count, dead cell count and viability percentage were obtained. From the results a dilution factor was calculated to obtain a live cell concentration of  $5 \times 10^4$  cells/ml.

### **2.4.4 Cryopreservation of cells**

Harvested cells were resuspended in freezing medium of 10% dimethyl sulphoxide (DMSO)(Sigma Aldrich, UK), 90% (v/v) growth media prior to pipetting  $1 \times 10^6$  cells into cryovials, which were placed in a Cryo 1°C freezing container (Nalgene, Hereford, UK) containing isopropanol in a -80°C freezer. Once cells were at -80°C, cryovials were transferred to liquid nitrogen storage. Cells were thawed by placing a cryovial in a 37°C incubator before adding cells to 5 mL of growth media prior to centrifugation at 1,200 rpm to remove DMSO. 1ml of pre-warmed complete medium was added to the cells and then quickly transferred to cell culture flasks (75cm<sup>2</sup>) containing 15mL pre-warmed complete culture media.

### **2.4.5 Aggrecan coating of plasticware for cell culture**

For culture of SHSY-5Y cell line, recombinant human aggrecan G1-IGD-G2 domain (R&D Systems, UK) was used to coat 24 well plates and 8 well chamber slides. The aggrecan stock solution was prepared by reconstituting of 25µg of aggrecan in 1 mL of sterile DPBS which was then filtered using a 0.2µm filter. Aggrecan solution (300µl) was added to wells to produce final concentrations ranging from 0 to 2.5µg/mL to cover the bottom of the wells and the plate then incubated at room temperature for 3 h. After this time the aggrecan/DPBS was removed and SHSY-5Y cells were seeded into the wells.

**Table 2-5: Human primary cells and secondary cell lines used in this study and their culture medium composition**

Name	Origin	Supplier	Culture Media
SHSY-5Y Neuroblastoma cell line	4 year-old Caucasian female, metastasised to the bone marrow	European cell culture collection	<ul style="list-style-type: none"> <li>• Dulbecco's Modified Eagle's Medium (DMEM)</li> <li>• 10% heated-inactivated foetal calf serum (HIFCS)</li> <li>• 1% (v/v) penicillin and streptomycin (P/S) (100u/mL/ 50µg/mL)</li> </ul>
CHME3 Microglia cell line	Human foetal	Prof Tardieu, Université Paris Sud, France	<ul style="list-style-type: none"> <li>• DMEM</li> <li>• 10% HIFCS</li> <li>• 1% (v/v) penicillin and streptomycin (P/S) (P/S) (100u/mL/ 50µg/mL)</li> </ul>
Primary astrocytes	Human	ScienCell™ Research Laboratories, UK	<ul style="list-style-type: none"> <li>• Basal astrocyte medium</li> <li>• 2% fetal bovine serum</li> <li>• 1% astrocyte growth supplement</li> <li>• 1% (v/v) penicillin and streptomycin (P/S) (P/S) (100u/mL/ 50µg/mL)</li> </ul>

## 2.4.6 Cytokine treatment of cells

Cells were seeded into 24-well plates at density of  $5 \times 10^4$  cells/well in 1mL of medium and left for 48 h to adhere. Recombinant cytokines IL-1 $\beta$ , IFN- $\gamma$  and TNF (Peprotech, UK) were diluted in serum-free media at concentrations of 0, 1, 10, 100 ng/mL (Appendix II). Media was removed and cells washed in serum free media prior to the addition of 1mL of each cytokine in triplicate wells for 24h. All experiments were repeated three times.

## 2.4.7 Mycoplasma Testing

Mycoplasma is a class of Mollicutes that represent a large group of specialized bacteria, distinguished by the absence of a cell wall. Mycoplasma are small and flexible, which make them able to pass through conventional microbiological filters (0.2 $\mu$ m). They depend on their hosts for many nutrients due to their limited biosynthetic capabilities (Drexler *et al.*, 2002). Mycoplasma has long been recognized as a common contaminant of cell lines in continuous culture and their presence may go undetected for months. As the mycoplasma competes with the cell lines for nutrients in complete culture media, this causes a reduction in the rate of cell proliferation and changes in cellular responses including gene expression (Dvorakova *et al.*, 2007).

The MycoAlert<sup>TM</sup> assay (Lonza, UK) was used to exploit the activity of certain mycoplasmal enzymes. The presence of these enzymes allows a rapid screening procedure, providing sensitive detection of contaminating bacteria in the test sample (Figure 2-6). The viable mycoplasma are lysed and the enzymes react with MycoAlert<sup>TM</sup> substrate catalysing the conversion of adenosine diphosphate (ADP) to adenosine triphosphate (ATP). The mycoplasma positive or negative samples can be detected by measuring ATP in specimens both before and after the addition of the MycoAlert<sup>TM</sup> substrate. If no mycoplasma enzymes are present, the second reading displays no increase over the first, while reaction of mycoplasma enzymes with their specific substrates leads to raised ATP levels, giving a positive result.

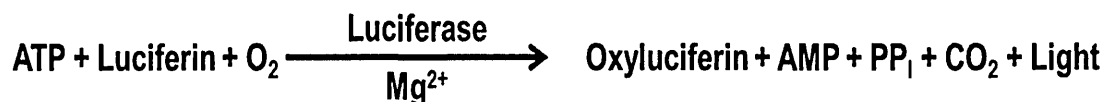


Figure 2-6: Modified from Promega. Luminescent reaction to detect ATP in mycoplasma test.

#### **2.4.7.1 Methodology**

MycoAlert™ reagent and substrate were reconstituted in MycoAlert™ assay buffer. 5mL of complete culture medium were transferred into a centrifuge tube, and spun at 200 X g for 10 mins. 100µl of cleared supernatant was transferred into white 96 well plates (Fisher Scientific), and 100µl MycoAlert™ reagent was added to each sample and incubated for 5 mins at room temperature. Following the incubation the plate was measured for luminescence (Reading A) using a Wallac Victor 21420 luminescence system. Following this, 100µl of MycoAlert™ substrate was added to each sample and incubated for a further 10 mins before re-measuring the luminescence (Reading B). The ratio was calculated for each well by dividing reading A by reading B (Ratio= Reading A/Reading B).

#### **2.4.8 Determination of cell viability by MTT assay**

Investigating the effect of specific conditions on the behaviour of cell lines *in vitro*, it is vital to determine if treatments have an effect on cell viability and proliferation. Cell viability was determined by a mitochondria enzyme dependent reaction of 3-(4, 5-dimethylthiazol-2yl)-2, 5- diphenyltetrazolium bromide, tetrazole (MTT) (Datki *et al.*, 2003; Cheung *et al.*, 2009). Briefly, all cell lines at a density of  $5 \times 10^4$  cells per well in 200µl media were cultured in 96-plates for 24h, after treatment, 10µl of MTT stock solution (5mg/ml) (Sigma, Aldrich, Uk) was added to each well (100µl) and left to incubate at 37°C for 3 hours. Metabolically active cells cleaved the yellow tetrazolium salt (MTT) to purple formazan crystal. At the end of the incubation time, the medium was removed and the formazan crystals were solubilized with 150µL of DMSO. The absorbance of the wells was measured at 570nm using Wallac Victor<sup>2</sup> plate reader spectrophotometer. These absorbance readings were then used in order to calculate fold-changes in cell number following treatment compared with untreated cells. All MTT assays were performed in triplicate.

#### **2.4.9 Immunocytochemistry of the CNS cells**

Immunocytochemistry is dependent on the affinity of an antibody for an antigen in a cell, where immunohistochemistry applies the same process, but in tissue sections. The antigen and antibody are held together by forces such as hydrogen bonding, hydrophobic interactions and ionic interactions and are reversible (Ramos-Vara, 2005).

The part of the antigen that is recognised by the antibody is known as the epitope and polyclonal antibodies can bind to more than one epitope, whereas monoclonal antibodies recognise a single epitope. Each antibody forms a complex which only occurs with the specific antigen, but some cross-reactivity can occur, however, in order to test the specificity of the antibodies used, immunoglobulin of the same class, namely isotype controls, can be used under the same experimental conditions (Delves *et al.*, 2006; Buchwalow *et al.*, 2011).

Cells were plated out into 24 well plates at a density of  $5 \times 10^4$  cells well/mL. Prior to ICC, cells were washed with two changes of PBS and then fixed in 4% (w/v) paraformaldehyde (PFA) for 10 mins. After 2 x 2 mins washes with PBS, the cells were placed in ice-cold acetone for 4 mins and subsequently left to air dry for 10-15 mins at RT. To enable permeabilisation of the cells for intracellular staining following acetone fixation, all antibodies were diluted in 0.5% Triton X-100 (Sigma, Aldrich, UK) in PBS. The neuroblastoma cell line (SHSY-5Y) and primary human astrocytes were labelled for specific phenotypic markers by indirect immunofluorescence. SHSY-5Y was labelled for neurofilaments (NF-L) and primary human astrocytes for GFAP, using monoclonal rabbit anti-human NF-L (1:100) and mouse anti-human GFAP directly conjugated (1:500) (Table 2-7). Fixed cells were also labelled for ADAMTS-9 using a polyclonal anti-goat antibody (1:100, Santa Cruz).

Cells were incubated in primary antibody (200 $\mu$ l, per well) overnight in the 4°C. The negative controls without the primary antibody were incubated with 20 $\mu$ l PBS with 0.5% Triton X-100 as for the primary antibody. After 2 x 2 mins washes with PBS, Alexa conjugated secondary antibodies (200 $\mu$ l per well, diluted in PBS) were applied to each well for 90 minutes. Table (2-6) provides the details of the primary antibodies used in this study and the secondary antibodies used were the same as in IHC for either monoclonal or polyclonal antibodies. Following a further 2 X 2 mins washes in PBS, cell nuclei were counterstained in a Vectashield mounting medium containing DAPI (Vector Labs, UK). Images were captured on an inverted stage fluorescence microscope (Olympus IX81) with Cool Snap digital camera (Olympus Media Cybernetics, Silver Spring, USA).

**Table 2-6: Details of primary and secondary antibodies used for dual immunocytochemical detection of GFAP, NF-L and ADAMTS-9 in the CNS cells**

Primary Antibody target	Species	Dilution	Incubation Time	Supplier
GFAP	Mouse (directly conjugated to Cy3)	1:500	overnight	Millipore, UK
NF-L	Rabbit	1:100	overnight	Cell Signalling, UK
ADAMTS-9	Goat	1:100	overnight	Santa Cruz, UK
<b>Secondary Antibody</b>				
anti-rabbit IgG Alexa Fluor 488	Donkey	1:1000	90 mins	Molecular Probes, Invitrogen , UK
anti-Goat IgG Alexa Fluor 488 or 568	Donkey	1:1000	90mins	Molecular Probes, Invitrogen , UK

Primary antibody against glial fibrillary acidic protein (GFAP) was directly conjugated to Cy3; primary antibodies against neurofilaments-L (NF-L) and ADAMTS-9 were detected by the appropriate fluorescently labelled secondary antibodies.

### 3.1 Introduction

The glial scar consists predominately of reactive astrocytes, microglia/macrophages and extracellular matrix molecules, especially CSPGs (Cregg *et al.*, 2014). CSPG aggrecan (Schmalfeldt *et al.*, 2000), versican (Schmalfeldt *et al.*, 2000), neurocan (Friedlander *et al.*, 1994) and phosphacan (Bovolenta *et al.*, 2000) are known to have growth-inhibitory effects, and are produced by almost all cell types at sites of CNS injury (especially by neurons and astrocytes) (Glatrey *et al.*, 2007). Recently, research groups provided grounds for optimism when they recognised growth-inhibitory components in CNS injury including CSPGs and myelin-derived proteins such as myelin associated glycoprotein (MAG), and myelin oligodendrocyte glycoprotein (MOG) which inhibits axonal growth. These molecules have been associated with glial scar that is actively formed following spinal cord injury (Rolls *et al.*, 2009; Sharma *et al.*, 2012).

The inhibitory nature of CSPGs on oligodendrocytes has also been shown in *in vivo* studies, in rat models of traumatic spinal cord injury, the accumulation of CSPGs is thought to inhibit OPC migration and their maturation into oligodendrocytes (Karimi *et al.*, 2012; Harlow *et al.*, 2014). CSPGs are found at the edge of active and expanding white matter lesions in MS (Sobel *et al.*, 2001). One study showed that the number of OPC outside such lesions is increased and that this change in OPC number may be an attempt at repair (Kuhlmann *et al.*, 2008). Various therapeutic approaches have been assessed to eliminate and reorganize the chemical components of the glial scar or regulate its negative effects. These include using degrading enzymes to eliminate scar components (especially CSPGs). Blocking by CSPGs can be reduced, but not eliminated, by removing chondroitin sulphate chains, indicating that multiple domains of CSPGs are involved in controlling axon regeneration (Bradbury *et al.*, 2002; Kwok *et al.*, 2008).

It is likely that cellular interactions between resident and inflammatory cells involved in glial scar formation are mediated by pro-inflammatory cytokines in MS. This leads to the production of increased amounts of proteolytic enzymes, which are the major effectors of the subsequent axon demyelination and resulting clinical symptoms (Kasper & Shoemaker, 2010). ADAMTS-mediated cleavage of aggrecan and versican in CNS ECM, via their glutamyl endopeptidase activity, could have a role in ECM degradation in glial scar formation in MS. The main aggrecanase cleavage site is Glu<sup>373</sup>-Ala<sup>374</sup>, and there are four additional cleavages sites in the GAG attachment region at

Glu<sup>1480</sup>-Gly<sup>1481</sup>, Glu<sup>1667</sup>-Gly<sup>1668</sup>, Glu<sup>1771</sup>-Ala<sup>1772</sup> and Glu<sup>1871</sup>-Leu<sup>1872</sup> (Figure 3-1) (Jones *et al.*, 2005; Porter *et al.*, 2005; Troeberg *et al.*, 2012). Westling and colleagues indicated that ADAMTS-4 could cleave versican V1 and V2 within GAGs (Glu<sup>405</sup>-Glu<sup>406</sup>) and (Glu<sup>441</sup>-Ala<sup>442</sup>) in neural tissue, which produced 70KDa and 64KDa fragments respectively (Westling *et al.*, 2004).

Previous studies in our laboratory reported the expression of ADAMTS-1, -4, -5 and TIMP-3 in MS CNS, and highlighted a possible role for ADAMTSs in lesion development in MS (Haddock *et al.*, 2006). This present study investigated intact CSPG expression and their breakdown by ADAMTSs, via production of aggrecan and versican fragments as an indicator of enzyme activity in MS tissue. Antibodies that recognize the neoepitopes produced by cleavage at specific sites, generated by proteolysis of the aggrecan and versican by glutamyl endopeptidases such as ADAMTS-4 and -9 neoepitopes antibodies, are now commercially available, and allow identification of regions of active enzyme activity within the CNS.

Our current state of knowledge suggests that glutamyl endopeptidases (GEP-ADAMTSs) may be important in MS pathogenesis because of their site of expression and their known and potential substrate specificities. Their effects may be detrimental in terms of the CNS ECM breakdown, enabling infiltration of immune and inflammatory cells and in myelin breakdown. Alternatively, they may be beneficial by enabling neurite outgrowth and neuronal repair. This chapter describes the detailed investigation of the expression of aggrecan, versican and their neoepitopes in both normal control and MS brain tissue (active, chronic inactive, chronic active lesions and NAWM), to further elucidate the role of CSPGs in MS pathogenesis.

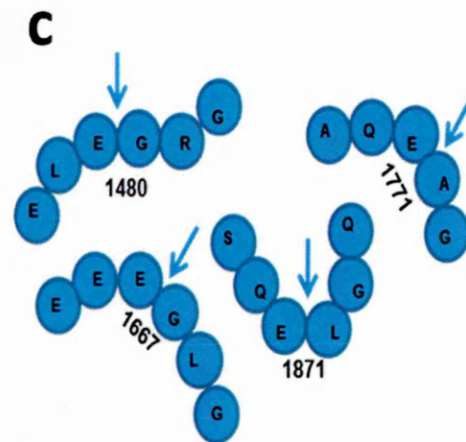
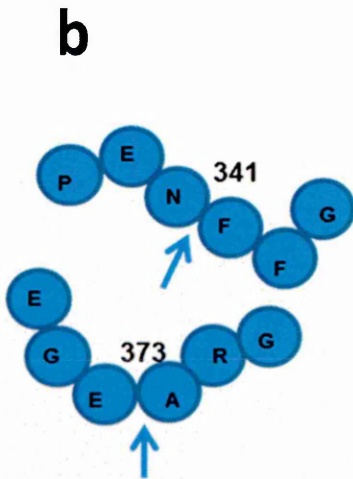
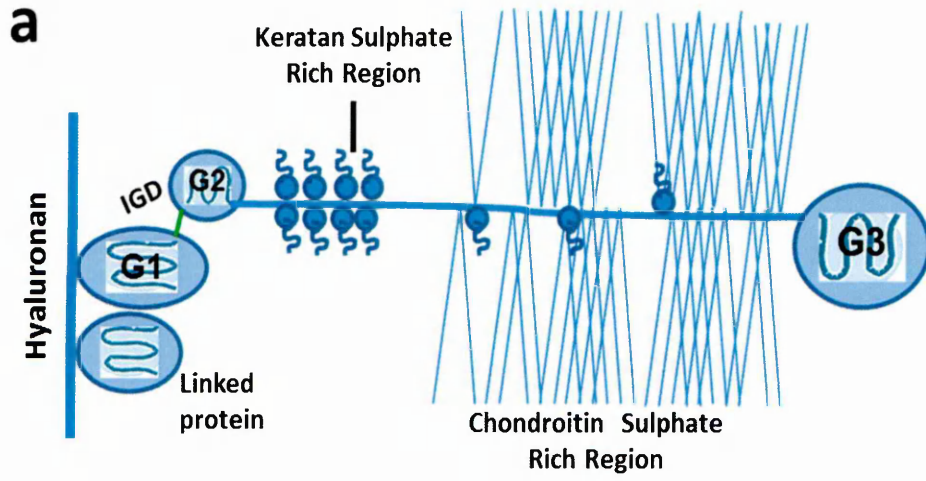
### 3.1.1 Aims of the study

The aims of this study were:

- To determine whether the expression levels of aggrecan and versican showed any differences in MS post-mortem tissue compared to normal control brain tissue using immunohistochemistry and western blotting.
- To study CSPG breakdown by ADAMTSs in *ex vivo* via the production of aggrecan and versican neoepitopes of ECM components in MS post-mortem tissue, compared to normal control brain tissue using immunohistochemistry and western blotting.

### **Figure 3-1: Aggrecan structure and ADAMTS cleavage sites**

Diagrammatic representation of aggrecan and its known cleavage sites; aggrecan has two cleavages sites located within the G1/G2 interglobular domain (IGD) (a). The Asn<sup>341</sup>-Phe<sup>342</sup> is the main MMP cleavage site, whereas the Glu<sup>373</sup>-Ala<sup>374</sup> is cleaved by aggrecanases including ADAMTS-9 (b). There are also four cleavage sites within the CSPG-rich region of aggrecan for ADAMTS-4 and ADAMTS-5; arrows indicate cleavage sites (c). Figure Adapted from Proter *et al*, (2005).



## **3.2 Results**

### **3.2.1 Tissue grading**

#### **3.2.1.1 H&E and ORO stains for the extent of inflammation and demyelination**

H&E staining was used to detect areas of inflammatory perivascular cuffs, within the brain tissue used for this study, and ORO was used to identify areas of demyelination. H&E and ORO stained sections were graded according to the extent of perivascular cuffing observed and myelin loss respectively, using a four point scale (Negative, +, ++ and +++). No inflammation or demyelination was seen in the majority of control brain tissues which were graded as negative (-). Tissue blocks graded from + through to +++ demonstrate immune cell infiltration and demyelination within MS lesions. These sections were also scored by Prof Nicola Woodroffe, following the initial scoring of the 80 blocks, scores were then compared and any results that did not match were re-assessed together to reach a consensus on the scoring. There was agreement of the scoring in > 90% of cases. The grading results for all tissue samples were further confirmed by immunohistochemistry investigations on serial sections using antibodies to HLA-DR and MOG, to demonstrate activated macrophages and loss of myelin respectively. Results of characterization of the blocks used, based on grading is illustrated in Figures (3-2) and (3-3), and are summarised in Table (3-1).

#### **3.2.1.2 HLA-DR expression for the extent of microglia activation**

Human leukocyte antigen (HLA) is expressed at the cell surface of antigen presenting cells and consists of a 34kDa (alpha) subunit and one of several 28kDa (beta) subunits, encoded by the MHC class II genes on chromosome 6 region 6p21.31 (Zephir *et al.*, 2009). The complex of HLA-DR and its ligands, peptides of 9 amino acids in length or longer, constitutes a ligand for T cell receptors (TCR). Several MHC class II genes are linked to autoimmune conditions, disease susceptibility and disease resistance. The primary function of HLA-DR is to present peptide antigen, potentially foreign in origin, to the immune system for the purpose of eliciting or suppressing T helper cell responses that eventually lead to T cell activation and production of antibodies by B cell against the same foreign peptide antigen (Racke, 2009).

CD8+ T cells use the CD8 molecules (in conjunction with their TCR) to recognize peptide MHC class I molecules HLA A, B or C in association with peptide and develop into cytotoxic T cells. CD4+ T cells develop into T<sub>h</sub>1 or T<sub>h</sub>2 cells; use the CD4 molecules to stabilize interactions with the peptide HLA-DR complex. Th17 are also differentiated from CD4+ in the presence of IL-6, TGF- $\beta$  and IL-21, they are characterised by the production of pro-inflammatory cytokines including IL-17, IL-21 and IL-23 (Christensen *et al.*, 2013). There are usually very low levels of HLA-DR expression in normal brain tissue, whereas in response to inflammatory stimuli in MS, microglia become activated and up regulate HLA-DR antigen expression (Handunnetthi *et al.*, 2010; Comabella & Khoury, 2012).

MS and control tissues used in this study were classified based on the criteria of Sobel *et al.*, (2001). In actively demyelinating lesions, HLA-DR positive cells were evenly distributed within the lesion, whereas in chronic active lesion HLA-DR positive cells were located at lesion edges rather than centrally. In chronic inactive lesions there were no HLA-DR positive cells either inside the lesion, at the edges of, or outside the demyelinating lesions. Lastly, in normal control and NAWM this was few HLA-DR positive cells. Results of human brain tissue classification according to HLA-DR immunostaining is illustrated in Figure (3-4), and summarised in Table (3-1).

### **3.2.1.3 MOG expression as a marker for the extent of demyelination**

MOG is a useful marker for classifying the type of lesion in MS based on the extent of demyelination and re-myelination (Lucchinetti *et al.*, 2005). In an active lesion, there is substantial reduction in MOG staining, whereas in chronic lesions there was no evidence of MOG staining in the centre (Sobel & Ahmed, 2001). Results of human brain tissue classification according to MOG immunostaining is illustrated in Figure (3-4), and summarised in Table (3-1).

### **3.2.2 Classification of the human brain tissue blocks**

Characterisation of the 89 blocks of MS and normal controls examined revealed 16 contained active lesions, 20 had chronic inactive lesions, 11 had chronic active lesions, 19 were NAWM, 16 were normal controls and 7 were poor structure (Table 3-1). Initially MS blocks were assessed for level of inflammation and 14 MS blocks displayed cuffs graded as (+). Control blocks also were assessed for inflammation and the

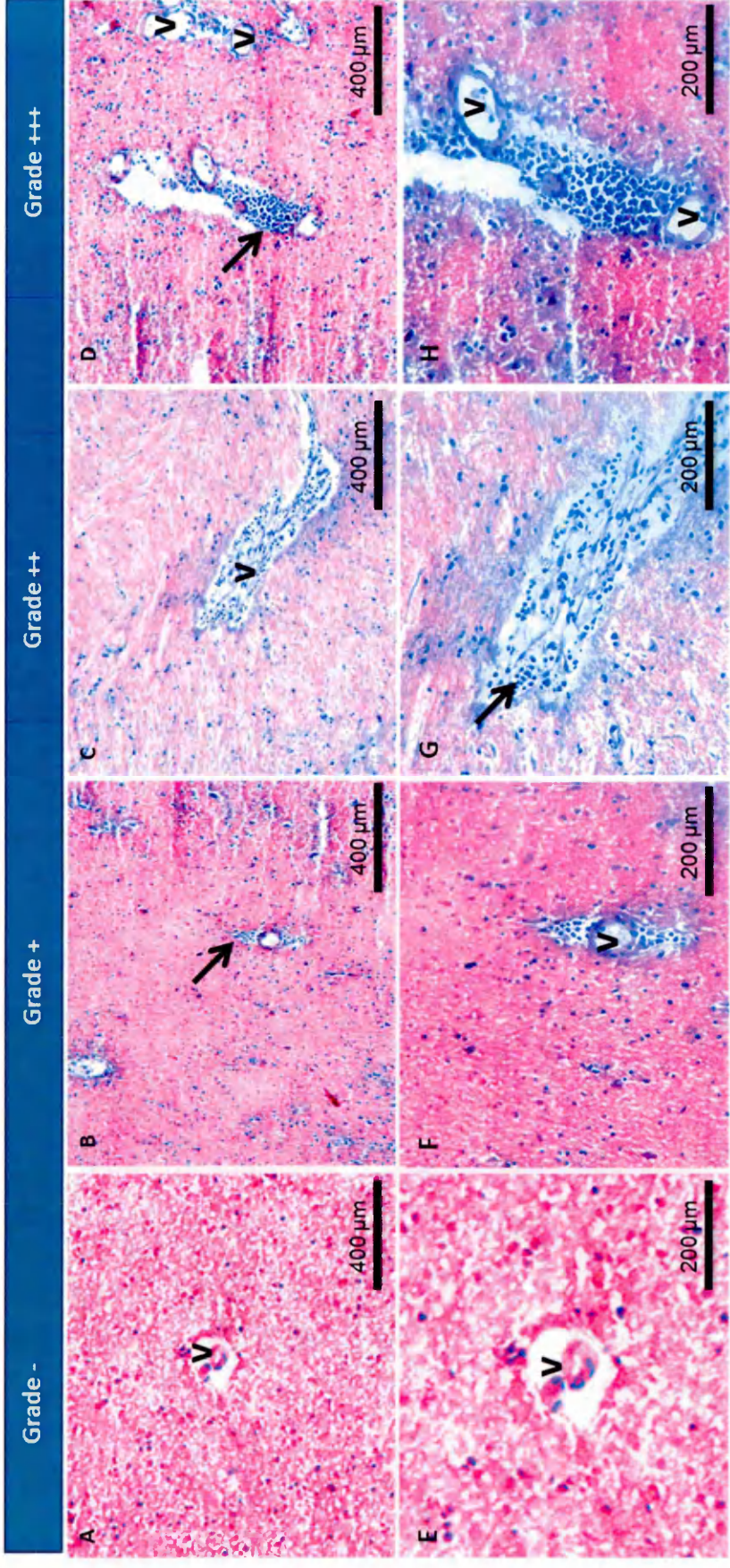
majority of blocks displayed no inflammation however 4 blocks displayed sparse perivascular lymphocytes and were graded as (+). The majority of MS tissue blocks showed varying degrees of inflammation and displayed cuffs at (++) except 9 blocks which displayed cuffs grade (+++). Figure (3-2) shows the varying degrees of inflammation (A) and (E) for normal control brain (NC014 P1E3) which shows a negative score (-), B and F were graded as there were a small numbers of cells in the perivascular region (+) and described as CAL (MS103 P1E4), D and H show (+++) H&E staining for a MS lesion with perivascular cellular infiltrate classified as an active lesions (MS092 P1E3).

All sections were stained with ORO, and the majority of tissue blocks were negative for ORO lipid-laden macrophages (Table 3-1). 9 MS blocks displayed weak ORO positive staining which was very sparse and graded as (+), while 18 blocks had one or more foci or cluster of ORO positive cells graded as (++) and were classified as active lesions. In 7 blocks however, ORO positive cells were abundant throughout the entire section graded (+++) and were also classified as active lesions (Figure 3-3).

16 blocks were classified as containing active lesions i.e. ongoing demyelination with or without ORO positive macrophages and increased HLA-DR staining in the absence of a hypo-cellular region. 11 blocks were classified as containing chronic-active lesions i.e. MOG loss entirely within the lesional centre with ORO positive macrophages and a rim of HLA-DR positive cells bordering the lesion with hyper-cellularity. 19 blocks were classified as NAWM i.e. displayed minimal inflammation, no ORO positive macrophages, normal MOG staining and resting microglia as indicating by HLA-DR staining. Figure (3-4) compares the expression of MOG and HLA-DR in NAWM and an active lesion to demonstrate the extent of demyelination and inflammation respectively.

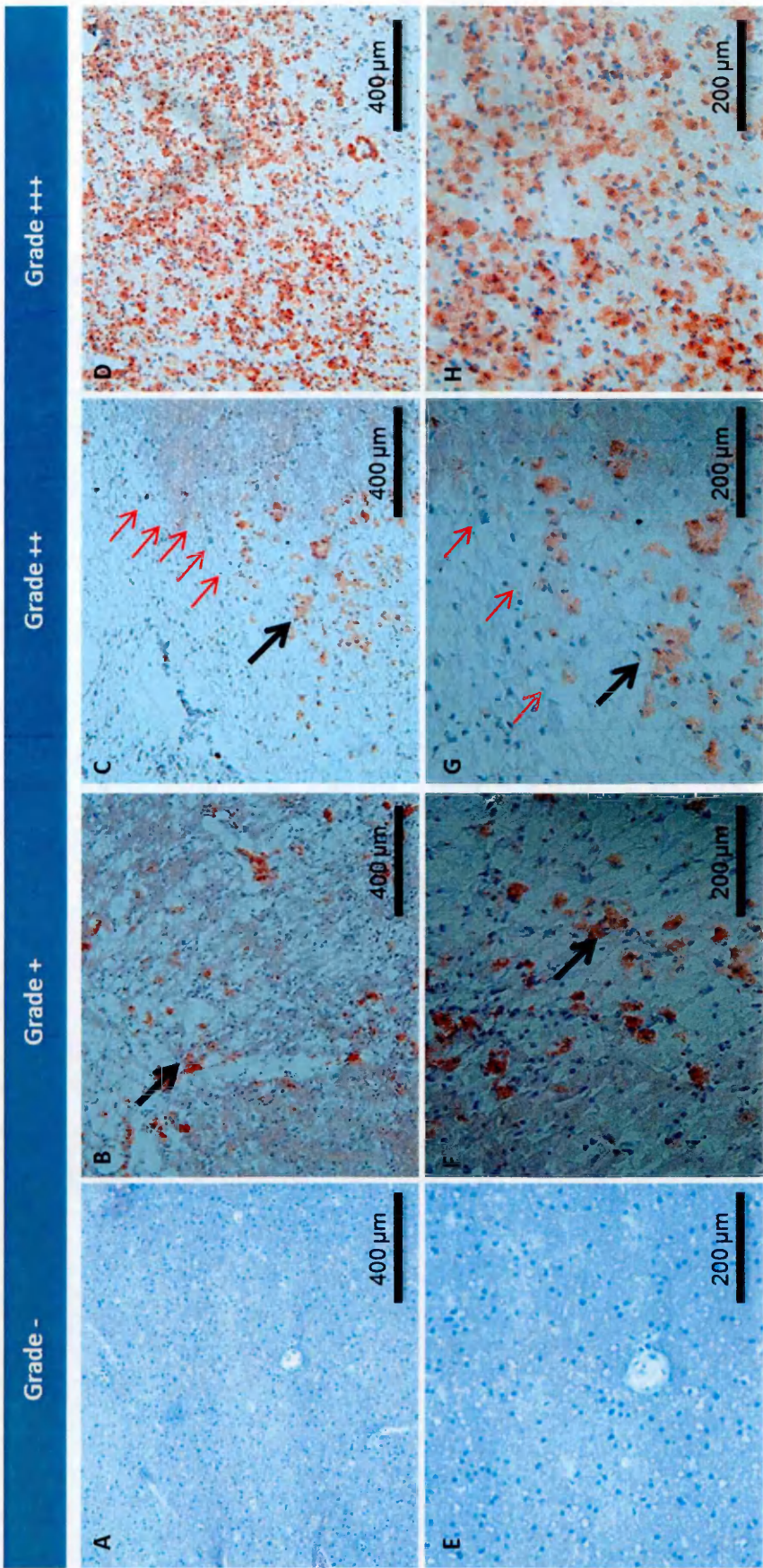
**Figure 3-2: Haematoxylin and eosin staining showing the different grades of inflammation observed in CNS MS and control white matter**

Olympus BX60 light microscope images of haematoxylin and eosin staining of frozen sections (10µm) showing different grades of inflammation observed in the CNS white matter. Control tissue (CO014 P1E3) showed no inflammation (A and E) while the majority of MS tissues showed an inflammatory burden of (+) (MS103 P1E4) (B and F), (++) (MS074 P1E2) (C and G), (+++) MS092 P1E3 (D and H). The black arrows indicate leukocytes that have breached the blood-brain barrier (BBB). The upper panel (A-D) shows a lower magnification and lower panel (E-H) shows a higher magnification of the same region. V=Vessel.



**Figure 3-3: ORO staining showing the different grades of lipid-laden macrophages in white matter CNS tissue**

Olympus BX60 light microscope images of Oil red O (ORO) staining showing the different grades of myelin breakdown in the activated lipid-laden macrophages in the CNS white matter. Nuclei were counterstained with haematoxylin (dark blue). Control tissue (CO014 P2D2) showed ORO negative staining (A and E), while some MS tissues sections showed a few ORO positive cells graded as + (MS050 P2C2) (B and F), ++ (MS081 P2C2) (C and G), +++ (MS074 P2D2) (D and H). Black arrows show lipid-laden macrophages with internalised myelin while red arrows indicate the plaque/lesion border. The upper panel (A-D) shows a lower magnification and lower panel (E-H) shows a higher magnification of the same region.



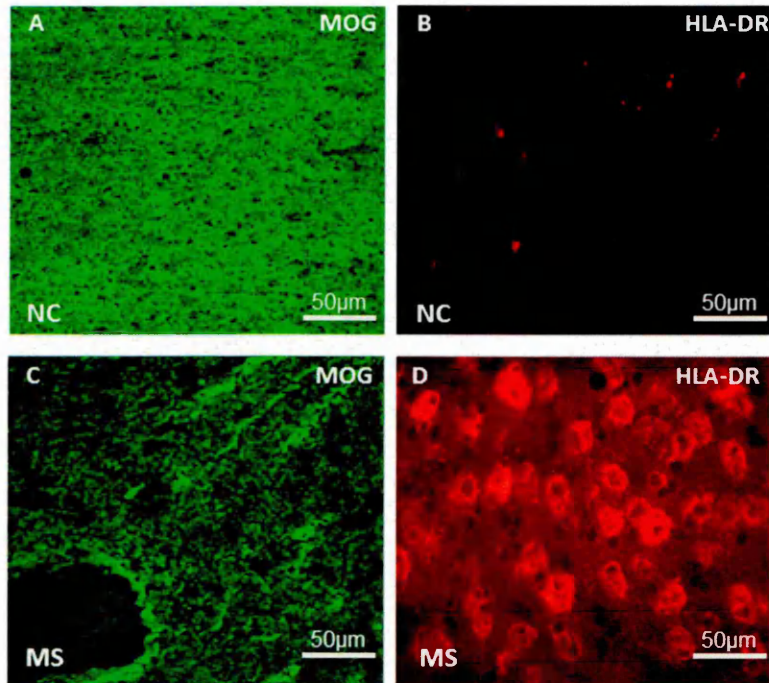


**Figure 3-4: MOG and HLA-DR expression in normal control (NC) and active MS lesion brain tissue**

Expression of MOG and HLA-DR assessed by IHC in NC and MS active lesion tissue to determine the extent of demyelination and inflammation respectively. (A-B) Normal control (CO037 A1B3) showed uniform expression of MOG and small numbers of evenly distributed HLA-DR+ cells respectively, whereas (C-D) active lesion (MS051 A1B3) shows disrupted MOG staining and positive HLA-DR immunoreactivity on abundant activated macrophages.

**Table 3-1: Human CNS tissue classification of MS and control blocks based on immunohistochemical studies used in this study**

Case No	Region	H+E	ORO	HLA-DR	MOG	Classification of lesion
MS049	A1B6	-	-	Mostly resting microglia	Negative in lesion	CL
	A1D6	-	-	Resting microglia	Normal	NAWM
MS050	P2C2	-	+	Resting microglia	Normal	CL
	P7C3	-	-	Resting microglia	Normal	NAWM
MS051	A1B3	++	++	Activated rounded up microglia	Disrupted in lesion	Small region AL, most of block is GM.
	P5C6	++	++	Mostly resting microglia, with small area of activated microglia at border	Negative in lesion	Small area is CAL
MS057	P4C1	++	++	Mostly resting microglia, some rounded up microglia	Disrupted in lesion	Small region AL, Most of block is GM.
	A2A3	-	-	Resting microglia	Normal	NAWM
MS058	A4E3	++	++	Mostly resting, some rounded up microglia	Disrupted	very small AL
	P1C1	+++	+++	Activated rounded up microglia	Disrupted	AL
	A2D2	+	-	Resting microglia	Negative in lesion	Small area CL, Mostly GM
	A2A4	--	--	--	--	Poor structure
MS060	A2F5	+	-	Resting microglia	Negative in lesion	CL
	A2E5	+	-	Resting microglia	Negative in lesion	CL
	A4D4	-	-	Resting microglia	Normal	NAWM
MS062	P1C3	+++	++	Activated rounded up microglia	Disrupted in lesion	AL
	P5D5	++	++	Activated rounded microglia and flattened in lesion	Negative in lesion	CAL
	A2C2	++	+	Resting microglia	Negative in lesion	CL
	A4C3	-	-	Resting microglia	Normal	NAWM
MS074	P1E2	++	++	Activated rounded up microglia	Disrupted	AL
	P2D2	+++	+++	Activated rounded up microglia	Disrupted	AL
	A5B5	+	-	Resting microglia	Normal	NAWM
	A4B6	-	-	Not clear	Not clear	Poor structure
MS076	P5B6	+	+	Resting microglia	Negative in lesion	CL
	A1B3	-	-	Resting microglia	Normal	NAWM
	P2A4	++	++	Activated rounded microglia at border	Negative in lesion	CAL

**Table 3-1: (Continued) Human CNS tissue classification of MS and control blocks based on immunohistochemical studies used in this study**

Case No	Region	H+E	ORO	HLA-DR	MOG	Classification of lesion
MS079	P2D2	+	+/-	Resting microglia	Negative in lesion	CL
	P3E4	+	+ /BV	Resting microglia	Negative in lesion	CL, Mainly GM
	P4B4	++	++	Activated rounded microglia	Disrupted	AL
MS080	P2B2	+++	++	Activated rounded microglia at border	Disrupted	AL
	P7C3	++	++	Activated rounded microglia	Negative in lesion	CAL
	A2C2	-	-	Resting microglia	Normal	NAWM, Mostly GM
MS081	A2B3	+	-	Resting microglia	Negative in lesion	CL
	P5C3	++	++	Activated rounded microglia	Disrupted in lesion	Very small AL, Mostly GM
	P2C2	++	++	Activated rounded microglia, flattened within lesion center	Negative in lesion	CAL.
	A4D4	++	++	Activated rounded microglia	Disrupted in lesion	Mainly AL, Mostly GM
MS090	P4C3	++	-/+	Resting microglia	Negative in lesion	CL
	P3D3	+++	++	Activated rounded up microglia	Disrupted in lesion	AL
	P3E3	++	++	Activated rounded up microglia	Disrupted in lesion	AL
	P1B4	+	-/+	Resting microglia	Negative in lesion	CL
MS092	P1E3	+++	+++	Activated rounded microglia	Disrupted in lesion	AL
	P4B3	-	-	Resting microglia	Normal	NAWM
MS094	P2C4	+	-	Resting microglia	Negative in lesion	Mainly CL, Mostly GM
	P3C7	++	-	Resting microglia	Negative in lesion	CL
	P4C2	-	-	Resting microglia	Normal	NAWM
MS100	P5D3	++	+++	Activated rounded up microglia at border	Negative in lesion	CAL
	A4C2	+	-	Resting microglia	Normal	NAWM
MS102	P5C6	+	-	Resting microglia	Negative in lesion	CL
	A2C5	-	-	Resting microglia	Normal	NAWM
MS103	P1E4	+	++	Mostly resting, with small area of activated microglia at border	ND	CAL
	P3C4	-	-	Resting microglia	Normal	NAWM, Mostly GM
MS104	P1B3	-	-	ND	ND	Poor structure
	P3E2	-	-	ND	ND	Poor structure
	P1E1	-	-	ND	ND	Poor structure
	P3E3	-	-	ND	ND	Poor structure
MS105	P1D3	-	-	Resting microglia	Normal	NAWM
	A4B3	-	-	Resting microglia	Normal	NAWM

**Table 3-1: (Continued) Human CNS tissue classification of MS and control blocks based on immunohistochemical studies used in this study**

Case No	Region	H+E	ORO	HLA-DR	MOG	Classification of lesion
MS106	P6D1	+	+	Resting microglia	Negative in lesion	CL
	P4B3	+++	++	Activated rounded microglia at border	Negative in lesion	CAL
	A2D1	++	-/+	Resting microglia	Negative in lesion	CL Hyper cellular at border
MS107	P2E2	-	-	ND	ND	Poor structure
	P5C7	-	-	Resting microglia	Normal	NAWM
MS121	P5B2	+++	+++	Activated rounded microglia	Disrupted	AL
MS122	A5B3	++	++	Activated rounded microglia, flattened within lesion centre	Negative in lesion	CAL.
	P5B7	++	++	Activated rounded microglia, flattened within lesion centre	Negative in lesion	CAL.
	A2E3	-	-	Resting microglia	Normal	NAWM
MS126	P4D2	-	-	Resting microglia	Normal	NAWM
	P5B3	-	-	Resting microglia	Normal	NAWM
MS153	P1C3	++	+	Activated rounded microglia and flattened in lesion	Negative in lesion	CAL
MS154	A2E6		-	Resting microglia	Negative in lesion	CL
	P3D5	+	-	Resting microglia	Negative in lesion	CL
MS160	P5A1	+++	+++	Activated rounded up microglia	Disrupted	AL
	A2D2	++	-	Resting microglia	Negative in lesion	CL
CO014	P1E3	-	-	Resting microglia	Normal	NAWM
	P2D2	-	-	Resting microglia	Normal	NAWM
CO022	P3D3	-	-	Resting microglia	Normal	NAWM
	P4C3	-	-	Resting microglia	Normal	NAWM
CO025	A4D4	+	-	Resting microglia	Normal	NAWM
	P3D4	-	-	Resting microglia	Normal	NAWM
CO026	A2D2	-	-	Resting microglia	Normal	NAWM
	P1A2	-	-	Resting microglia	Normal	NAWM
	P2A1	-	-	Resting microglia	Normal	NAWM
CO032	P5A2	-	-	Resting microglia	Normal	NAWM
	P1A1	-	-	Resting microglia	Normal	NAWM
CO036	P2A3	+	-	Resting microglia	Normal	NAWM
	P5A5	-	-	Resting microglia	Normal	NAWM
CO037	A1B3	+	-	Resting microglia	Normal	NAWM
	P5B2	+	-	Resting microglia	Normal	NAWM
CO039	A4B5	-	-	Resting microglia	Normal	NAWM

### 3.2.2.1 Immunohistochemical analysis of aggrecan and aggrecan

#### neoepitope expression in MS and control CNS tissue

Aggrecan and aggrecan neoepitope immunoreactivity were consistently demonstrated in normal control and MS tissue sections. Intense immunoreactivity for aggrecan and its neoepitope were seen in both active and chronic active lesions of MS tissue blocks as compared to NAWM, CLs and normal control white matter. In this study the expression of MOG in human brain tissue was used to determine the extent of demyelination. Omission of primary antibodies resulted in negative staining for all samples for aggrecan and its fragments indicating specificity of the antibodies used. Aggrecan and its neoepitope immunoreactivity were detected in 54 blocks of MS (44) and normal control (10). Aggrecan and its neoepitope immunostaining appeared heterogeneous in distribution both between samples and within the same section dependent on the contribution of AL, CL and CAL within the MS blocks.

Strong aggrecan immunoreactivity was observed in active lesions with ongoing demyelination and was associated with areas of activated microglia. Figure 3-5 shows normal control and NAWM with a uniform pattern of expression of MOG indicating intact myelin, low level of HLA-DR+ cells in areas where there was decreased expression of aggrecan and aggrecan neoepitope. In contrast, strong aggrecan and aggrecan neoepitope immunoreactivity were observed in areas of active lesions, assessed by increased HLA-DR expression, and the presence of myelin breakdown with ongoing demyelination evidenced by lack of MOG staining. Expression of aggrecan and its neoepitope within regions of interest on individual sections was quantified by Image J software on immunohistochemical staining for aggrecan and its neoepitope in control, NAWM and active lesion. As shown in Figure (3-5, d) much greater expression of aggrecan and aggrecan neoepitope in active lesions compared to NAWM and normal controls. Data are represented as the mean (control white matter, n=10; MS NAWM, n=10; MS active lesion, n=10)  $\pm$  SEM. A statistically significant differences between control white matter, MS NAWM and MS lesional tissue are indicated by asterisks (\*P< 0.05, \*\*P<0.01, \*\*\*P<0.001) (Kruskal-Wallis test) (Figure 3-5, d).

In chronic active lesions, aggrecan and its neoepitope expression was either weakly expressed or absent in areas of complete myelin loss and in the absence of microglia,

with strongest immunoreactivity observed in areas with thinning myelin and activated microglia at the lesion edge (Figure 3-6). In contrast, in chronic inactive lesions, aggrecan and its neopeptide expression was weak or absent in areas of complete myelin loss as well as in areas with thinning myelin and activated microglia (Figure 3-6). Image J software analysis of the level of aggrecan protein density from each region of CAL, CL, NAWM and NC showed much greater expression of aggrecan in active lesions compared to chronic lesions, NAWM and normal control brain tissue. Data represented as mean  $\pm$  SEM (10 blocks each CL and CAL).

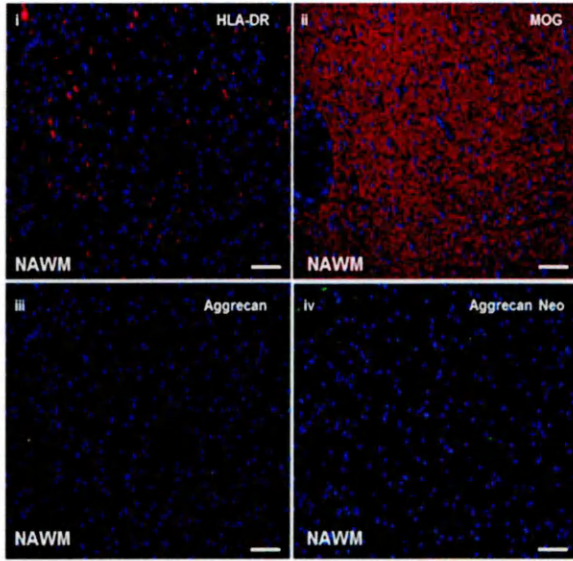
### **3.2.2.2 Western blot analysis of aggrecan and aggrecan neopeptide expression in MS and control tissue**

Following initial optimisation, SDS-PAGE was performed with 20 $\mu$ g protein/well before transferring separated proteins onto nitrocellulose membrane. Western blotting demonstrated that aggrecan and its neopeptide were present in all samples of MS active, NAWM and normal control brain tissue studied. Immunoblotting for  $\beta$ -actin (42kDa) was used as a reference protein. Two bands of 250 kDa and 70 kDa were observed for aggrecan and aggrecan neopeptide respectively, with the relevant antibodies. Figure 3-7 shows the variation in aggrecan and its neopeptide expression for all MS and normal brain samples examined, as determined by densitometry. Although expression was variable, overall there was a significant increase in aggrecan and aggrecan neopeptide expression in active lesions compared to NAWM and normal brain samples (\*\* $P < 0.001$ ,  $n=7$ ). Increase in levels of these proteins was due to increases in both the 250 kDa and 70 kDa bands. Densitometric analysis values are expressed as the density ratio of target (aggrecan or aggrecan neopeptide) to loading  $\beta$ -actin in arbitrary units for aggrecan and its fragment in control white matter, MS NAWM and MS active lesional brain tissue. As shown in figure 3-7, there was much greater expression of aggrecan and its neopeptide in active lesions compared to NAWM and normal control brain. Data was represented as the mean  $\pm$  SEM using Kruskal-Wallis analysis.

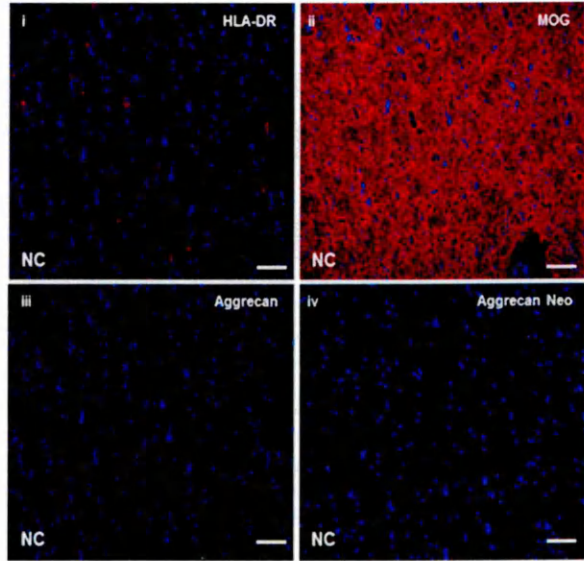
**Figure 3-5: Comparison of expression of aggrecan and its neoepitope between MS and control brain tissue by IHC**

Single and dual staining immunofluorescence microscopy of serial tissue sections stained with DAPI (blue) demonstrated cell nuclei, aggrecan and aggrecan neoepitope (green), MOG (red) and HLA-DR (red). Low levels of HLA-DR were observed in NAWM (MS094 P4C2) and normal control (NC022 P4C2) (a, i) and (b, i) respectively. Low levels of aggrecan and its neoepitope expression are seen in the same blocks as (a, iii) and (b, iii) respectively. In comparison to the active lesion (MS057 P4C1) (c, iii) showed high levels of these proteins in ongoing demyelination along with activated microglia (c, i) and (c, ii) respectively. Image J software analysis shows expression of aggrecan and its neoepitope in NC, NAWM and AL brain tissue (d). There is a greater expression of aggrecan and its neoepitope in the active lesion compared to NAWM and NC. Data represented as mean  $\pm$  SEM using Kruskal-Wallis, n=10, five readings for each region for each section (\*\*P<0.01, \*\*\*P<0.001, n=10). Scale bar 100 $\mu$ m

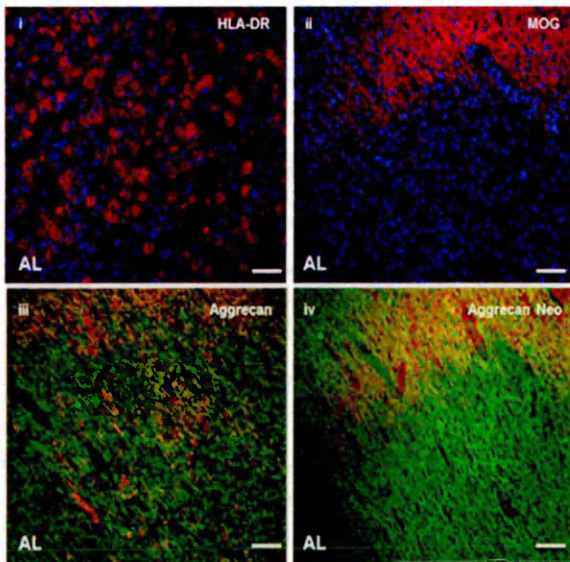
a



b



c



d

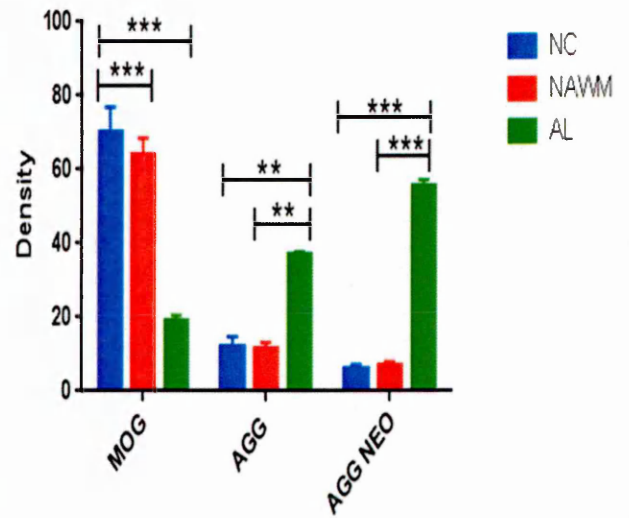


### **Figure 3-6: Expression of aggrecan and its neoepitope in CAL and CL brain tissue by IHC**

Immunofluorescence microscopy of serial tissue sections stained with DAPI (blue) demonstrated cell nuclei, aggrecan and aggrecan neoepitope (green), MOG (red) and HLA-DR (red). Low levels of HLA-DR were observed in areas of intact myelin in both CAL (MS051 P5C6) and CL (MS102 P5C6) (a, i) and (b, i) respectively. High levels of aggrecan and its neoepitope are present at the lesion edge in CAL (a; iii, iv) compared to CL (b; iii, iv). Areas of complete myelin loss were associated with absence of both microglia evidenced by HLA-DR and loss of aggrecan and aggrecan neoepitope in both CAL and CL. An abundance of aggrecan and aggrecan neoepitope are present at the lesion border in ongoing demyelination in CAL compared to the CL border. Low levels of aggrecan and its neoepitope at the lesional centre in both CAL and CL are associated with low levels of HLA-DR staining and absence entirely of MOG. Data is presented as Mean  $\pm$  SEM using Kruskal-Wallis, n= 10, five readings for each region for each section (c and d). Scale bar 100 $\mu$ m

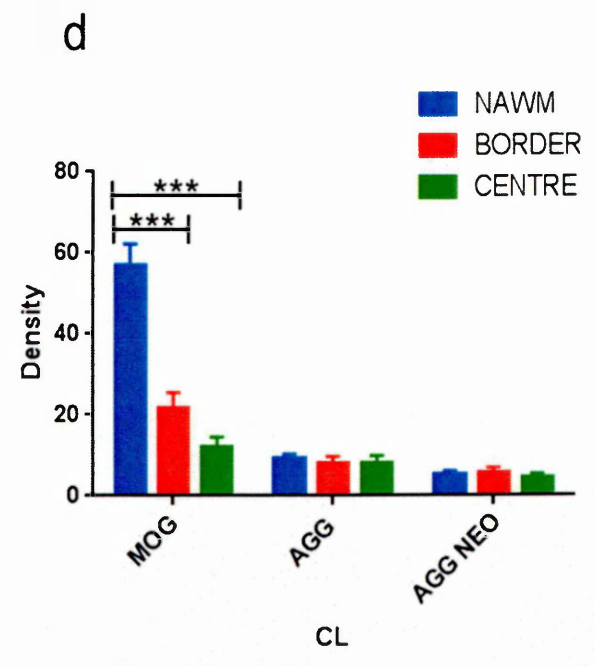
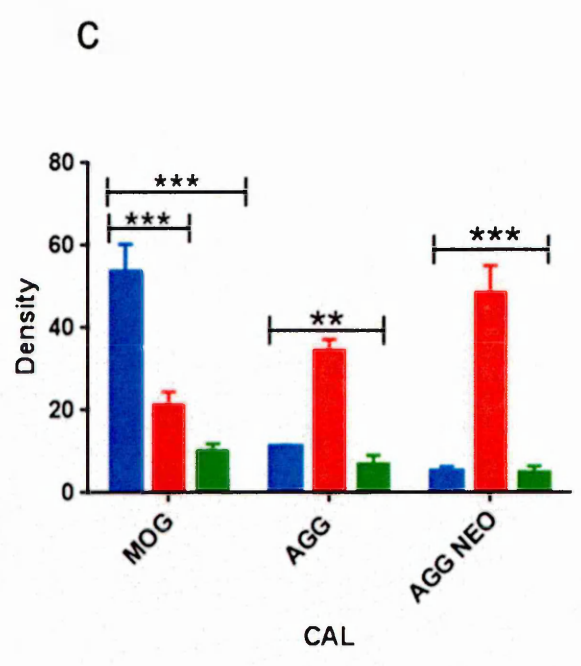
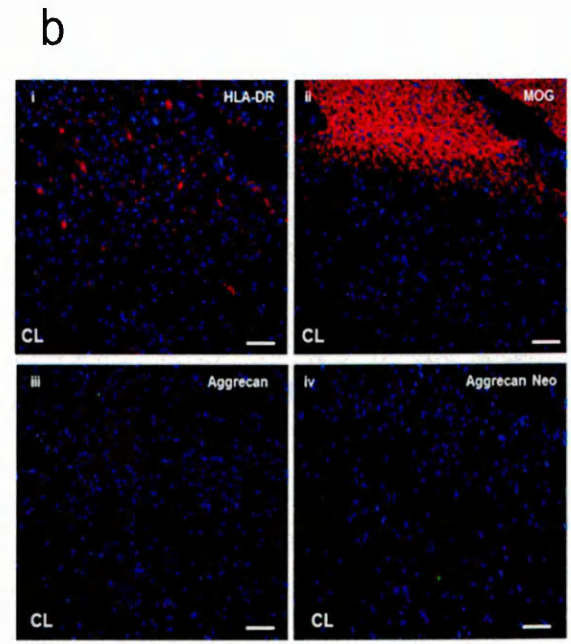
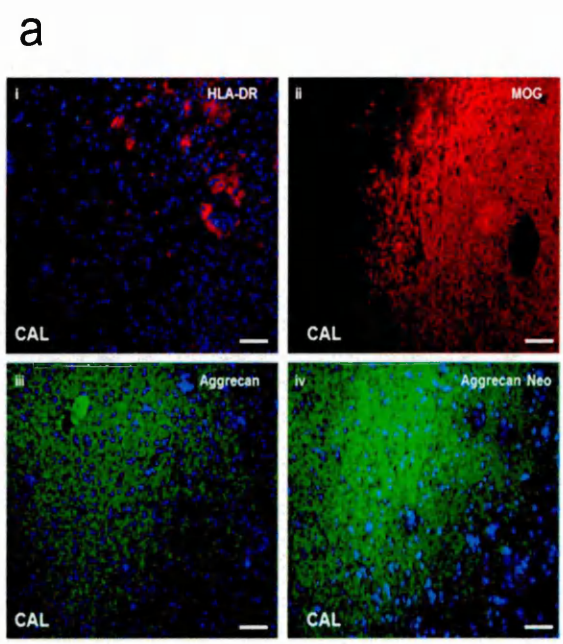
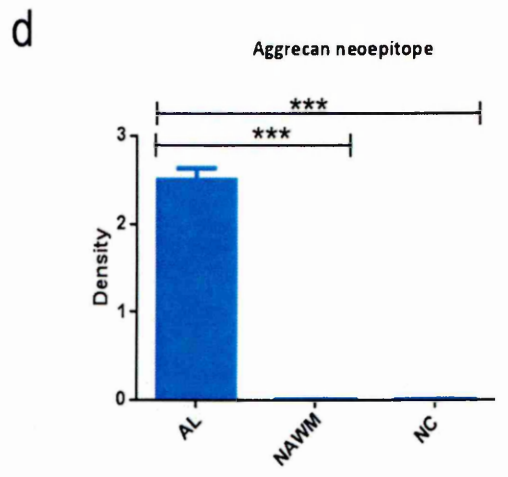
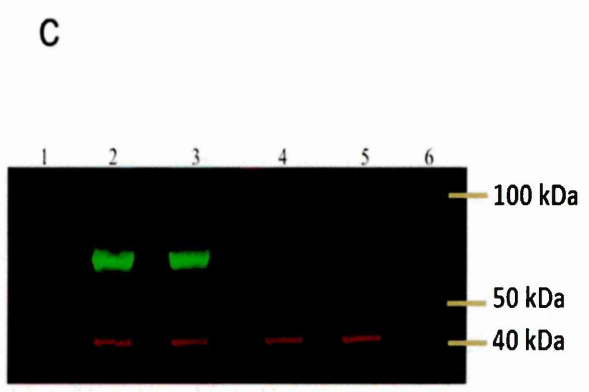
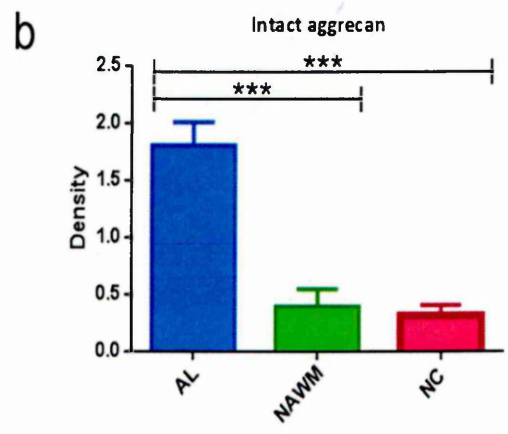
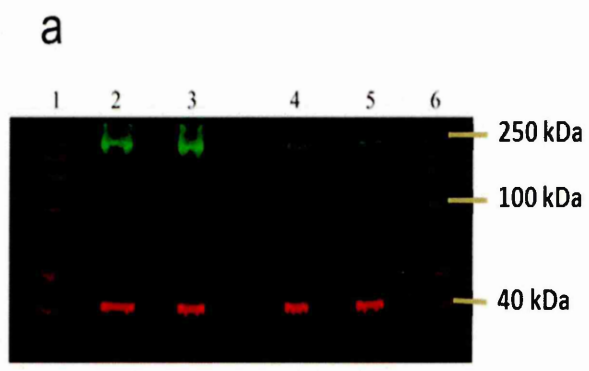


**Figure 3-7: Western blotting analysis of expression of aggrecan and its neoepitope in MS and control brain tissue**

Western blot of aggrecan (green), its neoepitope (green) and  $\beta$ -actin (red) from an active MS lesion (MS090 P3D3)( lanes 2, 3); control white matter (NC022 P3D3)( lane 4) and MS NAWM (MS103 P3C4)( lane 5). (Lane 1 and 6) represent standard molecular weight markers (40-300kDa) (Thermo Scientific, UK). (a) and (c) demonstrate expression of aggrecan (MW 250kDa) and aggrecan neoepitope (MW 70kDa) respectively in an active lesion, normal control and normal appearing white matter. Densitometric quantification shows much greater expression of aggrecan and its neoepitope in AL compared to NC and MS NAWM using Kruskal-Wallis (\*\*\*) $P < 0.001$ ,  $n = 7$  blocks) (b) and (d).



### **3.2.3 Expression of versican isoforms and versican neoepitope in human brain tissue**

#### **3.2.3.1 Immunohistochemical analysis of versican and versican neoepitope expression in MS and control tissue**

Intact versican and its fragment were identified using antibodies raised in rabbit; the immunogen for the neoepitope was a synthetic peptide corresponding to residue Glu<sup>405</sup>-Glu<sup>406</sup> which is a product of cleavage of versican V0/V2 generated by ADAMTSs. Intense immunoreactivity for both versican and the neoepitope was seen in active lesions of MS tissue blocks, as compared to NAWM, MS CL and control white matter tissue. Strong versican and neoepitope immunoreactivity was observed in active lesions with ongoing demyelination, evidenced by thinning of the myelin sheath, shown by disrupted MOG staining, and associated with areas of activated HLA-DR foamy macrophages/microglia. Figure (3-8, a) shows a normal control tissue (CO37 P5B2) with a uniform pattern of expression of MOG. Figure (3-8, c) lesional MS tissue (MS121 P5B2) shows loss and disruption of MOG. Loss of MOG staining was found in areas where there was increased expression of versican neoepitope, indicative of increased ADAMTS activity in lesional MS tissue (Figure 3-8, d).

MOG staining was absent within lesion centres and there was loss of ECM staining for versican, with dense intra-cytoplasmic granular staining in foamy macrophages. NAWM from MS blocks showed weak versican and versican neoepitope immunoreactivity, MOG staining was intact and normal in these cases. In chronic active lesions an increased gradient of versican immunoreactivity was observed starting at the inner edge of the hypercellular rim surrounding the hypocellular centre (Fig 3-9, a). There was less staining in chronic inactive lesions, although there was still an elevated expression compared to areas of NAWM (Figure 3-9, b). Furthermore, immunohistochemical analysis of versican and its neoepitope expression indicated much greater expression of versican isoforms (V0, V1 and V3) in active lesions compared to chronic and NAWM (Figure 3-9, c). Data represented as mean  $\pm$  SEM (10 blocks each CL and CAL). Statistically significant difference between control white matter, MS NAWM and MS AL tissue are marked by asterisks (\*\*\*) $P < 0.001$  using Kruskal-Wallis.

### 3.2.3.2 Western blot analysis of aggrecan and aggrecan neoepitope expression in MS and control CNS tissue

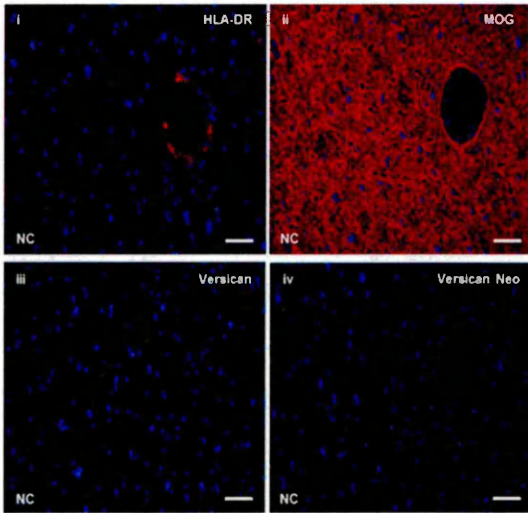
Western blotting analysis demonstrated that versican and its neoepitope were present in all samples of MS and normal control brain tissue studied. The versican antibody produced a triplet of bands at 300, 270 and 180 kDa. Figure (3-10, a) shows the variation in versican isoform expression for all the MS and normal brain samples examined (n=7), as determined by densitometry. Though expression was variable, overall there was a significant increase in versican isoform (V0, V1 and V2) expression in the MS active lesions compared to the NAWM and normal control brain samples. Increases in versican isoforms was due to increase in the 300, 270 and 180 kDa bands Figure (3-10, c).

Versican neoepitope bands at 64kDa represent the neoepitope sequence generated by the aggrecanase-mediated cleavage for versican V0/V2 in human samples (Westling *et al.*, 2004). This study was to determine whether lesional MS differed from NAWM and NC tissues in their ADAMTSs activity as determined by the presence of versican (V0/V2) neoepitopes by western blotting. Figure (3-10, b) shows that the expected 64kDa versican (V0/V2) neoepitope fragment (Westling *et al.*, 2004) is present and densitometric analysis values are expressed as the density ratio of target (versican neoepitope) to loading  $\beta$ -actin in arbitrary units for versican neoepitope and control white matter, MS NAWM and MS active lesional brain tissue. Much greater expression of versican neoepitope in active lesions is seen compared to NAWM and normal control (Figure 3-10, d). Data was represented as the mean  $\pm$  SEM using Kruskal-Wallis test (\*\*\*) $P < 0.001$ .

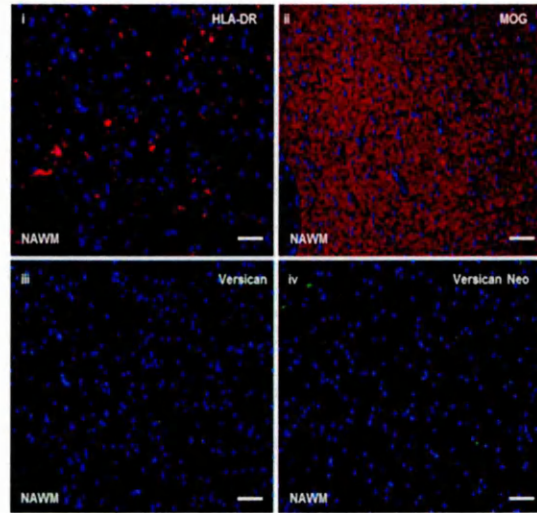
**Figure 3-8: Comparison of expression of versican and its neoepitope between MS and control brain tissue by IHC**

Single and dual staining immunofluorescence microscopy of serial tissue sections stained with DAPI (blue) demonstrating cell nuclei, versican and versican neoepitope (green), MOG (red) and HLA-DR (red). Low levels of HLA-DR were observed in normal control (NC037 P5B2) and NAWM (MS126 P5B3) (a, i) and (b, i) respectively. Low levels of versican and its neoepitope expression in the same blocks (a; ii, iii) and (b; ii, iii) is shown. In comparison to active lesion (MS121 P5B2) (c; ii, iii, iv), which shows high levels of versican and versican neoepitope in areas of ongoing demyelination along with activated microglia (c, i) and (c, ii) respectively. Image J software analysis shows expression of these proteins in NC, NAWM and AL brain tissue. There is a much greater expression of versican and its neoepitope in active lesions compared to NAWM and NC. Data represented as Mean  $\pm$  SEM using Kruskal-Wallis, n= 10, five readings for each region for each section (\*\*\*P<0.001). Scale bar 100 $\mu$ m

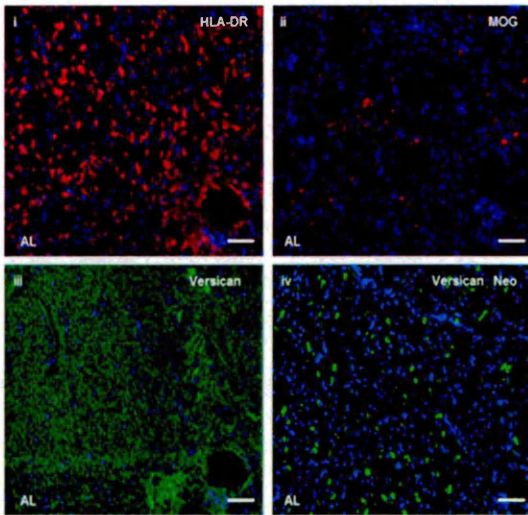
a



b



c



d

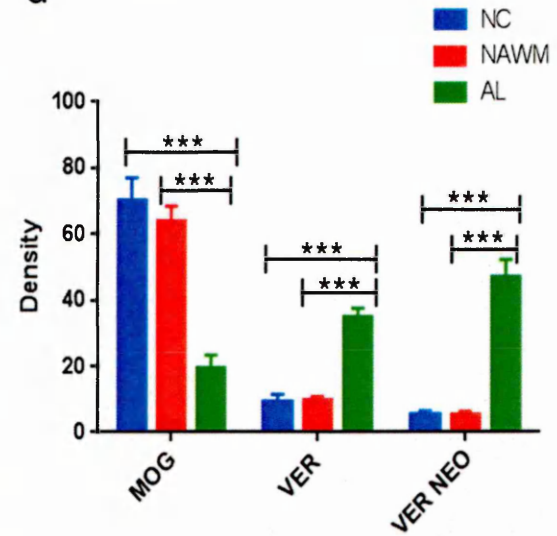


**Figure 3-9: Expression of versican and its neopeptide in CAL and CL MS brain tissue by IHC**

Immunofluorescence microscopy of serial tissue sections stained with DAPI (blue) demonstrated cell nuclei, versican and versican neopeptide (green), MOG (red) and HLA-DR (red). Low levels of HLA-DR staining were observed in areas of intact myelin in both CAL (MS050 P2C2) and CL (MS081 P2C2) (a, i) and (b, i) respectively. High levels of versican and its neopeptide at the lesion edge in CAL (a; iii, iv) compared to CL (b; iii, iv). Areas of complete MOG loss were associated with absence of both microglia evidenced by HLA-DR and loss of versican and versican neopeptide in both CAL and CL. Abundance of versican and versican neopeptide are present at the lesion border in ongoing demyelination in CAL compared to the chronic border lesion. Low levels of versican and its neopeptide are observed at the lesion centre in both CAL and CL, associated with low levels of HLA-DR staining and absence entirely of MOG. Data represented as Mean  $\pm$  SEM using Kruskal-Wallis, n= 10, five readings for each regions for each section (c and d). Scale bar 100 $\mu$ m

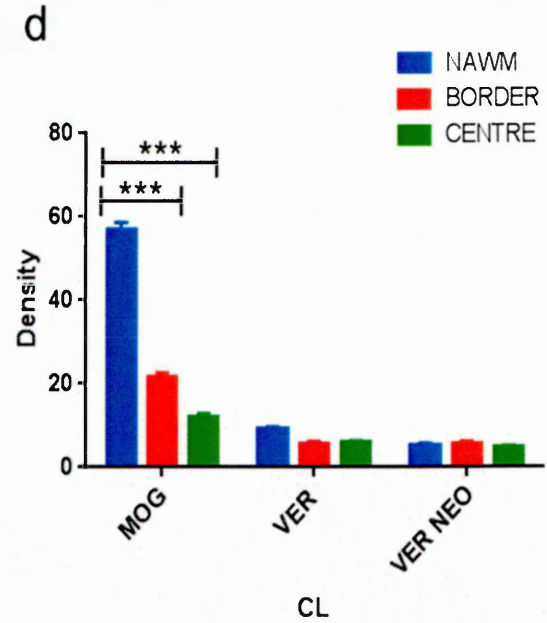
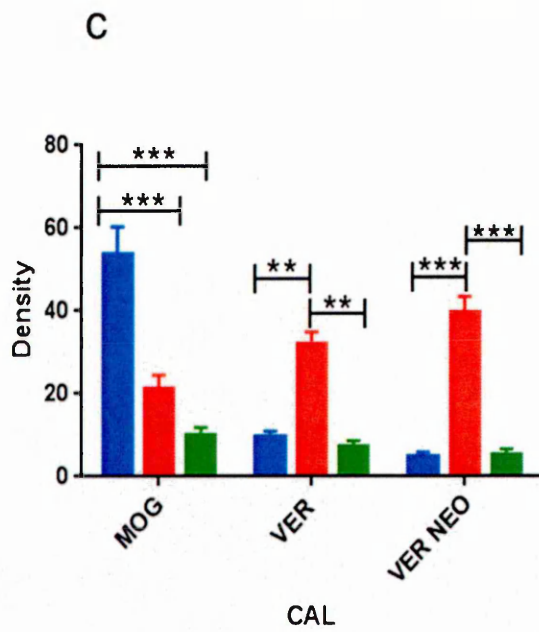
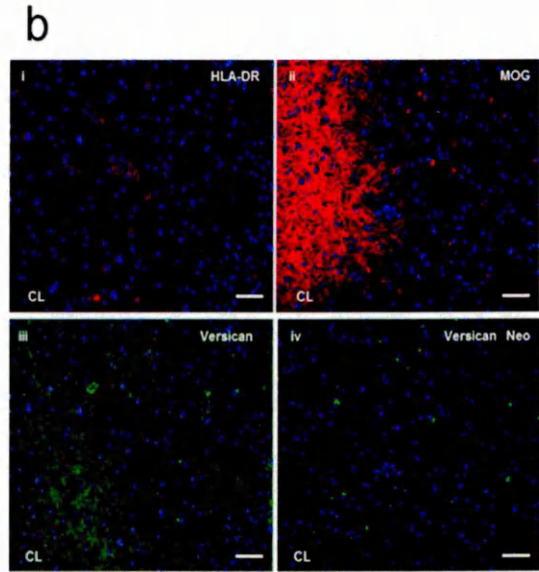
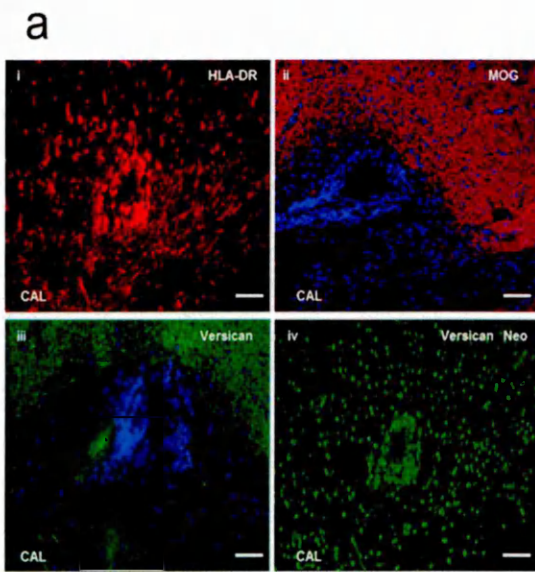


**Figure 3-10: Western blotting analysis of expression of versican isoforms and its neopeptide in MS and control brain tissue**

Western blot of versican isoforms and versican neopeptide (green) and  $\beta$ -actin (red) from an active MS lesion (MS090 P3D3) (lanes 2, 3); control white matter (NC022 P3D3) (lane 4) and MS NAWM (MS103 P3C4) (lane 5). (Lane 1 and 6) represent standard molecular weight markers (40-300KDa) (Thermo Scientific, UK). (a) and (c) demonstrated expression of versican isoforms (V0, V1 and V2) and versican neopeptide respectively in active lesion, normal control and normal appearing white matter. Densitometric quantification shows much greater expression of versican isoforms and its neopeptide in AL compared to NC and MS NAWM using Kruskal-Wallis, Mann Whitney (\*\*\*) $P < 0.001$ ,  $n = 7$  blocks) (b) and (d).

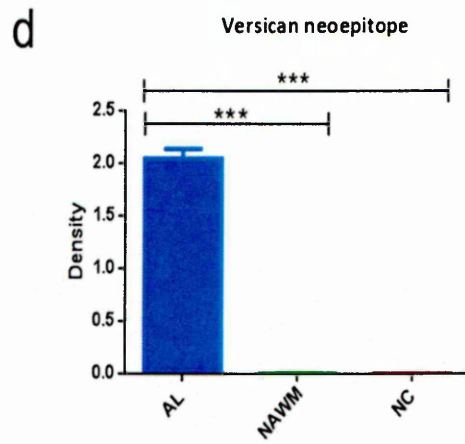
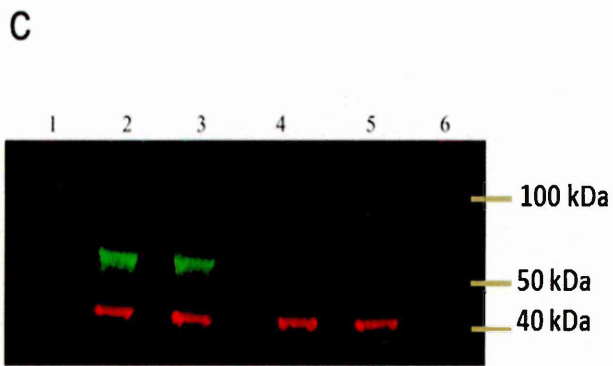
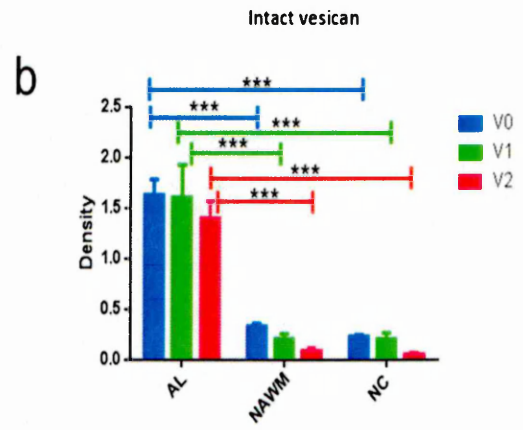
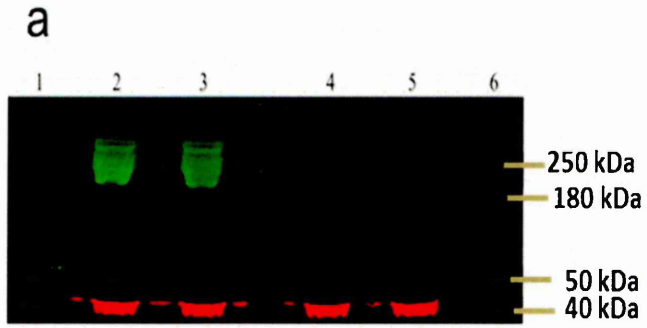


Table 3-2: Summary of extracellular matrix proteoglycan immunohistochemistry

CSPGs and its fragments	Normal control	MS NAWM	MS AL	MS CAL plaque edge	MS CAL plaque centre	MS CL plaque edge	MS CL plaque centre
Aggrecan	+	+	↑	↑	↓	↓	↓
Aggrecan Neo	+	+	↑	↑	↓	↓	↓
Versican	+	+	↑	↑	↓	↓	↓
Versican Neo	+	+	↑ Granular ECM aggregates	↑ Granular ECM aggregates	↓	↓	↓

+ = Normal positive staining; ↓ = loss of staining; ↑ = greater than normal staining

### 3.3 Discussion

Aggrecan and versican, two major components of the ECM in the CNS are widely expressed throughout the developing and adult CNS and have a role in guiding or limiting neurite outgrowth and cell migration (Sandy *et al.*, 2001; Sharma *et al.*, 2012). Alteration in the synthesis or breakdown of the ECM may contribute to disease processes (Asher *et al.*, 2001; Smith *et al.*, 2005). Thus, ADAMTS-mediated cleavage of CSPGs aggrecan and versican in CNS ECM, via their glutamyl endopeptidase activity, could have a role in normal turnover and ECM breakdown in MS (Westling *et al.*, 2004). To investigate this, here we demonstrated CSPG breakdown by ADAMTSs via production of aggrecan and versican neoepitopes as an indicator of enzyme activity. The objective in this project was to study CSPG protein expression and their breakdown by ADAMTSs *ex vivo* via the production of aggrecan and versican neoepitopes of ECM components in brain tissue. This was done by immunohistochemistry and western blotting. Also to show any differences, MS post-mortem tissue was compared to normal control brain tissue in terms of intact aggrecan and versican.

In this study, high levels of aggrecan, versican and their neoepitopes were found in areas of ongoing demyelination by immunohistochemistry, which has not previously been reported in MS compared to normal brain tissue. In comparison, much lower levels of these proteins were consistently found in NAWM of MS and control white matter tissue where there was no demyelination (Table 3-2). From a previous study, using the same anti-versican neoepitope antibody, a 64 KDa band indicated the presence of this neoepitope in MS active lesions (Westling *et al.*, 2004; Port *et al.*, 2005). Aggrecan and versican neoepitopes were increased, as observed by IHC and WB, in lesional tissue relative to normal control tissue, indicating that changes in ECM degradation may result from changes in ADAMTS activity level. The data provided cannot be used conclusively that aggrecan and versican neoepitopes present in active lesion were generated by ADAMTS-mediated cleavage. In this regard, there are two possible major cleavage sites at the C-termini on both aggrecan and versican G1 domains, which have been termed the "aggrecanase" site and the "MMP" site; however, these cleavage sites are approximately 30 residues apart in each case, and they generate species that are readily separated electrophoretically. An alignment of

this region of human versican V0, V1 and V2 domains suggests that there is no obvious equivalent MMP cleavage sites in these proteins, therefore most, or all of versicans from different species terminates at Glu<sup>405</sup>-Ala<sup>406</sup> following ADAMTS activity (Westling *et al.*, 2002; Demircan *et al.*, 2014). Since ADAMTS-4 cleaves brain aggrecan and versican, it is possible that this enzyme, as well as other aggrecanases including, ADAMTS-9 may play an important role in the processing of these molecules and other lecticans such as brevican, phosphacan and neurocan. It has been previously demonstrated that ADAMTS-4 is expressed in the CNS and shows an increased expression in MS active lesions compared to normal control white matter (Haddock *et al.*, 2006). Also further work from our group demonstrated that TIMP-3, which is an endogenous inhibitor for ADAMTSs is decreased in MS (Haddock *et al.*, 2006) and EAE (Plumb *et al.*, 2005). Sobel and Ahmed, (2001) demonstrated that intact versican was decreased in central lesions, in keeping with the observation of increased versican neoepitope expression in lesional MS described in this thesis.

In view of the abundance of ADAMTS enzymes and other ECM molecule-degrading enzymes in demyelinating areas, loss of aggrecan and versican in MS plaques is in line with previous observations (Lemons *et al.*, 2001; Westling *et al.*, 2004). We did not, however, anticipate identifying large granules of versican and its neoepitope within cells in active lesions. These granules likely are aggregates of the versican or products of its extracellular degradation by ADAMTS that is phagocytosed either by activated microglia or macrophages (Figure 3-8). Alternately, this staining pattern may represent synthesised versican prior to secretion by the cells (Sobel & Ahmed, 2001).

The striking increase in ECM proteoglycan immunostaining of the aggrecan and versican in active plaque edges suggests that their expression is increased as a consequence of the pro-inflammatory milieu of the borders of expanding acute lesions (Siebert *et al.*, 2014; Burda *et al.*, 2014). These increases are consistent with numerous studies which show enhancement of both mRNA and immunoreactivity of the lecticans and the major dermatan sulphate PGs, biglycan and decorin accompanying astrocytosis in CNS injury (Thon *et al.*, 2000; Jones *et al.*, 2002; Lau *et al.*, 2013). Furthermore, it has been indicated that TLRs are expressed by a variety of peripheral immune cells and resident cells of the CNS. TLRs play an important role in linking the innate to the adaptive immune response (Bell *et al.*, 2005). They have a significant role

in remodelling molecules in the CNS MS, as well as in EAE (Racke & Drew, 2009). In addition to lymphocytes that control adaptive immune responses, dendritic cells and tissue macrophages that regulate innate immune responses also play a crucial role in controlling MS pathogenesis (Takeda & Akira, 2005, Hacker *et al.*, 2006; Amor *et al.*, 2014). TLRs may be activated by fragments of the ECM molecules generated by proteolytic cleavage. The aggrecan neoepitope, versican neoepitope and short hyaluronan fragment could be a candidate for this binding to TLR on macrophages. Activation of TLRs induces the expression of proinflammatory cytokines such as IL-1, TNF, chemokines and adhesion molecules, which could induce production of ADAMTSs, amplifying ECM breakdown (Piccinini & Midwood, 2010).

Studies have emphasized that CSPGs can interact with adhesion molecules expressed on various cell types (Asfari *et al.*, 2010; Tan *et al.*, 2011). When axonal growth cones come into contact with CSPGs, they retract and collapse. This might be the reason for the abortive regenerative sprouting observed in spinal cord injury lesions (Profyris *et al.*, 2004; Fleming *et al.*, 2006). The interaction of CSPGs and neurons stimulates the Rho-associated protein kinase Rho-ROCK and/or protein kinase C (PKC) intracellular signalling cascades, which inhibit process extension. Also by blocking activation of the Rho-ROCK and PKC signalling pathways, the inhibitory effect of CSPGs could be observed (Lim *et al.*, 2013). While CSPGs are widely accepted to be inhibitory to axonal regeneration, the inhibitory nature of individual lectican molecules varies amongst the CSPGs. *In vitro*, purified brevican has been shown to be inhibitory to both axonal attachment and growth, while neurocan has been shown to interact with neuronal cell adhesion molecules (N-CAM) similarly inhibiting neurite outgrowth (Jones *et al.*, 2003; Yuan *et al.*, 2013).

At the molecular level, the inhibitory activity of CSPGs on neurite outgrowth and axon re-growth is mediated mainly by GAGs and their structural motifs. Treatment with chondroitinase ABC, an enzyme able to cleave the sugar side chains without altering the core protein structure, promotes axon re-growth both *in vivo* and *in vitro* (Properzi *et al.*, 2003). The ECM of the glial scar contains high level of CSPGs, Yiu *et al.*, (2006) demonstrated that neurons cannot cross the glial scar, in which CSPG levels are increased. Similarly, the increased expression of intact aggrecan and versican around sites of injury in MS lesions in this study might be involved in the inhibition of neurite

re-growth and axon elongation. The precise relationship of CSPG deposition to glial scarring and axon re-growth inhibition, binding to other ECM components and cell migration in the mature CNS are currently poorly understood. Previous studies performed in our laboratory demonstrated evidence for expression of ADAMTS-1, 4 and 5 in both normal and MS lesion with up-regulation of ADAMTS-4 at the protein level in MS lesions (Haddock *et al.*, 2006). Current knowledge suggests that these alterations may be beneficial, enabling neurite outgrowth and neuronal repair, since CSPGs inhibit neurite outgrowth, axonal regeneration and promote neural cell death. However, ADAMTS mediated degradation of CSPGs may increase access of inflammatory cells to sites of tissue destruction leading to detrimental outcomes (Inatani *et al.*, 2001; Cross *et al.*, 2006).

### **3.4 Conclusion**

Cleavage of white matter ECM components, versican and aggrecan, in MS plaques is up-regulated, in particular in active lesions and at chronic active border. This study provides evidence to suggest that CSPG breakdown is involved in MS pathogenesis; CSPGs are likely to contribute to the failure of axon regeneration and neurite outgrowth. ECM lectican abnormalities in the CNS of MS patients should be considered in the design of future interventional therapies and their breakdown by glutamyl endopeptidase ADAMTSs may be beneficial, enabling neurite outgrowth and neuronal repair.

**Chapter 4**  
**Expression of ADAMTS-9 in the CNS in MS:**  
**a pathological role**

## 4.1 Introduction

The ADAMTS enzyme family contains 20 individual gene products (Apte, 2004). Certain members of this family (ADAMTS-1, -4, -5, -8, -9 and 15) can proteolytically process aggrecan within the interglobulin domain (IGD) separating its globular G1 and G2 domains at a specific Glu<sup>373</sup>-Ala<sup>374</sup> bond or at one or more sites within the C-terminal glycosaminoglycan (GAG)-bearing region (Kuno *et al.*, 2000; Tortorella *et al.*, 1999). ADAMTS-9 was originally cloned by Clark *et al.*, (2000) who localized the gene to chromosome 3P14.2-P14.3. Of all ADAMTSs, ADAMTS-9 comprises the highest number of C-terminal TSP-1 like domains (Gottschall & Howell, 2015). This is indicative of a protein with the ability to bind to heparan sulphate proteoglycans (HSPGs) of the BBB basement membrane and glial scars as well as glycosphingolipid sulphatide, a lipid predominantly expressed in the brain (Zeng *et al.*, 2006).

ADAMTS-9 is widely expressed throughout the adult human body organs including brain, heart, placenta and others (Somerville *et al.*, 2003). Levels of pro-inflammatory cytokines TNF and IL-1 are up-regulated in the CNS in MS (Di Penta *et al.*, 2013) and ADAMTS-9 has been shown to be increased in response to these in chondrocytes and chondrosarcoma cells (Demircan *et al.*, 2005; Yaykasli *et al.*, 2009). Though, anti-inflammatory mediators such as TGFβ1 down-regulated ADAMTS-9 expression in prostate cells (Cross *et al.*, 2005).

Unlike other ADAMTSs, such as ADAMTS-1 and ADAMTS-4, pro-domain cleavage of ADAMTS-9 leads to reduced versicanase activity rather than enhancing the catalytic function, and pro-domain processing occurs outside the cytoplasm on the cell surface (Kumar *et al.*, 2012). It has been suggested that ADAMTS-9 degradation of CSPGs may increase access of inflammatory cells to the CNS and lead to axonal damage. Alternatively, breakdown of CSPGs, by ADAMTS-9 may enable axonal regeneration and neurite outgrowth, which is inhibited by CSPGs (Tauchi *et al.*, 2012). Several ADAMTSs have been shown to be elevated in human neurodegenerative disease and animal models of brain injury. ADAMTS-1, but not ADAMTS-5, appears to be up-regulated in Down's syndrome, Pick's disease and Alzheimer's disease (Miguel *et al.*, 2005) and ADAMTS-4 in MS (Haddock *et al.*, 2006).

### 4.1.1 Aim of study

Since in chapter 3, enzymatic degradation of aggrecan and versican was observed in MS lesions, the key aim of this study was to determine whether ADAMTS-9 is implicated in this ECM degradation; to develop an understanding of its activity by assessing its substrates *ex vivo*, which may then subsequently be exploited therapeutically through the design and application of molecules to increase or inhibit its activity. This study was designed to establish a reproducible protocol for the examination of ADAMTS-9 expression together with phenotypic markers of specific CNS cells. Snap-frozen autopsy brain tissue from the same blocks was used and classified as described in Chapter 3 (section 3.3.2). Image J software analysis of ADAMTS-9 expression by immunofluorescence was applied to establish differences in extent of ADAMTS-9 expression between NC, MS NAWM and MS AL. The major objectives addressed were:

- To determine whether ADAMTS-9 immunoreactivity is detectable in human snap frozen brain autopsy material.
- To investigate levels of ADAMTS-9 mRNA expression in MS AL brain tissue compared to levels in MS NAWM and control brain, using qRT-PCR.
- To Investigate the expression of ADAMTS-9 protein in MS AL compared to MS NAWM and normal control human brain tissue, using immunohistochemistry and western blotting.
- To identify the cell types within the brain associated with ADAMTS-9 expression, using dual staining immunohistochemistry.

## **4.2 Results**

### **4.2.1 ADAMTS-9 immunoreactivity within control and MS CNS white matter**

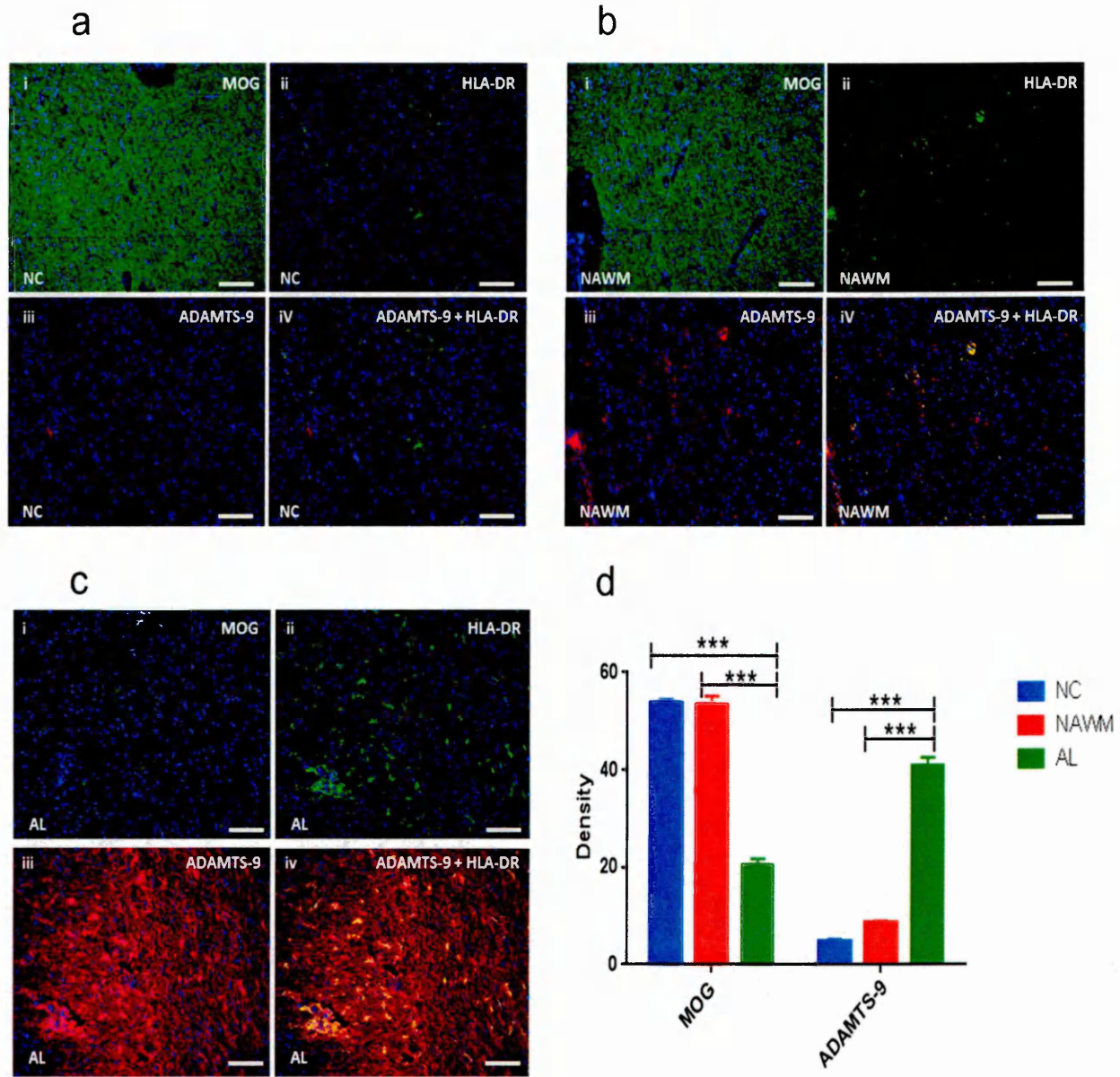
#### **4.2.1.1 Immunohistochemistry analysis of ADAMTS-9 in CNS tissue from MS and control**

Upon microscopic examination, ADAMTS-9 expression appeared to be associated with the cell body and elongated processes of parenchymal cells. Strong ADAMTS-9 immunoreactivity was observed in active MS lesions with ongoing demyelination and was associated with areas of activated microglia. Staining was quite extensive around some blood vessels (vWF+), which may indicate ADAMTS-9 is secreted by endothelial cells and binds to connective tissue components.

In normal control and NAWM with a uniform pattern of MOG staining, low levels of HLA-DR+ cells were found in areas where there were low levels of ADAMTS-9 expression (Figure 4-1). In contrast, strong ADAMTS-9 immunostaining was observed in areas with active lesions, assessed by increased HLA-DR+ cells, and myelin breakdown with ongoing demyelination. Expression of ADAMTS-9 within the region of interest on individual sections was quantified by image J software. Immunohistochemical analysis emphasized that ADAMTS-9 expression in NC, NAWM and AL. Much greater expression of ADAMTS-9 was observed in active lesion compared to NC and MS NAWM (Figure 4-1, d). Data are presented as the mean (n=10 each NC, NAWM and MS AL)  $\pm$  SEM. Statistically significant differences between control white matter, MS NAWM and MS active lesion are marked by asterisks \*\*\*P<0.001.

### **Figure 4-1: Detection of ADAMTS-9 in MS and control human brain tissue using IHC**

Single and dual staining immunofluorescence microscopy of serial tissue sections stained with DAPI (blue) demonstrating cell nuclei, ADAMTS-9 (red), MOG (green) and HLA-DR (green). Low levels of HLA-DR were observed in NAWM (MS076 A1B3) and normal control (NC37 A1B3) (a, ii) and (b, ii) respectively. Low levels of ADAMTS-9 expression in the same blocks (a, iii) and (b, iii) respectively. In comparison, active lesion (MS051 A1B3) shows high levels of ADAMTS-9 (c, iii) in areas of ongoing demyelination along with activated microglia (c, i) and (c, ii) respectively. Image J software analysis shows expression of ADAMTS-9 in control, NAWM and lesion brain tissue (d). Note the difference in graph, much greater expression of ADAMTS-9 in active lesions compared to NAWM and NC. Data represented as mean  $\pm$  SEM using Kruskal-Wallis,  $n=10$ , five reading for each region for each section (\*\* $P<0.01$ , \*\*\* $P<0.001$ ,  $n=10$ ). Scale bar 100 $\mu$ m



#### **4.2.1.2 Cellular localisation of ADAMTS-9 within MS active lesion**

ADAMTS-9 expression appeared to be associated with the cell body and the elongated processes of parenchymal astrocytes in active MS lesion. There were also increased levels of blood vessel associated ADAMTS-9 expression compared to NAWM and NC white matter, which appeared to be both endothelial and astrocytic-end-feet in origin. To determine the exact cellular distribution of ADAMTS-9, dual label immunofluorescence was carried out with polyclonal goat anti-ADAMTS-9 antibody and rabbit anti-NF or mouse anti HLA-DR or mouse anti-vWF or mouse anti-GFAP antibodies for identification of neurons, microglia/macrophages, endothelial cells and astrocytes respectively as described in chapter 2 (section 2.1.2.3). Immunofluorescence was carried out following the application of three different commercially available anti-GFAP antibodies to determine the cellular location of ADAMTS-9 protein expression within astrocytes cells, and to ensure there were no cross reactions (anti-GFAP, abcam, UK; anti-GFAP, Millipore, UK; anti-GFAP, invitrogen, UK). Following initial optimisation, mouse anti-GFAP antibody from Millipore was carried forward for use in this experiment.

Utilisation of the Zeiss 510 software enabled individual pixels to be scanned and viewed as a yellow colour if true co-localization existed between the two channels of interest. Co-localisation was observed with ADAMTS-9 and cerebral vascular endothelium in the lesion (Figure 4-2), compared to normal control human brain tissue (Appendix III). Co-localisation was also observed in the foamy macrophages and activated microglia in MS active lesion (Figure 4-3). Co-localisation of the astrocytic phenotypic marker (GFAP) with ADAMTS-9 provided definitive evidence of ADAMTS-9 expression by astrocyte cells within MS active lesions as shown in (Figure 4-5).

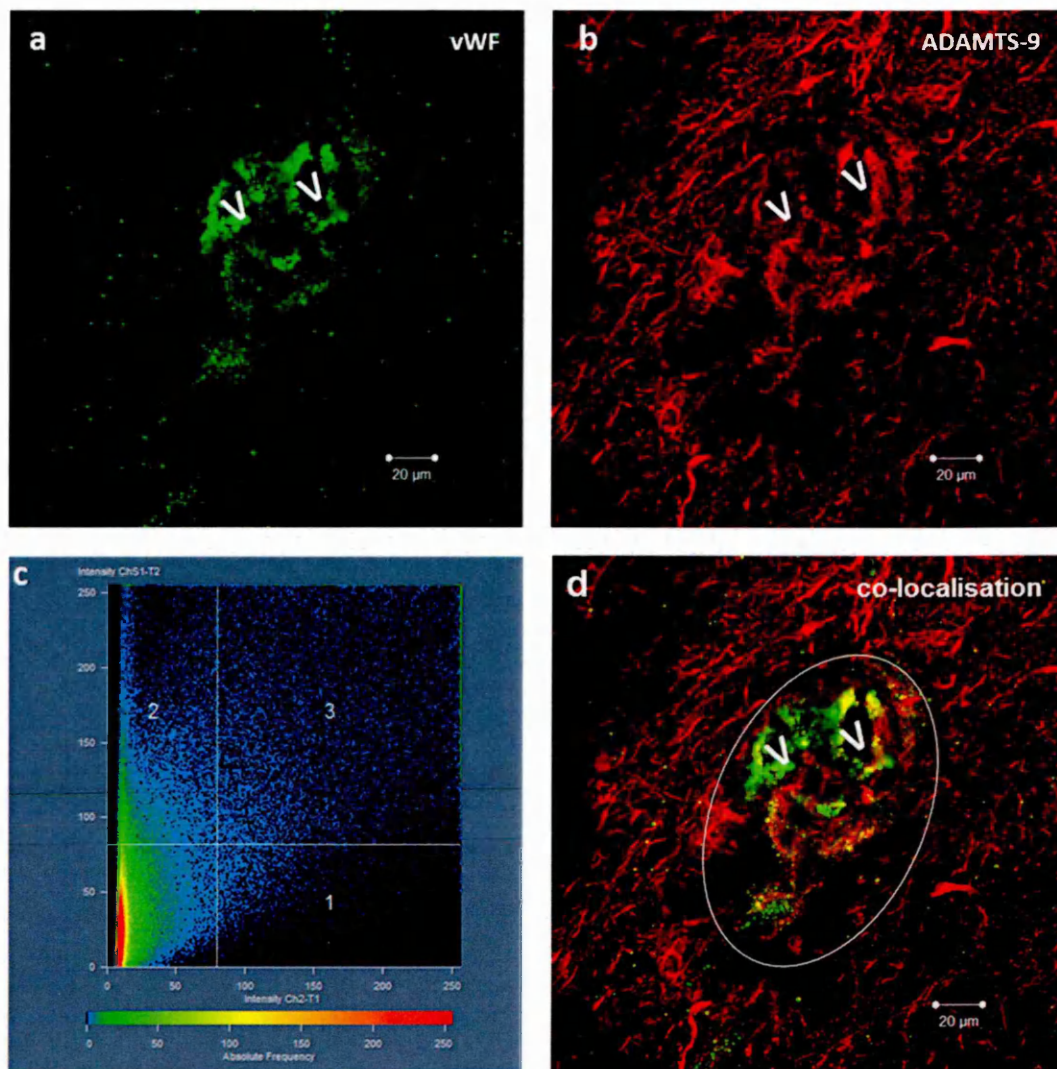


**Figure 4-2: Dual label immunofluorescence of ADAMTS-9 and vWF in MS AL brain tissue sections**

Dual label immunofluorescence for (a) vWF (green) and (b) ADAMTS-9 (red) in MS active lesion white matter (MS062 P1C3) with high levels of parenchymal ADAMTS-9 immunoreactivity. (C) Co-localisation is represented by the pixels in quadrant 3 on the graph and is demonstrated as yellow pixels in the composite image (d) following Zeiss 510 CSLM software reading of individual pixels for each fluorophore. V= vessel.

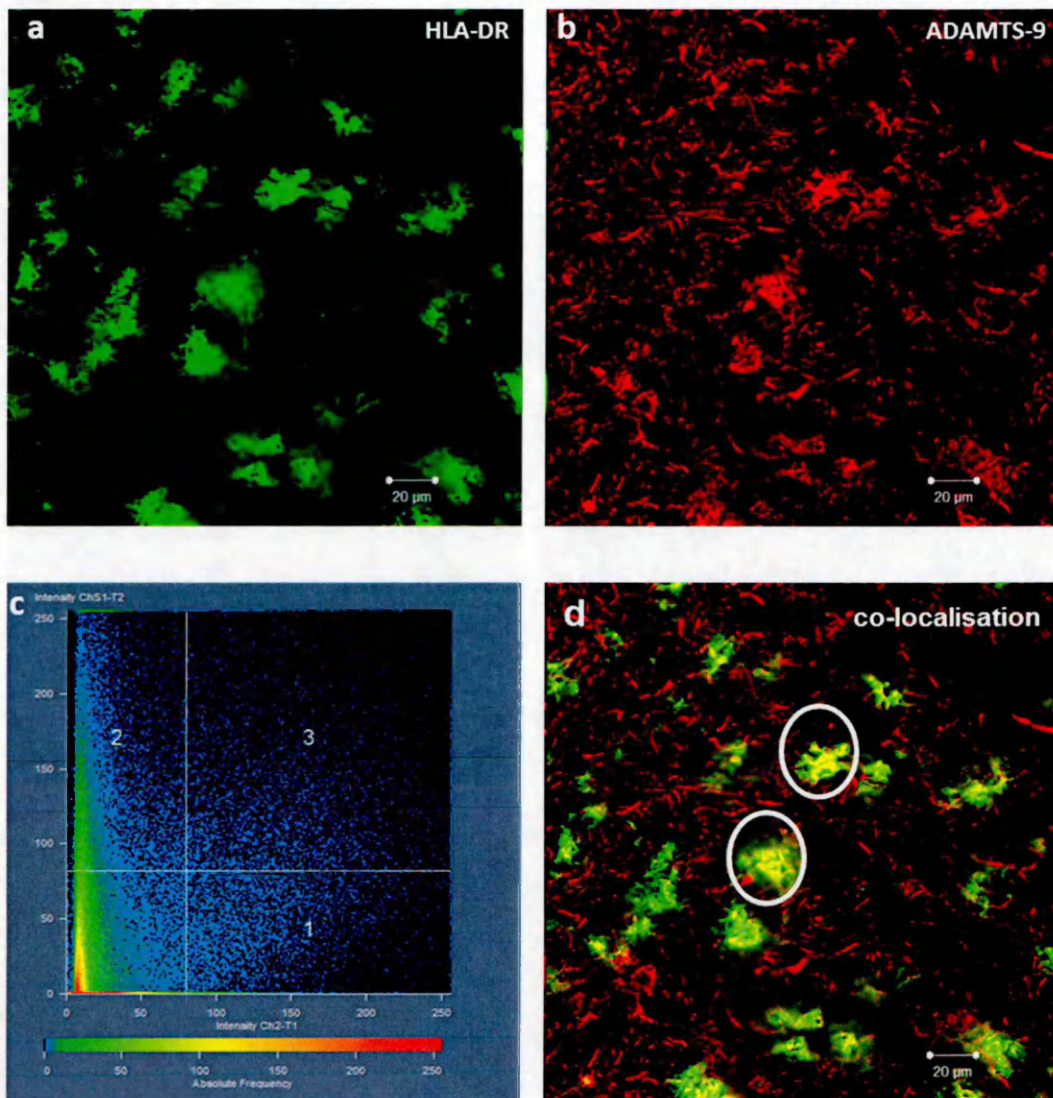


**Figure 4-3: Dual label immunofluorescence of ADAMTS-9 and HLA-DR in MS AL brain tissue**

Dual label immunofluorescence for (a) HLA-DR (green) and (b) ADAMTS-9 (red) in MS active lesion white matter (MS062 P1C3) with high levels of parenchymal ADAMTS-9 immunoreactivity. (c) Co-localization is represented by the pixels in quadrant 3 on the graph and is demonstrated as yellow pixels in the composite image (d) following Zeiss 510 CSLM software reading of individual pixels for each fluorophore. Areas circled indicate co-localisation of ADAMTS-9 to macrophages and activated microglia (stained yellow).

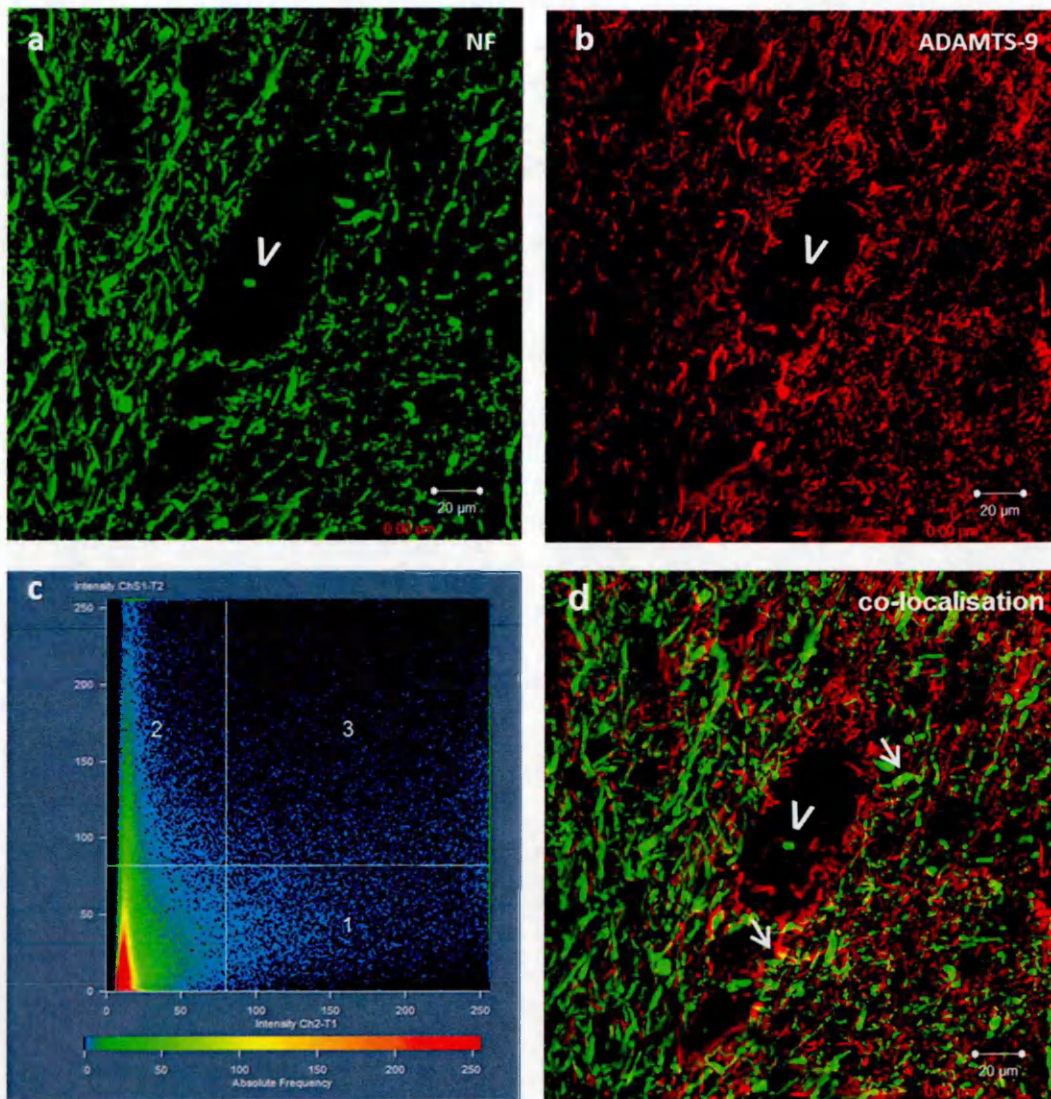


**Figure 4-4: Dual label immunofluorescence of ADAMTS-9 and NF in MS AL brain tissue**

Dual label immunofluorescence for (a) NF (green) and (b) ADAMTS-9 (red) in MS active lesion white matter (MS062 P1C3) with high levels of parenchymal ADAMTS-9 immunoreactivity. (c) Co-localization is represented by the pixels in quadrant 3 on the graph and is demonstrated as yellow pixels in the composite image (d) following Zeiss 510 CSLM software reading of individual pixels for each fluorophore. Arrows indicate co-localisation of ADAMTS-9 and NF on a few axons. V= vessel.

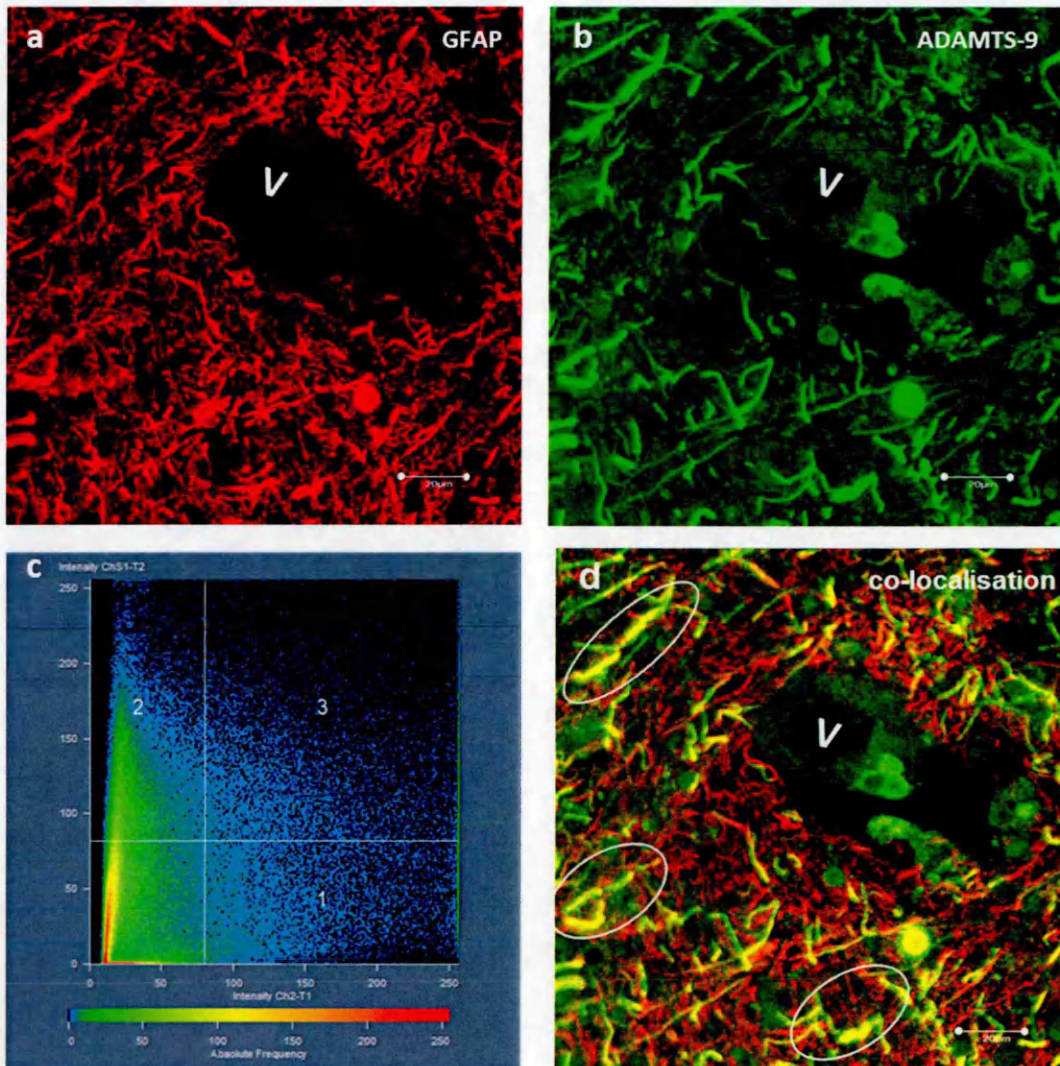


**Figure 4-5 Dual label immunofluorescence of ADAMTS-9 and GFAP in MS AL brain tissue**

Dual label immunofluorescence for (a) GFAP (red) and (b) ADAMTS-9 (green) in MS active lesion white matter (MS062 P1C3) with high levels of parenchymal ADAMTS-9 immunoreactivity. (C) Co-localization is represented by the pixels in quadrant 3 on the graph and is demonstrated as yellow pixels in the composite image (d) following Zeiss 510 CSLM software reading of individual pixels for each fluorophore. Areas circled indicate co-localisation of ADAMTS-9 to astrocytes (stained yellow). V= vessel.

### **4.2.1.3 Western blot analysis of ADAMTS-9 in CNS tissue from MS and control brain**

Western blotting of protein samples from CNS tissue homogenates indicated that ADAMTS-9 is constitutively expressed within MS and normal control tissue (Figure 4-6). As variations in the extent of ADAMTS-9 staining were detected within the white matter using IHC, and was not the grey matter, quantitation of protein samples were carried out due to the varying amount of white matter in the tissue blocks used. Anti-ADAMTS-9 antibody revealed a single band at approximately 180kDa, is an affinity purified goat polyclonal antibody raised against peptide mapping within internal region of ADAMTS-9 of human tissue (Cal *et al.*, 2002). The  $\beta$ -actin band (42 kDa) was used to verify the equal loading of the samples (Figure 4-6, a). The results demonstrated that ADAMTS-9 protein was present in both normal control and in MS human brain tissue. Densitometry analysis of this band showed a significant increase in ADAMTS-9 protein in the MS sample "active lesion" compared to the NAWM and normal control brain samples (Figure 4-6, b).

### **4.2.2 qRT-PCR analysis of mRNA expression of ADAMTS-9 in MS AL, MS NAWM and normal control brain tissue**

#### **4.2.2.1 Case selection**

A total of 30 tissue blocks were initially characterised for the study based on the histological and immunohistochemical assessment as described in chapter 3 (section 3.3.2). Histological evaluation identified 10 cases as having evidence of inflammation and ongoing demyelination considered as active lesions. Another 20 blocks identified as having no evidence of inflammation or demyelination were considered as normal control and NAWM samples (Table 3-1). RNA was extracted as described in chapter 2 (section 2.3.3.1), and then all samples were checked by agarose gel electrophoresis for RNA integrity as described in chapter 2 (section 2.3.4). Figure (4-7) shows a representative gel for extracted RNA with intact and good quality RNA as determined by the presence of 28S and 18s RNA subunit.

#### **4.2.2.2 qRT-PCR validation, normalisation and housekeeping genes**

It is essential to rule out variation between samples when detecting mRNA expression [(reverse transcription into cDNA as described in chapter 2 (section 2.3.5)]. Three widely used housekeeping genes (GAPDH, PPIA and HPRT-1) were tested for their stability across experimental samples and hence suitability as reference genes for normalisation of target gene expression in qRT-PCR as described in chapter 2 (section 2.3.6) (Vandesompele *et al.*, 2002). The expression of stability measure of CT values of the three stable genes was determined in each sample following cDNA synthesis. This demonstrated the suitability of PPIA, HPRT-1 and GAPDH to be used as reference genes; therefore all three genes were used in subsequent qRT-PCR experiments. Figure (4-8) shows representative amplification plots of qRT-PCR for housekeeping genes, all housekeeping gene CT values were between 18 -25 and for ADAMTS-9 CT values were > 30 indicating that the expression ADAMTS-9 was much lower than that of the housekeeping genes.

#### **4.2.2.3 Expression of ADAMTS-9 mRNA in human brain tissue**

qRT-PCR amplification of mRNA from normal and MS tissue blocks revealed that ADAMTS-9 was constitutively expressed at the mRNA level (Figure 4-8) in all samples studied. ADAMTS-9 was shown to be expressed at the mRNA level in control white matter, MS NAWM and MS AL. There was significantly higher ADAMTS-9 mRNA expression in the MS lesions compared to both NAWM and control white matter brain tissue using Kruskal-Wallis, n=7 (Figure 4-9).

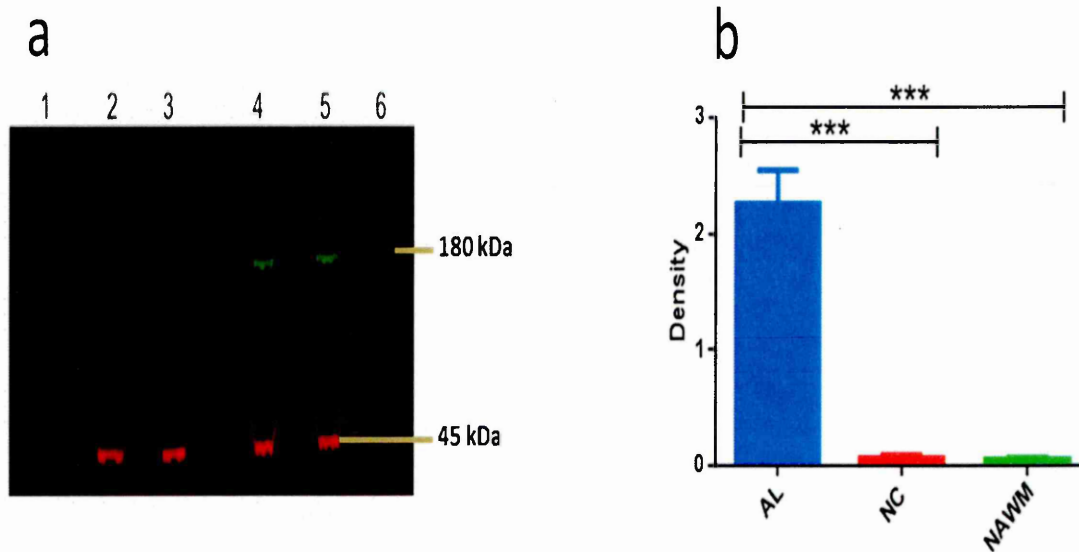


**Figure 4-6: Western blot analysis of ADAMTS-9 protein expression in MS and control CNS white matter protein extracts**

(a) Western blot of ADAMTS-9 (green 180KDa) and  $\beta$ -actin (red 42KDa) from; control white matter (lane 2) MS NAWM (lane 3) and active lesion (lanes 4 and 5). Lanes 1 and 6 represent standard molecular weight markers (40-300KDa) (Thermo Scientific, UK). (b) Densitometric quantification of ADAMTS-9 expression in active lesion, normal control and normal appearing white shows much greater expression of ADAMTS-9 in AL compared to NC and MS NAWM using Kruskal-Wallis,  $n=7$  (\*\*\*) $P<0.001$ ).

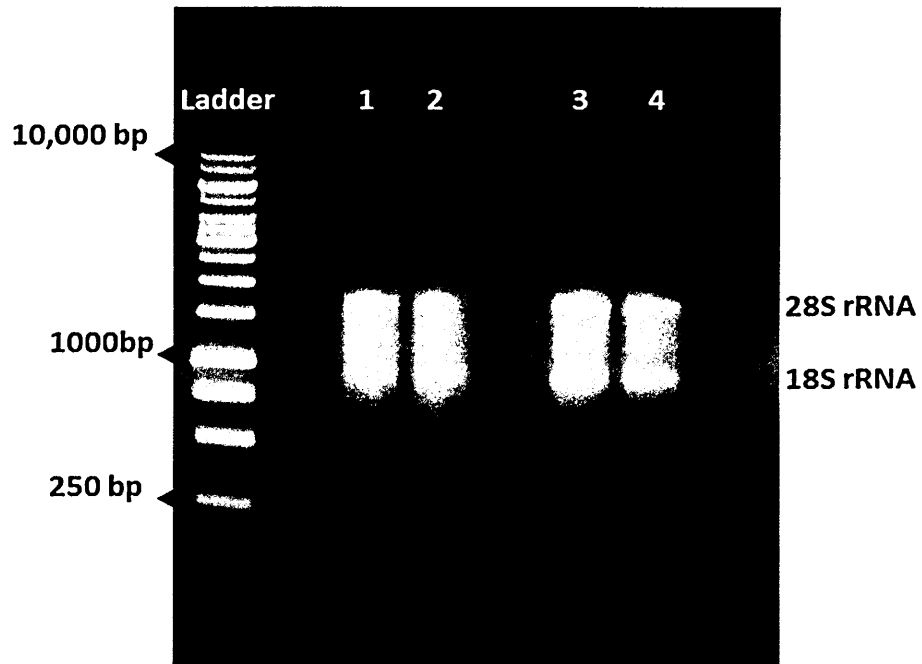
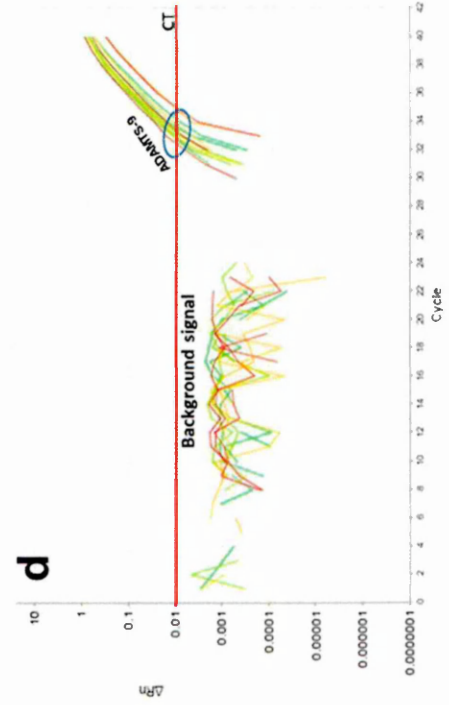
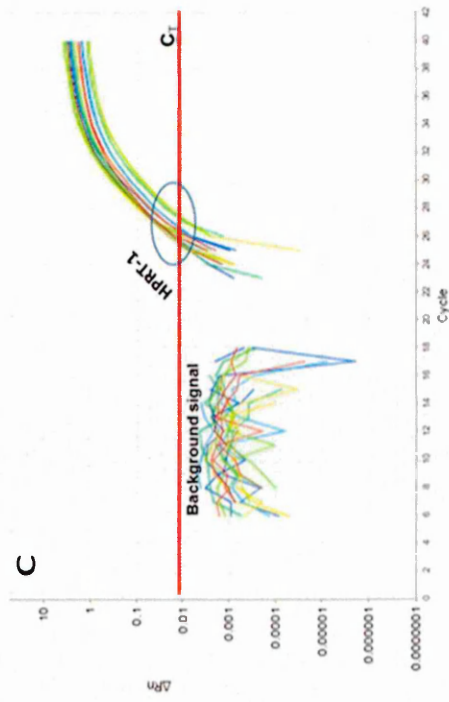
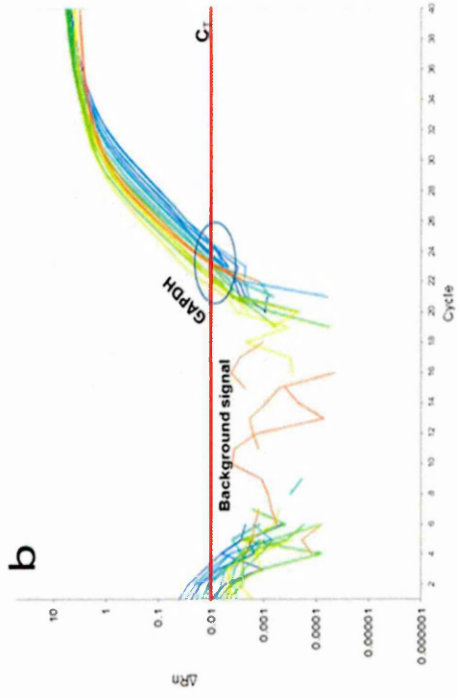
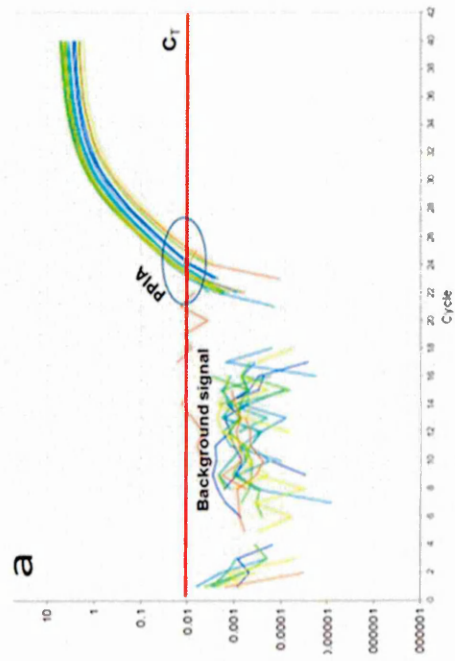


**Figure 4-7: Agarose gel electrophoresis pattern of total RNA extracted from control and MS human brain tissue**

Lanes (1 and 2) and (3 and 4) represent duplicate samples of RNA extracted from NC and MS white matter blocks respectively. 28S rRNA and 18S rRNA bands confirm RNA integrity. DNA marker contains thirteen markers between 250 and 10,000 bp, (Invitrogen, UK). bp= base pairs.

**Figure 4-8: Amplification plots from qRT-PCR data for housekeeping genes in MS and control human brain**

Amplification plots from qRT-PCR analysis of housekeeping genes (a) PPIA, (b) GAPDH, (c) HPRT-1 and (d) ADAMTS-9 in MS AL, NAWM and NC brain tissue showing exponential phase and plateau phase. The cycle threshold ( $C_T$ ) is represented by the red line at which point the fluorescence reaches above the threshold.  $\Delta Rn$  is the change in fluorescence.



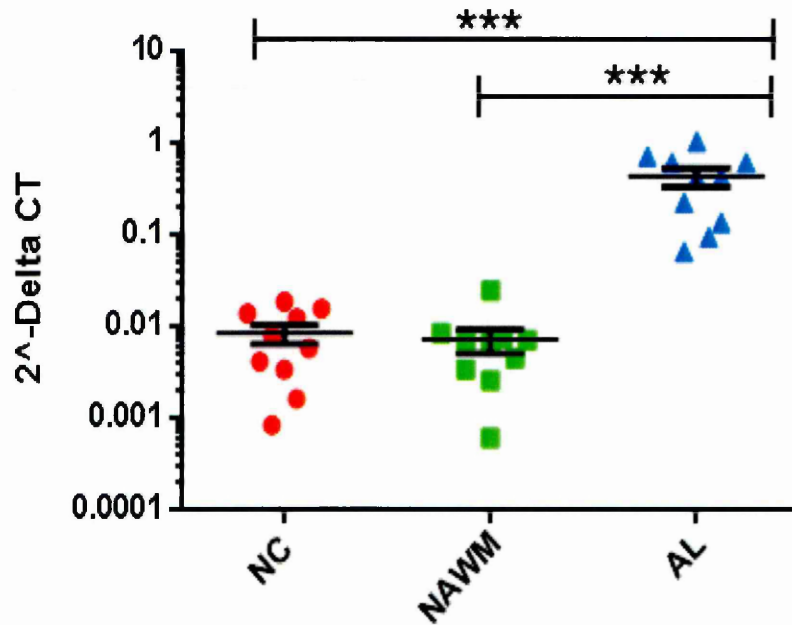


**Figure 4-9: Expression of ADAMTS-9 mRNA in human control and MS brain tissue assessed by qRT-PCR**

Real Time PCR (qRT-PCR) analysis showing ADAMTS-9 mRNA expression in NC, NAWM and MS active lesions. Much greater expression of ADAMTS-9 mRNA in MS lesions is seen compared to NC and MS NAWM. Data are presented as the mean (n=10 samples each NC, NAWM and MS AL) ± SEM. Statistically significant difference between control white matter, MS NAWM and MS active lesion are marked by asterisks \*\*\*P<0.001.

### 4.3 Discussion

The results presented here demonstrate the spectrum of ADAMTS-9 distribution in CNS tissue by IHC, along with image J software analysis of the relative level of ADAMTS-9 expression in normal control white matter, NAWM and the active lesions. Tissue was classified based on evidence of recent myelin breakdown and extent of cellular activation as determined by ORO staining and HLA-DR immunoreactivity, classification parameters as described by other authors (Sanders *et al.*, 1993; Van der Valk & De Groot, 2000). The first objective of this study was to determine whether ADAMTS-9 was expressed and then to establish a reproducible protocol for identification of ADAMTS-9 by immunofluorescence in snap frozen human autopsy brain material. Protein expression of ADAMTS-9 was further confirmed by western blotting following separation of proteins extracted from tissue homogenates by SDS PAGE as described in chapter 2 (section 2.2.4). Gene transcription for this protein was also demonstrated by reverse transcribing mRNA into cDNA followed by qRT-PCR.

High levels of ADAMTS-9 were found in areas of ongoing demyelination, which has not previously been reported in MS immunohistochemically. In comparison, much lower levels of this protein were consistently found in NAWM of MS and control white matter tissue where there was no evidence of demyelination. Previous studies using qRT-PCR indicated that ADAMTS-9 was expressed by differentiated neuroblastoma cells *in vitro* and significantly up-regulated following transient middle cerebral artery occlusion (tMCAo) in the rat (Reid *et al.*, 2009). ADAMTS-9 expression was associated with the endothelium of blood vessels and with the cell body and elongated processes of parenchymal astrocytes and the astrocytic end feet that encompass the cerebral vasculature. Co-localisation of ADAMTS-9 with the astrocyte phenotypic marker, GFAP, or the endothelial marker, vWF or neuronal marker, NF-L following dual labelled immunofluorescence, confirmed the morphological observations and clearly demonstrated that these three cell types are responsible for ADAMTS-9 expression. These observations confirm ADAMTS-9 expression within MS active lesions is similar to that for other MMPs reported previously e.g. ADAMTS-4 and ADAM 17 (Haddock *et al.*, 2006; Goddard *et al.*, 2001). ADAMTS-9 was also demonstrated to be expressed by activated macrophages/microglia cells in MS tissue and was upregulated in MS.

particularly in active lesions where ADAMTS-9 immunoreactivity is evident in numerous large foamy macrophages, implicating a possible role in the disease process.

The presence of ADAMTS-9 protein and mRNA was analysed by western blotting and qRT-PCR using protein and RNA extracted from 30 blocks (10 each NAWM, AL and NC). ADAMTS-9 was detected in all samples by a band at 180 kDa, probably corresponding to the mature form of the protein (Cal *et al.*, 2002). ADAMTS-9 protein expression was significantly increased, as observed by western blotting in MS active lesions. In addition, ADAMTS-9 mRNA was up-regulated in MS active lesion tissue; this suggests that translation of ADAMTS-9 increases in MS active lesions.

Changes in ADAMTS-9 reported in human chondrocytes in rheumatoid arthritis (RA) result from transcriptional changes in ADAMTS-9 or changes in protein activity due to up-regulation of aggrecan within injury sites (Demircan *et al.*, 2005). ADAMTS-9 may be involved in the loss of ECM by cleaving proteoglycans, as demonstrated for other ADAMTSs and other tissues (Sandy *et al.*, 2001; Lemarchant *et al.*, 2014) and as described here in chapter 3. Sobel and Ahmed, (2001) demonstrated that in active plaque centre and active lesions, CSPGs were decreased in the ECM and accumulated in foamy macrophages which is similar to our findings in chapter 3. This loss of CSPGs is related to the high levels of ADAMTS-9 observed in active MS plaques.

Transcriptional induction of ADAMTSs e.g. ADAMTS-1 and 9 in neurons and astrocytes following physical or toxic injury in the CNS has been reported and it was suggested that this expression at the site of injury may favour neurite outgrowth (Lemons *et al.*, 2001; Cau *et al.*, 2013). It has been reported that ADAMTS-4 cleaves versican *in vivo*, in a manner similar to the ADAMTS-mediated cleavage of aggrecan and versican in cartilage (Tortorella *et al.*, 2001; Demircan *et al.*, 2005), spinal cord (Fawcett, 2006; Lemons *et al.*, 2001) and brain tissue (Matthews *et al.*, 2000; Westling *et al.*, 2004). It was also reported that ADAMTS-4 was abundant in MS active lesions (Haddock *et al.*, 2006), in agreement with our reported observations for ADAMTS-9. Thus, ADAMTS-9 together with ADAMTS-4 expression in the CNS, may contribute to remodelling of the ECM in the brain in MS patients. On the other hand, others also suggest that the level of endogenous ADAMTSs is not sufficient to recover plasticity and functional recovery after human brain injury. The cleavage of CSPGs induced by glial cells may be achieved

not only by ADAMTS-9 but also by other ADAMTSs and MMPs, which are also upregulated after neuronal injuries (Nakamura *et al.*, 2000; Tauchi *et al.*, 2012). MMPs also cleave other matrix proteins, such as laminin and collagen, leading to loss of blood brain barrier integrity; enhancing the infiltration of immune cells which may worsen the pathology of MS (Rosenberg *et al.*, 1998).

ADAMTS-9 may play a role in a number of ways in the development of MS; proteolytic cleavages of ECM Heparan sulphate proteoglycan (HSPGs) of the BBB basement membrane and glial scar as well as cleavage of HGSPs into their soluble form, may create a chemotatic gradient for inflammatory cells to enter the CNS (Chen *et al.*, 2000; Zeng *et al.*, 2006). ADAMTSs are reported to cleave CSPGs and adhesion molecules from the luminal surface of blood vessels; however in MS, increased expression of CSPGs has been reported, suggesting an imbalance in enzyme/inhibitor activity. ADAMTS-9 expression has been demonstrated to be associated with astrocytes and activated macrophages/microglia and expressed at high levels in lesions with high level of cellular activity as gauged by HLA-DR and ORO expression. ADAMTS-9 cleaves CSPGs thereby possibly subjecting neurons to its cytotoxic effects (Cau *et al.*, 2013). CSPGs have been reported to inhibit myelin repair (Lau *et al.*, 2013) neurite outgrowth (Barrit *et al.*, 2006) and axon regeneration (Shen *et al.*, 2009; Brown *et al.*, 2012), which is investigated in chapter 5.

Following upregulation, ADAMTS-9 could be contributing to neuronal regeneration by two potential mechanisms; 1) promotion of neuronal differentiation/proliferation by enzymatic activity in the nucleus (Somerville *et al.*, 2003) or 2) operating as a peptidase on the cell surface of migrating CNS cells and clearing a path through the ECM or glial scar by degradation of CSPGs (Somerville *et al.*, 2003), enabling migration of oligodendrocyte precursor cells. Alternatively, the breakdown of CSPGs by ADAMTS-9 could have a damaging effect on the CNS by allowing the migration of inflammatory cells and activated macrophages to susceptible neurons. The efficiency by which ADAMTSs cleaves CSPGs does not appear to be as high as MMPs, perhaps limiting the impact of the peptidase as proteoglycanase in *ex vivo* (Somerville *et al.*, 2003). Therefore the up-regulation of ADAMTS-9 expression following stroke is not necessarily a bad thing because it is unlikely that the normal ECM structure will be significantly degraded by the peptidase.

The identification of the cells responsible for the synthesis of ADAMTS-9 is important when analysing the functional aspects of ADAMTS-9. ADAMTS-9 could be the sheddase responsible not only for CSPGs breakdown, but also for release of growth factors and adhesion molecules (Luan *et al.*, 2008). Moreover, astrocytes and macrophages can contribute to immune regulation through their role in resealing of the BBB and their direct effects on immune cell modulation molecules, such as TGF $\beta$ , and TNF and proteoglycans (Faulkner *et al.*, 2004; Rolls *et al.*, 2009). Proteoglycan, and principally CSPGs, are known for their immune-related activity in peripheral tissue. Owing to their adhesiveness to chemo-attractive agents and growth factors that are required for recruiting and activating immune cells, proteoglycans can capture these factors increasing their focal concentration and thereby targeting the immune response to the injured areas (Nandini *et al.*, 2006; Rolls *et al.*, 2009).

Reid *et al.*, (2009) provided evidence that IL-1 $\beta$  and TNF- $\alpha$  potentially up-regulated ADAMTS-9 in an astrocytic cell line (U373-MG) by activating transcription factor NF $\kappa$ B. This study provided strong evidence that ADAMTS-9 expression is modulated by pathological conditions that occur in response to CNS injury. The ADAMTS-9 data described here are consistent with previous studies of ADAMTS-1 and -4 expressions, which were both upregulated in MS. In contrast to ADAMTS-5 and -8, levels which were not significantly raised in response to experimental stroke or in MS (Chen *et al.*, 2000; Haddock *et al.*, 2006; Tian *et al.*, 2007). However, Luan *et al.*, (2008) indicated that specific blocking antibodies against IL-1 $\beta$  and TNF- $\alpha$  dramatically inhibited ADAMTS-7 and ADAMTS-12 induction in chondrocytes *in vitro*, and the suppression of TNF- $\alpha$  and IL-1 $\beta$  expression by siRNA in human chondrocytes prevented ADAMTS-7 and ADAMTS-12 mediated degradation of cartilage oligomeric matrix protein (COMP). Regardless of cell source, ADAMTS-9 expression by astrocytes and macrophages/microglia would allow cleavage of CSPGs resulting in promotion of a pro-inflammatory after acute CNS injury. These suggestions are in agreement with other reports indicating that, in the periphery, CSPGs regulate the motility and activation of macrophages (Hayashi *et al.*, 2001; Rolls *et al.*, 2008), dendritic cells (Kodaira *et al.*, 2000) and other immune cell types (Rolls *et al.*, 2006).

#### 4.4 Conclusion

In chapter 3 was reported that CSPGs including aggrecan and versican are up regulated in MS active lesions as were their neoepitopes indicative of ADAMTS-9 activity. Here we report the cellular origin and distribution of ADAMTS-9 expression within clinically and neuropathologically confirmed MS and normal control white matter, assessed by qRT-PCR, IHC and WB. ADAMTS-9 expression was associated predominantly with activated macrophages/microglia, parenchymal astrocytes and to lesser extent with blood vessel endothelium and axons in MS white matter. We demonstrated here that ADAMTS-9 expression at the mRNA and protein level was also increased in active inflammatory lesions with evidence of myelin breakdown, suggesting that up-regulation of ADAMTS-9 may be a general phenomenon induced by CNS injuries. ADAMTS-9 could degrade aggrecan and versican and reverse the neurite outgrowth inhibition mediated by human brain proteoglycans allowing OPCs to cross the glial scar to repair axons. However, as repair in MS is limited; this degradation of ECM proteins deposited in lesions does not allow the repair process to be complete. Further studies on this enzyme are now required to define its function in normal CNS physiology and in the pathological process of MS (See chapter 5).

**Chapter 5**  
**ADAMTS-9 expression and modulation**  
**in CNS cells *in vitro***

## 5.1 Introduction

In the CNS, inflammation is not a phenomenon that occurs spontaneously, it requires a stimulus (inflammatory or infection), to initiate pathways including intercellular communication by pro-inflammatory mediators such as cytokines and chemokines (Comabella & Khoury, 2012). Some of these molecules, such as interleukin-1 (IL-1), IL-2, IL-6, TNF- $\alpha$  and IFN- $\gamma$  are produced by many cell types such as monocytes, macrophages, NK cells, astrocytes and microglia (Imitola *et al.*, 2005; Ramesh *et al.*, 2013; Rossi *et al.*, 2013). They are all known proinflammatory factors and are found to be upregulated in MS (Lim & Constantinescu, 2010; Carminero *et al.*, 2011; Di Penta *et al.*, 2013). Additionally, when these molecules, especially IL-1, TNF- $\alpha$  and IFN- $\gamma$ , were injected into normal brain tissue, a significant amount of reactive astrogliosis was observed around the injection site (Abdelbassat *et al.*, 2011; Burda *et al.*, 2014; Siebert *et al.*, 2014).

Damage to the CNS, either by trauma or inflammation, initiates an increase in pro-inflammatory cytokines, which stimulate the upregulation of CSPGs expression, due to the induction of reactive gliosis (Yu *et al.*, 2012; Siebert *et al.*, 2014). Reactive astrocytes synthesise brevican, neurocan and phosphacan, while vascular macrophages, activated microglia and endogenous OPCs account for the increased expression of aggrecan, versican and NG2 (Asher *et al.*, 2002; Jones *et al.*, 2002; Viapiano *et al.*, 2006). CSPGs inhibit neurite outgrowth from embryonic chick and rodent neurons *in vitro* but the role of CSPGs on human neurons has been largely untested. Here, the effect of aggrecan on neurite outgrowth was investigated using neuroblastoma cell line (SHSY-5Y), cells grown on varying concentration of aggrecan to assess neurite extension (Hynds *et al.*, 1996; Cua *et al.*, 2013).

Enzymatic removal of the GAG chain from ECM core proteins by chondroitinase ABC permits some axonal regrowth; however the remaining intact core protein also possesses an inhibitory domain (Karimi *et al.*, 2012; Cua *et al.*, 2013). Because ADAMTSs can degrade the core protein of CSPGs, ADAMTS-9 was investigated for its capacity to overcome CSPG inhibition of neurite outgrowth in culture. ADAMTS-9 was selected for its known expression following inflammation in the CNS in MS as described in chapter 4.

Aggrecanase activity was previously described in rat astrocytes treated with IL-1 $\beta$ , and was also enhanced by TNF- $\alpha$  (Cross *et al.*, 2006; Rogerson *et al.*, 2010). Another study indicated that transforming growth factor alpha (TGF- $\alpha$ ) expressed by macrophages and transforming growth factor beta (TGF- $\beta$ ) expressed by both microglia and macrophages, resulted in the up-regulation and synthesis of both ADAMTS and their substrates CSPGs (Properzi *et al.*, 2005; Reid *et al.*, 2009). These data support the hypothesis that aggrecanases are active early in the disease process in MS or during acute inflammatory episodes (Merson *et al.*, 2010). In cartilage, ADAMTS-5 mRNA is strongly up-regulated by IL-1 $\beta$ , whereas ADAMTS-4 mRNA shows only a small degree of up-regulation (Ilic *et al.*, 2007). There is limited evidence as to the cellular source of ADAMTS-9 in the human brain. Furthermore, little is known about transcriptional regulation of ADAMTS-9 in the CNS, though in other tissues it appears to be modulated by pro-inflammatory mediators (Bevitt *et al.*, 2003; Demircan *et al.*, 2005).

In this study, the effect of pro-inflammatory cytokines (IL-1 $\beta$ , IFN- $\gamma$  and TNF- $\alpha$ ) on expression and modulation of ADAMTS-9 in astrocytes (primary human astrocytes), microglia (CHME3 human foetal cell line) and neuronal cells (SHSY-5Y) differentiated with RetA was assessed by ICC and WB. This may enable our understanding of the transcriptional initiators of ADAMTS-9 expression in the CNS in MS.

### 5.1.1 Aims of the study

- To confirm the effects of the RetA on neuroblastoma cell line SHSY-5Y differentiation
- To determine effects of varying concentrations of aggrecan on neurite outgrowth using in cell ELISA, ICC and WB detection of NF-L expression
- To optimise and validate methods to study ADAMTS-9 expression in SHSY-5Y cells grown on varying concentrations of aggrecan, at the mRNA level (qRT-PCR) and the protein level (ICC and WB).
- To determine the modulating effect of cytokine treatment on expression of ADAMTS-9 in all the cell types utilised in this study.

## 5.2 Methods

### 5.2.1 Neuroblastoma cell line differentiation with retinoic acid

Retinoic acid (RetA) is a metabolite of vitamin A that mediates the functions of vitamin A, which is required for cell growth and development and can control the expression of genes in the CNS (Clagett-Dame *et al.*, 2005). RetA treatment of SHSY-5Y cells has been shown to increase extension of neurites to produce a more neuronal phenotype comparable to *in vivo* neurons (Encinas *et al.*, 2000). Cells were cultured as described in chapter 2 (section 2.4.1). To induce differentiation of human neuroblastoma SHSY-5Y cells to become more mature neuronal cells, cells were seeded into 24 well plates at a density of  $5 \times 10^4$  cells/well in 1 mL culture medium containing 10  $\mu$ M RetA for 7 days (Cheung *et al.*, 2000). To confirm whether the cells had differentiated neuronal features, ICC was performed with anti-NF-L antibody as described in chapter 2 (section 2.4.9). NF-L is one of the intermediate filament protein subunits present in neurons, neuronal processes, and peripheral nerves and is a specific neuronal cell marker (Wang *et al.*, 2012). Figure 5.1 shows the difference in cell morphology between untreated and RetA treatment of the SHSY-5Y cells.

### 5.2.2 The effect of aggrecan on expression of ADAMTS-9 in the SHSY-5Y cells using in cell ELISA

After coating of aggrecan on plasticware as described in chapter 2.4.5, neuroblastoma cell line SHSY-5Y was plated into 96-well plates at a density of  $5 \times 10^4$ /200  $\mu$ l media/ well containing 10  $\mu$ M RetA for 7 days. Media were removed from the cells and then cells were washed with two changes of PBS. Following this, cells were fixed with 4% PFA for 10 mins and ice cold acetone for 4 mins. Cells were incubated with primary antibody to NF-L (1:1000),  $\beta$ -actin (1:1000) and ADAMTS-9 (1:100) overnight followed by appropriate secondary antibodies (Table 2-6) for 90mins. Nuclei were counterstained using DAPI. The double labelled in Cell-ELISA of NF-L with  $\beta$ -actin and ADAMTS-9 with  $\beta$ -actin were identified and imaged on the Odyssey infrared imaging system (LI-COR Bioscience, USA).

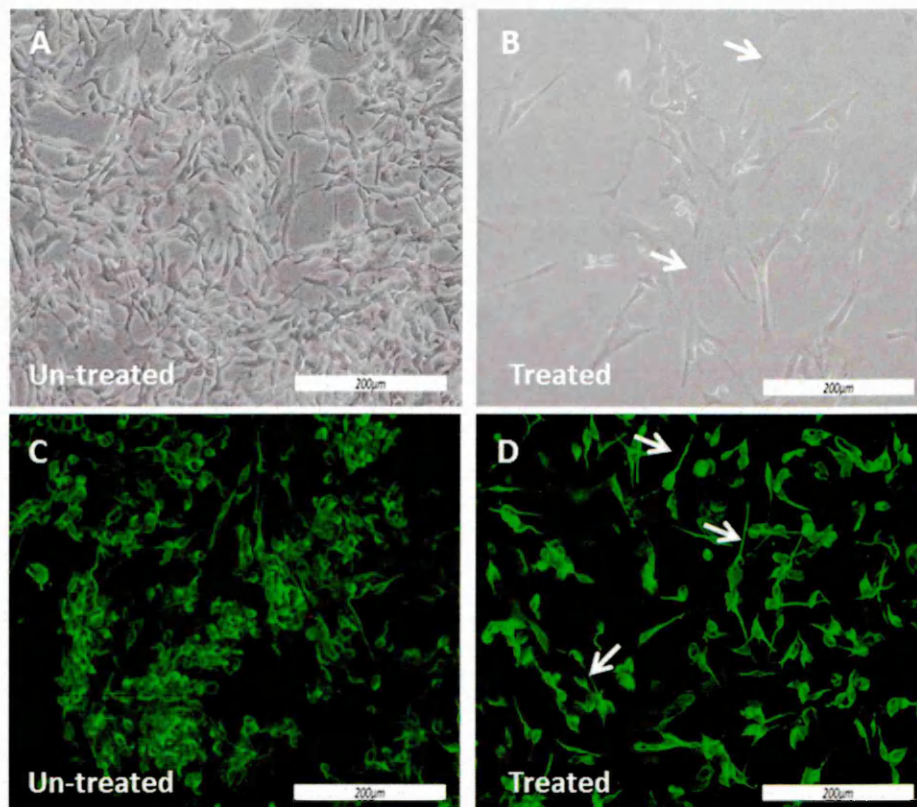


**Figure 5-1: Morphological effects of RetA on neuroblastoma cell line SHSY-5Y**

SHSY-5Y cell morphology A) untreated B) treated with RetA. Characterization of the neuroblastoma cell line SHSY-5Y with NF-L antibody staining (green). C) Untreated D) treated with RetA. White arrows indicate that RetA has enhanced neurite outgrowth. Images were captured on an inverted stage microscope (Olympus IX81 fluorescence microscope with Cool Snap digital camera (Olympus Media Cybernetics, Silver Spring, USA).

## **5.3 Results**

### **5.3.1 The effect of CSPGs on neurite outgrowth of the neuroblastoma cell line**

#### **5.3.1.1 Effect of aggrecan on the viability of differentiated SHSY-5Y cells**

The cell viability of differentiated SH-SY5Y cells grown on various concentrations of aggrecan on at 0  $\mu\text{g/ml}$ , 0.5, 1, 1.5, 1.75, 2 and 2.5 $\mu\text{g/ml}$  was determined by MTT assay and is shown as the percentage of values obtained for uncoated control wells at each concentration. The highest concentration of aggrecan that could be used in the experiment was determined as when cell viability was greater than 80% of their untreated controls (Datki *et al.*, 2003; Cheung *et al.*, 2009). The results showed that the highest concentration of aggrecan that could be used was 2 $\mu\text{g/ml}$ . Treatment of neuroblastoma cell line with aggrecan at 0.5, 1 and 1.5 $\mu\text{g/ml}$  resulted in smaller reductions of less than 8% in cell viability, whereas treatment with 2.5 $\mu\text{g/ml}$  caused more than 20% loss of cell viability compared to control untreated cells (Figure 5-2).

#### **5.3.1.2 The effect of aggrecan on expression of ADAMTS-9 in the differentiated SHSY-5Y cells using qRT-PCR**

##### **5.3.1.2.1 RNA integrity**

After growing cells on aggrecan as described in chapter 2.4.5, RNA was extracted from SHSY-5Y cells and the concentration was determined using a Nanodrop-1000 spectrophotometer. The absorbance ratios of A260/A280 were between 0.8 and 1.4 (data not shown) that reflected the purity of extracted RNA as described in chapter 2 (section 2.3.3). The RNA samples were separated by agarose gel electrophoresis as described in chapter 2 (section 2.3.4). All RNA samples showed two bands indicating 28S and 18S ribosomal RNA in a ratio of 2:1 by ethidium bromide staining indicating no degradation or contamination of extracted RNA had occurred (Figure 5-3).

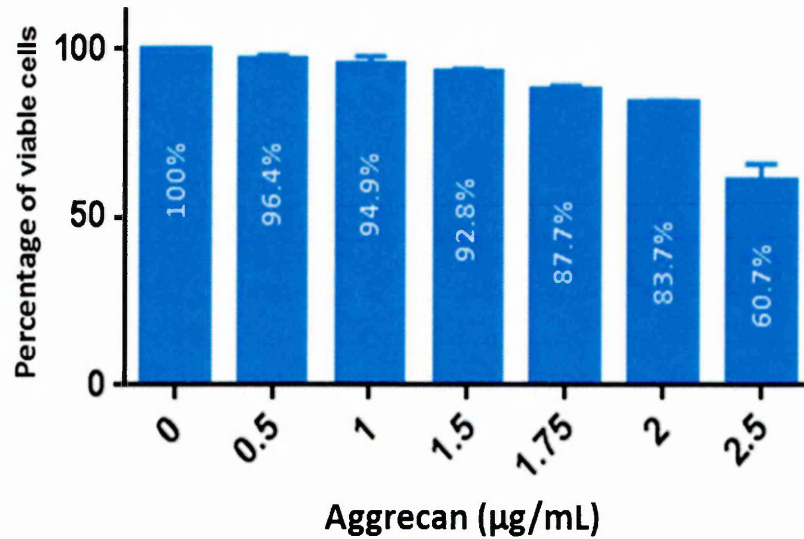


**Figure 5-2: Effect of aggrecan coating concentration on the viability of SHSY-5Y differentiated cells**

The percentage of viable cells on wells coated with aggrecan at different concentrations compared to control cells is shown. A decrease in cell viability was observed following coating with aggrecan at a concentration of 0.5µg/ml 3.6%, with a maximal decrease of 39.3% at 2.5µg/ml aggrecan coating. Data represented as mean ± SEM, n= 4 experiments in triplicate.

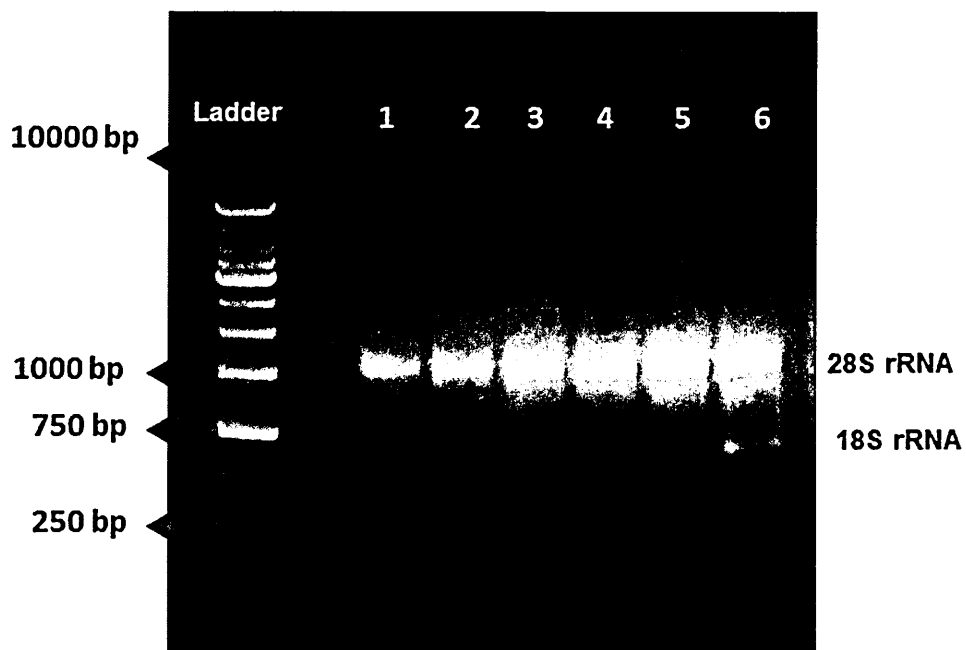


**Figure 5-3: Agarose gel electrophoresis of total RNA extracted from differentiated SHSY-5Y cells**

Visible bands of 28S and 18S ribosomal RNA indicating the integrity of RNA extracted from differentiated SHSY-5Y cells grown on coated and uncoated plates. Lanes 1, 2, 3, 4, 5 and 6 represent samples extracted from SHSY-5Y grown on aggrecan at varying concentrations 0, 0.5, 1, 1.5, 1.75 and 2 $\mu$ g/mL respectively. DNA marker contains thirteen markers between 250-10,000, (Invitrogen). bp= base pairs.

### **5.3.1.2.2 Selection of housekeeping genes as internal control genes**

The strategy here in this study to validate the qRT-PCR was by comparing mRNA expression of three housekeeping genes GAPDH, Cyclophilin-A and HPRT-1 in SHSY-5Y cells under the same conditions i.e. cells grown on varying concentrations of aggrecan from 0 to 2µg/mL as described in chapter 2 (section 2.4.5). The expression of ADAMTS-9 gene was also analysed in differentiated SHSY-5Y cells grown on aggrecan compared to uncoated control. Data showed that GAPDH was the most stable housekeeping gene as its relative mRNA expression was constant either when used as reference or as target gene compared to cells on control uncoated wells. When using HPRT-1 and Cyclophilin-A small changes in gene expression of HPRT-1 and Cyclophilin-A was observed under different test conditions although these were not statically significant with these housekeeping genes (data not shown). Statistical analysis for GAPDH gene expression was performed by Kruskal-Wallis test as described in the following section.

### **5.3.1.2.3 Comparison of ADAMTS-9 mRNA expression in SHSY-5Y in the presence of various concentrations of aggrecan**

The expression of ADAMTS-9 mRNA in differentiated cells grown on aggrecan was determined by qRT-PCR following 7 days *in vitro* exposed to 0.5µg/ml and 1µg/ml. There was an apparent increase in ribosomal RNA yield following aggrecan treatment of SHSY-5Y cells compared to those grown on uncoated plastic. This however, did not affect the real time PCR data as all target gene expression was normalised to housekeeping gene expression. No effect on the expression of the ADAMTS-9 mRNA relative to cells grown on control un-coated plates was seen. However, coating wells with aggrecan at 1.5µg/ml resulted in increased expression of ADAMTS-9 transcript, but this did not reach significant levels ( $P > 0.05$ ) after 7 days *in vitro*. However, high levels of ADAMTS-9 mRNA transcript were observed in SHSY-5Y cells plated on aggrecan at 1.75µg/ml and 2µg/ml compared to untreated cells respectively using Kruskal-Wallis test, (\*\* $P < 0.01$  and \*\*\* $P < 0.001$ ) (Figure 5-4).

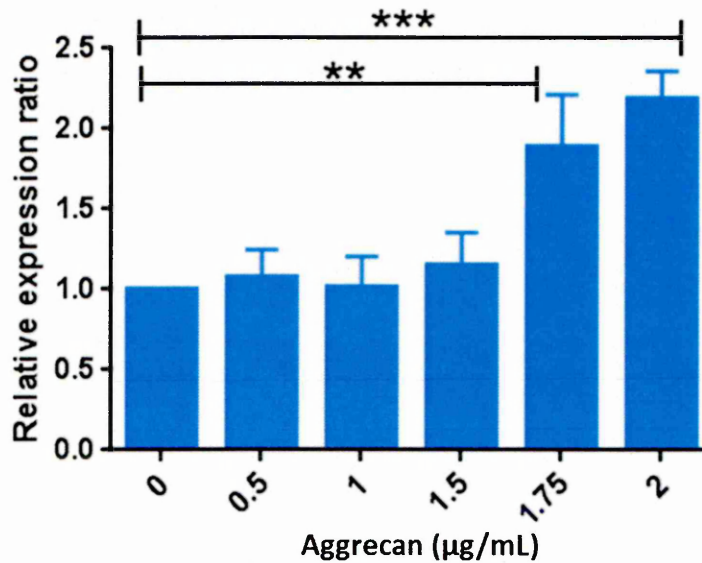


**Figure 5-4: ADAMTS-9 mRNA expression when differentiated SHSY-5Y cells were grown on various concentrations of aggrecan**

Relative fold change in ADAMTS-9 mRNA expression in SHSY-5Y cells following growth on aggrecan for 7 days (0-2 µg/mL). Expression was normalised to GAPDH mRNA level. An increase in ADAMTS-9 expression was observed following growth on aggrecan at concentrations 1.75 and 2 µg/mL using Kruskal-Wallis (\*\*P<0.01, \*\*\*P<0.001). Data represented as mean ± SEM, n=3 experiments with each one done in triplicate.

### **5.3.1.3 Immunocytochemical detection of NF-L and ADAMTS-9 in differentiated SHSY-5Y cells grown on aggrecan**

ICC was performed on differentiated SHSY-5Y cells in order to study the effect of aggrecan on neurite outgrowth and ADAMTS-9 expression following fixation in acetone to enable the intracellular localization of cell marker NF-L and ADAMTS-9. Negative controls were also performed whereby the primary antibody for both NF-L and ADAMTS-9 was omitted. With regards to the coating of plasticware with varying concentrations of aggrecan to assess neurite outgrowth and ADAMTS-9 expression, figure (5-5) illustrates the differences between the effects of varying aggrecan concentrations. There appears to be more neurofilament in the absence of aggrecan in image A, B and C compared with the cells grown on higher aggrecan concentration 2µg/ml in figure (5-5 J, K and L).

Images in figure (5-5) visualised using fluorescent microscopy showed that SHSY-5Y cells grown on wells coated with aggrecan at 0.5 and 1 µg/mL concentrations had no effect on the expression of ADAMTS-9 and NF-L proteins compared to control cells in uncoated wells. However, SHSY-5Y cells in wells coated with aggrecan at 2µg/mL had a higher abundance of ADAMTS-9 and lacked neurite outgrowth, with cells growing as clusters.

### **5.3.1.4 In cell-ELISA detection of NF-L and ADAMTS-9 in differentiated SHSY-5Y cell**

The expression of both ADAMTS-9 and NF-L in differentiated cells was also determined by in cell-ELISA and the results were similar to previous experiment 5.3.1.3. No staining was observed when primary antibody was omitted (replaced by PBS). Cells grown on wells coated with aggrecan at 0.5µg/ml and 1µg/ml had no effect on neurite outgrowth and ADAMTS-9 protein expression within SHSY-5Y cells relative to control cells in uncoated wells at day 7. In contrast, wells with aggrecan coating at 1.5µg/ml showed significant increase in ADAMTS-9 protein and low level expression of NF-L protein within SHSY-5Y cells as shown in Figure (5-6, B and E). Highest concentrations of aggrecan produced high level expression of ADAMTS-9 and low level expression of NF-L using Kruskal-Wallis (\*\*P<0.01, \*\*\*P<0.001) (Figure 5-6 C and F).

**Figure 5-5: Immunocytochemical detection of NF-L and ADAMTS-9 in differentiated SHSY-5Y cells grown on aggrecan**

Dual label immunofluorescence of the differentiated SHSY-5Y cells before and after growth on varying concentrations of aggrecan and expression of ADAMTS-9 (red). Differentiated SHSY-5Y cells stained (green) with anti-NF-L antibody. (A, B and C) cells were grown in the absence of aggrecan and showed normal expression of both NF-L and ADAMTS-9 respectively. (D, E and F) Cells were grown on aggrecan at 1 $\mu$ g/ml and showed no changes in both neurite outgrowth and ADAMTS-9 expression. (G, H and I) cells were grown on aggrecan at 1.5 $\mu$ g/ml and showed a lack of neurite outgrowth and no effect on ADAMTS-9. (J, K and L) cells that were grown on aggrecan at 2 $\mu$ g/ml had a higher level of ADAMTS-9 and lacked neurite outgrowth, cells grew as clusters compared to control SHSY-5Y cells on uncoated wells. Nuclei of the cells were counterstained using DAPI. Images were captured on an inverted stage microscope (Olympus IX81 fluorescence microscope with Cool Snap digital camera (Olympus Media Cybernetics, Silver Spring, USA)).

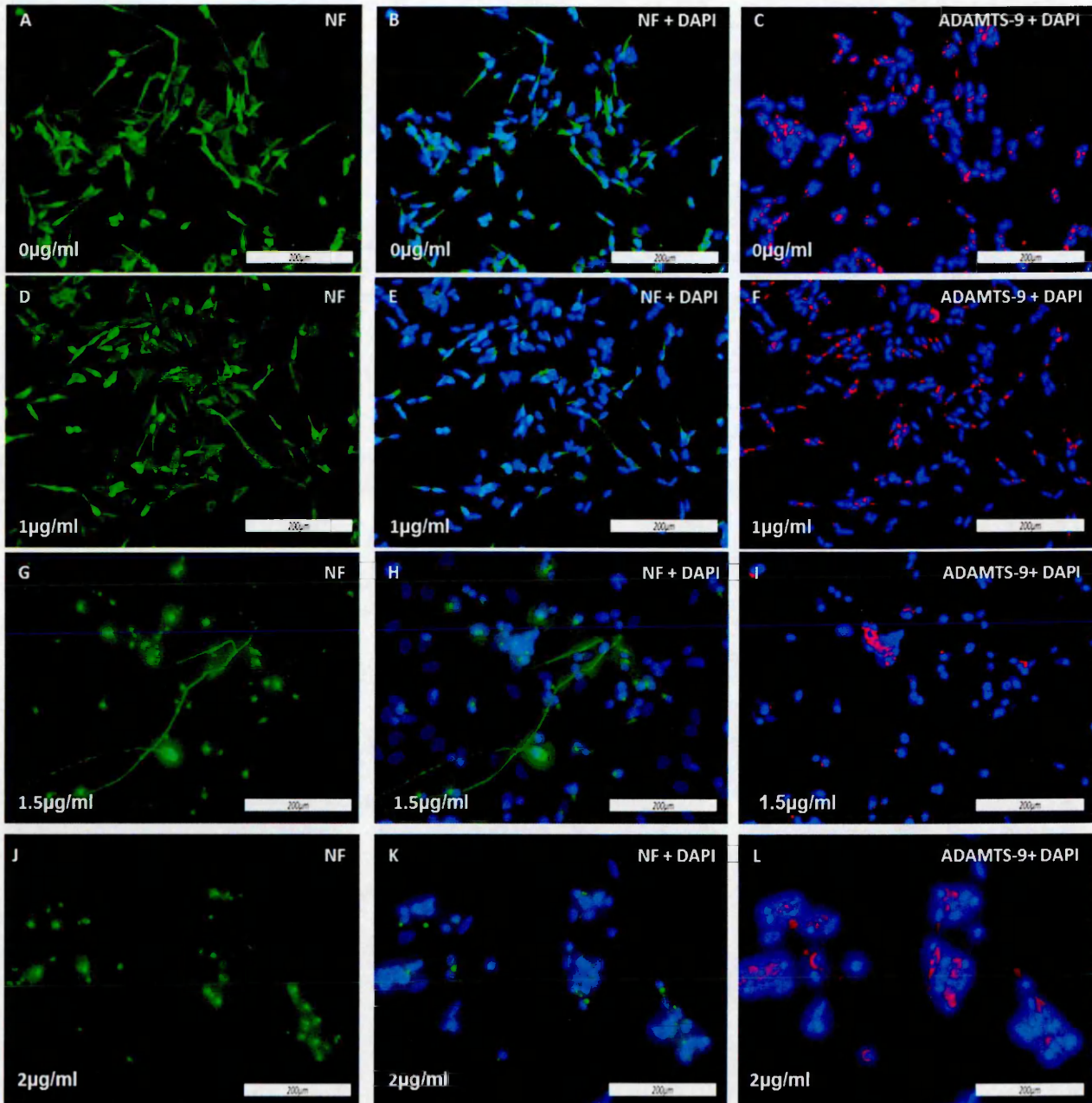
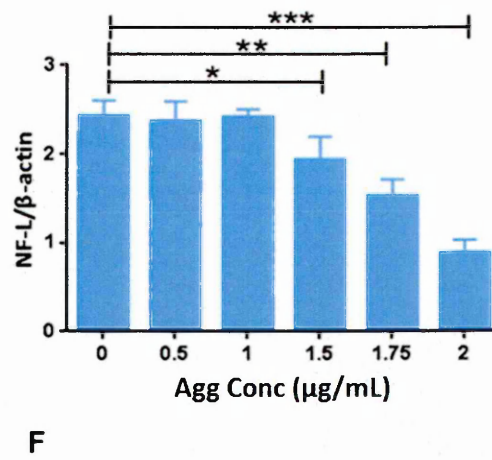
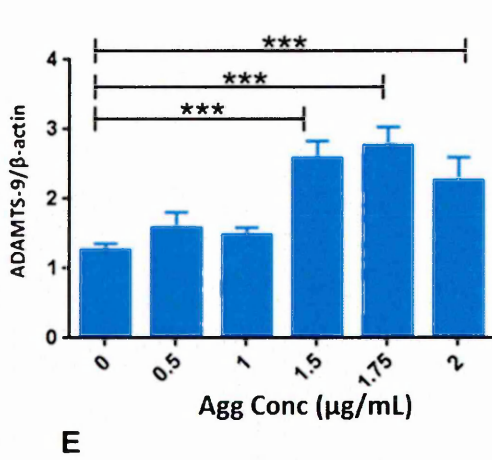
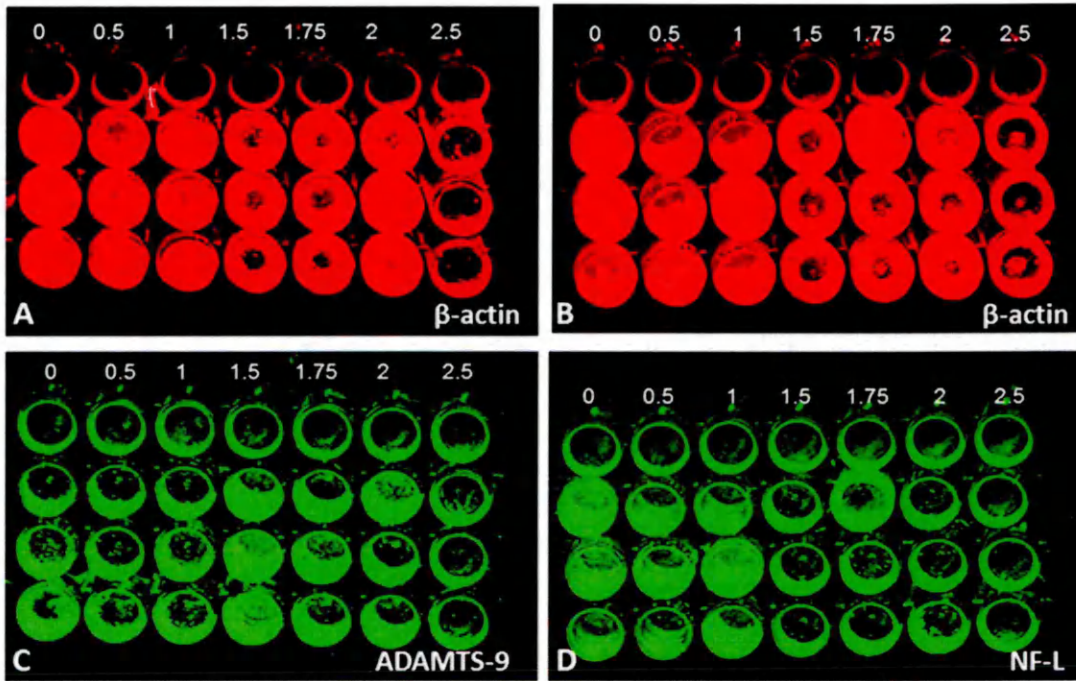


**Figure 5-6: Effect of aggrecan on ADAMTS-9 and NF-L protein expression using an in cell ELISA**

The double labelled in cell ELISA for  $\beta$ -actin (red) (A, B), ADAMTS-9 (green) (C) and NF-L (green) (D). Columns represent varying concentration of aggrecan 0, 0.5, 1, 1.5, 1.75, 2 and 2.5 $\mu$ g/ml respectively, each done in triplicate. The top row of each figure (A-D) shows no staining observed when primary antibody was omitted; the lower three rows show the primary antibody against ADAMTS-9 and NF-L (C) and (D) respectively. Not the difference in graphs (E) and (F), showing much greater expression of ADAMTS-9 is related to low levels of NF-L in cells grow on aggrecan at 1.5, 1.75 and 2 $\mu$ g/ml respectively, compared to control uncoated cells using Kruskal-Wallis, (\* $P < 0.05$ , \*\* $P < 0.01$ , \*\*\* $P < 0.001$ ). Data presented as mean  $\pm$  SEM, n=3 experiments, each one done in triplicate.



## **5.3.2 Effect of pro-inflammatory cytokines on ADAMTS-9 protein expression in CNS cells**

### **5.3.2.1 Effect of pro-inflammatory cytokines on cell viability**

#### **5.3.2.1.1 Human foetal microglial cell line CHME3**

Treatment of CHME3 cells with IL-1 $\beta$  at 100ng/mL resulted in a 15% decrease in viable cells compared to control untreated cells, similarly for 48h treatment with TNF- $\alpha$  at 100ng/mL an 11.3% decrease in viable cells compared to control was observed. Treatment with 100ng/mL IFN- $\gamma$  resulted in a 12.6% decrease in viable cells. A decrease in the percentage of viable cells was also observed following dual treatment of CHME3 cells with IL-1 $\beta$  and TNF- $\alpha$  at 10 and 100ng/mL, with maximal 10.3% reduction observed at 100ng/mL with both cytokines (Figure 5-7, a).

#### **5.3.2.1.2 Primary human astrocytes**

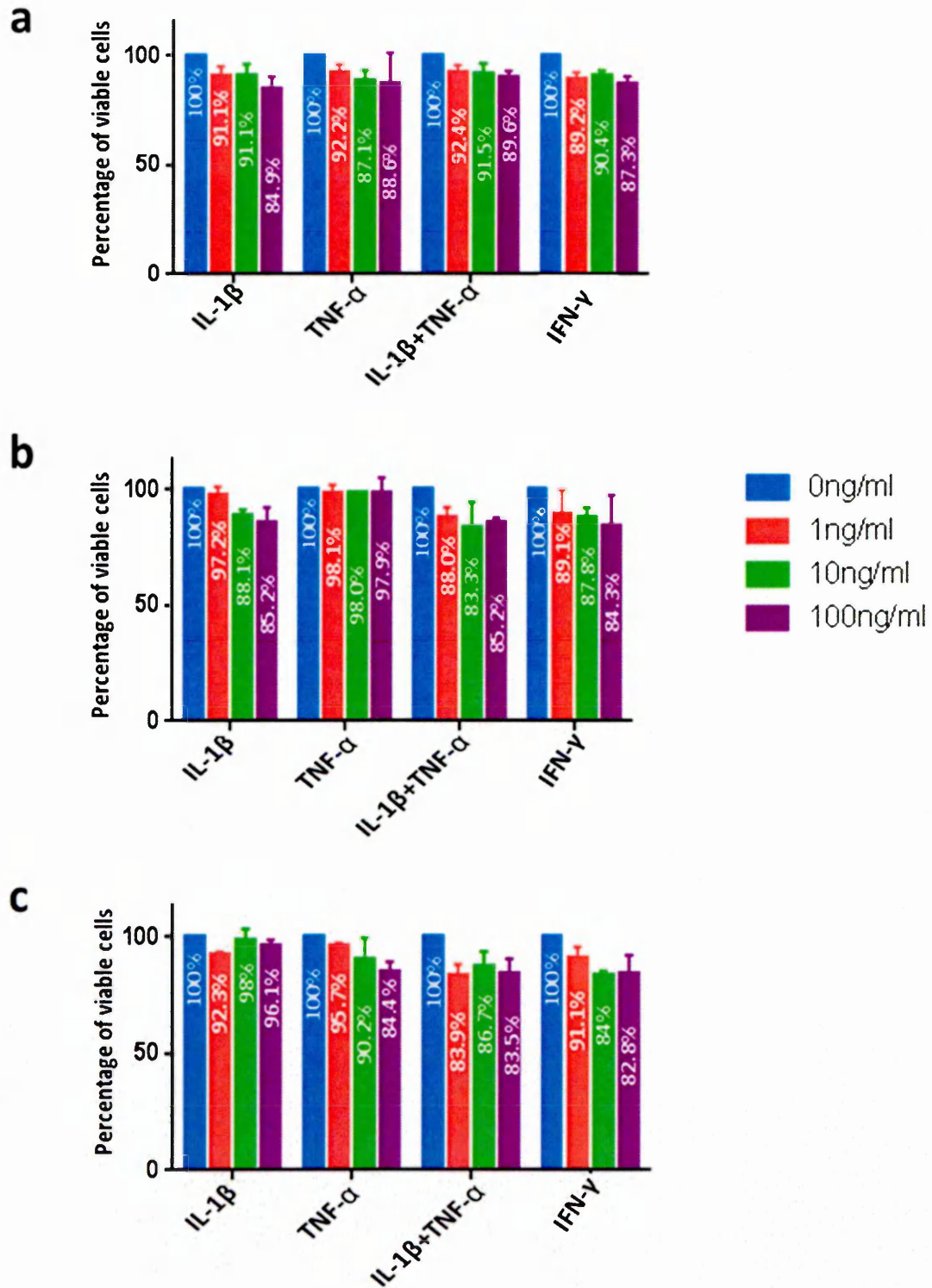
Treatment of primary astrocytes with 1ng/mL IL-1 $\beta$  for 48hr resulted in a small 2.7% decrease in the percentage of viable cells compared to untreated control cells, whereas dual treatment with 1ng/mL of IL-1 $\beta$  and TNF- $\alpha$  resulted in an 11.9% decrease in the number of viable cells compared to controls. Treatment of astrocytes with 100ng/mL of IL-1 $\beta$  + TNF- $\alpha$  or IL-1 $\beta$  alone for 48hrs resulted in a 14.7% decrease in the number of viable cells, whereas 100ng/mL of IFN- $\gamma$  caused a 15.6% reduction in the number of viable cells (Figure 5-7, b).

#### **5.3.2.1.3 SHSY-5Y differentiated cells**

TNF- $\alpha$  treatment of differentiated SHSY-5Y cells resulted in a decrease in cell number, with a maximal 15.5% decrease observed at 100ng/mL, similarly IFN- $\gamma$  treatment resulted in a decrease in viable cells, with maximal 15.9% decrease at 100ng/mL. Dual treatment of TNF- $\alpha$  and IL-1 $\beta$  resulted in a decrease in viable cells at all concentrations, with a maximal 16.0% decrease observed at 100ng/mL. Treatment of SHSY-5Y with IL-1 $\beta$  did not alter the viability of cells and percentage was less than 7% (Figure 5-7, c).

**Figure 5-7: Effect of pro-inflammatory cytokines on the viability of CNS cells *in vitro***

Effect of pro-inflammatory cytokines on the viability of CHME3 cells, (a) human astrocytes (b) and differentiated SHSY-5Y cells (c). 48hrs treatment with single and dual cytokines IL-1 $\beta$ , TNF- $\alpha$  and IFN- $\gamma$  at 0-100ng/ml. Data represented as mean  $\pm$  SEM, n=3 experiments, each done in triplicate.



### **5.3.2.2 Effect of pro-inflammatory cytokines on ADAMTS-9 protein expression in CNS cells using ICC**

To detect the modulation of ADAMTS-9 expression in CHME3, human primary astrocytes and SHSY-5Y cells, they were treated with pro-inflammatory cytokines (IL-1 $\beta$ , TNF- $\alpha$  and IFN- $\gamma$ ) which have been implicated in the pathogenesis of MS.

#### **5.3.2.2.1 Human foetal microglial cell line CHME3**

On treatment of human foetal microglia cell line (CHME3) with varying concentrations of pro-inflammatory cytokines to assess expression of ADAMTS-9, qualitative analysis via image J software showed that treatment of CHME3 with single pro-inflammatory cytokine IL-1 $\beta$  and IFN- $\gamma$  had no effect on the expression of ADAMTS-9 protein. Whereas, dual treatment of IL-1 $\beta$  and TNF- $\alpha$  at concentrations 10 and 100 ng/mL down-regulated ADAMTS-9 protein expression (figure 5-8).

#### **5.3.2.2.2 Primary human astrocytes**

Primary human astrocytes treated with single and dual cytokines IL-1 $\beta$  and TNF- $\alpha$  at all concentrations tested had no effect on expression of ADAMTS-9 (Appendix V). In comparison, IFN- $\gamma$  initiated an increase in ADAMTS-9 protein expression by primary astrocytes at 10 and 100ng/mL (Figure 5-9). Statistical analysis using Image J software confirmed this increase in ADAMTS-9 when astrocytes were treated with IFN- $\gamma$  at 10 and 100 ng/ml (Figure 5-10, b).

#### **5.3.2.2.3 SHSY-5Y differentiated cells**

Treatment of SHSY-5Y cell line with IL-1 $\beta$ , TNF- $\alpha$  and IFN- $\gamma$  had no statically significant effect on ADAMTS-9 expression at all concentrations tested (Data not shown). Culturing of cells, treatment of cells and ICC experimental procedure were identical to those adopted for the human primary astrocyte and CHME3 cells.

**Figure 5-8: Effect of pro-inflammatory cytokines on ADAMTS-9 expression in CHME3 cells**

Single immunofluorescence staining shows the expression of ADAMTS-9 in CHME3 cell line untreated and after treatment with varying concentrations (0-100ng/mL) of pro-inflammatory cytokines (IL-1 $\beta$ , TNF- $\alpha$  and IFN- $\gamma$ ). Images A, B and C cells were untreated. Images D, E and F show single and dual pro-inflammatory cytokines at concentration 1ng/ml. (G, H and I) and (J, K and L) with the same pro-inflammatory cytokines at concentrations 10 and 100ng/mL respectively. ADAMTS-9 (red), nuclei of the cells was counterstained using DAPI. Images were captured on an inverted stage microscope (Olympus IX81 fluorescence microscope with Cool Snap digital camera (Olympus Media Cybernetics, Silver Spring, USA)).

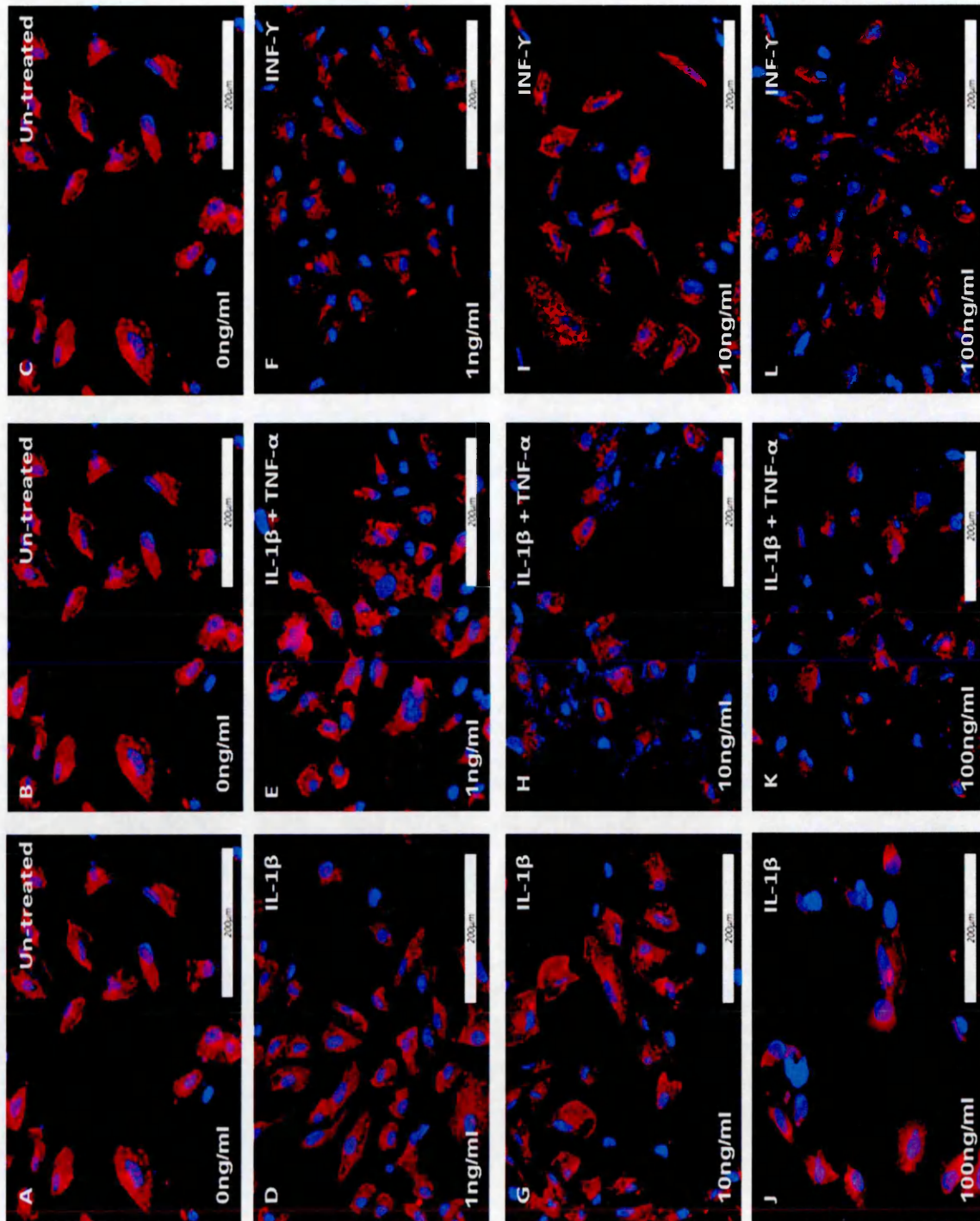


**Figure 5-9: Effect of pro-inflammatory cytokine interferon- $\gamma$  on ADAMTS-9 expression in human primary astrocytes**

Dual immunofluorescence shows the expression of GFAP (red) and ADAMTS-9 (green) in human primary astrocytes before and after treatment with varying concentrations (0-100ng/mL) of IFN- $\gamma$ . Images from A to D represent untreated cells. Images from E to H represent cells treated with IFN- $\gamma$  at a concentration 1ng/ml. (I, J, K and L) and (M, N, O and P) at concentration 10 and 100ng/mL respectively. Nuclei of the cells were counterstained using DAPI. Images were captured on inverted stage microscope (Olympus IX81 fluorescence microscope with Cool Snap digital camera (Olympus Media Cybernetics, Silver Spring, USA)).

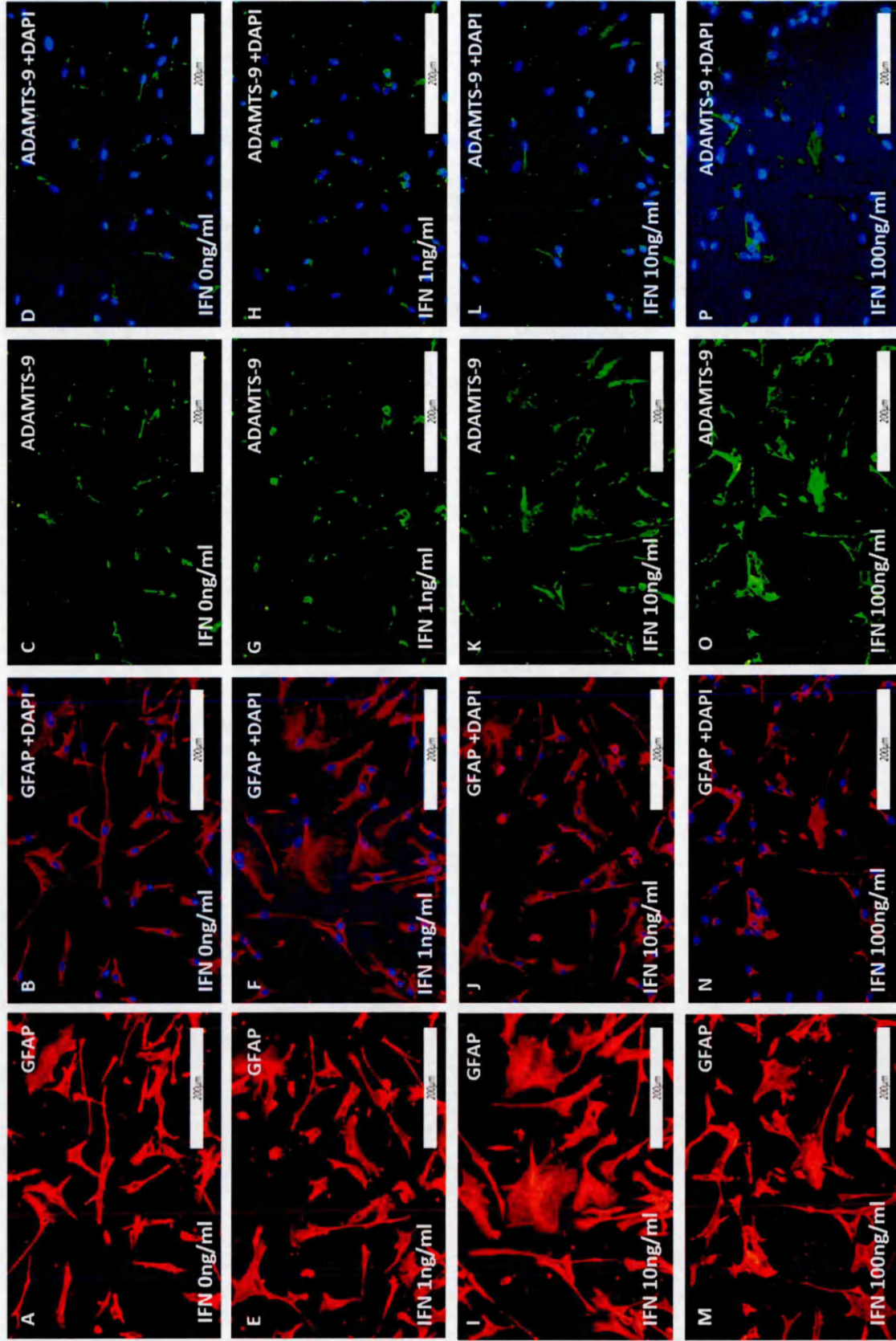
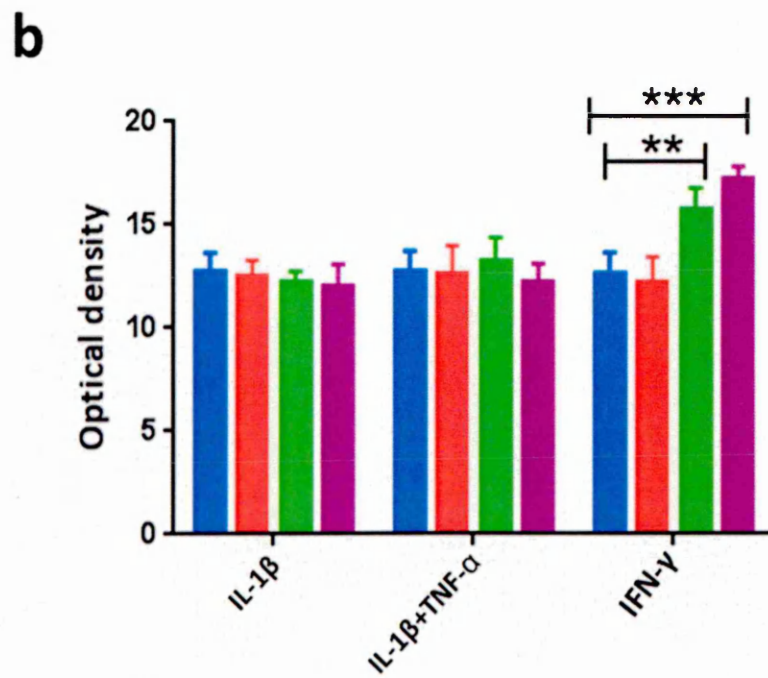
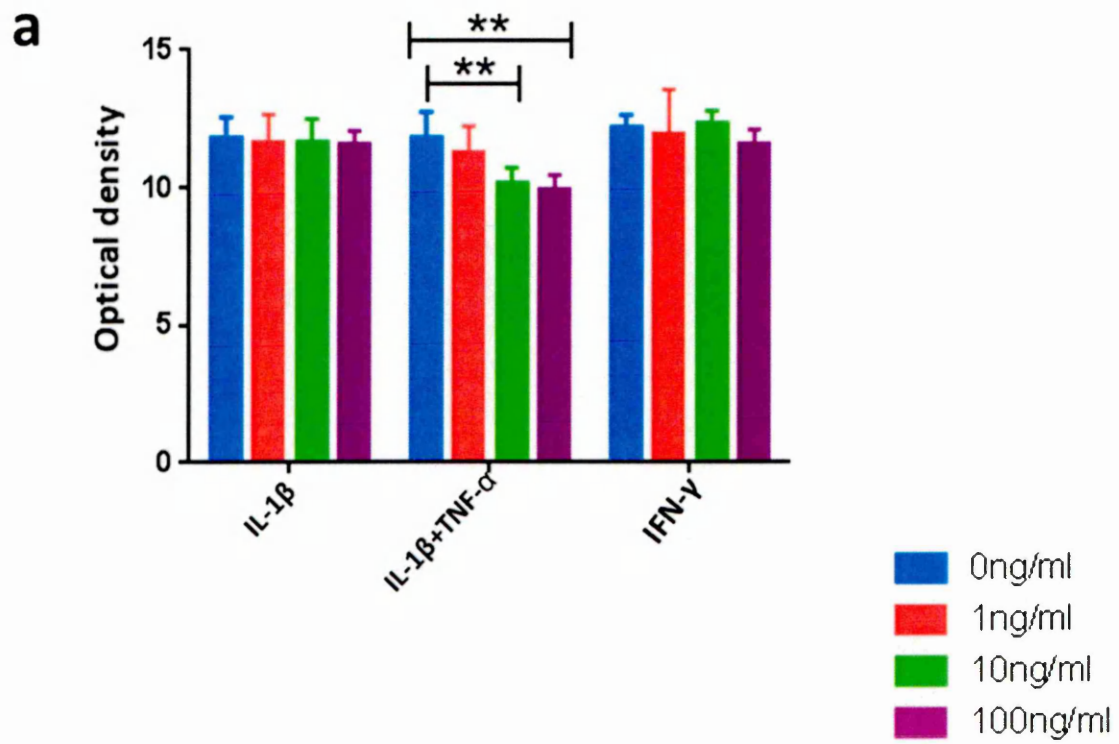


**Figure 5-10: Statistical analysis of the effect of pro-inflammatory cytokines on ADAMTS-9 expression in CHME3 cells and human primary astrocytes using ICC**

The effect of pro-inflammatory cytokines on ADAMTS-9 expression in CHME3 cells (a) and human astrocytes (b), after 48hrs treatment with single and dual cytokines with varying concentrations (0, 1, 10, 100ng/ml). Much lower expression of ADAMTS-9 in CHME3 treated with dual pro-inflammatory (IL-1 $\beta$  and TNF- $\alpha$ ) at concentrations 10 and 100ng/mL were seen (a). Treatment of astrocytes with IFN- $\gamma$  at 10 and 100ng/mL resulted in up-regulation of ADAMTS-9 expression (b). Data presented as mean  $\pm$  SEM, n=3 experiments, each done in triplicate, using Kruskal-Wallis, (\*\*P<0.01, \*\*\*P<0.001).



### 5.3.2.3 Effect of pro-inflammatory cytokines on ADAMTS-9 protein in

#### CNS cell using WB

The extracted proteins from CNS cells were quantified by Bradford assay as described in chapter 2.2.3, and the same amount of protein (20µg) was loaded per well on SDS-PAGE gels. Western blot analysis for all CNS cells utilised in this study was described in 2.2.4-2.2.7. The expression levels of ADAMTS-9 were investigated using quantitative two colour staining IRDye® 680 LT goat anti-mouse IgG for β-actin (red) and IRDye® CW donkey anti-goat IgG for ADAMTS-9 (green). Western blot analysis demonstrated that ADAMTS-9 was present in CHME3 cells (Figure 5-11, a), primary human astrocytes (Figure 5-11, b) and SHSY-5Y (Figure 5-11, c), and produced single bands at ~180KDa.

#### 5.3.2.3.1 Human foetal microglial cell line CHME3

Treatment of CHME3 cells with TNF-α and IL-1β for 48hrs at concentration of 1, 10 and 100ng/ml and treatment with IFN-γ at concentration of 1, 10 and 100ng/ml had no effect on the expression of ADAMTS-9 relative to control untreated cells (Figure a). However, the expression of ADAMTS-9 in the CHME3 was significantly down-regulated following dual treatment with IL-1β and TNF-α at 10 and 100ng/ml ( $P < 0.05$ , Kruskal-Wallis as shown in Figure 5-12, a).

#### 5.3.2.3.2 Human primary astrocytes

Dual treatment of human primary astrocytes with IL-1β for 48hrs at varying concentration (0-100ng/ml) had no effect on expression of ADAMTS-9. However, treatment with TNF-α at concentrations 10 and 100ng/ml resulted in an increase of ADAMTS-9, but this did not reach significant levels  $P > 0.05$  after 48hrs of treatment. High levels of ADAMTS-9 were expressed in astrocytes treated with IFN-γ at concentrations 10 and 100ng/ml ( $P < 0.001$ ) (Figure 5-12, b).

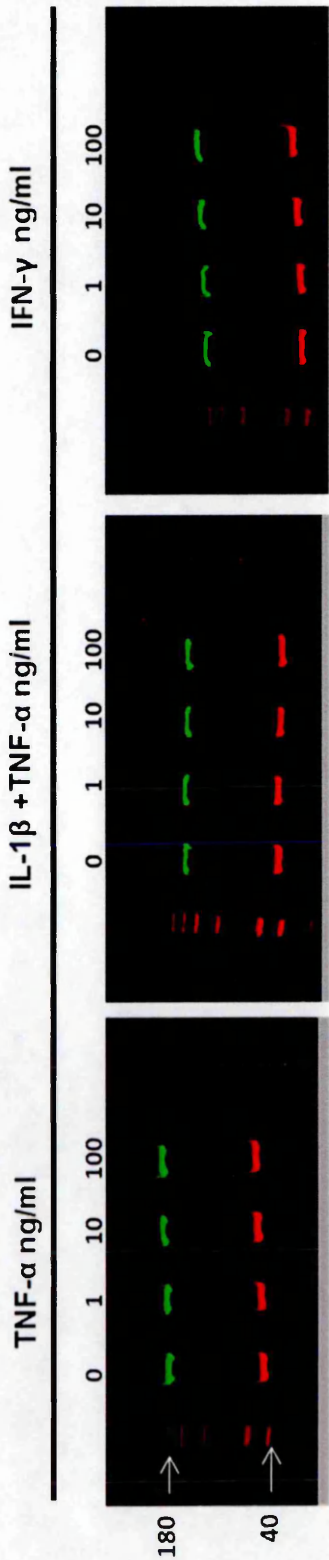
#### 5.3.2.3.3 SHSY-5Y cells

No statistically significant effect on ADAMTS-9 protein level expression was observed in differentiated SHSY-5Y cells following 0-100ng/ml of single or dual treatment with IL-1β, TNF-α and IFN-γ (Figure 5-12, c).

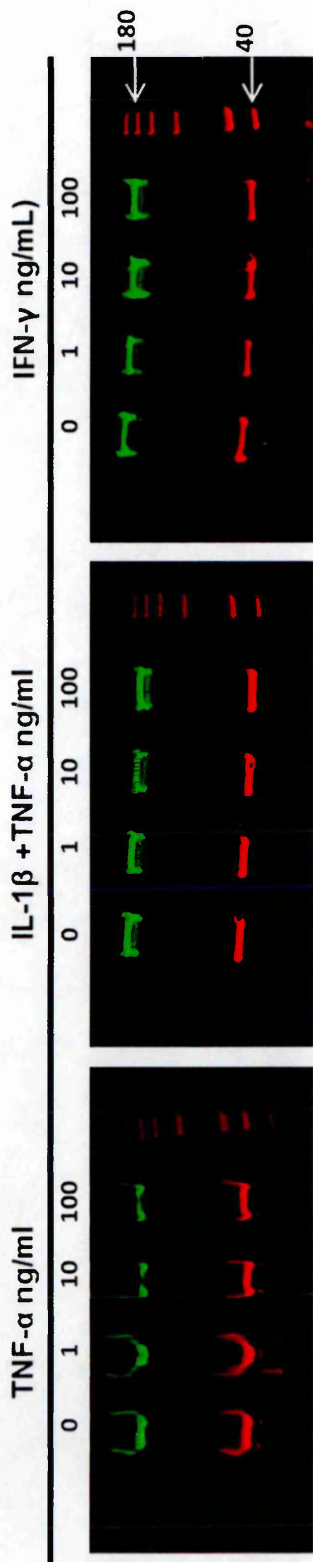
**Figure 5-11: Effect of Pro-inflammatory cytokines on expression of ADAMTS-9 in CNS cells assessed by WB**

The double labelled western blot for  $\beta$ -actin (red) and ADAMTS-9 (green), The ADAMTS-9 (~180KDa) and  $\beta$ -actin (~42KDa) were identified by a single band. Protein extracted from CNS cells following treatment with varying concentrations (0, 1, 10 and 100ng/ml) of pro-inflammatory cytokines IL-1 $\beta$ , TNF- $\alpha$  and IFN- $\gamma$ , (a) human microglia (CHME3), (b) human primary astrocytes and (c) differentiated neuroblastoma (SHSY-5Y).

a



b



c

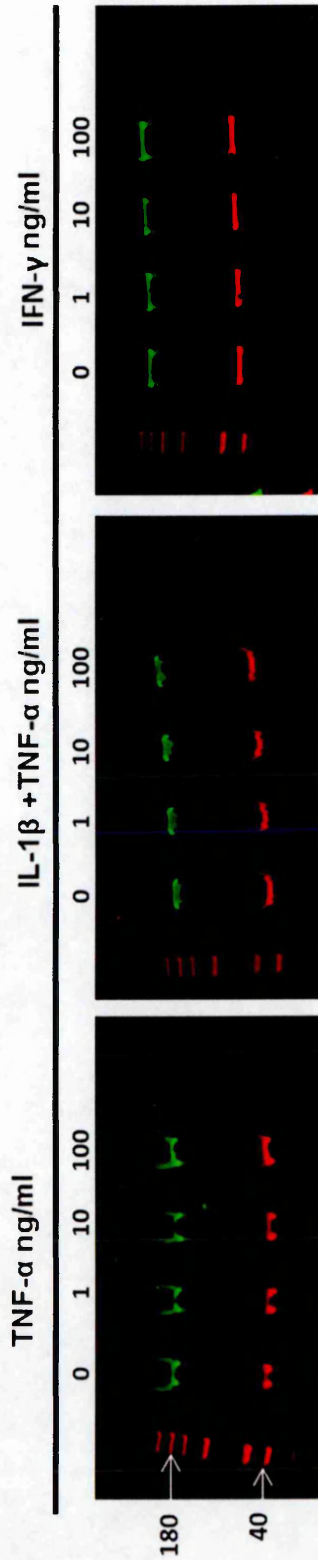


**Figure 5-12: Statistical analysis of the effect of pro-inflammatory cytokine treatment on expression of ADAMTS-9 in CNS cells assessed by WB**

The effect of pro-inflammatory cytokines on ADAMTS-9 expression in CHME3 (a), human astrocytes (b) and differentiated SHSY-5Y (c). Cells were treated for 48hrs with single and dual cytokines (IL-1 $\beta$ , TNF- $\alpha$  and IFN- $\gamma$ ) with varying concentrations (0, 1, 10, 100ng/ml). Lower expression of ADAMTS-9 in CHME3 cells treated with dual pro-inflammatory (IL-1 $\beta$  and TNF- $\alpha$ ) at concentrations 10 and 100ng/mL was observed (a). Treatment of astrocytes with INF- $\gamma$  at 10 and 100ng/mL resulted in up-regulation of ADAMTS-9 (b). Data presented as mean  $\pm$  SEM, n=3 experiments each done in triplicate, using Kruskal-Wallis test.

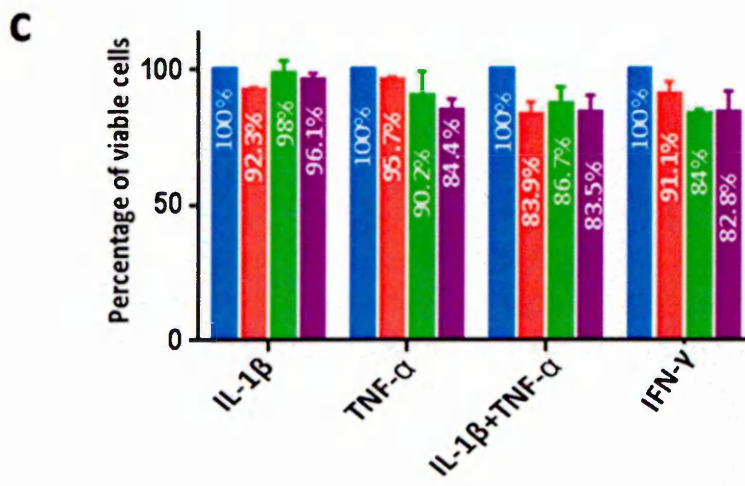
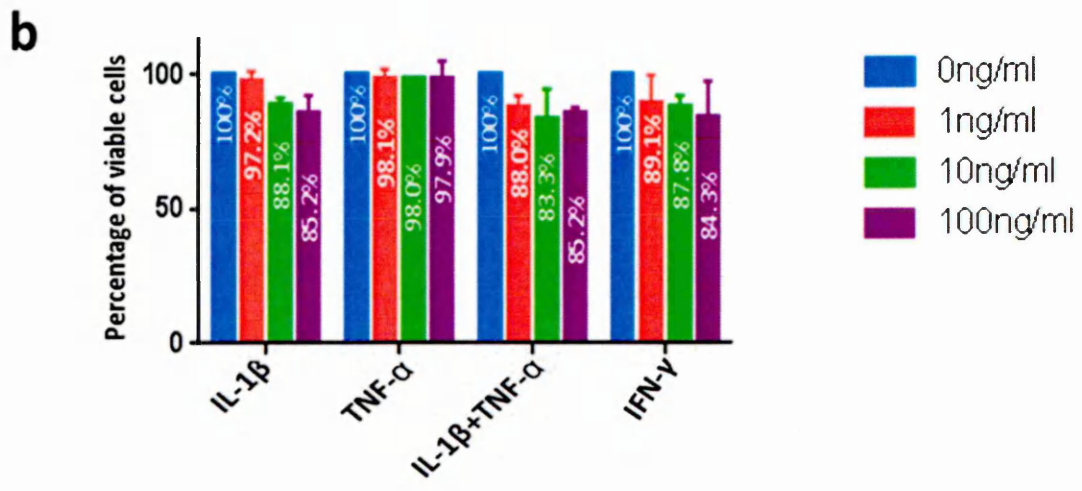
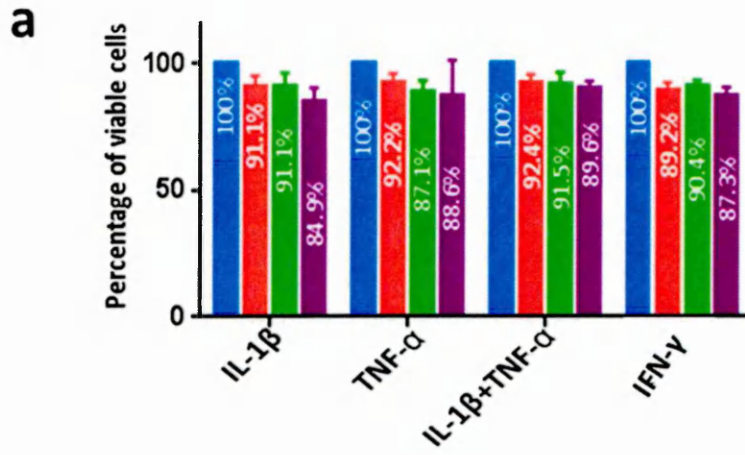


**Table 5-1: Summary of the effect of pro-inflammatory cytokines on ADAMTS-9 protein expression in CNS cell in *in vitro***

Pro-inflammatory cytokines could induce a significant change in ADAMTS-9 expression in CNS cells following treatment with varying cytokines concentration (1, 10 and 100ng/ml). IL-1 $\beta$  + TNF- $\alpha$  represents dual treatment with both cytokines. A significant decrease in expression is represented as  $\downarrow$ , whereas increase in expression is represented as  $\uparrow$ . No significant change is represented by: (-).

Cells	ICC/WB			
	IL-1 $\beta$	TNF- $\alpha$	IFN- $\gamma$	IL-1 $\beta$ +TNF- $\alpha$
CHME-3	-	-	-	$\downarrow$
Human primary astrocytes	-	-	$\uparrow$	-
SHSY-5Y	-	-	-	-

## 5.4 Discussion

### 5.4.1 Effect of aggrecan on neuronal phenotype; impact of ADAMTS-9

Neuronal growth cones integrate signals from outgrowth promoting molecules, e.g. laminin or fibronectin, and outgrowth-inhibiting molecules, e.g. CSPGs (Dickendesher *et al.*, 2012; Mammadov *et al.*, 2012; Tonge *et al.*, 2012). The CSPGs can inhibit neurite growth by several mechanisms such as binding to adhesion molecules (integrin  $\beta$ ) which are a bridge for cell-cell and cell ECM interactions (Tan *et al.*, 2011). Enzymatic cleavage of CSPG core protein has been reported to permit some axonal regrowth in CNS injury (Cua *et al.*, 2013). The objective of this current study was to determine whether ADAMTS-9 is expressed in CNS cells microglia (CHME3), primary astrocytes and differentiated neuronal cells (SHSY-5Y), under basal conditions. All the three cell types expressed ADAMTS-9 at the protein level. Previous studies in our laboratory revealed that CHME3, SHSY-5Y and primary astrocytes expressed mRNA for ADAMTS-1, -4, -5 and -9 (Cross *et al.*, 2006; Reid *et al.*, 2009).

The SHSY-5Y cell line has been widely used as an *in vitro* model of neurons since the early 1980s as these cells have many functional properties of neurons. They express neuronal marker enzyme activity tyrosine and dopamine- $\beta$  hydroxylases and express NF proteins (Skotake *et al.*, 2012). RetA is a metabolite of vitamin A that mediates functions of vitamin A, which are required for development and differentiation of neuronal cells and was used to differentiate (Clagett *et al.*, 2006). The SHSY-5Y cells were treated with RetA and visualised using light microscopy, showing a significant increase in the length of neurites containing neurofilaments compared to the control untreated cells, which supports results generated by other studies, regarding alterations in cellular morphology with RetA treatment (Encinas *et al.*, 2000; Clagett *et al.*, 2006).

Tucholski *et al.*, (2001) also reported increased neurite outgrowth with regards to number and length of neurites, and the necessary component of RetA-induced SHSY-5Y cell differentiation was simultaneously increased expression of active tissue transglutaminase which creates an inter or intramolecular bonds that are highly resistant to proteolysis (protein degradation)(Dwane *et al.*, 2013). Other studies in our group indicated that RetA differentiated SHSY-5Y cells showed a statistically significant

increase in ADAMTS-1 and -9 expression when compared to cells cultured without RetA (Reid *et al.*, 2009; Gibrel, 2012). A study by East *et al.*, (2007) showed increased ADAMTS-5 mRNA in cartilage explants treated with RetA. The increase in ADAMTS-9 in differentiated neuronal cells could lead to an increase in breakdown of CSPGs and allow neurite outgrowth as CSPGs are normally inhibitory. However, this study did not show any difference in levels of aggrecan expression or its neoepitope, in RetA treated SHSY-5Y cells compared to control untreated cells, thus suggesting that neuronal phenotype SHSY-5Y was not linked to increase ADAMTS-9 activity on aggrecan to generate the neoepitope. CSPG expression could be regulated at different stages including pre-transcriptional (e.g. cytokine modulation of mRNA expression) or post-transcriptional. Stability of the CSPG expression level in normal physiology prevents any changes that could result in neurodegenerative disease (Siebert *et al.*, 2014).

The response of neurons from animal models to the ECM molecules, LN and CSPGs, has been well studied *in vivo* and *in vitro* (Hynds *et al.*, 1999; Hynds *et al.*, 2001; Lau *et al.*, 2012; Cua *et al.*, 2013). In the present study, the effects of aggrecan on SHSY-5Y human neuroblastoma cell line, a well-accepted model of human neuronal differentiation, demonstrated CSPG was not permissive for neurite outgrowth from these cells at higher concentrations (2µg/ml), confirming previous studies (Hynds *et al.*, 1999; Lau *et al.*, 2013). Important and novel to this inquiry is the finding that aggrecan inhibited expression of NF-L and increased expression of ADAMTS-9 within these cells at concentrations of 2µg/ml. It is also similar to other studies which indicated that CSPGs decreased neurite initiation (number of neurites/cell, percentage of neurite-bearing cells) compared with cells plated on LN or control uncoated coverslip in SHSY-5Y cells (Hynds *et al.*, 1999). Many studies have established that CSPGs inhibit neurite outgrowth *in vitro* and they restrict axonal regeneration *in vivo* (Hynds *et al.*, 2001; Sandving *et al.*, 2004; Cua *et al.*, 2013).

Intrinsic attempts by axons to overcome CSPG inhibition through local ADAMTS-4 expression have been documented in CNS injury (Hamel *et al.*, 2008; Tauchi *et al.*, 2012), while there is no literature for ADAMTS-9 at this time. The results from in-cell ELISA analysis were interesting with regards to the cells in aggrecan coated wells having higher levels of ADAMTS-9 and lower levels of NF-L; this confirms that aggrecan is affecting neuronfilament subunit expression as well as ADAMTS-9 protein expression

by differentiated SHSY-5Y cells. Comparing data generated from qRT-PCR of SHSY-5Y cells with the data in figure (5-5/ICC) as well as Licor images of in-cell ELISA data in figure (5-6) with regards to expression of ADAMTS-9 and NF-L, shows that results were similar to those previously published (Schmalfedt *et al*, 2000; Yamada *et al*, 1997; Cua *et al*, 2013). They found that several MMPs as well as ADAMTS-4 were effective in degrading CSPGs and overcoming the promotion of neurite outgrowth observed on purified CSPGs and the neuronal ECM. The differences may be related to relative insensitivity of the neurite outgrowth where a large difference in aggrecan degradation may be required before an impact on neurite outgrowth can be observed. Alternatively, as different ADAMTSs can cleave the same substrates at different sites producing a different set of peptide fragments (Overall *et al.*, 2002); ADAMTS-9 could have produced aggrecan fragments, undetectable through the antibodies used in current western blotting that has growth-promoting properties reminiscent of certain CS-GAG chains (Clement *et al.*, 1999).

A previous study indicated that ADAMTS-4 could enhance neurite outgrowth from cultured rat neurons on both permissive and inhibitory substrates through a non-proteolytic mechanism that implicated the Erk1/2 MAP kinase cascade (Hamel *et al.*, 2008). This mechanism might not be a possibility in this study, where active ADAMTS-9 was not pre-incubated with aggrecan and was not available to interact with the cell surface or to act intracellularly. ADAMTS-9 may act through proteolytic mechanisms, as heat-inactivated ADAMTS-9 with no catalytic activity did not have the same efficacy. Aside from being processed by ADAMTS-9, aggrecan is also susceptible to cleavage by ADAMTS-1, ADAMTS-4 and ADAMTS-5 (Rauch, 2004). These other members of the ADAMTS family may demonstrate efficacy similar to ADAMTS-9 and would require further investigation.

ADAMTSs have been studied in adult CNS injury; the expression of ADAMTS-4 was altered in CNS white matter degeneration in MS (Haddock *et al.*, 2006). In a rat model of stroke, ADAMTS-4 correlated with a decrease in phosphacan accumulation (Haddock *et al.*, 2007). ADAMTS-9 is synergistically induced by interleukin-1 $\beta$  and TNF- $\alpha$  in OUMS-27 human chondrocytes (Demircan *et al.*, 2005). ADAMTS-9 mRNA was showed to be significantly up-regulated in tMCAo brain tissue compared to sham-operated animals at 24h post-ischemia (Reid *et al.*, 2009). ADAMTS-9 is upregulated in

MS active lesions, where a function would be to remodel the lesion microenvironment including potential clearance of CSPGs; however glial scars containing PGs still result and persist. The reason for incomplete clearance, include the inadequate production of ADAMTS-9, the overabundance of deposition of CSPGs in large lesions, the temporal mismatch between ADAMTS-9 and CSPG production, the presence of inhibitors (TIMP 3) that mitigate ADAMTS-9 activity and the likely requirement of other collaborative proteases. Further experiments are needed to address these possibilities. Finally, although the focus of this chapter is aggrecan, other ECM components including collagen, fibronectin, tenascins, proteoglycans and other classes of CSPGs are also deposited in lesions, and the capacity of ADAMTS-9, MMPs and other proteases to process these molecules in the context of CNS inflammation in MS remain to be investigated.

#### **5.4.2 Effect of pro-inflammatory cytokines on ADAMTS-9 expression in CNS cells**

*In vitro* studies with cytokine treatments such as IL-1 $\beta$  and TNF- $\alpha$ , which are implicated in MS pathogenesis could induce ADAMTSs (Siebert *et al.*, 2014). A previous study in our laboratory indicated that U373, U87-MG, primary astrocytes CHME3 microglia cells express ADAMTS-1, -4 and -5 (Cross *et al.*, 2006). The cloning of ADAMTS-9 from CNS cell cDNA library previously showed that the peptidase was expressed by such cells in the mouse (Clark *et al.*, 2000). These data in this study showed that ADAMTS-9 was expressed at the protein level by primary human astrocytes and the human foetal microglia cell line (CHME3). ICC, in-cell ELISA and WB also confirmed that ADAMTS-9 protein was expressed by the neuroblastoma cell line (SHSY-5Y) following differentiation. Overall, these data confirm that glial cells and neurons in the human CNS have the potential to constitutively express ADAMTS-9 *in vivo* as shown previously in chapter 4. This finding is in contrast to expression in CNS white matter with ADAMTS-1 which was not detected in differentiated SHSY-5Y cells, whereas Sasaki *et al.*, (2001) showed that neuroblastoma cell line (N1E-115) did express ADAMTS-1.

The effect of pro-inflammatory cytokines on expression of ADAMTS-9 in CNS cells was variable. This was highlighted by IFN- $\gamma$  which had no effect on ADAMTS-9 expression level in both CHME3 and SHSY-5Y cell lines but significantly up-regulation expression in

primary astrocyte cells. There was no modulation of ADAMTS-9 protein found in the differentiated SHSY-5Y cell line with either single treatment of IL-1 $\beta$ , TNF- $\alpha$  and IFN- $\gamma$  or dual treatment with IL-1 $\beta$  plus TNF- $\alpha$ . ADAMTS-9 expression could be regulated at different stages including pre-transcriptional (e.g. cytokines modulation expression), post-transcriptional (alternative splicing) and post-translational (e.g. pro-domain or c-terminal cleavage) (Gibrel *et al.*, 2012). In contrast to these findings, modulation of ADAMTS-9 expression by IL-1 $\beta$  and TNF- $\alpha$  has been reported previously by Demircan *et al.*, (2005) in chondrocytes and by Bevitt *et al.*, (2003) in retinal pigment epithelium (RPE)-derived cell line.

Expression of ADAMTS-9 was not modulated by single cytokine treatment with IL-1 $\beta$  or TNF- $\alpha$  in primary astrocytes. This finding further adds to previous data published by Haddock *et al.*, (2003), in that neither IL-1 $\beta$  nor TNF- $\alpha$  influenced ADAMTS-1, -4 or -5 mRNA expression level in U87-MG glioma cell line. In contrast, TGF- $\beta$ 1 was demonstrated in the same study to significantly down-regulate ADAMTS-1 expression level in this cell line, as reported here for dual treatment with IL-1 $\beta$  and TNF- $\alpha$  down-regulation of ADAMTS-9 expression in primary astrocytes. Data published by our group using qRT-PCR in the same cells SHSY-5Y and CHME3 proposed to a certain extent that ADAMTS-9 modulation is comparable to that of other ADAMTS aggrecanases in the CNS (Reid *et al.*, 2009). IL-1 $\beta$  had a similar effect on ADAMTS-1, 4 and -5 in CHME3 cells as it did on ADAMTS-9 in that no modulation was detected. In contrast to data obtained with ADAMTS-9, IL-1 $\beta$  and TNF modulated transcription of ADAMTS-1 and ADAMTS-4 in CHME3 and differentiated SHY-5Y cells (Cross *et al.*, 2006; Reid *et al.*, 2009).

The concentrations of cytokines used are very important to produce a statistically significant modulation of ADAMTS-9 protein in CNS cells, for instance, 1ng/ml, 10ng/ml and 100ng/ml (both IL-1 $\beta$  and TNF- $\alpha$ ) in SHSY-5Y, 1ng/mL (IFN- $\gamma$ ) in human primary astrocytes and 1ng/mL of both TNF- $\alpha$  and IL-1 $\beta$  in CHME3 cells were assessed. These concentrations of cytokines are likely to exceed physiological concentrations that are found in the normal human brain but exposure to a full combination of cytokines during CNS disease e.g. in MS, has a combined effect on the regulation of ADAMTS-9 (Gouze *et al.*, 2006). Cells were only tested following cytokine treatment for 48 h in this project, whereas *in vivo*, cytokine exposure is an ongoing phenomenon, thus

regulation of ADAMTS-9 may be potentially more marked. Another reason for not detecting modulation of ADAMTS-9 expression protein level following treatment with cytokines in certain CNS cells was perhaps because of the time-point studied. Furthermore, up-regulation of ADAMTS-9 could occur prior to any alteration in the pro-inflammatory cytokines. An alteration of ADAMTS-9 was identified in this study and also versican and aggrecan fragments similar to GHAP are produced (Westling *et al.*, 2004). The role of these neoepitopes is still not clear. It is suggested that these fragments could play an important role in MS pathogenesis, inducing an inflammatory response via TLR stimulation (Piccinini & Midwood, 2010).

## 5.5 Conclusion

The data presented in this chapter provide evidence that, a) ADAMTS-9 is expressed at the protein level by CNS cells *in vitro* under basal conditions, and this study offers preliminary evidence that ADAMTS-9 is implicated in normal physiological processes in the CNS, b) similar to results obtained from animal models, neurite outgrowth from SHSY-5Y cells is inhibited by aggrecan, c) this study suggests a role for ADAMTS-9 in overcoming aggrecan in the glial scar matrix to promote axonal regeneration in CNS by its up-regulation in the presence of aggrecan. Overcoming aggrecan inhibition may also have an impact on other aspects of nerve injury repair, such as remyelination, since the maturation of oligodendrocytes and myelin repair is inhibited by CSPGs (Lau *et al.*, 2013). d) ADAMTS-9 protein expression is up-regulated by IFN- $\gamma$  in the human primary astrocytes e) ADAMTS-9 expression level is downregulated in microglia (CHME3 cells) by IL-1 $\beta$  and TNF- $\alpha$ . f) The cytokines investigated had no effect on expression of ADAMTS-9 by SHSY-5Y cells.

Since IFN- $\gamma$  is the major proinflammatory cytokine produced by T cells, and IL-1 $\beta$  and TNF- $\alpha$  are predominantly secreted by monocyte/macrophage cell types, including microglia, the effects of these cytokines *in vivo* on resident CNS cell expression of ADAMTS-9 would reflect the inflammatory cell component present within lesions in the white matter in MS, based on these *in vitro* findings reported here.

**Chapter 6**  
**General Discussion**

## 6.1 Implications of this study

Given that CSPGs are a major barrier for remyelination and axon regeneration, a key experimental strategy for improving axonal regeneration and plasticity has been to modify the inhibitory extracellular environment (Lau *et al.*, 2013). This inhibitory activity of CSPGs could be reduced, but not eliminated by removing GAG-side chains, indicating that multiple domains of CSPGs are involved in controlling axon regeneration (Cua *et al.*, 2013; Zhao *et al.*, 2013). ADAMTS-9 is a recently discovered peptidase which has been studied mainly in embryogenesis because it has highly similar structure to *C. elegans* gonadal morphogenesis proteinase GON-1. However, it also generated proteoglycan fragments following spinal cord injury (SCI) in mouse (Demircan *et al.*, 2013). Despite ADAMTS-9 protein being expressed in the developing and injured adult CNS and having the ability to cleave CSPGs present in brain ECM, it has not been studied previously in MS tissue (Reid *et al.*, 2009).

The main overall aim of this thesis was to investigate the role of ADAMTS-9 in the pathogenesis of MS, in particular its role in the breakdown of CSPGs. This involved a three-pronged approach. The first part of this study involved detailed investigation into the expression of aggrecan, versican and their neopeptide fragment proteins using antibodies which specially recognise ADAMTS cleavage-derived aggrecan and versican neopeptides or intact protein in post mortem MS and control CNS tissue. The second part of the study involved a detailed investigation into the expression of ADAMTS-9 in post-mortem MS and control brain tissue in order to determine the cell types expressing ADAMTS-9 and any difference in the level of ADAMTS-9 mRNA and protein expression between MS and control brain tissue. The third part of this study involved an *in vitro* investigation into the expression of ADAMTS-9 in CNS cells and treatment of these cells with pro-inflammatory cytokines to determine if cytokines are implicated in the modulation of ADAMTS-9. In addition, the effect of CSPGs on ADAMTS-9 expression and neurite outgrowth using SHSY-5Y cells plated on aggrecan coated wells was investigated.

## 6.2 Postmortem studies

CSPGs are upregulated rapidly in the tissue surrounding a lesion site, due to the induction of reactive gliosis (Siebert *et al.*, 2014) (see figure 6-1). There are many

members of the CSPG family and individual CSPGs are synthesised by different cell types and at different time points following CNS injury (Siebert *et al.*, 2014). The results from this thesis confirmed previous findings, that aggrecan and versican are increased in MS brain tissue compared to control brain tissue (Westeling *et al.*, 2004). *In vitro* studies demonstrated that CSPGs can interact with adhesion molecules expressed on neuronal cells (Afshari *et al.*, 2010; Tan *et al.*, 2011). When axonal growth cones come into contact with CSPGs, they collapse and retract. This is expected to be reason for the abortive regenerative neuronal sprouting observed in MS. The interaction of CSPGs and neurons activates the Rho-ROCK and/or protein kinase C (PKC) intracellular signalling cascades, which inhibit process extension (Sharma *et al.*, 2012; Cua *et al.*, 2013).

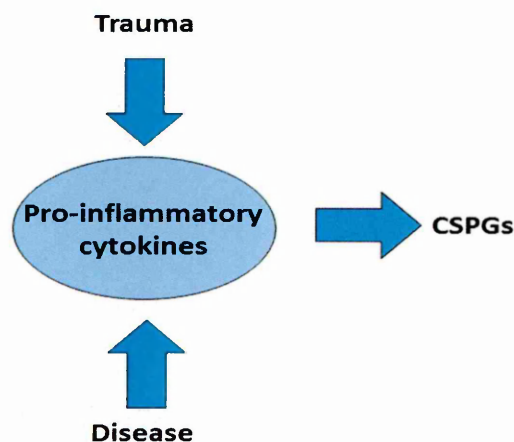


**Figure 6-1: CSPG Deposition at CNS lesions**

Damage of the CNS, either by disease or trauma mechanism initiates an increase in pro-inflammatory cytokines, which stimulate the up-regulation of CSPG family expression (adapted from Siebert *et al.*, (2014).

Though the inhibitory effects of CSPGs on axons have been known for some time, the effects they exert on other cell populations, such as oligodendrocytes have only been recently deliberated. *In vivo*, CSPG expression can modulate the migration and differentiation of endogenous OPCs that are attracted to glial scars and accumulation of OPCs at the edges of a lesion can be observed after spinal cord injury (Karimi *et al.*, 2012; Lau *et al.*, 2013). ADAMTS mediated cleavage of aggrecan, versican and brevican

in the CNS ECM, via their glutamyl endopeptidase (GEP) activity, could have a potential role in MS pathogenesis. Detection of neoepitopes of aggrecan and versican (V0/V2) using antibody specific for the new C-terminal sequence generated by cleavage of aggrecan and versican at Glu373-Ala374 and Glu405-Gln406 respectively were performed. IHC and western blotting results showed increased aggrecan and versican neoepitopes in lesional MS compared to normal control. This result is in agreement with Westling *et al.*, (2004) who observed a similar sized fragment with this antibody on versican V0/V2 cleavage by ADAMTS-4, which locally promoted motor function after spinal cord injury.

It has been reported that ADAMTS-9 may be involved in the loss of ECM by cleaving CSPGs, as demonstrated in other tissues (Demircan *et al.*, 2013). Sobel and Ahmed, (2001) showed that in the active lesion core, versican, aggrecan and neurocan were decreased in the ECM. The findings in this study are consistent with this report suggesting that the breakdown of versican in the lesion core in MS is due to excess ADAMTSs cleavage. Furthermore levels of ADAMTS-9 mRNA and protein were significantly increased, as observed by qRT-PCR, immunohistochemistry and western blotting in MS active lesions compared to normal control tissue from the same blocks used for CSPGs investigation in chapter 3. Intense ADAMTS-9 immunoreactivity was observed in areas of active lesions, assessed by increased HLA-DR expression and the presence of myelin breakdown in the activated lipid-laden macrophages stained with ORO. Staining was more intense in the active lesion core and ADAMTS-9 expression was highly upregulated associated with aggrecan and versican up-regulation. Strong ADAMTS-9 immunoreactivity was found associated with cells that phenotypically were identified as GFAP+ astrocytes, HLA-DR+ microglia and vWF+ endothelia, localized in active demyelinating MS lesions. The data suggests that the aggrecan and versican neoepitopes were generated by ADAMTS-9 mediated cleavage. Since ADAMTS-9 cleaves the Glu373-Ala374 and Glu405-Glu406 bonds of aggrecan and versican respectively, it is likely that this enzyme, as well as other described aggrecanases (ADAMTS-1, -4 or -5), play a crucial role in the processing of these molecules and other lecticans including brevican, neurocan and phosphacan in the CNS *in vivo* (Westling *et al.*, 2004).

### 6.3 *In vitro* studies

The findings in chapter 3 showed that versican and aggrecan neoepitopes were generated by characteristic ADAMTS (aggrecanase) cleavage. Data in chapter 4 also showed that ADAMTS-9 protein was expressed by astrocytes, endothelium, neurons and activated microglia with up-regulation in active lesions compared to the normal control in *ex vivo* CNS tissue, indicating that ADAMTS-9 secreted from these cells could play a part in ECM remodelling, particularly of aggrecan and versican. However, it has been demonstrated that expression of a number of ADAMTS enzymes can be modulated by a range of mediators (e.g. cytokines) in different CNS cell types (Cross *et al.*, 2006; Reid *et al.*, 2009). ADAMTS-1 and -4 expressions in astrocytes and neurons has been reported following physical or toxic injury to the CNS and it was modulated by pro-inflammatory cytokines, suggesting that this expression at the site of injury may support neurite outgrowth (Cross *et al.*, 2006; Cua *et al.*, 2013).

The data in chapter 5 demonstrated that ADAMTS-9 is expressed under basal conditions by human primary astrocytes, a foetal human microglia cell line and a neuroblastoma cell line differentiated with RetA *in vitro*, which suggests that ADAMTS-9 may be constitutively expressed in brain. There is evidence from this current study to show that ADAMTS-9 expression is upregulated by external factors including CSPGs and pro-inflammatory cytokines as summarised in figure 6-2. Each of the factors exerted different effects on ADAMTS-9 protein expression across the cell-types suggesting that *in vivo* modulation of the protein expression is complex. Three of the pro-inflammatory cytokines (TNF- $\alpha$ , IL-1 $\beta$  and IFN- $\gamma$ ) highly reported to be involved in CNS inflammation modulated ADAMTS-9 expression suggesting this is a key event in pathogenesis of MS (reviewed by Siebert *et al.*, 2014). Support for this finding was the demonstration that ADAMTS-9 expression was significantly increased in MS active lesions compared to normal controls as well as its up-regulation following treatment with INF- $\gamma$  in primary astrocytes.

However, no modulation in the expression of ADAMTS-9 was observed in SHSY-5Y cells with pro-inflammatory cytokines in this current study (Table 5-1). This result is in agreement with Gibrel, (2012) who found similar results with ADAMTS-1. A previous *in vitro* study demonstrated no modulation of ADAMTS-9 mRNA expression by TNF- $\alpha$  in an astrocytoma cell line (U87-MG) (Reid *et al.*, 2009). This current study also showed

that IL-1 $\beta$  and TNF- $\alpha$  did not significantly alter ADAMTS-9 expression in primary astrocytes but down-regulated ADAMTS-9 expression in CHME3 cell line. Cross *et al.*, (2006) showed that IL-1 $\beta$  treatment did not significantly alter the mRNA expression level of ADAMTS-1, -5 and TIMP in astrocytes, although there was increased expression of ADAMTS-9 on treatment with IL-1 $\beta$  and TNF- $\alpha$  in other systems (Demircan *et al.*, 2005).

To further understand the role of ADAMTS-9 within the CNS, in particular its role in breakdown of CSPGs, it would be important to detect where the protein is localised in cells *in vitro*. ICC of SHSY-5Y cells cultured in wells coated with aggrecan demonstrated that ADAMTS-9 was up-regulated and localised within the nucleus and possibly in intracellular vesicles but not in the ECM. Unfortunately, ICC and WB detection of the aggrecan and versican neoepitope were not performed in this study due to the limit of detection of protein expressed. However, this may have been because the experiment (ICC) was performed on monolayer cells after 48 h treatment, which was unlikely to have synthesised high levels of ECM within the time frame of the experiment. Others have indicated that ADAMTS-9 is a secreted protein which remains localised to the cell surface, potentially in the pericellular matrix, which is an area of ECM closely associated with the plasma membrane (Koo *et al.*, 2007). The results here provide support for this since ADAMTS-9 was shown to be significantly raised in SHSY-5Y cells grown on plates coated with aggrecan at a concentration 2 $\mu$ g/ml and it was not found more widely associated with the ECM by ICC.

#### **6.4 Future Directions**

To further understand the functional role of ADAMTS-9 and its substrates in MS, both an *in vivo* and *in vitro* approach should be considered.

There is evidence from this current study indicating a functional role of ADAMTSs as determined by an increase in the levels of aggrecan and versican neoepitopes in MS active lesions, compared to normal control brain tissue, which is a result of their cleavage by ADAMTS-9 possibly as a result of increased production and/or activity. Other studies indicated that ADAMTS-4 as well as other aggrecanases (ADAMTS-1 and -5), may play a crucial role in MS pathogenesis by degradation of other lecticans including brevican, neurocan and phosphacan (Westling *et al.*, 2004; Haddock *et al.*,

2007; Tauchi *et al.*, 2012). Brevican and neurocan are degraded by ADAMTSs; their neoepitopes could be detected with specific antibodies in further investigations (Matthews *et al.*, 2000, Tauchi *et al.*, 2012). CSPG fragments similar to glial hyaluronate binding protein fragments (GHAP) are produced following ADAMTS cleavage and the functional role of these fragments is still unknown (Westling *et al.*, 2004). However, the CSPG degradation products reported here may result in activation of TLRs inducing inflammatory responses in the same way as GHAP fragments (Piccinini & Midwood, 2010). TLR expression and the effect of synthetic GHAP could be studied in CNS cells *in vitro* on parameters such as cytokine and ADAMTS expression.

To further clarify the role of ADAMTS-9 in MS, it would be important to focus on functional studies *in vitro*. Using ADAMTS-9 knock-out mice would be a useful tool to assess the role of ADAMTS-9 in normal physiology not just in MS. It also would be informative to assess neurite outgrowth in transfected neuronal cells over expressing ADAMTS-9 enzyme. ADAMTS-9 could be stably transfected using an inducible expression vector system into the neuronal cell line and could be induced by the addition of low level protein. Hamel *et al.*, (2008) described over expression of ADAMTS-4 following transfection in primary astrocytes. In addition to over expression, these authors also added ADAMTS-4 enzymes to neuronal cells grown in culture as well as in co-culture with astrocytes. This approach could also be taken as part of future work to investigate ADAMTS-9 function.

Changes in ECM after neuronal injury can inhibit remyelination, an ADAMTS-9 approach that normalises the level of ECM components such as CSPGs and hyaluronan may form part of novel therapies to enhance the repair of myelin. A promising approach to promote remyelination is the use of enzymatic clearance of deposited ECM components using hyaluronidases to remove excess inhibitory hyaluronan and CSPGs from lesion sites. Further studies are necessary to determine the balance of the potential beneficial and inhibitory roles of hyaluronidases in the context of remyelination (reviewed by Lau *et al.*, 2013).

Another approach to reduce the deposition of inhibitory ECM components would be to prevent the transport of these components into the extracellular environment. CSPG biosynthesis is catalysed by a series of intracellular enzymes including

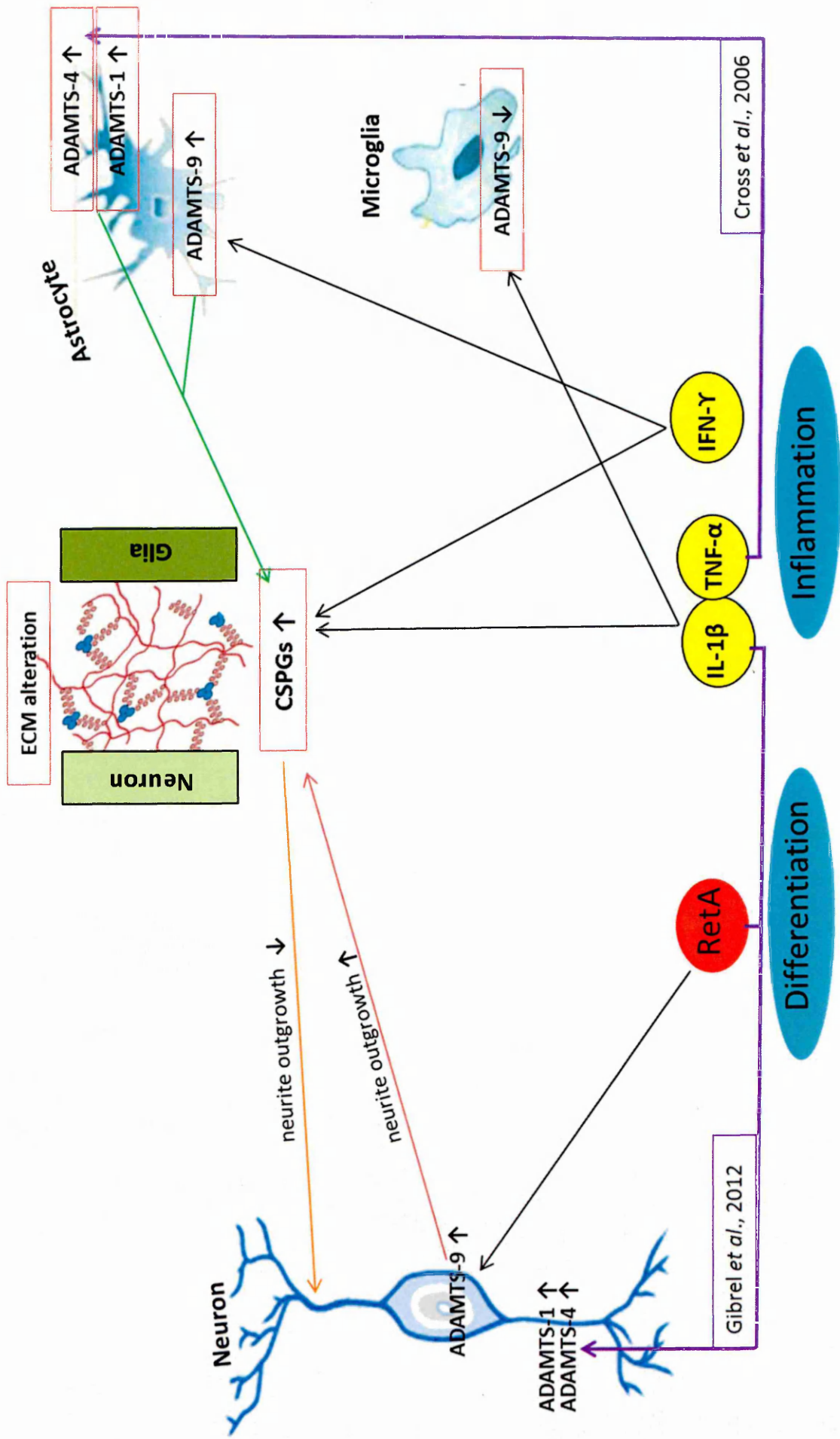
xylosyltransferase-1 which initiates GAG polymerisation on the core protein to complete formation of the PGs for secretion into the ECM (Grimpe *et al.*, 2004). Targeting of xylosyltransferase-1 mRNA with locally applied novel DNA deoxyribose molecules has been shown to disrupt CSPG synthesis resulting in increased neurite outgrowth and axonal regeneration around CNS lesions (reviewed by Gloster *et al.*, 2012).

## 6.5 Conclusion

The study documented in this thesis provides evidence that CSPGs, including aggrecan and versican are upregulated in MS active lesions. These CSPGs are also upregulated after spinal cord injury and they probably contribute to the failure of axon regeneration and neurite outgrowth (Jones *et al.*, 2003; Tauchi *et al.*, 2012). It also provides evidence that ADAMTS-9 expression was increased in active lesions associated with CNS cell injury. ADAMTS-9 could degrade aggrecan and versican and reverse the neurite outgrowth inhibition mediated by human brain CSPGs. On the contrary they may be detrimental by increasing inflammatory cell access to the site of injury. *In vitro* studies showed that ADAMTS-9 is constitutively expressed in CNS cells (human foetal microglia cell line CHME3, primary astrocytes and neuroblastoma cell line SHSY-5Y) suggesting that ADAMTS-9 has the potential to be implicated in both normal physiology and pathology in the CNS. It also demonstrated that ADAMTS-9 expression was up-regulated in differentiated SHSY-5Y cell line grown on plates coated with aggrecan. ADAMTS-9 was also modulated by pro-inflammatory cytokines in both astrocytes and microglia. Further investigation of the primary neuronal cells is required to elucidate further the role of neuronal ADAMTSs in MS pathogenesis.

### Figure 6-2: Modulation of ADAMTS-9 expression in the CNS

ADAMTS-9 mediated cleavage of lecticans aggrecan and versican in the CNS ECM, via their glutamyl endopeptidase (GEP) activity, could have a potential role in normal ECM turnover and ECM in MS (Ahmed & Sobel, 2001). To support this suggestion and demonstrate the activity of these ADAMTSs and determine their functional role an *ex vivo* study on human CNS tissue was performed. Data illustrated an upregulation of versican and aggrecan neopeptide in MS lesion indicative of ADAMTS involvement in ECM breakdown (Green arrow). Data also demonstrated that ADAMTS-9 was expressed predominantly by astrocytes, macrophages, endothelium and neurons with increased expression within MS active lesion suggesting its role in this breakdown. In addition, previous studies by Cross *et al.*, 2006 showed an increase in ADAMTS-1 and ADAMTS-4 by TNF- $\alpha$  in astrocytes (purple arrow). This study provided evidence that neurite outgrowth from SHSY-5Y cells was inhibited by aggrecan *in vitro* (orange arrow); this inhibition was associated with a high level of expression of ADAMTS-9. This could be beneficial as ADAMTS-9 could degrade CSPGs enabling neuronal outgrowth and/or migration of neuronal precursor cells (Cua *et al.*, 2013). Based on the results generated *in vitro* study, ADAMTS-9 was expressed by neuronal cell line SHSY-5Y, human foetal microglia (CHME3) and primary astrocytes. Modulation of ADAMTS-9 expression in the brain is likely to be complex and multifactorial as represented in the figure. ADAMTS-9 was modulated to a certain extent by IL-1 $\beta$ , TNF- $\alpha$  and IFN- $\gamma$  (yellow ovals) which are factors shown to be important in CNS inflammation thus providing preliminary evidence that the peptidase could be implicated in MS pathogenesis. An increase in expression is indicated with a  $\uparrow$  arrow and a decrease in expression is indicated with a  $\downarrow$  arrow.



- Abbott, N. J., Patabendige, A. A., Dolman, D. E., Yusof, S. R., & Begley, D. J. (2010). Structure and function of the blood–brain barrier. *Neurobiology of Disease*, *37*(1), 13-25.
- Abd-El-Basset, E., & Abd-El-Barr, M. M. (2011). Effect of Interleukin-1 $\beta$  on the expression of actin isoforms in cultured mouse astroglia. *The Anatomical Record*, *294*(1), 16-23.
- Afshari, F. T., Kwok, J. C., White, L., & Fawcett, J. W. (2010). Schwann cell migration is integrin-dependent and inhibited by astrocyte-produced aggrecan. *Glia*, *58*(7), 857-869.
- Akenami, F. O., Koskiniemi, M., & Vaheri, A. (2000). Plasminogen activation in multiple sclerosis and other neurological disorders. *Fibrinolysis and Proteolysis*, *14*(1), 1-14.
- Albert, M., Antel, J. Brück, W., & Stadelmann, C. (2007). Extensive cortical remyelination in patients with chronic multiple sclerosis. *Brain Pathology*, *17*(2), 129-138.
- Alexander, J., Harris, M., Wells, S., Mills, G., Chalamidas, K., Ganta, V., Minagar, A. (2010). Alterations in serum MMP-8, MMP-9, IL-12p40 and IL-23 in multiple sclerosis patients treated with interferon- $\beta$ 1b. *Multiple Sclerosis*, *16*(7), 801-809.
- Algeciras, M. E., Takahara, H., & Bhattacharya, S. K. (2008). Mechanical stretching elevates peptidyl arginine deiminase 2 expression in astrocytes. *Current Eye Research*, *33*(11-12), 994-1001.
- Allinson, T. M., Parkin, E. T., Turner, A. J., & Hooper, N. M. (2003). ADAMs family members as amyloid precursor protein  $\alpha$ -secretases. *Journal of Neuroscience Research*, *74*(3), 342-352.
- Aloisi, F., Serafini, B., Magliozzi, R., Howell, O. W., & Reynolds, R. (2010). Detection of Epstein–Barr virus and B-cell follicles in the multiple sclerosis brain: what you find depends on how and where you look. *Brain*, *223*.
- Alter, A., Duddy, M., Hebert, S., Biernacki, K., Prat, A., Antel, J. P., Bar-Or, A. (2003). Determinants of human B cell migration across brain endothelial cells. *Journal of Immunology*, *170*(9), 4497-4505.
- Altmann, D.M., Boyton, R.J 2004. Models of multiple sclerosis. Drug discovery today. Disease models 4: 405-410.

- Alvarez, J. I., Cayrol, R., & Prat, A. (2011). Disruption of central nervous system barriers in multiple sclerosis. *Biochimica et Biophysica Acta (BBA)-Molecular Basis of Disease*, 1812(2), 252-264.
- Andreini, C., Banci, L., Bertini, I., Elmi, S., & Rosato, A. (2005). Comparative analysis of the ADAM and ADAMTS families. *Journal of Proteome Research*, 4(3), 881-888.
- Antel, J., Antel, S., Caramanos, Z., Arnold, D. L., & Kuhlmann, T. (2012). Primary progressive multiple sclerosis: Part of the MS disease spectrum or separate disease entity? *Acta Neuropathologica*, 123(5), 627-638.
- Apte, S. S. (2004). A disintegrin-like and metalloprotease (reprolysin type) with thrombospondin type 1 motifs: The ADAMTS family. *The International Journal of Biochemistry & Cell Biology*, 36(6), 981-985.
- Apte, S. S. (2009). A disintegrin-like and metalloprotease (reprolysin-type) with thrombospondin type 1 motif (ADAMTS) superfamily: Functions and mechanisms. *The Journal of Biological Chemistry*, 284(46), 31493-31497.
- Aravalli, R. N., Peterson, P. K., & Lokensgard, J. R. (2007). Toll-like receptors in defence and damage of the central nervous system. *Journal of Neuroimmune Pharmacology*, 2(4), 297-312.
- Armstrong, R. C., Dorn, H. H., Kufta, C. V., Friedman, E., & Dubois-Dalq, M. E. (1992). Pre-oligodendrocytes from adult human CNS. *The Journal of Neuroscience*, 12(4), 1538-1547.
- Ascherio, A., Munger, K. L., & Simon, K. C. (2010). Vitamin D and multiple sclerosis. *The Lancet Neurology*, 9(6), 599-612.
- Asher, R. A., Morgenstern, D. A., Fidler, P. S., Adcock, K. H., Oohira, A., Braistead, J. E., Fawcett, J. W. (2000). Neurocan is upregulated in injured brain and in cytokine-treated astrocytes. *The Journal of Neuroscience*, 20(7), 2427-2438.
- Asher, R. A., Morgenstern, D. A., Moon, L. D., & Fawcett, J. W. (2001). Chondroitin sulphate proteoglycans: Inhibitory components of the glial scar. *Progress in Brain Research*, 132, 611-619.
- Asher, R. A., Morgenstern, D. A., Shearer, M. C., Adcock, K. H., Pesheva, P., & Fawcett, J. W. (2002). Versican is upregulated in CNS injury and is a product of oligodendrocyte lineage cells. *The Journal of Neuroscience*, 22(6), 2225-2236.

- Avolio, C., Ruggieri, M., Giuliani, F., Liuzzi, G. M., Leante, R., Riccio, P., Trojano, M. (2003). Serum MMP-2 and MMP-9 are elevated in different multiple sclerosis subtypes. *Journal of Neuroimmunology*, *136*(1), 46-53.
- Aulchenko, Y. S., Hoppenbrouwers, I. A., Ramagopalan, S. V., Broer, L., Jafari, N., Hillert, J., & Goossens, D. (2008). Genetic variation in the KIF1B locus influences susceptibility to multiple sclerosis. *Nature genetics*, *40*(12), 1402-1403.
- Back, S. A., Tuohy, T. M., Chen, H., Wallingford, N., Craig, A., Struve, J., Chang, A. (2005). Hyaluronan accumulates in demyelinated lesions and inhibits oligodendrocyte progenitor maturation. *Nature Medicine*, *11*(9), 966-972.
- Bahlo, M., Booth, D. R., Broadley, S. A., Brown, M. A., Foote, S. J., Griffiths, L. R., ... & Rubio, J. P. (2009). Genome-wide association study identifies new multiple sclerosis susceptibility loci on chromosomes 12 and 20. *Nature genetics*, *41*(7), 824-828.
- Baranzini, S. E., Wang, J., Gibson, R. A., Galwey, N., Naegelin, Y., Barkhof, F., Oksenberg, J. R. (2009). Genome-wide association analysis of susceptibility and clinical phenotype in multiple sclerosis. *Human Molecular Genetics*, *18*(4), 767-778.
- Barritt, A. W., Davies, M., Marchand, F., Hartley, R., Grist, J., Yip, P., Bradbury, E. J. (2006). Chondroitinase ABC promotes sprouting of intact and injured spinal systems after spinal cord injury. *The Journal of Neuroscience*, *26*(42), 10856-10867.
- Barros, C. S., Franco, S. J., & Muller, U. (2011). Extracellular matrix: Functions in the nervous system. *Cold Spring Harbor Perspectives in Biology*, *3*(1), a005108.
- Bartus, K., James, N., Bosch, K., & Bradbury, E. (2012). Chondroitin sulphate proteoglycans: Key modulators of spinal cord and brain plasticity. *Experimental Neurology*, *235*(1), 5-17.
- Bashinskaya, V. V., Kulakova, O. G., Boyko, A. N., Favorov, A. V., & Favorova, O. O. (2015). A review of genome-wide association studies for multiple sclerosis: classical and hypothesis-driven approaches. *Human Genetics*, *134*(11-12), 1143-1162.
- Bear, M. F., Connors, B. W., & Paradiso, M. A. (2007). *Neuroscience* Lippincott Williams & Wilkins.
- Bebo, B. F., Adlard, K., Schuster, J. C., Unsicker, L., Vandenbark, A. A., & Offner, H. (1999). Gender differences in protection from EAE induced by oral tolerance with a peptide analogue of MBP-Ac1-11. *Journal of Neuroscience*, *55*(4), 432-440.

- Bekku, Y., Vargova, L., Goto, Y., Vorisek, I., Dmytrenko, L., Narasaki, M., Oohashi, T. (2010). Bral1: Its role in diffusion barrier formation and conduction velocity in the CNS. *The Journal of Neuroscience: 30*(8), 3113-3123.
- Bell, J. K., Botos, I., Hall, P. R., Askins, J., Shiloach, J., Segal, D. M., & Davies, D. R. (2005). The molecular structure of the toll-like receptor 3 ligand-binding domain. *Proceedings of the National Academy of Sciences of the United States of America, 102*(31), 10976-10980.
- Bellail, A. C., Hunter, S. B., Brat, D. J., Tan, C., & Van Meir, E. G. (2004). Microregional extracellular matrix heterogeneity in brain modulates glioma cell invasion. *The International Journal of Biochemistry & Cell Biology, 36*(6), 1046-1069.
- Benveniste, E. N., Tang, L. P., & Law, R. M. (1995). Differential regulation of astrocyte TNF- $\alpha$  expression by the cytokines TGF- $\beta$ , IL-6 and IL-10. *International Journal of Developmental Neuroscience, 13*(3), 341-349.
- Bevitt, D. J., Mohamed, J., Catterall, J. B., Li, Z., Arris, C. E., Hiscott, P., Clarke, M. P. (2003). Expression of ADAMTS metalloproteinases in the retinal pigment epithelium derived cell line ARPE-19: Transcriptional regulation by TNF $\alpha$ . *Biochimica et Biophysica Acta (BBA)-Gene Structure and Expression, 1626*(1), 83-91.
- Biname, F., Sakry, D., Dimou, L., Jolivel, V., & Trotter, J. (2013). NG2 regulates directional migration of oligodendrocyte precursor cells via rho GTPases and polarity complex proteins. *The Journal of Neuroscience: 33*(26), 10858-10874.
- Boche, D., Perry, V., & Nicoll, J. (2013). Review: Activation patterns of microglia and their identification in the human brain. *Neuropathology and Applied Neurobiology, 39*(1), 3-18.
- Bonneh-Barkay, D., & Wiley, C. A. (2009). Brain extracellular matrix in neurodegeneration. *Brain Pathology, 19*(4), 573-585.
- Bornstein, P. (1992). Thrombospondins: Structure and regulation of expression. *FASEB Journal: 6*(14), 3290-3299.
- Bradbury, E. J., Moon, L. D., Popat, R. J., King, V. R., Bennett, G. S., Patel, P. N., McMahon, S. B. (2002). Chondroitinase ABC promotes functional recovery after spinal cord injury. *Nature, 416*(6881), 636-640.
- Brodal, P. (2004). *The central nervous system: Structure and function* Oxford University Press.

- Brosnan, C. F., & John, G. R. (2009). Revisiting notch in remyelination of multiple sclerosis lesions. *The Journal of Clinical Investigation*, *119*(1), 10-13.
- Brosnan, C. F., & Raine, C. S. (2013). The astrocyte in multiple sclerosis revisited. *Glia*, *61*(4), 453-465.
- Brown, J. M., Xia, J., Zhuang, B., Cho, K. S., Rogers, C. J., Gama, C. I., Hsieh-Wilson, L. C. (2012). A sulfated carbohydrate epitope inhibits axon regeneration after injury. *Proceedings of the National Academy of Sciences of the United States of America*, *109*(13), 4768-4773.
- Brück, W., Porada, P., Poser, S., Rieckmann, P., Hanefeld, F., Kretzschmarch, H. A., & Lassmann, H. (1995). Monocyte/macrophage differentiation in early multiple sclerosis lesions. *Annals of Neurology*, *38*(5), 788-796.
- Bsibsi, M., Persoon-Deen, C., Verwer, R. W., Meeuwse, S., Ravid, R., & Van Noort, J. M. (2006). Toll-like receptor 3 on adult human astrocytes triggers production of neuroprotective mediators. *Glia*, *53*(7), 688-695.
- Buchwalow, I., Samoilova, V., Boecker, W., & Tiemann, M. (2011). Non-specific binding of antibodies in immunohistochemistry: Fallacies and facts. *Scientific Reports*, *1*
- Burda, J. E., & Sofroniew, M. V. (2014). Reactive gliosis and the multicellular response to CNS damage and disease. *Neuron*, *81*(2), 229-248.
- Burton, J. M., Kimball, S., Vieth, R., Bar-Or, A., Dosch, H. M., Cheung, R., O'Connor, P. (2010). A phase I/II dose-escalation trial of vitamin D3 and calcium in multiple sclerosis. *Neurology*, *74*(23), 1852-1859.
- Bustin, S. A. (2002). Quantification of mRNA using real-time reverse transcription PCR (RT-PCR): Trends and problems. *Journal of Molecular Endocrinology*, *29*(1), 23-39.
- Cal, S., Obaya, A. J., Llamazares, M., Garabaya, C., Quesada, V., & López-Otín, C. (2002). Cloning, expression analysis, and structural characterization of seven novel human ADAMTSs, a family of metalloproteinases with disintegrin and thrombospondin-1 domains. *Gene*, *283*(1), 49-62.
- Caminero, A., Comabella, M., & Montalban, X. (2011). Tumor necrosis factor alpha (TNF- $\alpha$ ), anti-TNF- $\alpha$  and demyelination revisited: An ongoing story. *Journal of Neuroimmunology*, *234*(1), 1-6.

- Carvey, P. M., Hendey, B., & Monahan, A. J. (2009). The blood–brain barrier in neurodegenerative disease: A rhetorical perspective. *Journal of Neurochemistry*, *111*(2), 291-314.
- Chandler, S., Miller, K., Clements, J., Lury, J., Corkill, D., Anthony, D., Gearing, A. (1997). Matrix metalloproteinases, tumor necrosis factor and multiple sclerosis: An overview. *Journal of Neuroimmunology*, *72*(2), 155-161.
- Chang, A., Tourtellotte, W. W., Rudick, R., & Trapp, B. D. (2002). Premyelinating oligodendrocytes in chronic lesions of multiple sclerosis. *New England Journal of Medicine*, *346*(3), 165-173.
- Charil, A., Yousry, T. A., Rovaris, M., Barkhof, F., De Stefano, N., Fazekas, F., Polman, C. (2006). MRI and the diagnosis of multiple sclerosis: Expanding the concept of “no better explanation”. *The Lancet Neurology*, *5*(10), 841-852.
- Chen, H., Herndon, M. E., & Lawler, J. (2000). The cell biology of thrombospondin-1. *Matrix Biology*, *19*(7), 597-614.
- Cheung, Y., Lau, W. K., Yu, M., Lai, C. S., Yeung, S., So, K., & Chang, R. C. (2009). Effects of all-trans-retinoic acid on human SH-SY5Y neuroblastoma as *in vitro* model in neurotoxicity research. *Neurotoxicology*, *30*(1), 127-135.
- Choi, N., Kim, B., Park, C., Han, Y. J., Lee, H. W., Choi, J. H., Song, J. J. (2009). Multiple-layer substrate zymography for detection of several enzymes in a single sodium dodecyl sulfate gel. *Analytical Biochemistry*, *386*(1), 121-122.
- Choi, S. S., Lee, H. J., Lim, I., Satoh, J., & Kim, S. U. (2014). Human astrocytes: Secretome profiles of cytokines and chemokines. *PLoS One*, *9*(4), e92325.
- Christensen, J. R., Börnsen, L., Ratzner, R., Piehl, F., Khademi, M., Olsson, T & Sellebjerg, F. (2013). Systemic inflammation in progressive multiple sclerosis involves follicular T-helper, Th17-and activated B-cells and correlates with progression. *PLoS one*, *8*(3), e57820.
- Clagett-Dame, M., McNeill, E. M., & Muley, P. D. (2006). Role of all-trans retinoic acid in neurite outgrowth and axonal elongation. *Journal of Neurobiology*, *66*(7), 739-756.
- Clark, M. E., Kelner, G. S., Turbeville, L. A., Boyer, A., Arden, K. C., & Maki, R. A. (2000). ADAMTS9, a novel member of the ADAM-TS/metallospodin gene family. *Genomics*, *67*(3), 343-350.

- Clement, A. M., Sugahara, K., & Faissner, A. (1999). Chondroitin sulfate E promotes neurite outgrowth of rat embryonic day 18 hippocampal neurons. *Neuroscience Letters*, *269*(3), 125-128.
- Colige, A. (2010). ADAMTS-2: Procollagen processing and implications in genetic and acquired diseases. *XVIIIème Congrès Annuel, Société Française De Biologie De La Matrice Extracellulaire*.
- Comabella, M., & Khoury, S. J. (2012). Immunopathogenesis of multiple sclerosis. *Clinical Immunology*, *142*(1), 2-8.
- Constantinescu, C. S., Farooqi, N., O'Brien, K., & Gran, B. (2011). Experimental autoimmune encephalomyelitis (EAE) as a model for multiple sclerosis (MS). *British Journal of Pharmacology*, *164*(4), 1079-1106.
- Constantinescu, C. S., Tani, M., Ransohoff, R. M., Wysocka, M., Hilliard, B., Fujioka, T., Trinchieri, G. (2005). Astrocytes as antigen-presenting cells: Expression of IL-12/IL-23. *Journal of Neurochemistry*, *95*(2), 331-340.
- Crawley, J. T., de Groot, R., Xiang, Y., Luken, B. M., & Lane, D. A. (2011). Unraveling the scissile bond: How ADAMTS13 recognizes and cleaves von Willebrand factor. *Blood*, *118*(12), 3212-3221.
- Cregg, J. M., DePaul, M. A., Filous, A. R., Lang, B. T., Tran, A., & Silver, J. (2014). Functional regeneration beyond the glial scar. *Experimental Neurology*, *253*, 197-207.
- Crocker, S. J., Whitmire, J. K., Frausto, R. F., Chertboonmuang, P., Soloway, P. D., Whitton, J. L., & Campbell, I. L. (2006). Persistent macrophage/microglial activation and myelin disruption after experimental autoimmune encephalomyelitis in tissue inhibitor of metalloproteinase-1-deficient mice. *The American Journal of Pathology*, *169*(6), 2104-2116.
- Cross, N., Chandrasekharan, S., Jokonya, N., Fowles, A., Hamdy, F., Buttle, D., & Eaton, C. (2005). The expression and regulation of ADAMTS-1,-4,-5,-9, and-15, and TIMP-3 by TGFβ1 in prostate cells: Relevance to the accumulation of versican. *The Prostate*, *63*(3), 269-275.
- Cua, R. C., Lau, L. W., Keough, M. B., Midha, R., Apte, S. S., & Yong, V. W. (2013). Overcoming neurite-inhibitory chondroitin sulfate proteoglycans in the astrocyte matrix. *Glia*, *61*(6), 972-984.
- Daneman, R. (2012). The blood–brain barrier in health and disease. *Annals of Neurology*, *72*(5), 648-672.

- Daneman, R., Zhou, L., Kebede, A. A., & Barres, B. A. (2010). Pericytes are required for blood-brain barrier integrity during embryogenesis. *Nature*, 468(7323), 562-566.
- Dankowski, T., Buck, D., Andlauer, T. F., Antony, G., Bayas, A., Bechmann, L., & Gold, R. (2015). Successful Replication of GWAS Hits for Multiple Sclerosis in 10,000 Germans Using the Exome Array. *Genetic epidemiology*, 39(8), 601-608.
- Datki, Z., Juhász, A., Gálfi, M., Soós, K., Papp, R., Zádori, D., & Penke, B. (2003). Method for measuring neurotoxicity of aggregating polypeptides with the MTT assay on differentiated neuroblastoma cells. *Brain Research Bulletin*, 62(3), 223-229.
- Davalos, D., Grutzendler, J., Yang, G., Kim, J. V., Zuo, Y., Jung, S., ... & Gan, W. B. (2005). ATP mediates rapid microglial response to local brain injury in vivo. *Nature neuroscience*, 8(6), 752-758.
- de Pablos, R. M., Espinosa-Oliva, A. M., & Herrera, A. J. (2013). Immunohistochemical detection of microglia. *Microglia* (pp. 281-289) Springer.
- Deller, T., Haas, C. A., & Frotscher, M. (2000). Reorganization of the rat fascia dentata after a unilateral entorhinal cortex lesion: Role of the extracellular matrix. *Annals of the New York Academy of Sciences*, 911(1), 207-220.
- Demircan, K., Hirohata, S., Nishida, K., Hatipoglu, O. F., Oohashi, T., Yonezawa, T., Ninomiya, Y. (2005). ADAMTS-9 is synergistically induced by interleukin-1 $\beta$  and tumor necrosis factor  $\alpha$  in OUMS-27 chondrosarcoma cells and in human chondrocytes. *Arthritis & Rheumatism*, 52(5), 1451-1460.
- Demircan, K., Topcu, V., Takigawa, T., Akyol, S., Yonezawa, T., Ozturk, G., Akyol, O. (2014). ADAMTS4 and ADAMTS5 knockout mice are protected from versican but not aggrecan or brevican proteolysis during spinal cord injury. *BioMed Research International*, 2014
- Demircan, K., Yonezawa, T., Takigawa, T., Topcu, V., Erdogan, S., Ucar, F., Hirohata, S. (2013). ADAMTS1, ADAMTS5, ADAMTS9 and aggrecanase-generated proteoglycan fragments are induced following spinal cord injury in mouse. *Neuroscience Letters*, 544, 25-30.
- Di Penta, A., Moreno, B., Reix, S., Fernandez-Diez, B., Villanueva, M., Errea, O., Villoslada, P. (2013). Oxidative stress and proinflammatory cytokines contribute to demyelination and axonal damage in a cerebellar culture model of neuroinflammation. *PLoS One*, 8(2), e54722.

Dick, G., Tan, C. L., Alves, J. N., Ehlert, E. M., Miller, G. M., Hsieh-Wilson, L. C., Kwok, J. C. (2013). Semaphorin 3A binds to the perineuronal nets via chondroitin sulfate type E motifs in rodent brains. *The Journal of Biological Chemistry*, 288(38), 27384-27395.

Dickendesher, T. L., Baldwin, K. T., Mironova, Y. A., Koriyama, Y., Raiker, S. J., Askew, K. L., Liepmann, C. D. (2012). NgR1 and NgR3 are receptors for chondroitin sulfate proteoglycans. *Nature Neuroscience*, 15(5), 703-712.

Drexler, H. G., & Uphoff, C. C. (2002). Mycoplasma contamination of cell cultures: Incidence, sources, effects, detection, elimination, prevention. *Cytotechnology*, 39(2), 75-90.

Dunn, J. R., Reed, J., Du Plessis, D., Shaw, E., Reeves, P., Gee, A., Walker, C. (2006). Expression of ADAMTS-8, a secreted protease with antiangiogenic properties, is downregulated in brain tumours. *British Journal of Cancer*, 94(8), 1186-1193.

Dvorakova, L. V., & Reichelova, M. (2007). Detection of mycoplasma contamination in cell cultures and bovine sera, 50(6), 262-268.

Dwane, S., Durack, E., & Kiely, P. A. (2013). Optimising parameters for the differentiation of SH-SY5Y cells to study cell adhesion and cell migration. *BMC Research Notes*, 6, 366-0500-6-366.

Dyment, D. A., Ebers, G. C., & Sadovnick, A. D. (2004). Genetics of multiple sclerosis. *The Lancet Neurology*, 3(2), 104-110.

Edgar, J. M., McLaughlin, M., Yool, D., Zhang, S. C., Fowler, J. H., Montague, P., Griffiths, I. R. (2004). Oligodendroglial modulation of fast axonal transport in a mouse model of hereditary spastic paraplegia. *The Journal of Cell Biology*, 166(1), 121-131.

Encinas, M., Iglesias, M., Liu, Y., Wang, H., Muhaisen, A., Cena, V., Comella, J. X. (2000). Sequential treatment of SH-SY5Y cells with retinoic acid and brain-derived neurotrophic factor gives rise to fully differentiated, neurotrophic factor-dependent, human neuron-like cells. *Journal of Neurochemistry*, 75(3), 991-1003.

Engelhardt, B., & Ransohoff, R. M. (2005). The ins and outs of T-lymphocyte trafficking to the CNS: Anatomical sites and molecular mechanisms. *Trends in Immunology*, 26(9), 485-495.

Fisher, D., Xing, B., Dill, J., Li, H., Hoang, H. H., Zhao, Z., Li, S. (2011). Leukocyte common antigen-related phosphatase is a functional receptor for chondroitin

sulfate proteoglycan axon growth inhibitors. *The Journal of Neuroscience*, 31(40), 14051-14066.

Fleige, S., & Pfaffl, M. W. (2006). RNA integrity and the effect on the real-time qRT-PCR performance. *Molecular Aspects of Medicine*, 27(2), 126-139.

Fleming, J. C., Norenberg, M. D., Ramsay, D. A., Dekaban, G. A., Marcillo, A. E., Saenz, A. D., Weaver, L. C. (2006). The cellular inflammatory response in human spinal cords after injury. *Brain*, 129(Pt 12), 3249-3269.

Fletcher, J., Lalor, S., Sweeney, C., Tubridy, N., & Mills, K. (2010). T cells in multiple sclerosis and experimental autoimmune encephalomyelitis. *Clinical & Experimental Immunology*, 162(1), 1-11.

Forgione, N., & Fehlings, M. G. (2014). Rho-ROCK inhibition in the treatment of spinal cord injury. *World Neurosurgery*, 82(3), e535-e539.

Francis, K., Van Beek, J., Canova, C., Neal, J. W., & Gasque, P. (2003). Innate immunity and brain inflammation: the key role of complement. *Expert reviews in molecular medicine*, 5(15), 1-19.

Fukata, M., Vamadevan, A. S., & Abreu, M. T. (2009). Toll-like receptors (TLRs) and nod-like receptors (NLRs) in inflammatory disorders. *Seminars in Immunology*, 21(4) 242-253.

Fünfschilling, U., Supplie, L. M., Mahad, D., Boretius, S., Saab, A. S., Edgar, J., Möbius, W. (2012). Glycolytic oligodendrocytes maintain myelin and long-term axonal integrity. *Nature*, 485(7399), 517-521.

Galtrey, C. M., & Fawcett, J. W. (2007). The role of chondroitin sulfate proteoglycans in regeneration and plasticity in the central nervous system. *Brain Research Reviews*, 54(1), 1-18.

Garton, K. J., Gough, P. J., Blobel, C. P., Murphy, G., Greaves, D. R., Dempsey, P. J., & Raines, E. W. (2001). Tumor necrosis factor- $\alpha$ -converting enzyme (ADAM17) mediates the cleavage and shedding of fractalkine (CX3CL1). *Journal of Biological Chemistry*, 276(41), 37993-38001.

Gibrel, G. G. (2012). The Role of ADAMTS-1,-4 and-5 in Multiple Sclerosis, PhD thesis Sheffield Hallam University.

Gingras, D., Pagé, M., Annabi, B., & Béliveau, R. (2000). Rapid activation of matrix metalloproteinase-2 by glioma cells occurs through a posttranslational MT1-MMP-

- dependent mechanism. *Biochimica et Biophysica Acta (BBA)-Molecular Cell Research*, 1497(3), 341-350.
- Ginhoux, F., Lim, S., Hoeffel, G., Low, D., & Huber, T. (2013). Origin and differentiation of microglia. *Frontiers in cellular neuroscience*, 7.
- Glezer, I., Simard, A., & Rivest, S. (2007). Neuroprotective role of the innate immune system by microglia. *Neuroscience*, 147(4), 867-883.
- Gloster, T. M., & Vocadlo, D. J. (2012). Developing inhibitors of glycan processing enzymes as tools for enabling glycobiology. *Nature Chemical Biology*, 8(8), 683-694.
- Goddard, D. R., Bunning, R. A., & Woodroffe, M. N. (2001). Astrocyte and endothelial cell expression of ADAM 17 (TACE) in adult human CNS. *Glia*, 34(4), 267-271.
- Goldberg, P., Fleming, M., & Picard, E. (1986). Multiple sclerosis: Decreased relapse rate through dietary supplementation with calcium, magnesium and vitamin D. *Medical Hypotheses*, 21(2), 193-200.
- Gooz, M. (2010). ADAM-17: The enzyme that does it all. *Critical Reviews in Biochemistry and Molecular Biology*, 45(2), 146-169.
- Gottschall, P. E., & Howell, M. D. (2015). ADAMTS expression and function in central nervous system injury and disorders. *Matrix Biology*, 44, 70-76.
- Gourraud, P., Harbo, H. F., Hauser, S. L., & Baranzini, S. E. (2012). The genetics of multiple sclerosis: An up-to-date review. *Immunological Reviews*, 248(1), 87-103.
- Gray, E., Thomas, T. L., Betmouni, S., Scolding, N., & Love, S. (2008). Elevated matrix metalloproteinase-9 and degradation of perineuronal nets in cerebrocortical multiple sclerosis plaques. *Journal of Neuropathology and Experimental Neurology*, 67(9), 888-899.
- Grimpe, B., & Silver, J. (2004). A novel DNA enzyme reduces glycosaminoglycan chains in the glial scar and allows microtransplanted dorsal root ganglia axons to regenerate beyond lesions in the spinal cord. *The Journal of Neuroscience*, 24(6), 1393-1397.
- Gu, Z., Kaul, M., Yan, B., Kridel, S. J., Cui, J., Strongin, A., Lipton, S. A. (2002). S-nitrosylation of matrix metalloproteinases: Signaling pathway to neuronal cell death. *Science*, 297(5584), 1186-1190.

- Gunson, R., Collins, T., & Carman, W. (2006). Practical experience of high throughput real time PCR in the routine diagnostic virology setting. *Journal of Clinical Virology*, 35(4), 355-367.
- Haas, J., Korporal, M., Schwarz, A., Balint, B., & Wildemann, B. (2011). The interleukin-7 receptor  $\alpha$  chain contributes to altered homeostasis of regulatory T cells in multiple sclerosis. *European Journal of Immunology*, 41(3), 845-853.
- Hacker, H., Redecke, V., Blagoev, B., Kratchmarova, I., Hsu, L., Wang, G., Hacker, G. (2006). Specificity in toll-like receptor signalling through distinct effector functions of TRAF3 and TRAF6. *Nature*, 439(7073), 204-207.
- Haddock, G., Cross, A. K., Plumb, J., Surr, J., Buttle, D. J., Bunning, R. A., & Woodroffe, M. N. (2006). Expression of ADAMTS-1, -4, -5 and TIMP-3 in normal and multiple sclerosis CNS white matter. *Multiple Sclerosis*, 12(4), 386-396.
- Haddock, G., Cross, A., Allan, S., Sharrack, B., Callaghan, J., Bunning, R., Woodroffe, M. (2007). Brevican and phosphacan expression and localization following transient middle cerebral artery occlusion in the rat. *Biochemical Society Transactions*, 35(4), 692.
- Haider, L., Fischer, M. T., Frischer, J. M., Bauer, J., Hoftberger, R., Botond, G., Lassmann, H. (2011). Oxidative damage in multiple sclerosis lesions. *Brain*, 134, 1914-1924.
- Hamel, M. G., Ajmo, J. M., Leonardo, C. C., Zuo, F., Sandy, J. D., & Gottschall, P. E. (2008). Multimodal signaling by the ADAMTSs (a disintegrin and metalloproteinase with thrombospondin motifs) promotes neurite extension. *Experimental Neurology*, 210(2), 428-440.
- Hamm, S., Dehouck, B., Kraus, J., Wolburg-Buchholz, K., Wolburg, H., Risau, W., Dehouck, M. (2004). Astrocyte mediated modulation of blood-brain barrier permeability does not correlate with a loss of tight junction proteins from the cellular contacts. *Cell and Tissue Research*, 315(2), 157-166.
- Handel, A. E., Giovannoni, G., Ebers, G. C., & Ramagopalan, S. V. (2010). Environmental factors and their timing in adult-onset multiple sclerosis. *Nature Reviews Neurology*, 6(3), 156-166.
- Handunnetthi, L., Ramagopalan, S. V., Ebers, G. C., & Knight, J. C. (2010). Regulation of major histocompatibility complex class II gene expression, genetic variation and disease. *Genes and Immunity*, 11(2), 99-112.

- Harlow, D. E., & Macklin, W. B. (2014). Inhibitors of myelination: ECM changes, CSPGs and PTPs. *Experimental Neurology*, *251*, 39-46.
- Hayashi, K., Kadomatsu, K., & Muramatsu, T. (2001). Requirement of chondroitin sulfate/dermatan sulfate recognition in midkine-dependent migration of macrophages. *Glycoconjugate Journal*, *18*(5), 401-406.
- Haynes, S. E., Hollopeter, G., Yang, G., Kurpius, D., Dailey, M. E., Gan, W. B., & Julius, D. (2006). The P2Y<sub>12</sub> receptor regulates microglial activation by extracellular nucleotides. *Nature neuroscience*, *9*(12), 1512-1519.
- Hedström, A. K., Hillert, J., Olsson, T., & Alfredsson, L. (2013). Smoking and multiple sclerosis susceptibility. *European Journal of Epidemiology*, *28*(11), 867-874.
- Hedstrom, A. K., Olsson, T., & Alfredsson, L. (2012). High body mass index before age 20 is associated with increased risk for multiple sclerosis in both men and women. *Multiple Sclerosis*, *18*(9), 1334-1336.
- Hickey, W. F. (1999). The pathology of multiple sclerosis: A historical perspective. *Journal of Neuroimmunology*, *98*(1), 37-44.
- Higgins, E. S., & George, M. S. (2013). *Neuroscience of clinical psychiatry: The pathophysiology of behavior and mental illness* Lippincott Williams & Wilkins.
- Hilario, J. D., Rodino-Klapac, L. R., Wang, C., & Beattie, C. E. (2009). Semaphorin 5A is a bifunctional axon guidance cue for axial motoneurons *in vivo*. *Developmental Biology*, *326*(1), 190-200.
- Hill, K. E., Zollinger, L. V., Watt, H. E., Carlson, N. G., & Rose, J. W. (2004). Inducible nitric oxide synthase in chronic active multiple sclerosis plaques: Distribution, cellular expression and association with myelin damage. *Journal of Neuroimmunology*, *151*(1), 171-179.
- Holdt, L. M., Thiery, J., Breslow, J. L., & Teupser, D. (2008). Increased ADAM17 mRNA expression and activity is associated with atherosclerosis resistance in LDL-receptor deficient mice. *Arteriosclerosis, Thrombosis and Vascular Biology*, *28*(6), 1097-1103.
- Holman, D. W., Klein, R. S., & Ransohoff, R. M. (2011). The blood–brain barrier, chemokines and multiple sclerosis. *Biochimica et Biophysica Acta (BBA)-Molecular Basis of Disease*, *1812*(2), 220-230.

- Hoppenbrouwers, I., Aulchenko, Y., Ebers, G. C., Ramagopalan, S., Oostra, B., Van Duijn, C., & Hintzen, R. (2008). EVI5 is a risk gene for multiple sclerosis. *Genes and Immunity*, *9*(4), 334-337.
- Howell, M. D., Torres-Collado, A. X., Iruela-Arispe, M. L., & Gottschall, P. E. (2012). Selective decline of synaptic protein levels in the frontal cortex of female mice deficient in the extracellular metalloproteinase ADAMTS1. *PloS one*, *7*(10).
- Huijbregts, S. C., Kalkers, N. F., de Sonnevile, L. M., de Groot, V., & Polman, C. H. (2006). Cognitive impairment and decline in different MS subtypes. *Journal of the Neurological Sciences*, *245*(1), 187-194.
- Hunanyan, A. S., Garcia-Alias, G., Alessi, V., Levine, J. M., Fawcett, J. W., Mendell, L. M., & Arvanian, V. L. (2010). Role of chondroitin sulfate proteoglycans in axonal conduction in mammalian spinal cord. *The Journal of Neuroscience*, *30*(23), 7761-7769.
- Hynds, D. L., & Snow, D. M. (1999). Neurite outgrowth inhibition by chondroitin sulfate proteoglycan: Stalling/stopping exceeds turning in human neuroblastoma growth cones. *Experimental Neurology*, *160*(1), 244-255.
- Hynds, D. L., & Snow, D. M. (2001). Fibronectin and laminin elicit differential behaviors from SH-SY5Y growth cones contacting inhibitory chondroitin sulfate proteoglycans. *Journal of Neuroscience Research*, *66*(4), 630-642.
- Ibáñez, C. F., & Simi, A. (2012). p75 neurotrophin receptor signaling in nervous system injury and degeneration: Paradox and opportunity. *Trends in Neurosciences*, *35*(7), 431-440.
- Ilic, M. Z., East, C. J., Rogerson, F. M., Fosang, A. J., & Handley, C. J. (2007). Distinguishing aggrecan loss from aggrecan proteolysis in ADAMTS-4 and ADAMTS-5 single and double deficient mice. *The Journal of Biological Chemistry*, *282*(52), 37420-37428.
- Imitola, J., Chitnis, T., & Khoury, S. J. (2005). Cytokines in multiple sclerosis: From bench to bedside. *Pharmacology & Therapeutics*, *106*(2), 163-177.
- Inatani, M., Honjo, M., Otori, Y., Oohira, A., Kido, N., Tano, Y., Tanihara, H. (2001). Inhibitory effects of neurocan and phosphacan on neurite outgrowth from retinal ganglion cells in culture. *Investigative Ophthalmology & Visual Science*, *42*(8), 1930-1938.

International Multiple Sclerosis Genetics Consortium, & Wellcome Trust Case Control Consortium 2. (2011). Genetic risk and a primary role for cell-mediated immune mechanisms in multiple sclerosis. *Nature*, 476(7359), 214-219.

İndüklenmesi, G. E. D. (2014). Early induction of ADAMTS1,-4,-5 and-9 in IL-1 stimulated mouse astrocytes. *Turk Neurosurg*, 24(4), 519-524.

Isik, B., ERDEMLI, H. K., Comertoglu, I., Akyol, S., Firat, R., Kaya, M., Demircan, K. (2015). Changes of the expressions of orphan and gon-ADAMTS in chondrosarcoma cells. *International Journal of Hematology & Oncology*, 25(3).

Jack, C. S., Arbour, N., Blain, M., Meier, U. C., Prat, A., & Antel, J. P. (2007). Th1 polarization of CD4+ T cells by toll-like receptor 3-activated human microglia. *Journal of Neuropathology and Experimental Neurology*, 66(9), 848-859.

Jack, C., Ruffini, F., Bar-Or, A., & Antel, J. P. (2005). Microglia and multiple sclerosis. *Journal of Neuroscience Research*, 81(3), 363-373.

Jander, S., Schroeter, M., Fischer, J., & Stoll, G. (2000). Differential regulation of microglial keratan sulfate immunoreactivity by proinflammatory cytokines and colony-stimulating factors. *Glia*, 30(4), 401-410.

Jiang, D., Liang, J., & Noble, P. W. (2007). Hyaluronan in tissue injury and repair. *Cell Dev. Biol.*, 23, 435-461.

Johnson, M. H., & De Haan, M. (2015). *Developmental cognitive neuroscience: An introduction* John Wiley & Sons.

Jones, G. C., & Riley, G. P. (2005). ADAMTS proteinases: A multi-domain, multi-functional family with roles in extracellular matrix turnover and arthritis. *Arthritis*, 7(4), 160-169.

Jones, L. L., & Tuszynski, M. H. (2002). Spinal cord injury elicits expression of keratan sulfate proteoglycans by macrophages, reactive microglia, and oligodendrocyte progenitors. *The Journal of Neuroscience*, 22(11), 4611-4624.

Jones, L. L., Margolis, R. U., & Tuszynski, M. H. (2003). The chondroitin sulfate proteoglycans neurocan, brevican, phosphacan, and versican are differentially regulated following spinal cord injury. *Experimental Neurology*, 182(2), 399-411.

Jones, L. L., Yamaguchi, Y., Stallcup, W. B., & Tuszynski, M. H. (2002). NG2 is a major chondroitin sulfate proteoglycan produced after spinal cord injury and is expressed by macrophages and oligodendrocyte progenitors. *The Journal of Neuroscience*, 22(7), 2792-2803.

- Kadomatsu, K., & Sakamoto, K. (2014). Mechanisms of axon regeneration and its inhibition: Roles of sulfated glycans. *Archives of Biochemistry and Biophysics*, *558*, 36-41.
- Kaltsonoudis, E., Voulgari, P. V., Konitsiotis, S., & Drosos, A. A. (2014). Demyelination and other neurological adverse events after anti-TNF therapy. *Autoimmunity Reviews*, *13*(1), 54-58.
- Karimi-Abdolrezaee, S., Schut, D., Wang, J., & Fehlings, M. G. (2012). Chondroitinase and growth factors enhance activation and oligodendrocyte differentiation of endogenous neural precursor cells after spinal cord injury. *PLoS One*, *7*(5), e37589.
- Kashiwagi, M., Enghild, J. J., Gendron, C., Hughes, C., Caterson, B., Itoh, Y., & Nagase, H. (2004). Altered proteolytic activities of ADAMTS-4 expressed by C-terminal processing. *The Journal of Biological Chemistry*, *279*(11), 10109-10119.
- Kassmann, C. M., & Nave, K. A. (2008). Oligodendroglial impact on axonal function and survival - a hypothesis. *Current Opinion in Neurology*, *21*(3), 235-241.
- Kettenmann, H., & Verkhratsky, A. (2008). Neuroglia: The 150 years after. *Trends in Neurosciences*, *31*(12), 653-659.
- Khodosevich, K., & Monyer, H. (2010). Signaling involved in neurite outgrowth of postnatally born subventricular zone neurons in vitro. *BMC Neuroscience*, *11*, 18-2202-11-18.
- Kieseier, B. C., Pischel, H., Neuen-Jacob, E., Tourtellotte, W. W., & Hartung, H. (2003). ADAM-10 and ADAM-17 in the inflamed human CNS. *Glia*, *42*(4), 398-405.
- Killar, L., White, J., Black, R., & Peschon, J. (1999). Adamalysins: A family of metzincins including TNF- $\alpha$  converting enzyme (TACE). *Annals of the New York Academy of Sciences*, *878*(1), 442-452.
- Kim, S., Takahashi, H., Lin, W., Descargues, P., Grivennikov, S., Kim, Y., Karin, M. (2009). Carcinoma-produced factors activate myeloid cells through TLR2 to stimulate metastasis. *Nature*, *457*(7225), 102-106.
- Klegeris, A., & McGeer, P. L. (2005). Non-steroidal anti-inflammatory drugs (NSAIDs) and other anti-inflammatory agents in the treatment of neurodegenerative disease. *Current Alzheimer Research*, *2*(3), 355-365.

- Klein, T., & Bischoff, R. (2010). Active metalloproteases of the A disintegrin and metalloprotease (ADAM) family: Biological function and structure. *Journal of Proteome Research*, 10(1), 17-33.
- Kodaira, Y., Nair, S. K., Wrenshall, L. E., Gilboa, E., & Platt, J. L. (2000). Phenotypic and functional maturation of dendritic cells mediated by heparan sulfate. *Journal of Immunology*, 165(3), 1599-1604.
- Kohm, A. P., & Miller, S. D. (2003). Role of ICAM-1 and P-selectin expression in the development and effector function of CD4 CD25 regulatory T cells. *Journal of Autoimmunity*, 21(3), 261-271.
- Koizumi, S., Shigemoto-Mogami, Y., Nasu-Tada, K., Shinozaki, Y., Ohsawa, K., Tsuda, M., & Inoue, K. (2007). UDP acting at P2Y6 receptors is a mediator of microglial phagocytosis. *Nature*, 446(7139), 1091-1095.
- Kolb, W. P., & Granger, G. A. (1968). Lymphocyte in vitro cytotoxicity: Characterization of human lymphotoxin. *Proceedings of the National Academy of Sciences of the United States of America*, 61(4), 1250-1255.
- Koo, B. H., Longpre, J. M., Somerville, R. P., Alexander, J. P., Leduc, R., & Apte, S. S. (2007). Regulation of ADAMTS9 secretion and enzymatic activity by its propeptide. *The Journal of Biological Chemistry*, 282(22), 16146-16154.
- Koprivica, V., Cho, K. S., Park, J. B., Yiu, G., Atwal, J., Gore, B., He, Z. (2005). EGFR activation mediates inhibition of axon regeneration by myelin and chondroitin sulfate proteoglycans. *Science*, 310(5745), 106-110.
- Kouwenhoven, M., Özenci, V., Gomes, A., Yarilin, D., Giedraitis, V., Press, R., & Link, H. (2001). Multiple sclerosis: Elevated expression of matrix metalloproteinases in blood monocytes. *Journal of Autoimmunity*, 16(4), 463-470.
- Krstic, D., Rodriguez, M., & Knuesel, I. (2012). Regulated proteolytic processing of reelin through interplay of tissue plasminogen activator (tPA), ADAMTS-4, ADAMTS-5, and their modulators.
- Krüger, P. (2001). Mast cells and multiple sclerosis: A quantitative analysis. *Neuropathology and Applied Neurobiology*, 27(4), 275-280.
- Kucharova, K., Chang, Y., Boor, A., Yong, V. W., & Stallcup, W. B. (2011). Reduced inflammation accompanies diminished myelin damage and repair in the NG2 null mouse spinal cord. *J Neuroinflammation*, 8, 158.

- Kuhlmann, T., Miron, V., Cui, Q., Wegner, C., Antel, J., & Bruck, W. (2008). Differentiation block of oligodendroglial progenitor cells as a cause for remyelination failure in chronic multiple sclerosis. *Brain*, *131*(Pt 7), 1749-1758.
- Kumar, S., Rao, N., & Ge, R. (2012). Emerging roles of ADAMTSs in angiogenesis and cancer. *Cancers*, *4*(4), 1252-1299.
- Kuno, K., Iizasa, H., Ohno, S., & Matsushima, K. (1997). The exon/intron organization and chromosomal mapping of the mouse ADAMTS-1 gene encoding an ADAM family protein with TSP motifs. *Genomics*, *46*(3), 466-471.
- Kuno, K., Okada, Y., Kawashima, H., Nakamura, H., Miyasaka, M., Ohno, H., & Matsushima, K. (2000). ADAMTS-1 cleaves a cartilage proteoglycan, aggrecan. *FEBS Letters*, *478*(3), 241-245.
- Kurazono, S., Okamoto, M., Sakiyama, J., Mori, S., Nakata, Y., Fukuoka, J., Matsui, H. (2001). Expression of brain specific chondroitin sulfate proteoglycans, neurocan and phosphacan, in the developing and adult hippocampus of Ihara's epileptic rats. *Brain Research*, *898*(1), 36-48.
- Kurien, B. T., & Scofield, R. H. (2006). Western blotting. *Methods*, *38*(4), 283-293.
- Kurien, B. T., Dorri, Y., Dillon, S., Dsouza, A., & Scofield, R. H. (2011). An overview of western blotting for determining antibody specificities for immunohistochemistry. *Signal transduction immunohistochemistry* (pp. 55-67) Springer.
- Kurzepa, J., Bartosik-Psujek, H., Suchozebrska-Jesioneck, D., Rejdak, K., Stryjecka-Zimmer, M., & Stelmasiak, Z. (2005). Role of matrix metalloproteinases in the pathogenesis of multiple sclerosis. *Neurologia i Neurochirurgia Polska*, *39*(1), 63-67.
- Kwok, J. C., Afshari, F., Garcia-Alias, G., & Fawcett, J. W. (2008). Proteoglycans in the central nervous system: Plasticity, regeneration and their stimulation with chondroitinase ABC. *Restorative Neurology and Neuroscience*, *26*(2), 131.
- Kwok, J. C., Dick, G., Wang, D., & Fawcett, J. W. (2011). Extracellular matrix and perineuronal nets in CNS repair. *Developmental Neurobiology*, *71*(11), 1073-1089.
- Kwok, J., Warren, P., & Fawcett, J. (2012). Chondroitin sulphate: A key molecule in the brain matrix. *The International Journal of Biochemistry & Cell Biology*, *44*(4), 582-586.
- Lappe-Siefke, C., Goebbels, S., Gravel, M., Nicksch, E., Lee, J., Braun, P. E., Nave, K. (2003). Disruption of Cnp1 uncouples oligodendroglial functions in axonal support and myelination. *Nature Genetics*, *33*(3), 366-374.

- Larochelle, C., Alvarez, J. I., & Prat, A. (2011). How do immune cells overcome the blood–brain barrier in multiple sclerosis? *FEBS Letters*, *585*(23), 3770-3780.
- Larsen, P. H., Wells, J. E., Stallcup, W. B., Opdenakker, G., & Yong, V. W. (2003). Matrix metalloproteinase-9 facilitates remyelination in part by processing the inhibitory NG2 proteoglycan. *The Journal of Neuroscience*, *23*(35), 11127-11135.
- Lassmann, H., & van Horssen, J. (2011). The molecular basis of neurodegeneration in multiple sclerosis. *FEBS Letters*, *585*(23), 3715-3723.
- Lau, L. W., Cua, R., Keough, M. B., Haylock-Jacobs, S., & Yong, V. W. (2013). Pathophysiology of the brain extracellular matrix: A new target for remyelination. *Nature Reviews Neuroscience*, *14*(10), 722-729.
- Lau, L. W., Keough, M. B., Haylock-Jacobs, S., Cua, R., Döring, A., Sloka, S., Yong, V. W. (2012). Chondroitin sulfate proteoglycans in demyelinated lesions impair remyelination. *Annals of Neurology*, *72*(3), 419-432.
- Lemarchant, S., Pruvost, M., Hébert, M., Gauberti, M., Hommet, Y., Briens, A., Petite, D. (2014). tPA promotes ADAMTS-4-induced CSPG degradation, thereby enhancing neuroplasticity following spinal cord injury. *Neurobiology of Disease*, *66*, 28-42.
- Lemarchant, S., Pruvost, M., Montaner, J., Emery, E., Vivien, D., Kanninen, K., & Koistinaho, J. (2013). ADAMTS proteoglycanases in the physiological and pathological central nervous system. *Journal of Neuroinflammation*, *10*, 133-2094-10-133.
- Lemons, M. L., Sandy, J. D., Anderson, D. K., & Howland, D. R. (2001). Intact aggrecan and fragments generated by both aggrecanase and metalloproteinase-like activities are present in the developing and adult rat spinal cord and their relative abundance is altered by injury. *The Journal of Neuroscience*, *21*(13), 4772-4781.
- Leppert, D., Lindberg, R. L., Kappos, L., & Leib, S. L. (2001). Matrix metalloproteinases: Multifunctional effectors of inflammation in multiple sclerosis and bacterial meningitis. *Brain Research Reviews*, *36*(2), 249-257.
- Lassmann, H., van Horssen, J., & Mahad, D. (2012). Progressive multiple sclerosis: pathology and pathogenesis. *Nature Reviews Neurology*, *8*(11), 647-656.
- Levi-Montalcini, R., & Calissano, P. (2013). Nerve growth factor. *Neuroscience Year: Supplement 2 to the Encyclopedia of Neuroscience*, 110.

- Levine, J. M., Reynolds, R., & Fawcett, J. W. (2001). The oligodendrocyte precursor cell in health and disease. *Trends in Neurosciences*, 24(1), 39-47.
- Libbey, J. E., McCoy, L. L., & Fujinami, R. S. (2007). Molecular mimicry in multiple sclerosis. *International Review of Neurobiology*, 79, 127-147.
- Lill, C. M., Luessi, F., Alcina, A., Sokolova, E. A., Ugidos, N., de la Hera, B., & Mescheriakova, J. Y. (2015). Genome-wide significant association with seven novel multiple sclerosis risk loci. *Journal of medical genetics*, jmedgenet-2015.
- Lim, H., & Joe, Y. A. (2013). A ROCK inhibitor blocks the inhibitory effect of chondroitin sulfate proteoglycan on morphological changes of mesenchymal stromal/stem cells into neuron-like cells. *Biomolecules & Therapeutics*, 21(6), 447.
- Lim, S., & Constantinescu, C. S. (2010). TNF- $\alpha$ : A paradigm of paradox and complexity in multiple sclerosis and its animal models. *Open Autoimmun J*, 2, 160-170.
- Lima, T. F. R., Braga, V. L. L., Silva, J. T. D., Simplício, G. N., de Oliveira, Samira Ádila Abreu, Barros, R. R., dos Santos, Maria do Socorro Vieira. (2015). The HLA-DRB1 alleles effects on multiple sclerosis: A systematic review. *International Archives of Medicine*, 8
- Lin, R., Rosahl, T. W., Whiting, P. J., Fawcett, J. W., & Kwok, J. (2011). 6-sulphated chondroitins have a positive influence on axonal regeneration. *PLoS One*, 6(7), e21499.
- Lindberg, R. L., De Groot, C. J., Montagne, L., Freitag, P., van der Valk, P., Kappos, L., & Leppert, D. (2001). The expression profile of matrix metalloproteinases (MMPs) and their inhibitors (TIMPs) in lesions and normal appearing white matter of multiple sclerosis. *Brain: A Journal of Neurology*, 124(Pt 9), 1743-1753.
- Linnartz, B., Bodea, L., & Neumann, H. (2012). Microglial carbohydrate-binding receptors for neural repair. *Cell and Tissue Research*, 349(1), 215-227.
- Liu, B. P., Cafferty, W. B., Budel, S. O., & Strittmatter, S. M. (2006). Extracellular regulators of axonal growth in the adult central nervous system. *Philosophical Transactions of the Royal Society of London. Series B, Biological Sciences*, 361(1473), 1593-1610.
- Liu, K. J., & Rosenberg, G. A. (2005). Matrix metalloproteinases and free radicals in cerebral ischemia. *Free Radical Biology and Medicine*, 39(1), 71-80.

- Livak, K. J., & Schmittgen, T. D. (2001). Analysis of relative gene expression data using real-time quantitative PCR and the 2- $\Delta\Delta$ CT method. *Methods*, 25(4), 402-408.
- Lleo, A., Galea, E., & Sastre, M. (2007). Molecular targets of non-steroidal anti-inflammatory drugs in neurodegenerative diseases. *Cellular and Molecular Life Sciences*, 64(11), 1403-1418.
- Longpre, J. M., & Leduc, R. (2004). Identification of prodomain determinants involved in ADAMTS-1 biosynthesis. *The Journal of Biological Chemistry*, 279(32), 33237-33245.
- Loughlin, A. J., Woodroffe, M. N., & Cuzner, M. L. (1993). Modulation of interferon-gamma-induced major histocompatibility complex class II and fc receptor expression on isolated microglia by transforming growth factor-beta 1, interleukin-4, noradrenaline and glucocorticoids. *Immunology*, 79(1), 125-130.
- Love, S., Louis, D., & Ellison, D. W. (2008). *Greenfield's neuropathology eighth edition* CRC Press.
- Luan, Y., Kong, L., Howell, D. R., Ilalov, K., Fajardo, M., Bai, X., Liu, C. (2008). Inhibition of ADAMTS-7 and ADAMTS-12 degradation of cartilage oligomeric matrix protein by alpha-2-macroglobulin. *Osteoarthritis and Cartilage*, 16(11), 1413-1420.
- Lucchinetti, C. F., Popescu, B. F., Bunyan, R. F., Moll, N. M., Roemer, S. F., Lassmann, H & Weigand, S. D. (2011). Inflammatory cortical demyelination in early multiple sclerosis. *New England Journal of Medicine*, 365(23), 2188-2197.
- Lublin, F. D., & Reingold, S. C. (1996). Defining the clinical course of multiple sclerosis: Results of an international survey. national multiple sclerosis society (USA) advisory committee on clinical trials of new agents in multiple sclerosis. *Neurology*, 46(4), 907-911.
- Lucas, R. M., Ponsonby, A. L., Dear, K., Valery, P. C., Pender, M. P., Taylor, B. V., McMichael, A. J. (2011). Sun exposure and vitamin D are independent risk factors for CNS demyelination. *Neurology*, 76(6), 540-548.
- Lucchinetti, C. F., Parisi, J., & Bruck, W. (2005). The pathology of multiple sclerosis. *Neurologic Clinics*, 23(1), 77-105.
- Lucchinetti, C., Bruck, W., Parisi, J., Scheithauer, B., Rodriguez, M., & Lassman, H. (2000). Heterogeneity of multiple sclerosis lesions: Implications for the pathogenesis of demyelination. *Annals of Neurology*, 47(6), 707-717.

- Luissint, A., Artus, C., Glacial, F., Ganeshamoorthy, K., & Couraud, P. (2012). Tight junctions at the blood brain barrier: Physiological architecture and disease-associated dysregulation, *9*(1), 23.
- Luitse, M. J., Biessels, G. J., Rutten, G. E., & Kappelle, L. J. (2012). Diabetes, hyperglycaemia, and acute ischaemic stroke. *The Lancet Neurology*, *11*(3), 261-271.
- Luo, L. (2000). Rho GTPases in neuronal morphogenesis. *Nature Reviews Neuroscience*, *1*(3), 173-180.
- Ma, Q., Manaenko, A., Khatibi, N. H., Chen, W., Zhang, J. H., & Tang, J. (2011). Vascular adhesion protein-1 inhibition provides antiinflammatory protection after an intracerebral hemorrhagic stroke in mice. *Journal of Cerebral Blood Flow & Metabolism*, *31*(3), 881-893.
- Maeda, N. (2015). Proteoglycans and neuronal migration in the cerebral cortex during development and disease. *Frontiers in Neuroscience*, *9*
- Maier, L. M., Lowe, C. E., Cooper, J., Downes, K., Anderson, D. E., Severson, C., Aubin, C. (2009). IL2RA genetic heterogeneity in multiple sclerosis and type 1 diabetes susceptibility and soluble interleukin-2 receptor production. *PLoS Genet*, *5*(1), e1000322.
- Majerus, E. M., Zheng, X., Tuley, E. A., & Sadler, J. E. (2003). Cleavage of the ADAMTS13 propeptide is not required for protease activity. *The Journal of Biological Chemistry*, *278*(47), 46643-46648.
- Mammadov, B., Mammadov, R., Guler, M. O., & Tekinay, A. B. (2012). Cooperative effect of heparan sulfate and laminin mimetic peptide nanofibers on the promotion of neurite outgrowth. *Acta Biomaterialia*, *8*(6), 2077-2086.
- Mandal, M., Mandal, A., Das, S., Chakraborti, T., & Chakraborti, S. (2003). Clinical implications of matrix metalloproteinases. *Molecular and Cellular Biochemistry*, *252*(1-2), 305-329.
- Markovic-Plese, S., Pinilla, C., & Martin, R. (2004). The initiation of the autoimmune response in multiple sclerosis. *Clinical Neurology and Neurosurgery*, *106*(3), 218-222.
- Martins, T. B., Rose, J. W., Jaskowski, T. D., Wilson, A. R., Husebye, D., Seraj, H. S., & Hill, H. R. (2011). Analysis of proinflammatory and anti-inflammatory cytokine serum concentrations in patients with multiple sclerosis by using a multiplexed immunoassay. *American Journal of Clinical Pathology*, *136*(5), 696-704.

- Matthews, R. T., Gary, S. C., Zerillo, C., Pratta, M., Solomon, K., Arner, E. C., & Hockfield, S. (2000). Brain-enriched hyaluronan binding (BEHAB)/brevican cleavage in a glioma cell line is mediated by a disintegrin and metalloproteinase with thrombospondin motifs (ADAMTS) family member. *The Journal of Biological Chemistry*, 275(30), 22695-22703.
- McFarland, H. F., & Martin, R. (2007). Multiple sclerosis: A complicated picture of autoimmunity. *Nature Immunology*, 8(9), 913-919.
- McKerracher, L., Ferraro, G. B., & Fournier, A. E. (2012). Rho signaling and axon regeneration. *Int Rev Neurobiol*, 105, 117-140.
- McQuaid, S., Cunnea, P., McMahon, J., & Fitzgerald, U. (2009). The effects of blood-brain barrier disruption on glial cell function in multiple sclerosis. *Biochemical Society Transactions*, 37(1), 329.
- Medana, I., Martinic, M. A., Wekerle, H., & Neumann, H. (2001). Transection of major histocompatibility complex class I-induced neurites by cytotoxic T lymphocytes. *The American Journal of Pathology*, 159(3), 809-815.
- Merson, T. D., Binder, M. D., & Kilpatrick, T. J. (2010). Role of cytokines as mediators and regulators of microglial activity in inflammatory demyelination of the CNS. *Neuromolecular Medicine*, 12(2), 99-132.
- Miguel, R. F., Pollak, A., & Lubec, G. (2005). Metalloproteinase ADAMTS-1 but not ADAMTS-5 is manifold overexpressed in neurodegenerative disorders as down syndrome, alzheimer's and pick's disease. *Molecular Brain Research*, 133(1), 1-5.
- Miller, D. H., Weinshenker, B. G., Filippi, M., Banwell, B. L., Cohen, J. A., Freedman, M. S., Polman, C. H. (2008). Differential diagnosis of suspected multiple sclerosis: A consensus approach. *Multiple Sclerosis*, 14(9), 1157-1174.
- Milo, R., & Kahana, E. (2010). Multiple sclerosis: Geoepidemiology, genetics and the environment. *Autoimmunity Reviews*, 9(5), A387-A394.
- Minagar, A., & Alexander, J. S. (2003). Blood-brain barrier disruption in multiple sclerosis. *Multiple Sclerosis*, 9(6), 540-549.
- Minagar, A., Shapshak, P., Fujimura, R., Ownby, R., Heyes, M., & Eisdorfer, C. (2002). The role of macrophage/microglia and astrocytes in the pathogenesis of three neurologic disorders: HIV-associated dementia, Alzheimer disease, and multiple sclerosis. *Journal of the Neurological Sciences*, 202(1), 13-23.

- Mittelbronn, M., Dietz, K., Schluesener, H., & Meyermann, R. (2001). Local distribution of microglia in the normal adult human central nervous system differs by up to one order of magnitude. *Acta Neuropathologica*, *101*(3), 249-255.
- Mohan, H., Krumbholz, M., Sharma, R., Eisele, S., Junker, A., Sixt, M., Lassmann, H. (2010). Extracellular matrix in multiple sclerosis lesions: Fibrillar collagens, biglycan and decorin are upregulated and associated with infiltrating immune cells. *Brain Pathology*, *20*(5), 966-975.
- Moore, C. S., Abdullah, S. L., Brown, A., Arulpragasam, A., & Crocker, S. J. (2011). How factors secreted from astrocytes impact myelin repair. *Journal of Neuroscience Research*, *89*(1), 13-21.
- Morawski, M., Brückner, G., Arendt, T., & Matthews, R. (2012). Aggrecan: Beyond cartilage and into the brain. *The International Journal of Biochemistry & Cell Biology*, *44*(5), 690-693.
- Mueller, B. K., Mack, H., & Teusch, N. (2005). Rho kinase, a promising drug target for neurological disorders. *Nature Reviews Drug Discovery*, *4*(5), 387-398.
- Muir, E., Adcock, K., Morgenstern, D., Clayton, R., Von Stillfried, N., Rhodes, K., Rogers, J. (2002). Matrix metalloproteinases and their inhibitors are produced by overlapping populations of activated astrocytes. *Molecular Brain Research*, *100*(1), 103-117.
- Munger, K. L. (2013). Childhood obesity is a risk factor for multiple sclerosis. *Multiple Sclerosis*, *19*(13), 1800.
- Nair, A., Frederick, T. J., & Miller, S. D. (2008). Astrocytes in multiple sclerosis: A product of their environment. *Cellular and Molecular Life Sciences*, *65*(17), 2702-2720.
- Nakamura, H., Fujii, Y., Inoki, I., Sugimoto, K., Tanzawa, K., Matsuki, H., Okada, Y. (2000). Brevican is degraded by matrix metalloproteinases and aggrecanase-1 (ADAMTS4) at different sites. *The Journal of Biological Chemistry*, *275*(49), 38885-38890.
- Nandini, C. D., & Sugahara, K. (2006). Role of the sulfation pattern of chondroitin sulfate in its biological activities and in the binding of growth factors. *Advances in Pharmacology*, *53*, 253-279.
- Nave, K. (2010). Myelination and support of axonal integrity by glia. *Nature*, *468*(7321), 244-252.

- Nicholls, J., & Saunders, N. (1996). Regeneration of immature mammalian spinal cord after injury. *Trends in Neurosciences*, *19*(6), 229-234.
- Nicholson, A. C., Malik, S. B., Logsdon, J. M., Jr, & Van Meir, E. G. (2005). Functional evolution of ADAMTS genes: Evidence from analyses of phylogeny and gene organization. *BMC Evolutionary Biology*, *5*, 11.
- Nieto-Sampedro, M. (1999). Neurite outgrowth inhibitors in gliotic tissue. *The functional roles of glial cells in health and disease* (pp. 207-224) Springer.
- Nimmerjahn, A., Kirchhoff, F., & Helmchen, F. (2005). Resting microglial cells are highly dynamic surveillants of brain parenchyma *in vivo*. *Science (New York, N.Y.)*, *308*(5726), 1314-1318.
- Noda, M., Nakanishi, H., Nabekura, J., & Akaike, N. (2000). AMPA–kainate subtypes of glutamate receptor in rat cerebral microglia. *The Journal of Neuroscience*, *20*(1), 251-258.
- Norton, W. T. (1996). Do oligodendrocytes divide? *Neurochemical Research*, *21*(4), 495-503.
- Novak, U., & Kaye, A. H. (2000). Extracellular matrix and the brain: Components and function. *Journal of Clinical Neuroscience*, *7*(4), 280-290.
- Okada, K., Kuroda, E., Yoshida, Y., Yamashita, U., Suzumura, A., & Tsuji, S. (2005). Effects of interferon- $\beta$  on the cytokine production of astrocytes. *Journal of Neuroimmunology*, *159*(1), 48-54.
- Oki, T., Takahashi, S., Kuwabara, S., Yoshiyama, Y., Mori, M., Hattori, T., & Suzuki, N. (2004). Increased ability of peripheral blood lymphocytes to degrade laminin in multiple sclerosis. *Journal of the Neurological Sciences*, *222*(1), 7-11.
- Olson, J. K., Croxford, J. L., Calenoff, M. A., Dal Canto, M. C., & Miller, S. D. (2001). A virus-induced molecular mimicry model of multiple sclerosis. *The Journal of Clinical Investigation*, *108*(2), 311-318.
- Orlando, C., Pinzani, P., & Pazzagli, M. (1998). Developments in quantitative PCR. *Clinical Chemistry and Laboratory Medicine*, *36*(5), 255-269.
- Orton, S., Herrera, B. M., Yee, I. M., Valdar, W., Ramagopalan, S. V., Sadovnick, A. D., Canadian Collaborative Study Group. (2006). Sex ratio of multiple sclerosis in Canada: A longitudinal study. *The Lancet Neurology*, *5*(11), 932-936.
- Overall, C. M. (2002). Molecular determinants of metalloproteinase substrate specificity. *Molecular Biotechnology*, *22*(1), 51-86.

- Park, K. K., Liu, K., Hu, Y., Kanter, J. L., & He, Z. (2010). PTEN/mTOR and axon regeneration. *Experimental Neurology*, 223(1), 45-50.
- Paolicelli, R. C., Bolasco, G., Pagani, F., Maggi, L., Scianni, M., Panzanelli, P & Ragozzino, D. (2011). Synaptic pruning by microglia is necessary for normal brain development. *Science*, 333(6048), 1456-1458.
- Passi, A., Negrini, D., Albertini, R., Miserocchi, G., & De Luca, G. (1999). The sensitivity of versican from rabbit lung to gelatinase A (MMP-2) and B (MMP-9) and its involvement in the development of hydraulic lung edema. *FEBS Letters*, 456(1), 93-96.
- Patani, R., Balaratnam, M., Vora, A., & Reynolds, R. (2007). Remyelination can be extensive in multiple sclerosis despite a long disease course. *Neuropathology and Applied Neurobiology*, 33(3), 277-287.
- Patrikios, P., Stadelmann, C., Kutzelnigg, A., Rauschka, H., Schmidbauer, M., Laursen, H., Lassmann, H. (2006). Remyelination is extensive in a subset of multiple sclerosis patients. *Brain*, 129, 3165-3172.
- Paulissen, G., Rocks, N., Gueders, M. M., Crahay, C., Quesada-Calvo, F., Bekaert, S., Noel, A. (2009). Role of ADAM and ADAMTS metalloproteinases in airway diseases, *10(127)*, 101-186.
- Pellerin, L., & Magistretti, P. (2005). The central role of astrocytes in neuroenergetics. *Neuroglia. Oxford University Press, Oxford*, , 367-376.
- Pender, M. P., & Greer, J. M. (2007). Immunology of multiple sclerosis. *Current Allergy and Asthma Reports*, 7(4), 285-292.
- Pendleton, J. C., Shambloott, M. J., Gary, D. S., Belegu, V., Hurtado, A., Malone, M. L., & McDonald, J. W. (2013). Chondroitin sulfate proteoglycans inhibit oligodendrocyte myelination through PTP $\sigma$ . *Experimental Neurology*, 247, 113-121.
- Persidsky, Y., Ramirez, S. H., Haorah, J., & Kanmogne, G. D. (2006). Blood–brain barrier: Structural components and function under physiologic and pathologic conditions. *Journal of Neuroimmune Pharmacology*, 1(3), 223-236.
- Petty, M. A., & Lo, E. H. (2002). Junctional complexes of the blood–brain barrier: Permeability changes in neuroinflammation. *Progress in Neurobiology*, 68(5), 311-323.
- Piaton, G., Aigrot, M. S., Williams, A., Moyon, S., Tepavcevic, V., Moutkine, I., Lubetzki, C. (2011). Class 3 semaphorins influence oligodendrocyte precursor

recruitment and remyelination in adult central nervous system. *Brain*, 134(Pt 4), 1156-1167.

Piccinini, A. M., & Midwood, K. S. (2010). DAMPening inflammation by modulating TLR signalling. *Mediators of Inflammation*, 2010.

Pierrot-Deseilligny, C., & Souberbielle, J. C. (2010). Is hypovitaminosis D one of the environmental risk factors for multiple sclerosis?. *Brain*, 133(7), 1869-1888.

Pittas, F., Ponsonby, A., van der Mei, Ingrid AF, Taylor, B. V., Blizzard, L., Groom, P., Dwyer, T. (2009). Smoking is associated with progressive disease course and increased progression in clinical disability in a prospective cohort of people with multiple sclerosis. *Journal of Neurology*, 256(4), 577-585.

Plemel, J. R., Keough, M. B., Duncan, G. J., Sparling, J. S., Yong, V. W., Stys, P. K., & Tetzlaff, W. (2014). Remyelination after spinal cord injury: Is it a target for repair? *Progress in Neurobiology*, 117, 54-72.

Plumb, J., Cross, A. K., Surr, J., Haddock, G., Smith, T., Bunning, R. A., & Woodroffe, M. N. (2005). ADAM-17 and TIMP3 protein and mRNA expression in spinal cord white matter of rats with acute experimental autoimmune encephalomyelitis. *Journal of Neuroimmunology*, 164(1), 1-9.

Plumb, J., McQuaid, S., Cross, A. K., Surr, J., Haddock, G., Bunning, R. A., & Woodroffe, M. N. (2006). Upregulation of ADAM-17 expression in active lesions in multiple sclerosis. *Multiple Sclerosis*, 12(4), 375-385.

Polman, C. H., Reingold, S. C., Banwell, B., Clanet, M., Cohen, J. A., Filippi, M., Kappos, L. (2011). Diagnostic criteria for multiple sclerosis: 2010 revisions to the McDonald criteria. *Annals of Neurology*, 69(2), 292-302.

Porter, S., Clark, I., Kevorkian, L., & Edwards, D. (2005). The ADAMTS metalloproteinases. *Biochem. J*, 386, 15-27.

Prat, A., & Antel, J. (2005). Pathogenesis of multiple sclerosis. *Current Opinion in Neurology*, 18(3), 225-230.

Probert, L., & Akassoglou, K. (2001). Glial expression of tumor necrosis factor in transgenic animals: How do these models reflect the "normal situation"? *Glia*, 36(2), 212-219.

Profyris, C., Cheema, S. S., Zang, D., Azari, M. F., Boyle, K., & Petratos, S. (2004). Degenerative and regenerative mechanisms governing spinal cord injury. *Neurobiology of Disease*, 15(3), 415-436.

- Properzi, F., Asher, R. A., & Fawcett, J. W. (2003). Chondroitin sulphate proteoglycans in the central nervous system: Changes and synthesis after injury. *Biochemical Society Transactions*, 31(2), 335-336.
- Properzi, F., Carulli, D., Asher, R. A., Muir, E., Camargo, L. M., Van Kuppevelt, T. H., Sugahara, K. (2005). Chondroitin 6-sulphate synthesis is up-regulated in injured CNS, induced by injury-related cytokines and enhanced in axon-growth inhibitory glia. *European Journal of Neuroscience*, 21(2), 378-390.
- Purves, D., Brannon, E. M., Cabeza, R., Huettel, S. A., LaBar, K. S., Platt, M. L., Woldorff, M. G. (2008). *Principles of cognitive neuroscience* Sinauer Associates Sunderland, MA.
- Racke, M. K. (2009). Immunopathogenesis of multiple sclerosis. *Annals of Indian Academy of Neurology*, 12(4), 215-220.
- Racke, M. K., & Drew, P. D. (2009). Toll-like receptors in multiple sclerosis. *Toll-like receptors: Roles in infection and neuropathology* (pp. 155-168) Springer.
- Ramesh, G., MacLean, A. G., & Philipp, M. T. (2013). Cytokines and chemokines at the crossroads of neuroinflammation, neurodegeneration, and neuropathic pain. *Mediators of Inflammation*, 2013
- Ramos-Vara, J. A. (2005). Technical aspects of immunohistochemistry. *Veterinary Pathology*, 42(4), 405-426.
- Ransohoff, R. M. (2011). Microglia and monocytes: 'tis plain the twain meets in the brain. *Nature neuroscience*, 14(9), 1098-1100.
- Rauch, U. (2004). Extracellular matrix components associated with remodeling processes in brain. *Cellular and Molecular Life Sciences*, 61(16), 2031-2045.
- Rawlings, N. D., Waller, M., Barrett, A. J., & Bateman, A. (2014). MEROPS: The database of proteolytic enzymes, their substrates and inhibitors. *Nucleic Acids Research*, 42(Database issue), D503-9.
- Reid, M. J., Cross, A. K., Haddock, G., Allan, S. M., Stock, C. J., Woodroffe, M. N., Bunning, R. A. (2009). ADAMTS-9 expression is up-regulated following transient middle cerebral artery occlusion (tMCAo) in the rat. *Neuroscience Letters*, 452(3), 252-257.
- Ren, P., Zhang, L., Xu, G., Palmero, L. C., Albin, P. T., Coselli, J. S., LeMaire, S. A. (2013). ADAMTS-1 and ADAMTS-4 levels are elevated in thoracic aortic aneurysms and dissections. *The Annals of Thoracic Surgery*, 95(2), 570-577.

- Renart, J., Reiser, J., & Stark, G. R. (1979). Transfer of proteins from gels to diazobenzoyloxymethyl-paper and detection with antisera: A method for studying antibody specificity and antigen structure. *Proceedings of the National Academy of Sciences of the United States of America*, 76(7), 3116-3120.
- Reynolds, R., Roncaroli, F., Nicholas, R., Radotra, B., Gveric, D., & Howell, O. (2011). The neuropathological basis of clinical progression in multiple sclerosis. *Acta Neuropathologica*, 122(2), 155-170.
- Rivera, S., Khrestchatisky, M., Kaczmarek, L., Rosenberg, G. A., & Jaworski, D. M. (2010). Metzincin proteases and their inhibitors: Foes or friends in nervous system physiology? *The Journal of Neuroscience*, 30(46), 15337-15357.
- Rodríguez, D., Morrison, C. J., & Overall, C. M. (2010). Matrix metalloproteinase: What do they not do? New substrates and biological roles identified by murine models and proteomics. *Biochimica et Biophysica Acta (BBA)-Molecular Cell Research*, 1803(1), 39-54.
- Roelofs, R. F., Fischer, D. F., Houtman, S. H., Sluijs, J. A., Van Haren, W., Van Leeuwen, F. W., & Hol, E. M. (2005). Adult human subventricular, subgranular, and subpial zones contain astrocytes with a specialized intermediate filament cytoskeleton. *Glia*, 52(4), 289-300.
- Rogerson, F. M., Chung, Y. M., Deutscher, M. E., Last, K., & Fosang, A. J. (2010). Cytokine-induced increases in ADAMTS-4 messenger RNA expression do not lead to increased aggrecanase activity in ADAMTS-5-deficient mice. *Arthritis & Rheumatism*, 62(11), 3365-3373.
- Rolls, A., Cahalon, L., Bakalash, S., Avidan, H., Lider, O., & Schwartz, M. (2006). A sulfated disaccharide derived from chondroitin sulfate proteoglycan protects against inflammation-associated neurodegeneration. *FASEB Journal*, 20(3), 547-549.
- Rolls, A., Shechter, R., & Schwartz, M. (2009). The bright side of the glial scar in CNS repair. *Nature Reviews Neuroscience*, 10(3), 235-241.
- Rolls, A., Shechter, R., London, A., Segev, Y., Jacob-Hirsch, J., Amariglio, N., Schwartz, M. (2008). Two faces of chondroitin sulfate proteoglycan in spinal cord repair: A role in microglia/macrophage activation. *PLoS Med*, 5(8), e171.
- Roloff, F., Scheiblich, H., Dewitz, C., Dempewolf, S., Stern, M., & Bicker, G. (2015). Enhanced neurite outgrowth of human model (NT2) neurons by small-molecule inhibitors of Rho/ROCK signaling. *PloS One*, 10(2)

- Rosenberg, G. A. (2002). Matrix metalloproteinases in neuroinflammation. *Glia*, 39(3), 279-291.
- Rosenberg, G. A., Estrada, E. Y., & Dencoff, J. E. (1998). Matrix metalloproteinases and TIMPs are associated with blood-brain barrier opening after reperfusion in rat brain. *Stroke; a Journal of Cerebral Circulation*, 29(10), 2189-2195.
- Ross, M., & Pawlina, W. *Histology A text and atlas*. 2006.
- Rossi, S., Furlan, R., De Chiara, V., Motta, C., Studer, V., Mori, F., Bernardi, G. (2012). Interleukin-1 $\beta$  causes synaptic hyperexcitability in multiple sclerosis. *Annals of Neurology*, 71(1), 76-83.
- Roy, I., Evans, D. B., & Dwinell, M. B. (2014). Chemokines and chemokine receptors: Update on utility and challenges for the clinician. *Surgery*, 155(6), 961-973.
- Sadovnick, A. D. (2013). Differential effects of genetic susceptibility factors in males and females with multiple sclerosis. *Clinical Immunology*, 149(2), 170-175.
- Sanders, V., Conrad, A. J., & Tourtellotte, W. W. (1993). On classification of post-mortem multiple sclerosis plaques for neuroscientists. *Journal of Neuroimmunology*, 46(1), 207-216.
- Sandy, J. D., Westling, J., Kenagy, R. D., Iruela-Arispe, M. L., Verscharen, C., Rodriguez-Mazaneque, J. C., Clowes, A. W. (2001). Versican V1 proteolysis in human aorta in vivo occurs at the Glu441-Ala442 bond, a site that is cleaved by recombinant ADAMTS-1 and ADAMTS-4. *The Journal of Biological Chemistry*, 276(16), 13372-13378.
- Sasaki, M., Seo-Kiryu, S., Kato, R., Kita, S., & Kiyama, H. (2001). A disintegrin and metalloprotease with thrombospondin type1 motifs (ADAMTS-1) and IL-1 receptor type 1 mRNAs are simultaneously induced in nerve injured motor neurons. *Molecular Brain Research*, 89(1), 158-163.
- Sato, W., Tomita, A., Ichikawa, D., Lin, Y., Kishida, H., Miyake, S., Yamamura, T. (2012). CCR2(+)CCR5(+) T cells produce matrix metalloproteinase-9 and osteopontin in the pathogenesis of multiple sclerosis. *Journal of Immunology*, 189(10), 5057-5065.
- Sawcer, S., Franklin, R. J., & Ban, M. (2014). Multiple sclerosis genetics. *The Lancet Neurology*, 13(7), 700-709.
- Schaefer, L., & Schaefer, R. M. (2010). Proteoglycans: From structural compounds to signaling molecules. *Cell and Tissue Research*, 339(1), 237-246.

- Scheller, J., Chalaris, A., Garbers, C., & Rose-John, S. (2011). ADAM17: A molecular switch to control inflammation and tissue regeneration. *Trends in Immunology*, 32(8), 380-387.
- Schmalefeldt, M., Bandtlow, C. E., Dours-Zimmermann, M. T., Winterhalter, K. H., & Zimmermann, D. R. (2000). Brain derived versican V2 is a potent inhibitor of axonal growth. *Journal of Cell Science*, 113, 807-816.
- Schutz-Geschwender, A., Zhang, Y., Holt, T., McDermitt, D., & Olive, D. M. (2004). Quantitative, two-color western blot detection with infrared fluorescence. *LI-COR Biosciences*,
- Scott, A. J., O'Dea, K. P., O'Callaghan, D., Williams, L., Dokpesi, J. O., Tatton, L., Takata, M. (2011). Reactive oxygen species and p38 mitogen-activated protein kinase mediate tumor necrosis factor alpha-converting enzyme (TACE/ADAM-17) activation in primary human monocytes. *The Journal of Biological Chemistry*, 286(41), 35466-35476.
- Serres, S., Mardiguan, S., Campbell, S. J., McAteer, M. A., Akhtar, A., Krapitchev, A., Sibson, N. R. (2011). VCAM-1-targeted magnetic resonance imaging reveals subclinical disease in a mouse model of multiple sclerosis. *FASEB Journal*, 25(12), 4415-4422.
- Sharma, K., Selzer, M. E., & Li, S. (2012). Scar-mediated inhibition and CSPG receptors in the CNS. *Experimental Neurology*, 237(2), 370-378.
- Shen, Y., Tenney, A. P., Busch, S. A., Horn, K. P., Cuascut, F. X., Liu, K., Flanagan, J. G. (2009). PTPsigma is a receptor for chondroitin sulfate proteoglycan, an inhibitor of neural regeneration. *Science*, 326(5952), 592-596.
- Sherman, L. S., & Back, S. A. (2008). A 'GAG' reflex prevents repair of the damaged CNS. *Trends in Neurosciences*, 31(1), 44-52.
- Shimoda, M., & Khokha, R. (2013). Proteolytic factors in exosomes. *Proteomics*, 13(10-11), 1624-1636.
- Shiomi, T., Lemaître, V., D'Armiento, J., & Okada, Y. (2010). Matrix metalloproteinases, a disintegrin and metalloproteinases, and a disintegrin and metalloproteinases with thrombospondin motifs in non-neoplastic diseases. *Pathology International*, 60(7), 477-496.
- Shivane, A. G., & Chakrabarty, A. (2007). Multiple sclerosis and demyelination. *Current Diagnostic Pathology*, 13(3), 193-202.

- Shokrgozar, M. A., Sarial, S., Amirzargar, A., Shokri, F., Rezaei, N., Arjang, Z., Lotfi, J. (2009). IL-2, IFN- $\gamma$ , and IL-12 gene polymorphisms and susceptibility to multiple sclerosis. *Journal of Clinical Immunology*, 29(6), 747-751.
- Shute, J. (2012). Glycosaminoglycan and chemokine/growth factor interactions. *Heparin-A century of progress*, 307-324.
- Siebert, J. R., Conta Steencken, A., & Osterhout, D. J. (2014). Chondroitin sulfate proteoglycans in the nervous system: Inhibitors to repair. *BioMed Research International*, 2014
- Skotak, M., Wang, F., & Chandra, N. (2012). An in vitro injury model for SH-SY5Y neuroblastoma cells: Effect of strain and strain rate. *Journal of Neuroscience Methods*, 205(1), 159-168.
- Sloane, J. A., Batt, C., Ma, Y., Harris, Z. M., Trapp, B., & Vartanian, T. (2010). Hyaluronan blocks oligodendrocyte progenitor maturation and remyelination through TLR2. *Proceedings of the National Academy of Sciences of the United States of America*, 107(25), 11555-11560.
- Smith, G. M., & Strunz, C. (2005). Growth factor and cytokine regulation of chondroitin sulfate proteoglycans by astrocytes. *Glia*, 52(3), 209-218.
- Sofroniew, M. V., & Vinters, H. V. (2010). Astrocytes: Biology and pathology. *Acta Neuropathologica*, 119(1), 7-35.
- Somerville, R. P., Longpre, J. M., Jungers, K. A., Engle, J. M., Ross, M., Evanko, S., Apte, S. S. (2003). Characterization of ADAMTS-9 and ADAMTS-20 as a distinct ADAMTS subfamily related to caenorhabditis elegans GON-1. *The Journal of Biological Chemistry*, 278(11), 9503-9513.
- Sorokin, L. (2010). The impact of the extracellular matrix on inflammation. *Nature Reviews Immunology*, 10(10), 712-723.
- Sospedra, M., & Martin, R. (2005). Immunology of multiple sclerosis. *Immunol.*, 23, 683-747.
- Sotgiu, S., Pugliatti, M., Fois, M. L., Arru, G., Sanna, A., Sotgiu, M. A., & Rosati, G. (2004). Genes, environment, and susceptibility to multiple sclerosis. *Neurobiology of Disease*, 17(2), 131-143.
- Stanton, H., Melrose, J., Little, C. B., & Fosang, A. J. (2011). Proteoglycan degradation by the ADAMTS family of proteinases. *Biochimica Et Biophysica Acta (BBA)-Molecular Basis of Disease*, 1812(12), 1616-1629.

- Steinman, L. (2009). A molecular trio in relapse and remission in multiple sclerosis. *Nature Reviews Immunology*, 9(6), 440-447.
- Sternlicht, M. D., & Werb, Z. (2001). How matrix metalloproteinases regulate cell behavior. *Annual Review of Cell and Developmental Biology*, 17, 463-516.
- Stratton, C. W., & Wheldon, D. B. (2006). Multiple sclerosis: An infectious syndrome involving chlamydia pneumoniae. *Trends in Microbiology*, 14(11), 474-479.
- Strober, W. (2001). Trypan blue exclusion test of cell viability. *Current Protocols in Immunology*.
- Sugahara, K., & Mikami, T. (2007). Chondroitin/dermatan sulfate in the central nervous system. *Current Opinion in Structural Biology*, 17(5), 536-545.
- Suvarna, S. K., Layton, C., & Bancroft, J. D. (2013). Bancroft's theory and practice of histological techniques, expert consult: *Bancroft's theory and practice of histological techniques* Elsevier Health Sciences.
- Szabo, K. A., Ablin, R. J., & Singh, G. (2004). Matrix metalloproteinases and the immune response. *Clinical and Applied Immunology Reviews*, 4(5), 295-319.
- Takahashi, H., & Craig, A. M. (2013). Protein tyrosine phosphatases PTP $\delta$ , PTP $\sigma$ , and LAR: Presynaptic hubs for synapse organization. *Trends in Neurosciences*, 36(9), 522-534.
- Takeda, K., & Akira, S. (2005). Toll-like receptors in innate immunity. *International Immunology*, 17(1), 1-14.
- Takeda, S., Takeya, H., & Iwanaga, S. (2012). Snake venom metalloproteinases: Structure, function and relevance to the mammalian ADAM/ADAMTS family proteins. *Biochimica Et Biophysica Acta (BBA)-Proteins and Proteomics*, 1824(1), 164-176.
- Tan, C. L., Kwok, J. C., Patani, R., French-Constant, C., Chandran, S., & Fawcett, J. W. (2011). Integrin activation promotes axon growth on inhibitory chondroitin sulfate proteoglycans by enhancing integrin signaling. *The Journal of Neuroscience*, 31(17), 6289-6295.
- Tang, B. L. (2001). ADAMTS: A novel family of extracellular matrix proteases. *The International Journal of Biochemistry & Cell Biology*, 33(1), 33-44.

- Tauchi, R., Imagama, S., Natori, T., Ohgomori, T., Muramoto, A., Shinjo, R., Kadomatsu, K. (2012). The endogenous proteoglycan-degrading enzyme ADAMTS-4 promotes functional recovery after spinal cord injury. *J Neuroinflammation*, 9, 53.
- Tauchi, R., Imagama, S., Ohgomori, T., Natori, T., Shinjo, R., Ishiguro, N., & Kadomatsu, K. (2012). ADAMTS-13 is produced by glial cells and upregulated after spinal cord injury. *Neuroscience Letters*, 517(1), 1-6.
- Taylor, B. V. (2011). The major cause of multiple sclerosis is environmental: Genetics has a minor role--yes. *Multiple Sclerosis*, 17(10), 1171-1173.
- Thon, N., Haas, C. A., Rauch, U., Merten, T., Fässler, R., Frotscher, M., & Deller, T. (2000). The chondroitin sulphate proteoglycan brevican is upregulated by astrocytes after entorhinal cortex lesions in adult rats. *European Journal of Neuroscience*, 12(7), 2547-2558.
- Tian, Y., Zhang, P., Xiao, X., Zhang, J., Zhao, J., Kang, Q., Liu, Y. (2007). The quantification of ADAMTS expression in an animal model of cerebral ischemia using real-time PCR. *Acta Anaesthesiologica Scandinavica*, 51(2), 158-164.
- Tong, J., Liu, W., Wang, X., Han, X., Hyrien, O., Samadani, U., Huang, J. H. (2013). Inhibition of nogo-66 receptor 1 enhances recovery of cognitive function after traumatic brain injury in mice. *Journal of Neurotrauma*, 30(4), 247-258.
- Tonge, D. A., de Burgh, H. T., Docherty, R., Humphries, M. J., Craig, S. E., & Pizzey, J. (2012). Fibronectin supports neurite outgrowth and axonal regeneration of adult brain neurons *in vitro*. *Brain Research*, 1453, 8-16.
- Tortorella, M. D., Burn, T. C., Pratta, M. A., Abbaszade, I., Hollis, J. M., Liu, R., Arner, E. C. (1999). Purification and cloning of aggrecanase-1: A member of the ADAMTS family of proteins. *Science*, 284(5420), 1664-1666.
- Tortorella, M. D., Pratta, M., Liu, R. Q., Austin, J., Ross, O. H., Abbaszade, I., Arner, E. (2000). Sites of aggrecan cleavage by recombinant human aggrecanase-1 (ADAMTS-4). *The Journal of Biological Chemistry*, 275(24), 18566-18573.
- Tortorella, M., Malfait, A., Deccico, C., & Arner, E. (2001). The role of ADAM-TS-4 (aggrecanase-1) and ADAM-TS-5 (aggrecanase-2) in a model of cartilage degradation. *Osteoarthritis and Cartilage*, 9(6), 539-552.
- Trapp, B. D., Peterson, J., Ransohoff, R. M., Rudick, R., Mörk, S., & Bö, L. (1998). Axonal transection in the lesions of multiple sclerosis. *New England Journal of Medicine*, 338(5), 278-285.

- Trendelenburg, G., & Dirnagl, U. (2005). Neuroprotective role of astrocytes in cerebral ischemia: focus on ischemic preconditioning. *Glia*, *50*(4), 307-320.
- Troeberg, L., & Nagase, H. (2012). Proteases involved in cartilage matrix degradation in osteoarthritis. *Biochimica et Biophysica Acta (BBA)-Proteins and Proteomics*, *1824*(1), 133-145.
- Tullman, M. J. (2013). Overview of the epidemiology, diagnosis, and disease progression associated with multiple sclerosis, *19*(2), S15-20.
- Van der Valk, P., & De Groot, C. (2000). Staging of multiple sclerosis (MS) lesions: Pathology of the time frame of MS. *Neuropathology and Applied Neurobiology*, *26*(1), 2-10.
- Van Horssen, J., Dijkstra, C. D., & De Vries, H. E. (2007). The extracellular matrix in multiple sclerosis pathology. *Journal of Neurochemistry*, *103*(4), 1293-1301.
- Van Leeuwen, F., Salehi, A., Giger, R., Holtmaat, A., & Verhaagen, J. (1998). Semaphorin-mediated neuronal growth cone guidance. *Neuronal Degeneration and Regeneration*, *117*, 115.
- Vandesompele, J., De Preter, K., Pattyn, F., Poppe, B., Van Roy, N., De Paepe, A., & Speleman, F. (2002). Accurate normalization of real-time quantitative RT-PCR data by geometric averaging of multiple internal control genes. *Genome Biology*, *3*(7).
- Verslegers, M., Lemmens, K., Van Hove, I., & Moons, L. (2013). Matrix metalloproteinase-2 and-9 as promising benefactors in development, plasticity and repair of the nervous system. *Progress in Neurobiology*, *105*, 60-78.
- Viapiano, M. S., & Matthews, R. T. (2006). From barriers to bridges: Chondroitin sulfate proteoglycans in neuropathology. *Trends in Molecular Medicine*, *12*(10), 488-496.
- Viegas, M., Martins, T., Seco, F., & Do Carmo, A. (2009). An improved and cost-effective methodology for the reduction of autofluorescence in direct immunofluorescence studies on formalin-fixed paraffin-embedded tissues. *European Journal of Histochemistry*, *51*(1), 59-66.
- Von Bernhardi, R., & Ramirez, G. (2001). Microglia astrocyte interaction in alzheimer's disease: Friends or foes for the nervous system? *Biological Research*, *34*(2), 123-128.
- Vong, S., & Kalluri, R. (2011). The role of stromal myofibroblast and extracellular matrix in tumor angiogenesis. *Genes & Cancer*, *2*(12), 1139-1145.

Wågsäter, D., Björk, H., Zhu, C., Björkegren, J., Valen, G., Hamsten, A., & Eriksson, P. (2008). ADAMTS-4 and -8 are inflammatory regulated enzymes expressed in macrophage-rich areas of human atherosclerotic plaques. *Atherosclerosis*, *196*(2), 514-522.

Wake, H., Moorhouse, A. J., & Nabekura, J. (2011). Functions of microglia in the central nervous system—beyond the immune response. *Neuron glia biology*, *7*(01), 47-53.

Wang, H., Wu, M., Zhan, C., Ma, E., Yang, M., Yang, X., & Li, Y. (2012). Neurofilament proteins in axonal regeneration and neurodegenerative diseases. *Neural Regeneration Research*, *7*(8), 620.

Wang, P., Tortorella, M., England, K., Malfait, A. M., Thomas, G., Arner, E. C., & Pei, D. (2004). Proprotein convertase furin interacts with and cleaves pro-ADAMTS4 (aggrecanase-1) in the trans-golgi network. *The Journal of Biological Chemistry*, *279*(15), 15434-15440.

Wang, T., Liu, B., Qin, L., Wilson, B., & Hong, J. (2004). Protective effect of the SOD/catalase mimetic MnTMPyP on inflammation-mediated dopaminergic neurodegeneration in mesencephalic neuronal-glial cultures. *Journal of Neuroimmunology*, *147*(1), 68-72.

Weber, S., Wetzel, S., Prox, J., Lehmann, T., Schneppenheim, J., Donners, M., & Saftig, P. (2013). Regulation of adult hematopoiesis by the a disintegrin and metalloproteinase 10 (ADAM10). *Biochemical and Biophysical Research Communications*, *442*(3), 234-241.

Weishaupt, A., Kreiss, M., Gold, R., & Herrmann, T. (2004). Modulation of experimental autoimmune encephalomyelitis by administration of cells expressing antigenic peptide covalently linked to MHC class II. *Journal of Neuroimmunology*, *152*(1), 11-19.

Westling, J., Fosang, A. J., Last, K., Thompson, V. P., Tomkinson, K. N., Hebert, T., Sandy, J. D. (2002). ADAMTS4 cleaves at the aggrecanase site (Glu373-Ala374) and secondarily at the matrix metalloproteinase site (Asn341-Phe342) in the aggrecan interglobular domain. *The Journal of Biological Chemistry*, *277*(18), 16059-16066.

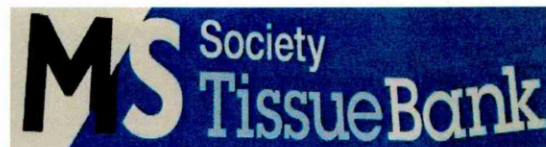
Westling, J., Gottschall, P., Thompson, V., Cockburn, A., Perides, G., Zimmermann, D., & Sandy, J. (2004). ADAMTS4 (aggrecanase-1) cleaves human brain versican V2 at Glu405-Gln406 to generate glial hyaluronate binding protein. *Biochem.J*, *377*, 787-795.

- Wiese, S., Karus, M., & Faissner, A. (2012). Astrocytes as a source for extracellular matrix molecules and cytokines. *Frontiers in Pharmacology*, 3, 120.
- Wójciak-Stothard, B., Entwistle, A., Garg, R., & Ridley, A. J. (1998). Regulation of TNF- $\alpha$ -induced reorganization of the actin cytoskeleton and cell-cell junctions by rho, rac, and Cdc42 in human endothelial cells. *Journal of Cellular Physiology*, 176(1), 150-165.
- Wu, Y. J., LA Pierre, D. P., Jin, W., Albert, J. Y., & Burton, B. Y. (2005). The interaction of versican with its binding partners. *Cell Research*, 15(7), 483-494.
- Yamada, H., Fredette, B., Shitara, K., Hagihara, K., Miura, R., Ranscht, B., Yamaguchi, Y. (1997). The brain chondroitin sulfate proteoglycan brevican associates with astrocytes ensheathing cerebellar glomeruli and inhibits neurite outgrowth from granule neurons. *The Journal of Neuroscience*, 17(20), 7784-7795.
- Yang, Y., & Rosenberg, G. A. (2011). Blood-brain barrier breakdown in acute and chronic cerebrovascular disease. *Stroke; a Journal of Cerebral Circulation*, 42(11), 3323-3328.
- Yang, Y., Estrada, E. Y., Thompson, J. F., Liu, W., & Rosenberg, G. A. (2007). Matrix metalloproteinase-mediated disruption of tight junction proteins in cerebral vessels is reversed by synthetic matrix metalloproteinase inhibitor in focal ischemia in rat. *Journal of Cerebral Blood Flow & Metabolism*, 27(4), 697-709.
- Yao, P. J., O'Herron, T. M., & Coleman, P. D. (2003). Immunohistochemical characterization of clathrin assembly protein AP180 and synaptophysin in human brain. *Neurobiology of Aging*, 24(1), 173-178.
- Yaykasli, K. O., Oohashi, T., Hirohata, S., Hatipoglu, O. F., Inagawa, K., Demircan, K., & Ninomiya, Y. (2009). ADAMTS9 activation by interleukin 1 $\beta$  via NFATc1 in OUMS-27 chondrosarcoma cells and in human chondrocytes. *Molecular and Cellular Biochemistry*, 323(1-2), 69-79.
- Yiu, G., & He, Z. (2006). Glial inhibition of CNS axon regeneration. *Nature Reviews Neuroscience*, 7(8), 617-627.
- Yong, V. W. (2005). Metalloproteinases: Mediators of pathology and regeneration in the CNS. *Nature Reviews Neuroscience*, 6(12), 931-944.
- Yong, V. W., Power, C., Forsyth, P., & Edwards, D. R. (2001). Metalloproteinases in biology and pathology of the nervous system. *Nature Reviews Neuroscience*, 2(7), 502-511.

- Yu, P., Wang, H., Katagiri, Y., & Geller, H. M. (2012). An in vitro model of reactive astrogliosis and its effect on neuronal growth. *Astrocytes*, 327-340.
- Yuan, Y., & He, C. (2013). The glial scar in spinal cord injury and repair. *Neuroscience Bulletin*, 29(4), 421-435.
- Zako, M., Shinomura, T., Ujita, M., Ito, K., & Kimata, K. (1995). Expression of PG-M(V3), an alternatively spliced form of PG-M without a chondroitin sulfate attachment in region in mouse and human tissues. *The Journal of Biological Chemistry*, 270(8), 3914-3918.
- Zamanian, J. L., Xu, L., Foo, L. C., Nouri, N., Zhou, L., Giffard, R. G., & Barres, B. A. (2012). Genomic analysis of reactive astrogliosis. *The Journal of Neuroscience*, 32(18), 6391-6410.
- Zeng, W., Corcoran, C., Collins-Racie, L. A., LaVallie, E. R., Morris, E. A., & Flannery, C. R. (2006). Glycosaminoglycan-binding properties and aggrecanase activities of truncated ADAMTSs: Comparative analyses with ADAMTS-5,-9,-16 and-18. *Biochimica et Biophysica Acta -General Subjects*, 1760(3), 517-524.
- Zephir, H., Fajardy, I., Outteryck, O., Blanc, F., Roger, N., Fleury, M., de Seze, J. (2009). Is neuromyelitis optica associated with human leukocyte antigen? *Multiple Sclerosis*, 15(5), 571-579.
- Zhao, R., & Fawcett, J. W. (2013). Combination treatment with chondroitinase ABC in spinal cord injury—breaking the barrier. *Neuroscience Bulletin*, 29(4), 477-483.
- Zheng, J., Lan, Y., Zhang, J., Guo, Y., & Luo, Y. (2000). *In vitro* culture and immunohistochemical identification of astrocytes of infantile optic nerve, 16(3), 203-207.
- Zhong, Y., Kinio, A., & Saleh, M. (2013). Functions of NOD-like receptors in human diseases. *Frontiers in Immunology*, 4.
- Zimmermann, D. R., & Dours-Zimmermann, M. T. (2008). Extracellular matrix of the central nervous system: From neglect to challenge. *Histochemistry and Cell Biology*, 130(4), 635-653.
- Zuvich, R., McCauley, J., Pericak-Vance, M., & Haines, J. (2009). Genetics and pathogenesis of multiple sclerosis. *Seminars in Immunology*, , 21(6) 328-333.

# Appendices

## Appendix I



### **MS Society Tissue Bank**

Wolfson Neuroscience Laboratories  
Imperial College London  
Hammersmith Hospital Campus  
160 Du Cane Road  
London W12 0NN  
Phone+ 44(0)20 7594 9734  
Fax + 44(0) 20 7594 9735  
UKmstissuebank@imperial.ac.uk  
WWW.UKmstissuebank. imperial.ac.uk

7 March 2013

Nicola Woodroofe  
Sheffield Hallam University  
Biomedical Research Centre  
Floor 7 Owen building  
Howard Street  
Sheffield S1 1WB

Dear Prof Nicola Woodroofe

Study Title: The role of ADAMTS-1, 4 and 9 and associated changes in the extracellular matrix in the pathogenesis of multiple sclerosis

REC Reference number: 08/MRE09/31

Tissue supplied for the project: 84 snap frozen block of human brain tissue from 28 MS and 8 control cases.

## **Appendix II**

### **Buffers and Solutions**

#### **4% Paraformaldehyde**

Phosphate buffer 0.2M

(Solution A)

Weight out 11.36g  $\text{Na}_2\text{HPO}_4$  and dissolve in 400ml of distilled  $\text{H}_2\text{O}$

(Solution B)

3.2 g  $\text{NaH}_2\text{PO}_4 \cdot 2\text{H}_2\text{O}$  in 100ml  $\text{dH}_2\text{O}$

0.2M phosphate buffer was made by mixing solution A& B above

in fume hood, 16g of paraformaldehyde was added to 100mL of distilled  $\text{H}_2\text{O}$  and heated to  $60^\circ\text{C}$  then add 2M  $\text{N}_2\text{OH}$  to dissolve. Added distilled  $\text{H}_2\text{O}$  to make a total volume of 200ml. Add 200ml of 0.2M phosphate buffer and pH to 7.2.

#### **Preparation instruction of Chondroitinase**

Reconstitute in a 0.01% bovine serum albumin aqueous solution. Subsequent dilutions can be made into a buffer containing 50mM Tris, pH 8.0, 60mM sodium acetate and 0.02% bovine serum albumin. Solutions should be prepared fresh.

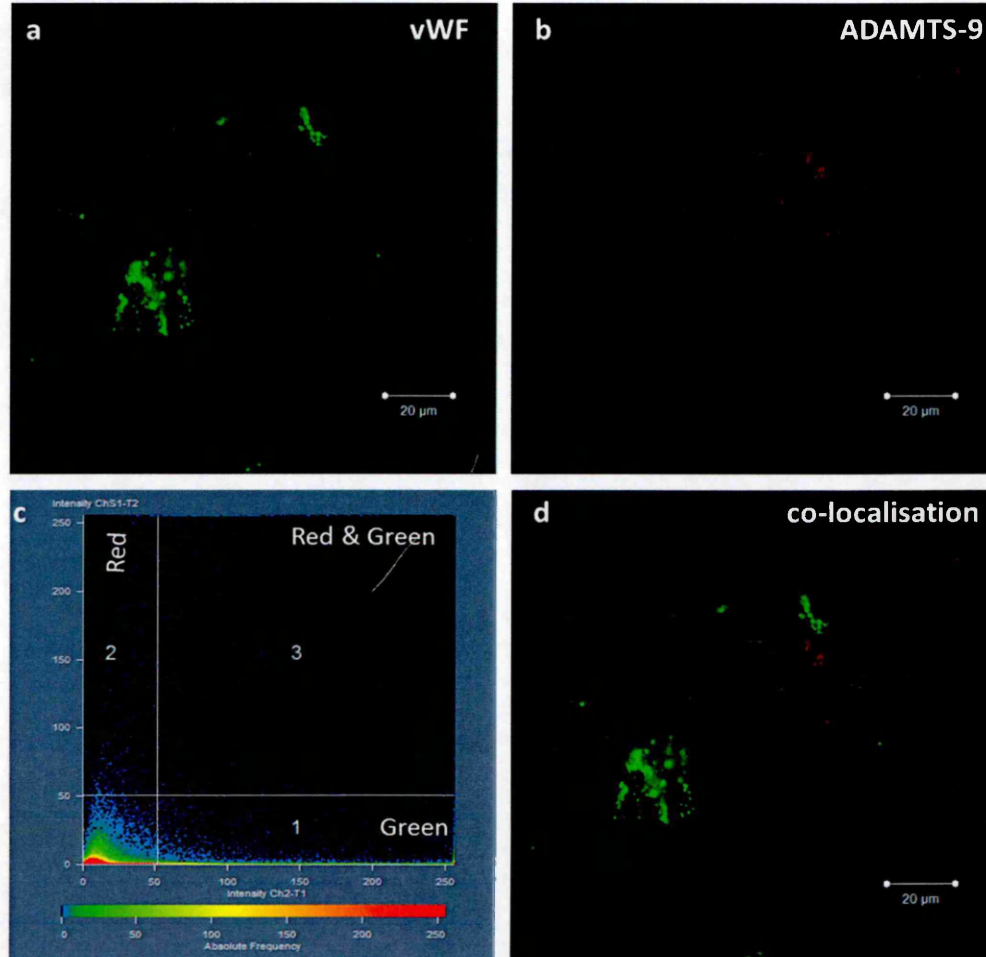
#### **Running Buffer 1x**

Running Buffer was made by mixing 100ml methanol, 850mL  $\text{H}_2\text{O}$  and 50mL running buffer 20X (invitrogen, UK)

#### **Reconstitution of cytokine**

Recombinant cytokines IL- $\beta$  (50 $\mu\text{g}$ ), TNF- $\alpha$  (50 $\mu\text{g}$ ) and IFN- $\gamma$  (20  $\mu\text{g}$ ) were reconstituted from lyophilised powder in 500 $\mu\text{L}$ , 500  $\mu\text{L}$ , 200  $\mu\text{L}$  PBS respectively, to give final stock concentration of 100 $\mu\text{g}/\text{mL}$ . These stock solutions of cytokines were stored in 20 $\mu\text{L}$  aliquots at  $-20^\circ\text{C}$  for further dilution on the day of experiments.

## Appendix III



Dual label immunofluorescence of ADAMTS-9 and vWF in normal control brain tissue

Dual-label immunofluorescence for (a) vWF (green) and (b) ADAMTS-9 (red) in normal control brain tissue white matter with low levels of parenchymal ADAMTS-9 immunoreactivity. (c) Co-localisation is not represented by pixels in quadrant 3 on the graph and is not demonstrated as yellow pixels in the composite image as shown in chapter 4.

Co-localisation software of the Zeiss 510 CSLM was utilised to conclude whether or not individual pixels were truly co-localised for the ADAMTS-9. The software produce as spectra dot plots that displays channel 1 pixels in quadrant 2, channel 2 pixels in quadrant 1 and pixels that are both channel 1 + 2 in quadrant 3.

## Appendix IV

### Published Abstracts

- Abuneeza E, Cross AK, Haddock G, Bunning RAD and Woodroofe MN. Expression of ADAMTS-9 in the central nervous system in multiple sclerosis and its relationship to cleavage of aggrecan and versican. Poster presented at International society of neuroimmunology, 9-13<sup>th</sup> November 2014, Esni Course-European School of Neuroimmunology, Mainz, Germany. International Journal of Neuroimmunology.
- Abuneeza E, Cross AK, Haddock G, Bunning RAD and Woodroofe MN. Changes in extracellular matrix chondroitin sulphate proteoglycan in multiple sclerosis white matter lesions: a role for ADAMTS-9. Poster presented at British Society for immunology Congress 2<sup>nd</sup> - 5<sup>th</sup> December 2013, The Arena & Convention Centre, Liverpool, UK.

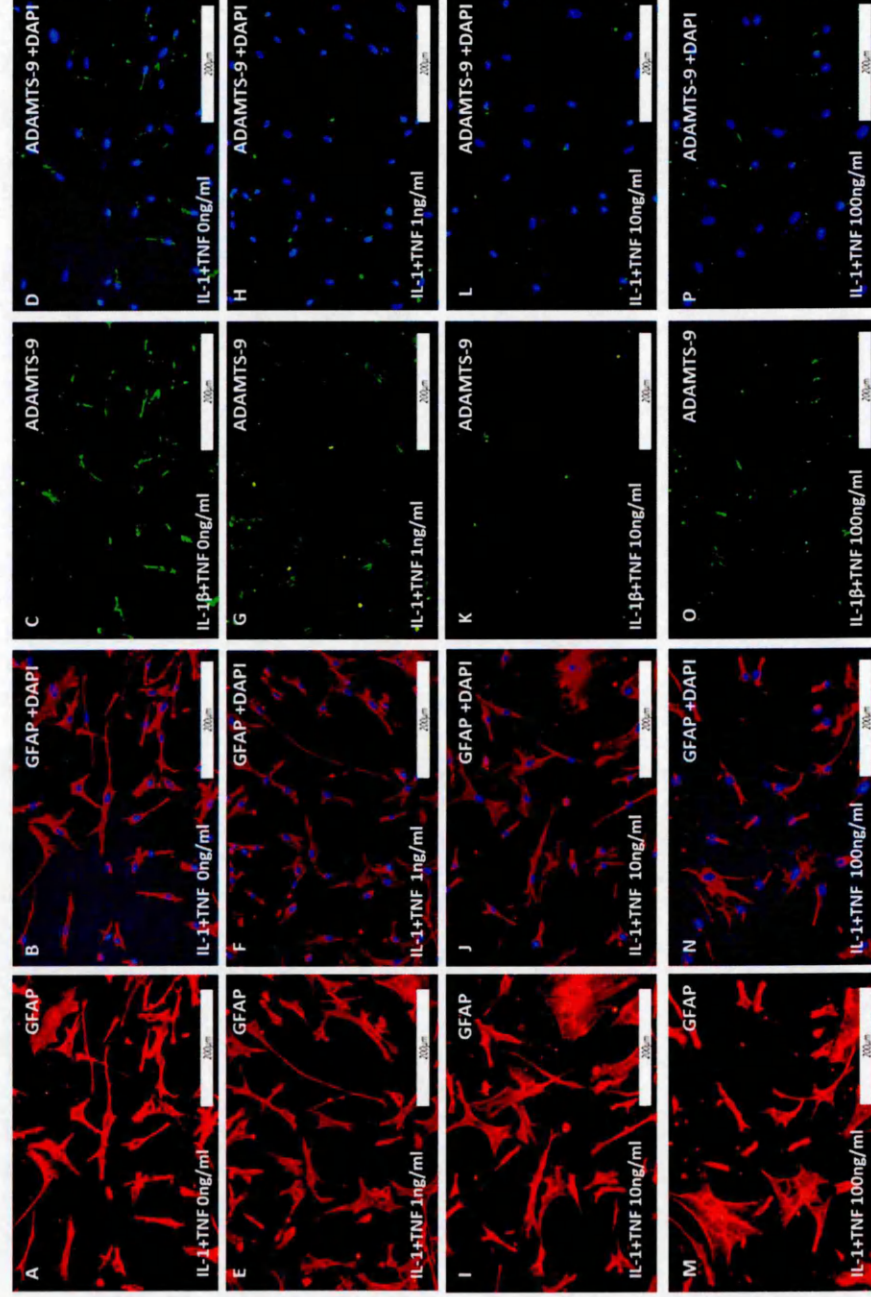
### Department Oral Presentation (BMRC)

- Final year presentation: February 2015
- Second year presentation: August 2014
- First year presentation: March 2013
- Introductory oral presentation: July 2012

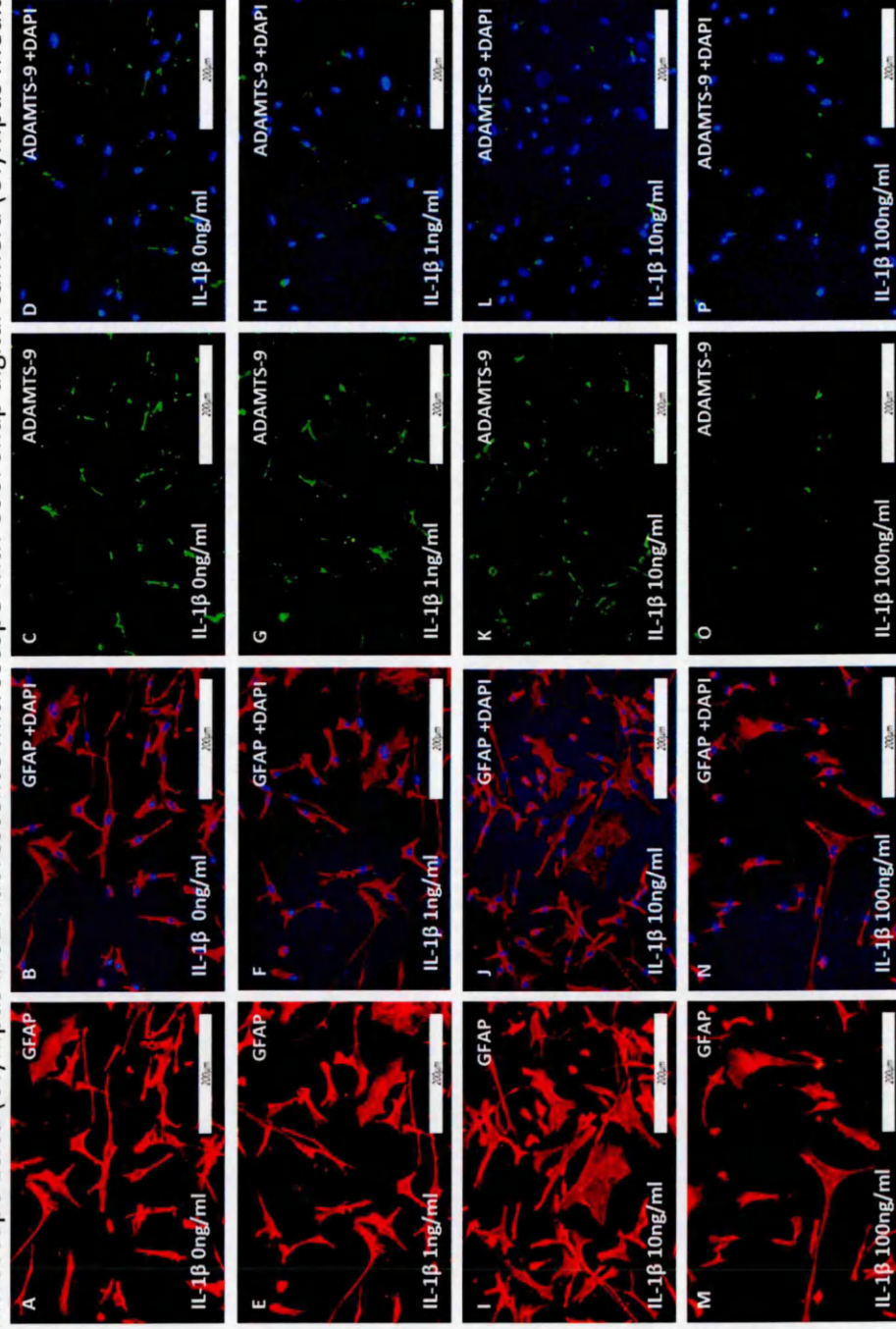
### Conference attendance

- Yorkshire Immunology Group Symposium 12<sup>th</sup> June 2013, Alfred Denny Biology LT1, University of Sheffield, Sheffield, UK.
- BMRC/MERI Winter Poster session 17<sup>th</sup> December 2013, Sheffield Hallam University, Sheffield, UK.
- British Society for immunology Congress 2<sup>nd</sup> - 5<sup>th</sup> December 2013, The Arena & Convention Centre, Liverpool, UK.
- British Society for immunology Summer School 29 July- 1 August 2013, University of Newcastle, Newcastle, UK.
- The first BMRC PhD Summer Research Conference 9<sup>th</sup> July 2012, Sheffield Hallam University, Sheffield, UK.

**Appendix V :** Dual immunofluorescence showing expression of GFAP (red) and ADAMTS-9 (green) in human primary astrocytes untreated and after dual treatment with varying concentrations (0-100mg/mL) of IL-1 $\beta$  and TNF- $\alpha$ . Images from A to D represent cells not treated. Images from E to H represented cells dual treated with cytokines at concentration 1ng/ml. (I, J, K and L) and (M, N, O and P) cells treated with the same pro-inflammatory cytokines at concentrations 10 and 100ng/mL respectively. Nuclei of the cells were counterstained using DAPI. Images were captured on an inverted stage microscope Leica (Olympus IX81 fluorescence microscope with Cool Snap digital camera (Olympus Media Cybernetics, Silver Spring, USA)).



**Appendix V ( Continued):** Dual immunofluorescence showing expression of GFAP (red) and ADAMTS-9 (green) in human primary astrocytes untreated and after treatment with varying concentrations (0-100mg/mL) of IL-1 $\beta$ . Images from A to D represent cells not treated. Images from E to H represented cells dual treated with cytokines at concentration 1ng/ml. (I, J, K and L) and (M, N, O and P) cells treated with the same pro-inflammatory cytokine at concentrations 10 and 100ng/mL respectively. Nuclei of the cells were counterstained using DAPI. Images were captured on an inverted stage microscope Leica (Olympus IX81 fluorescence microscope with Cool Snap digital camera (Olympus Media Cybernetics, Silver Spring, USA).



## Appendix VI-A

### Directory of suppliers for the reagents used in this thesis

Supplier	Address
Abcam	330 Cambridge Science Park, Cambridge, Milton Rd, CB4 0FL, UK
Applied Bioscience	Lingley House, 120 Birchwood Boulevard, Warrington, WA3 7QH, UK
Bioline	16 The Edge Business Centre, Humber Rd., London, NW2 6EW
Dako	Denmark House, Angel Drove, Ely, Cambridgshire, CB7 4ET, UK
Fisher Scientific Inc	Bishop Meadow Rd., Loughborough, Leicestershire, LE11 5RG, UK
Invitrogen	3 Fountain Drive, Inchinnan Business Park, Paisley, PA4 9RF, UK
Leica	Larch House, Woodlands Business Park, Breckland, Linford Wood, Milton Keynes, MK14 6FG, UK
Lonza	Muenchensteinerstrasser 38, CH – 4002, Basel, Switzerland
Millipore	Suite 3 & 5, Building 6, Croxley Green Business Park, Watford, WD18 8YH, UK
Sigma-Aldrich	The Old Brickyard, New Road, Gillingham, Dorset, SP8 4XT, UK
LI-COR Biosciences Ltd	John's Innovation Centre, Cowley Road, Cambridge, CB4 0WS, UK
Vector Laboratories Ltd	3 Accent Park, Bakewell Road, Orton Southgate, Peterborough, PE2 6XS, U.K
Fisher Scientific Inc	Bishop Meadow Rd., Loughborough, Leicestershire, LE11 5RG, UK;
Santa Cruz	2145 Delaware Ave, California, 95060, USA

**Appendix VI-A: Directory of suppliers for the reagents used in this thesis  
(continued)**

Supplier	Address
Peprotech EC Ltd	Peprotech House, 29 Margravine Rd., London, W6 8LL, UK
R&D systems	19 Barton Lane, Abingdon Science Park, Abingdon, OX14 3NB, UK
Mettler-Toledo	Mettler-Toledo Ltd., 64 Boston Road, Beaumont Leys, Leicester, LE4 1AW , UK
ScienceCell™ Research laboratories	6076 Corte Del Cedro, Carlsbad, CA 92011, California, USA
TAAB Equipment Laboratories	SciQuip LTD Newtown Wem Shropshire SY4 5NU, UK
Cell Path Ltd	80 Mochdre Enterprise Park, Newtown, Powys, SY16 4LE, UK
Grant Equipment Ltd	Grant Instruments (Cambridge) Ltd, Shepreth, Cambridgeshire SG8 6GB, UK
Raymond A lamb Ltd	4-5, Park View Industrial Estate, Alder Cl, Eastbourne, East Sussex BN23 6QE, UK
Heraeus Instrument	Postfach 1561, Hanau, D-63450, Germany

### Appendix VI-B: Materials and their supplier utilised in this project

No	Material	Catalogue No	supplier	Methodology
1	Acetone	A/0560/17	Fisher Scientific,UK	IHC
2	Anti- Actin ( $\beta$ - actin antibody produced in mouse)	8H10D10	Cell Signaling Technology	WB
3	Anti- Glial Fibrillary Acidic Protein (GFAP) Antibody	MAB3402C3	Millipore	IHC
4	Anti-Human ADAMTS-9 (C-19) Antibody	SC-21502	Santa Cruz Biotechnology	IHC/WB
5	Anti-Human Leukocyte Antigen (HLA-DR) Antibody	NCL-LN3	Leica, UK	IHC
6	Anti-Human Aggrecan antibody	AB3778	Abcam, UK	IHC/WB
7	Anti-Human Aggrecan Neopeptide Antibody	PA1-1746	ThermoFisher Scientific, UK	IHC/WB
8	Anti-Human Versican antibody	AB111072	Abcam, UK	IHC/WB
9	Anti-Human Versican V0/V2 Neopeptide Antibody	PA3-119	ThermoFisher Scientific, UK	IHC/WB
10	Anti-Myelin Oligodendrocyte Glycoprotein (MOG) Antibody	-	Gift. Glasgow-University	IHC
11	Anti-Neurofilament-L (NF-L) Antibody	C28E10	Cell Signalling, UK	IHC/WB/Cell culture
12	Anti-Von Willebrand factor (vWF) Antibody	M0616	Dako, UK	IHC
13	Alexa fluor 488 Donkey anti-rabbit	A21206	Invitrogen,UK	IHC
14	Alexa fluor 488 Goat-anti-rabbit	A11008	Invitrogen,UK	IHC
15	Alexa fluor 488 Rabbit anti-mouse	A11050	Invitrogen,UK	IHC
16	Alexa fluor 568 Rabbit anti-mouse	A11061	Invitrogen,UK	IHC
17	Alexa fluor 568 Goat anti-mouse	A11004	Invitrogen,UK	IHC

**Appendix VI-B: Materials utilised in this project (Continued)**

No	Material	Catalogue No	Supplier	Methodology
18	Alexa fluor 568 Donkey anti-goat	A11057	Invitrogen, UK	IHC
19	Alexa fluor 488 Donkey anti-goat	A11055	Invitrogen, UK	IHC
20	Agarose	Bio-41026	Bioline	RNA gel electrophoresis
21	Astrocyte growth supplement	1852	ScienCell™ Research Laboratories	Cell culture
22	Basal astrocyte medium	1801	ScienCell™ Research Laboratories	Cell culture
23	Bovine serum albumin (BSA)	A/3059-50G	Sigma-Aldrich, UK	IHC
24	Chondroitinase ABC from <i>Protues vulgaris</i>	C3667	Sigma-Aldrich, UK	IHC
25	Coverslip 22x50mm	FB58661	Fisher Scientific, UK	H&E
26	Choloroform	C2432	Sigma-Aldrich, UK	RNA Extraction
27	Coverslip glasses 22X22mm	FB58633	Fisher Scientific, UK	IHC
28	Cryo M bed	CO28	TAAB Laboratories Equipment, UK	IHC
29	Cryo spray freezer spray	KNA-0173-00A	Cell Path Ltd	IHC
30	Dimethyl sulphoxide (DMSO)	D4540	Sigma-Aldrich, UK	Cell preservation
31	Disposable centrifuge tube, sterile, polypropylene	05-539-12	Fisher Scientific, UK	Cell culture
32	Deoxynucleotide triphosphate (dNTP)	Bio39026	invitrogen, UK	cdNA synthesis

**Appendix VI-B: Materials utilised in this project (Continued)**

<b>No</b>	<b>Material</b>	<b>Catalogue No</b>	<b>Supplier</b>	<b>Methodology</b>
33	Donkey anti-rabbit IRDye®800CW	C30417-02	Li-COR Biosciences	WB
34	DPX mountant	44581	Sigma-Aldrich, UK	H&E
35	Dulbecco's modified eagle medium DMEM	31965-023	Invitrogen, UK	Cell culture
36	Dulbecco's phosphate buffered saline (D-PBS)	14200-067	Invitrogen, UK	Cell culture, WB, IHC
37	Eosin Y solution	HT 110116	Sigma-Aldrich, UK	H&E
38	Ethanol	M/4450/17	Fisher Scientific, UK	H+E
39	Foetal bovine serum (astrocytes cell culture)	0010	ScienCell™ Research Laboratories	Cell culture
40	Foetal bovine serum	10106-169	Invitrogen, UK	Cell culture
41	Glass racks	E98	Raymond A Lamb limited	IHC
42	Glycerol gelatin	GG1	Sigma-Aldrich, UK	ORO
43	Goat anti-mouse IRDye® 680 LT 0.5mg	C20927-05	LiCOR-Bioscience	WB
44	Harris's Haematoxylin	HHS32	Sigma-Aldrich, UK	H&E & ORO
45	Hybond-C extra	RPN203E	GE Healthcare, LTD, UK	WB
46	ImmEdge hydrophobic barrier pen	H-4000	Vector Laboratories UK Ltd	IHC
47	Instant Blue™ Coomassie Based staining solution	CB22-7GX	Sigma-Aldrich, UK	Protein Gel
48	Immuno slide staining tray	E103-3	Fisher Scientific, UK	ICC

**Appendix VI-B: Materials utilised in this project (Continued)**

No	Material	Catalogue No	Supplier	Methodology
49	Methanol	M/3950/17	Fisher Scientific, UK	WB
50	Micro Amp optical 96-well plate reaction with bar code	3414320	Applied Biosystem, UK	qRT-PCR
51	MycAlert™ reagent (Lyophilized)	LT-27-217	Lonza	Mycoplasma test
52	MycAlert™ assay buffer	LT27-218	Lonza	Mycoplasma test
53	MycAlert™ substrate (Lyophilized)	LT27-221	Lonza	Mycoplasma test
54	Normal goat serum	Ab7481	Abcam, UK	IHC
55	Normal donkey serum	Ab7475	Abcam, UK	IHC
56	Nuclease free water	W3513	Sigma-Aldrich, UK	qRT-PCR
57	Nunclon™ delta surface cell culture flask, T25	156367	Fisher Scientific,UK	Cell culture
58	Nunclon™ delta surface cell culture flask, T75	156499	Fisher Scientific,UK	Cell culture
59	Nunclon™ delta surface cell culture plates with lid, 24-well	142475	Fisher Scientific,UK	Cell culture
60	Nunclon™ delta surface cell culture plates with lid, 6-well	140675	Fisher Scientific,UK	Cell culture
61	Nupage 7% Tris-Acetate gel 1.0mm x10 well	EA0355BOX	Invitrogen,UK	WB
62	Nupage anti-oxidant	NP0005	Invitrogen, UK	WB
63	Nupage LDS sample buffer (4X)	NP0007	Invitrogen, UK	WB

**Appendix VI-B: Materials utilised in this project (Continued)**

No	Material	Catalogue No	Supplier	Methodology
64	Nupage Tris-acetate Running Buffer (20X)	LA0041	Invitrogen, UK	WB
65	Nupage Transfer buffer (20X)	NP0006-1	Invitrogen, UK	WB
66	Oil Red O (ORO)	625	Sigma-Aldrich, UK	H&E
67	Olympus BX60 fluorescence microscope with Cool SNAP colour digital camera	-	-	IHC
68	Olympus BX51 fluorescence microscope with colorView III digital color camera	-	-	ICC
69	Phosphate buffer saline (PBS)	14190-094	Invitrogen, UK	IHC, H&E
70	Paraformaldehyde (PFA) Powder 95%	158127	Sigma-Aldrich, UK	IHC/ICC
71	Penicillin/streptomycin solution liquid (5000units/ml)	5070-063	Invitrogen, UK	Cell Culture
72	Penicillin/streptomycin solution (Astrocyte cell culture)	0503	ScienCell Research Laboratories	Cell Culture
73	Propanol for molecular biology	19516	Sigma-Aldrich, UK	RNA extraction
74	Protease inhibitor cocktail	P2714	Sigma-Aldrich, UK	Protein extraction
75	Random primer 9 unite	48190-011	Invitrogen, UK	cDNA synthesis
76	Recombinant human interferon gamma	300-02	Pepro Tech, UK	Cytokine treatment
77	Recombinant human interleukin-1 beta	200-01B	Pepro Tech, UK	Cytokine treatment
78	Recombinant human Tumour Necrosis Factor alpha B	300-01A	Pepro Tech, UK	Cytokine treatment
79	Retinoic acid >98% powder	R2625	Sigma-Aldrich, UK	SHSY5Y Differentiation

**Appendix VI-B: Materials utilised in this project (Continued)**

<b>NO</b>	<b>Material</b>	<b>catalogue NO</b>	<b>supplier</b>	<b>Methodology</b>
80	Corning® Small Cell Scraper	3010	Corning incorporated caster®	Cell culture
81	Sodium acetate trihydrate	S-7670	Sigma-Aldrich, UK	IHC (Deglycosylation)
82	Sodium hydroxide	BH15ITD	BDH Lab. Supplies,UK	H&E & ORO stain
83	Sudan Black B stain	199664	Sigma-Aldrich, UK	IHC
84	Thiazolyl Blue Tetrazolium Bromide	M5655-500MG	Sigma-Aldrich, UK	MTT
85	Taq man fast advanced master mix 1ml	112009	Invitrogen, UK	qRT-PCR
86	Taq man gene expression assay (ADAMTS-9)	Hs00172025_ml	Applied Biosystem, UK	qRT-PCR
87	Taq man gene expression assay (GAPDH)	Hs999999905_ml	Applied Biosystem, UK	qRT-PCR
88	Taq man gene expression assay (HPRT-1)	Hs999999909_ml	Applied Biosystem, UK	qRT-PCR
89	Taq man gene expression assay (PIIA)	Hs999999904_ml	Applied Biosystem, UK	qRT-PCR
90	Vectashield mount medium with DAPI	CA94010	Vector laboratories,UK	IHC
91	Wallac Victor 21420 Luminescence system	-	-	Cell culture, WB
92	Xylene	534056	Sigma-Aldrich, UK	H+E